INSTITUTO CARLOS CHAGAS
Doutorado em Biociências e Biotecnologia

CARACTERIZAÇÃO FUNCIONAL DE DZIP1 EM CÉLULAS DE LINHAGEM HELA E CÉLULAS-TRONCO DERIVADAS DE TECIDO ADIPOSO HUMANO

PATRÍCIA SHIGUNOV

CURITIBA/PR
2013

Ministério da Saúde

FIOCRUZ
Fundação Oswaldo Cruz

INSTITUTO CARLOS CHAGAS
Pós-Graduação em Biociências e Biotecnologia

Patrícia Shigunov

CARACTERIZAÇÃO FUNCIONAL DE DZIP1 EM CÉLULAS DE LINHAGEM HELA E CÉLULAS-TRONCO DERIVADAS DE TECIDO ADIPOSO HUMANO

Tese apresentada ao Instituto Carlos Chagas como parte dos requisitos para obtenção do título de Doutora em Biociências e Biotecnologia.

Orientadores: Prof. Dr. Bruno Dallagiovanna
Prof. Dr. Alejandro Correa

CURITIBA/PR
2013

Ficha catalográfica elaborada pela
Biblioteca de Ciências Biomédicas/ ICICT / FIOCRUZ - RJ

S555 Shigunov, Patrícia

Caracterização funcional de DZIP1 em células de linhagem hela e células-tronco derivadas de tecido adiposo humano / Patrícia Shigunov. – Curitiba, 2013.

xv, 133 f. : il. ; 30 cm.

Tese (Doutorado) – Instituto Carlos Chagas, Pós-Graduação em Biociências e Biotecnologia, 2013.
Bibliografia: f. 80-86

1. DAZ interacting protein 1 (DZIP1). 2. Células hela. 3. Células-tronco derivadas de tecido adiposo humano. 4. Complexos ribonucleoprotéicos. I. Título.

CDD 572.84

FUNDAÇÃO OSWALDO CRUZ
Instituto Carlos Chagas
Coordenação Curso de Pós-Graduação em Biociências e Biotecnologia
Rua Prof. Algacyr Munhoz Mader 3775
Cidade Industrial / 81350-010 Curitiba, PR
Tel. / Fax: (041) 3316-3230 / 3316-3267

Instituto Carlos Chagas

Ata da Sessão Pública de exame de dissertação para obtenção do grau de **Doutorado** em Biociências e Biotecnologia.

Aos vinte e três dias do mês de setembro de dois mil e treze , às 13 horas, nas dependências do Instituto Carlos Chagas/Fiocruz Paraná, reuniu-se a Banca Examinadora designada pelo Colegiado do Programa de Pós-Graduação em Biociências e Biotecnologia, composta pelos Professores: Dr. Samuel Goldenberg, Dr. Giordano Wosgrau Calloni e Dra. Lysangela Ronalte Alves com a finalidade de julgar a tese da candidata Patricia Shigunov, intitulada: **"Caracterização funcional de DZIP1 em células de linhagem Hela e células-tronco derivadas de tecido adiposo humano",** para obtenção do grau de Doutor em Biociências e Biotecnologia. A candidata teve até 45 (quarenta e cinco) minutos para a apresentação, e cada examinador teve um tempo máximo de arguição de 30 (trinta) minutos, seguido de 30 (trinta) minutos para resposta do candidato ou de 60 (sessenta) minutos quando houve diálogo na arguição. O desenvolvimento dos trabalhos seguiu o roteiro de sessão de defesa, estabelecido pela Coordenação do Programa, com abertura, condução e encerramento da sessão solene de defesa feito pelo Presidente **Dr. Samuel Goldenberg.** Após haver analisado o referido trabalho e arguido o candidato, os membros da banca examinadora deliberaram pela "APROVAÇÃO....", habilitando-a ao título de Doutor em Biociências e Biotecnologia, condicionada à implementação das correções sugeridas pelos membros da Banca Examinadora e ao cumprimento integral das exigências estabelecidas no Regimento Interno deste Programa de Pós-Graduação.

Prof. Dr. Giordano Wosgrau Calloni
UFSC

Prof. Dr. Samuel Goldenberg
ICC

Profª. Dra. Lysangela Ronalte Alves
ICC

Conferido com o original

Karin Goebel
Analista de Gestão em Saúde
Matrícula Siape 1956267
Instituto Carlos Chagas - Fiocruz PR

Ao meu companheiro Eduardo,
Á minha amada Íris,
Aos meus pais e irmãos.

AGRADECIMENTOS

Ao meu esposo, Eduardo Cezar Santos, agradeço o companheirismo, paciência e compreensão.

Aos meus pais, Claudinéia e Nicolau Shigunov, pelo amor incondicional e por sempre terem acreditado em mim.

À minha irmã, Vanessa Shigunov, pela amizade e apoio.

Ao Dr. Bruno Dalagiovanna por orientar minha formação científica desde a iniciação científica ao doutoramento. Agradeço por toda a sabedoria transmitida nesse período e pela amizade.

Aos membros da banca examinadora: Dr. Samuel Goldenberg, Dr. Giordano Calloni e Dra. Lysangela Ronalte Alves pela revisão criteriosa do presente trabalho.

Ao Dr. Marco Stimamiglio pelo suporte nas plataformas de citometria e microscopia confocal.

Ao Dr. Jose Sotelo-Silveira pelos ensinamentos nas análises de microarranjo de DNA.

Aos Dr. Fabricio Marchini e Dr. Michel Batista pelo suporte na plataforma de proteômica.

À todos do Laboratório de Biologia Básica de Células-Tronco: Dr. Alejandro Correa Dominguez, Crisciele Kuligovski, Dra. Alessandra Melo de Aguiar, Andressa Vaz Schittini, Dra. Ana Paula Abud, Dra. Jaiesa Zych, Axel Cofré, Ana Carolina Origa, Bruna Marcon, Anny Robert, Dra. Elizabeth de Moraes, Addeli Angulski e Thamile Reus. Pelos ensinamentos e pela amizade.

Ao pessoal técnico, administrativo e de manutenção do Instituto Carlos Chagas por propiciarem excelentes condições de trabalho.

À toda a equipe do Núcleo de Tecnologia Celular da Pontifícia Universidade Católica do Paraná, em especial Alexandra Senegaglia, Carmen Rebellato, Paula Hansen, Fabiane Barchick e ao Paulo Brofman.

À todos os amigos e pesquisadores do Instituto Carlos Chagas pelos ensinamentos e amizade.

Às agências financiadoras FIOCRUZ, CNPq, CAPES e FUNDAÇÃO ARAUCÁRIA pelo auxílio financeiro.

RESUMO

A regulação da expressão gênica em células eucariontes pode ser feita em nível transcricional e pós-transcricional. Em nível pós-transcricional, famílias de proteínas de união ao RNA participam desse processo. Muitos estudos têm apontado a família de proteínas DAZ (Deleted in Azoospermia) como estabilizadora de mRNAs e com um papel central no controle da autorrenovação de células-tronco. DZIP1 (DAZ-interacting protein) é uma proteína capaz de interagir com DAZ em células-tronco embrionárias e germinativas humanas. Em zebrafish, a proteína DZIP1 tem sido descrita como um dos reguladores da via de sinalização Hedgehog (Hh). No entanto, as funções de DZIP1 não foram descritas e há poucos dados sobre os mecanismos em que essa proteína participa. Dessa forma, o presente estudo visa a caracterização funcional de DZIP1 utilizando células HeLa e células-tronco derivadas de tecido adiposo (CTA). O trabalho é dividido em duas grandes partes: (1) Caracterização funcional de DZIP1 em células HeLa e (2) Caracterização de DZIP1 em CTA. Na primeira parte, a localização celular de DZIP1 foi determinada e é predominantemente citoplasmática com um padrão granular. A fim de identificar o tipo desses grânulos, ensaios de co-localização de DZIP1 com DCP1 (*p-bodies*) foram realizados e resultaram em não co-localização. Ensaio de imunofluorescência em células sob estresse oxidativo mostrou a co-localização de DZIP1 e TIA1 (marcador de grânulos de estresse). Estes resultados sugeriram que DZIP1 é um componente de complexos ribonucleoprotéicos (pelo menos em condições de estresse). Com o objetivo de identificar os mRNAs associados com DZIP1 foram realizadas imunoprecipitações dessa proteína e os mRNAs identificados por hibridação de microarranjos de DNA. As redes gênicas formadas pelos mRNAs alvos de DZIP1 indicam funções envolvendo o controle do ciclo celular e expressão gênica. O silenciamento de DZIP1 resultou em aumento no número de células em ensaio de curva de crescimento. Ensaios de EMSA utilizando sondas de homoribopolímeros sugerem que DZIP1 não interage diretamente com o RNA. A proteína DZIP1 está envolvida na via de sinalização Hh e um bloqueador específico dessa via é a ciclopamina. Observamos que a localização de DZIP1 sofre mudanças após a inibição da via Hh. Ainda, a expressão dos mRNAs associados a DZIP1 foi avaliada por qRT-PCR em células tratadas com ciclopamina e observou-se que a expressão deles aumenta com o tratamento. Porém, quando DZIP1 é silenciado ou superexpresso em células HeLa, o nível de expressão dos mRNAs associados não é afetado de forma significativa. Ainda assim, ensaios de decaimento de RNA com ActD foram realizados e demonstraram que DZIP1 não afeta a vida média dos mRNAs avaliados. Para estudar a associação de DZIP1 aos polissomos, extratos citoplasmáticos foram separados em gradiente de sacarose e a presença de DZIP1 nas frações polissomais foi visualizada por western blot. Na segunda parte deste trabalho, a localização de DZIP1 foi avaliada nas CTA em diferentes condições: normal, sob estresse oxidativo, com a via Hh bloqueada e ativada. DZIP1 apresentou um padrão de expressão granular e principalmente citoplasmático como observado em células HeLa. De maneira geral, os diferentes tratamentos não afetaram a localização de DZIP1. Em conclusão, a proteína DZIP1 participa de um complexo ribonucleoprotéico que transita nos compartimentos núcleo e citoplasma, está associada à maquinaria da tradução e sob estresse oxidativo está presente em grânulos de estresse. Estes resultados sugerem que a função de DZIP1 estaria associada ao transporte de mRNAs entre diferentes compartimentos funcionais, participando do ciclo de vida do mRNA na célula.

ABSTRACT

Regulation of gene expression in eukaryotic cells occurs both at the transcriptional and post-transcriptional level. At the post-transcriptional level, RNA-binding proteins families participate in this process. Many studies pointed to the DAZ (Deleted in Azoospermia) family as stabilizing mRNAs with a central role in controlling stem cells self-renewal. DZIP1 (DAZ-interacting protein) is a protein able to interact with DAZ in human embryonic and germ stem cells. In zebrafish, DZIP1 has been described as one of the regulators of the hedgehog signaling pathway (Hh). However, DZIP1 molecular function has not been described and there is little information about the mechanisms in which this protein is involved. This study aims to characterize the function of DZIP1 in HeLa and adipose stem cells (ASC). The work is divided into two major parts: (1) Functional characterization of DZIP1 in HeLa cells and (2) characterization of DZIP1 in ASCs. First, the cellular localization of DZIP1 was determined. The protein is predominantly cytoplasmic showing a granular pattern. In order to identify the class of these granules, localization assays of DZIP1 and DCP1 (p-bodies) were conducted and resulted in no co-localization. Immunofluorescence assays in cells under oxidative stress showed co-localization of DZIP1 and TIA1 (a stress granule marker). These results suggested that DZIP1 is a component of a ribonucleoprotein complex (at least under stress conditions). Aiming to identify mRNAs associated with DZIP1 we performed immunoprecipitation assays of the protein and the associated mRNAs were identified by hybridization of DNA microarrays. The genetic networks formed by mRNAs associated with DZIP1 indicate functions including the control of cell cycle, proliferation and gene expression. DZIP1 silencing resulted in an increase in the number of cells in growth curve assays. EMSA using homoribopolymer probes suggests that DZIP1 does not interact directly with RNA. DZIP1 protein is involved in the Hh signaling pathway of which cyclopamine is a specific inhibitor. We observed that the cellular location of DZIP1 undergoes changes after inhibition of the Hh pathway. Furthermore, the expression of mRNAs associated with DZIP1 was evaluated by qRT-PCR in cyclopamine-treated cells where they showed increased expression with treatment. When DZIP1 is silenced or overexpressed in HeLa cells, the expression level of associated mRNAs is not significantly affected. Moreover, RNA decay assays were performed with ActD showing that DZIP1 do not affect the half life of mRNAs. To study the association of DZIP1 with polysomes, cytoplasmic extracts were separated on sucrose gradient and the presence of DZIP1 in polysomal fractions was visualized by western blot. Regarding the characterization of DZIP1 in stem cells, its location was evaluated in ASCs under different conditions: normal, oxidative stress, activated and blocked Hh pathway. DZIP1 showed a pattern of granular cytoplasmic expression as observed in HeLa cells. In general, the different treatments did not affect the cellular location of DZIP1. In conclusion, the protein DZIP1 is part of a ribonucleoprotein complex that transits the nucleus and cytoplasm compartments and is associated with the translation machinery and under oxidative stress is present in stress granules. These results suggest that the function of DZIP1 be associated with the transport of mRNAs among different functional compartments, participating in the cycling of mRNAs in the cell.

LISTA DE FIGURAS

LISTA DE TABELAS

LISTA DE ABREVIATURAS E SIGLAS

BSA: albumina de soro bovino (“Bovine Serum Albumin”)

$CaCl_2$: cloreto de cálcio

cDNA: DNA complementar

DAPI: 4,6-diamidino-2-phenylindole

DNA: ácido desoxirribonucleico

DNase: desoxirribonuclease

dNTP: desoxirribonucleospideo trifosfato

E-64: L-transepoxisuccinil-leucilamido (4-guanidino)butano

EDTA: ácido etileno-diamino-tetracético

EMSA: ensaio de mobilidade eletroforética (“Eletrophoretic Mobility Shift Assay”)

kb: quilobase

kDa: quiloDalton

LB: meio Luria-Bertani

M: molar

mg: miligrama

mL: mililitro

mM: milimolar

mRNA: RNA mensageiro

mRNP: ribonucleoproteína mensageira

$Na_2HPO_4.7H_2O$: fosfato dibásico de sódio heptahidratado

NaCl: cloreto de sódio

NCBI: “National Center for Biotechnology Information”

ng: nanograma

ORF: região aberta de leitura (“Open Reading Frame”)

pb: pares de base

P-bodies: grânulos de processamento (“Processing bodies”)

PBS: solução salina tamponada (“Phosphate Buffered Saline”)

PCR: reação em cadeia da polimerase (“Polymerase Chain Reaction”)

pH: potencial hidrogeniônico

PMSF: fluoreto de fenilmetilsulfonil

RBD: domínio de ligação ao RNA (“RNA Binding Domain”)

RBP: proteína de ligação ao RNA (“RNA Binding Protein”)

RNA: ácido ribonucleico

RNase: ribonuclease

RNP: ribonucleoproteína

rpm: rotações por minuto

rRNA: RNA ribossomal

SDS: dodocil sulfato de sódio

SDS-PAGE: eletroforese em gel de poliacrilamida

Tris: hidroximetil aminometano

tRNA: RNA transportador

μg: micrograma

μL: microlitro

μm: micrômetro

μM: micromolar

UTR: região não-traduzida (“UnTranslated Region”)

V: volts

SUMÁRIO

1. INTRODUÇÃO

O corpo humano possui aproximadamente 210 tipos de células diferentes e todas as células do nosso corpo possuem a mesma informação genética (Strachan, 1999). Isso implica em uma série de questionamentos de como pode essa mesma informação originar células tão diferentes. O neurônio, por exemplo, possui características fenotípicas únicas para realizar a condução do impulso nervoso pelo corpo, assim como uma célula muscular cardíaca é capaz de gerar uma diferença no potencial elétrico em sua membrana, sincronizando seu movimento com milhares de outras células com um único objetivo comum, contrair o miocárdio para o bombeamento do sangue para todo o corpo. As duas células descritas acima refletem uma pequena parcela do que um genoma bem coordenado é capaz de fazer.

Atualmente, sabe-se que os seres humanos possuem cerca de 21.000 genes que codificam em proteínas (Frazer, 2012), informações suficientes para originar um organismo complexo. Dependendo de quais genes e quanto estão ativados determinará o tipo de célula. Por exemplo, as células musculares possuem as proteínas miosinas, extremamente importantes para a contração muscular. Se o gene que codifica essa proteína está desligado nas células musculares, essas células não serão capazes de fazer a contração, resultando na falência do organismo. Esse exemplo demonstra a importância desses genes estarem coordenados perfeitamente para manter um organismo com tamanha diversidade celular. As células devem regular seu próprio genoma para ativar e desativar genes dependendo de sua localização espaço-temporal propiciando seu fenótipo característico, como tamanho, estruturas, função, ciclo celular, entre outros. O controle dessas características é realizado por diversos mecanismos de regulação da expressão gênica.

1.1 Mecanismos de Regulação da Expressão Gênica

As características fenotípicas descritas acima dependem do conjunto de genes particulares que a célula expressa. A expressão dos genes significa a transformação da informação contida no DNA em moléculas de RNA, que por sua vez podem ser traduzidas em proteínas. Portanto, uma célula pode controlar as proteínas que produz pelo controle de quando e como um determinado gene é transcrito, também conhecido como controle transcricional.

A transcrição dos genes é realizada pelas enzimas RNA polimerase I (transcreve genes de RNAs ribossômicos), RNA polimerase II (transcreve genes que serão traduzidos em proteínas ou microRNAs) e RNA polimerase III (transcreve pequenos RNAs, como o tRNA)

(Vannini & Cramer, 2012). Todas as etapas da expressão de um gene podem ser reguladas (Figura 1.1). Entretanto, alguns trabalhos demonstram que em eucariotos superiores existe um controle pós-transcricional elaborado, onde cada etapa do metabolismo do mRNA está sujeita a uma regulação mRNA-específica (Matoulkova et al, 2012).

1.2 Regulação pós-transcricional da expressão gênica

O mRNA possui características intrínsecas como regiões que não são traduzidas em proteína e estão localizadas nas porções 5´ e 3' (5´-UTR e 3´-UTR). Essas regiões são alvos para as proteínas reguladoras envolvidas na modulação pós-transcricional (Matoulkova et al, 2012). No processamento do mRNA, uma guanosina metilada é adicionada à região 5´ (conhecida como "cap") e uma cauda com poli-adeninas (poli-A) na região 3´-UTR. O "cap" e a cauda poli-A são importantes para a exportação do mRNA para o citoplasma, tradução e prevenção da degradação por exonucleases, garantindo a estabilidade do mRNA na célula. A incorporação destas duas estruturas reflete uma das primeiras etapas da regulação pós-transcricional.

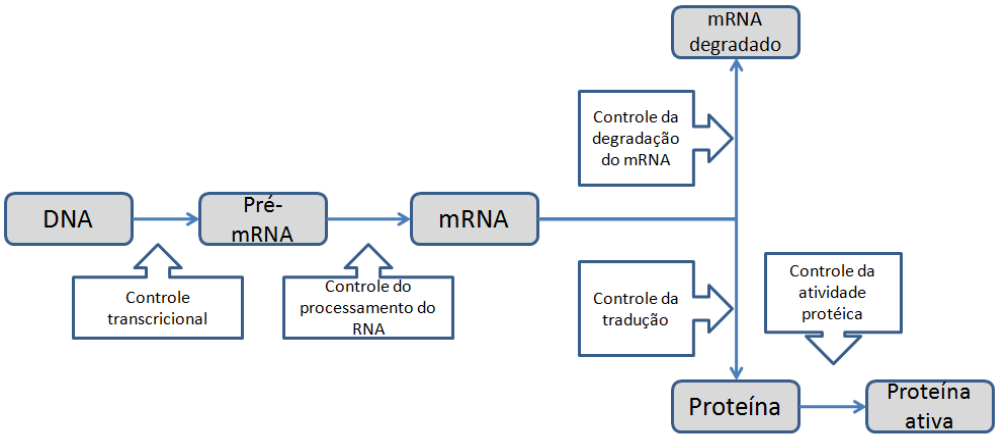

Figura 1.1 Mecanismos de controle da expressão gênica. Adaptado de Unwin & Whetton, 2006.

A transcrição do gene resulta na formação de um transcrito primário, um pré-RNA mensageiro (mRNA) contendo íntrons e éxons, e é necessário que este seja processado para originar um mRNA maduro (De Conti et al, 2013). Esse processamento é o processo de remoção dos íntrons que também é conhecido como "splicing" e é regulado por diversas proteínas e RNAs. As sequências dos íntrons são removidas do RNA por meio de duas reações sequenciais de transferência de fosforil, as quais unem dois éxons, enquanto removem o íntron na forma de uma alça (De Conti et al, 2013). O "splicing" do RNA também permite que os eucariotos superiores tenham a capacidade de sintetizar várias proteínas diferentes a

partir do mesmo gene. Ou seja, os transcritos sofrem "splicing" em regiões diferentes, produzindo grupos distintos de mRNAs, permitindo, assim, que um grupo correspondente de diferentes proteínas seja produzido. Esse processo é denominado "splicing" alternativo (Djebali et al, 2012).

Em eucariotos, a exportação de mRNA e proteínas do núcleo para o citoplasma é um processo regulado que permite o controle da expressão de proteínas. As proteínas que são transportadas do núcleo para o citoplasma, e vice-versa, possuem sinais de localização nuclear e/ou sinais de exportação nuclear, e algumas delas podem carregar sub populações de mRNAs como parte de um complexo ribonucleoprotéico (mRNP – "mRNA-protein complex") (Jansen & Niessing, 2012).

A estabilidade do mRNA desempenha um papel importante na expressão do gene em células de mamíferos, afetando as taxas em que os mRNAs são degradados e acumulados. Uma série de fatores exógenos (hormônios, citocinas, íons, estresse, virus e entre outros) influenciam a meia vida do mRNA (Keene, 2010). Os mecanismos de decaimento do RNA incluem interações entre os elementos agindo em *cis* e *trans*. Os principais elementos *cis* que afetam a taxa de decaimento incluem os elementos ricos em AU (ARE), elementos responsivos ao ferro, "stem-loops", determinantes da região codificante, elementos de resposta aos jun-quinases, íntrons retidos, junções exon e tamanho da cauda poli-A (Wu & Brewer, 2012). Fatores *trans* que controlam o decaimento dos mRNAs incluem as RNAses, proteínas de união ao RNA, siRNA, miRNA e piRNA (Wu & Brewer, 2012).

Outro ponto de controle da expressão gênica envolve o acoplamento do mRNA com a os ribossomos. No citoplasma, os mRNAs maduros são reconhecidos pelos fatores de iniciação eucariótico (eIF), proteínas envolvidas na fase inicial de tradução. Os fatores participam na formação de um complexo juntamente com a subunidade ribossomal 40S e Met-tRNA inicial chamado de complexo de pré iniciação 43S (Alekhina & Vassilenko, 2012). O eIF-4E reconhece o "cap" na porção 5´, enquanto eIF-4G reconhece as proteínas de união a cauda poli-A (PABP – "poly(A) binding protein"), promovendo a circularização do mRNA (Mazumder et al, 2003). Essa etapa é importante para a certificação da integridade do mRNA que será traduzido. O complexo percorre a região 5´-UTR até encontrar o códon AUG, recrutando a subunidade ribossomal 60S e formando o complexo 80S, dando início ao processo de elongação da tradução.

Considerando que o mRNA é um intermediário nas mudanças fenotípicas numa célula, agindo como mensageiro para a síntese de proteína (Unwin & Whetton, 2006), os mecanismos que regulam a tradução do mRNA em proteína são altamente controlados por elementos *cis* e *trans*. Alguns fatores devem ser levados em consideração quando se trata de

mudanças na expressão de proteínas, como: processamento, localização e estabilidade do mRNA, proteínas reguladoras da tradução, razão de tradução, estabilidade da proteína, modificações pós-traducionais e localização celular da proteína (Auweter et al, 2006).

A contribuição dos elementos regulatórios nas regiões não traduzidas do mRNA para a expressão do gene em células eucarióticas inclui trato de oligopirimidina terminal, sítio interno de entrada do ribossomo, janelas abertas de leitura a montante, elementos de poliadenilação citoplasmáticos, elementos ricos em AU (que modulam a estabilidade e tradução do mRNA (Pichon *et al.*, 2012), entre outros. Esses elementos regulatórios no mRNA podem adotar estruturas secundárias e/ou contêm motivos que permitem sua interação com uma diversidade de proteínas regulatórias e RNAs (Figura 1.2). As interações resultantes são sensíveis ao contexto molecular e celular, ou seja, com resposta sensível e rápida aos sinais celulares como exposição a hormônios ou estresse citotóxico.

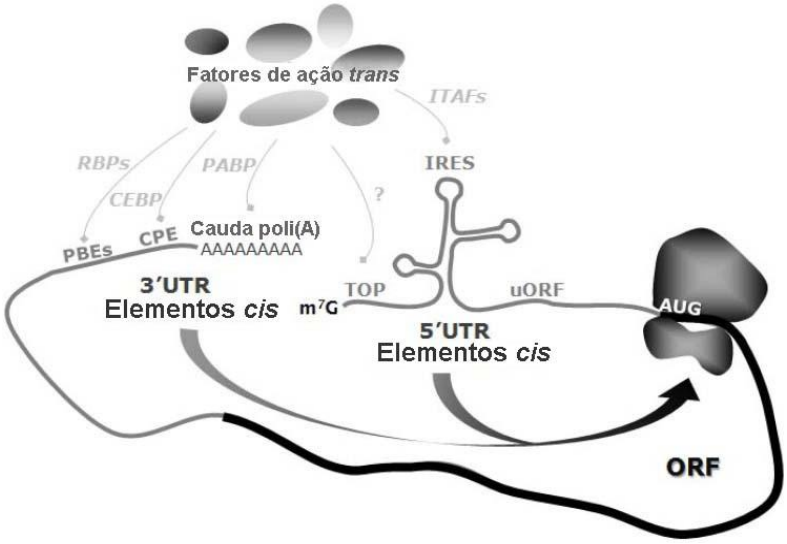

Figura 1.2 Esquema representativo da regulação do início da tradução através de elementos *cis* e fatores agindo em *trans* nas regiões 5´-UTR e 3´-UTR. Regulação através da porção 5´-UTR pode ocorrer via motivo 5´trato oligopirimidina terminal (TOP - "Terminal Oligopyrimidine tracts"), sítios internos de entrada do ribossomo (IRES), seus fatores agindo em *trans* e janelas abertas de leitura a montante (uORFs). Regulação através da 3´-UTR pode ocorrer via interação de proteínas de interação ao RNA (RBPs), a interação de proteínas de ligação a elementos de poliadenilação citoplasmático (CPE) e também via interação de proteínas de ligação a poli-A (PABP), que leva a circularização do mRNA. Adaptado de (Pichon et al, 2012).

A regulação da expressão gênica ocorre em diversos níveis nos organismos eucariotos e é um processo altamente controlado. O metabolismo do mRNA é mediado pela interação de fatores em *trans*, como a classe de proteínas de ligação ao RNA ("RNA-binding proteins" – RBPs) e pequenos RNAs não codificantes (Janga, 2012).

1.3 Pequenos RNAs não codificantes

Recentemente, os trabalhos de sequenciamento do genoma vêm apresentando um número cada vez maior de RNAs não codificantes e que possui uma importância funcional crucial para o desenvolvimento normal, fisiologia e doenças (Alexander et al, 2010). A relevância funcional do genoma não codificante de proteínas é particularmente evidente para a classe de pequenos RNAs não codificantes (ncRNAs) chamados microRNAs (miRNAs).

Em mamíferos, os miRNAs são reguladores essenciais que determinam a atividade de proliferação, apoptose, diferenciação, entre outras funções (Chen & Lodish, 2005; Esau et al, 2004). Até o momento, de acordo com o banco de dados miRBase, cerca de 30.424 miRNAs maduros foram identificados em 206 espécies (Kozomara & Griffiths-Jones, 2011).

Os miRNAs são moléculas de RNA fita simples de 19-25 nucleotídeos que agem como potentes reguladores pós-transcricionais da expressão gênica em plantas e animais (Kim, 2005). Os miRNAs exercem seus efeitos regulatórios ligando-se geralmente à região 3' não traduzida de mRNA-alvo. Este mecanismo de atuação permite a redução dos níveis protéicos de seus genes-alvos, raramente afetando o nível de expressão transcricional (Kim, 2005).

Esses pequenos RNAs passam por processamentos gerados por etapas de clivagens catalisadas por dois complexos distintos: Drosha, encontrado no núcleo, e Dicer encontrado no citoplasma (Filipowicz et al, 2008). Após a clivagem por Dicer, a forma madura do miRNA (~22 nucleotídeos) é incorporada a um complexo de silenciamento induzido por RNA (*RNA-induced silencing complex* – RISC), que inclui as proteínas Argonauta como principais componentes (Filipowicz et al, 2008). Apenas uma das fitas do miRNA permanece no complexo RISC para controlar a expressão pós-transcricional de genes alvo (Schwarz et al, 2003).

Os miRNAs podem interferir no transcrito por dois mecanismos diferentes: degradação do mRNA ou repressão da tradução. A regulação pós-transcricional exercida pelos miRNAs na região 3' não traduzida depende do grau de complementaridade com o mRNA-alvo. O pareamento de modo imperfeito com o mRNA acarreta a inibição traducional do alvo, sendo o mecanismo principal de atuação dos miRNAs em mamíferos (Brennecke et al, 2005). Alguns estudos indicam que um único miRNA possa regular cerca de duzentos RNAs apresentando funções totalmente diversas. Desta forma, os miRNAs constituem uma enorme e complexa rede regulatória da sinalização celular (Valencia-Sanchez et al, 2006). Além disso, através da regulação global da expressão gênica celular e associação a diferentes

funções, torna-se evidente que os miRNAs podem alterar o progresso de diversas patologias (Jones et al, 2012).

1.4 Proteínas de ligação ao RNA

As proteínas com domínios de ligação ao RNA (RBPs – "RNA binding protein") possuem funções em todo o aspecto que compreende a biologia do RNA, da transcrição, "splicing" do transcrito e poliadenilação até as modificações, transporte, localização, tradução e estabilidade do RNA. As RBPs não somente influenciam nesses processos, mas também estabelecem as conexões entre eles (Glisovic et al, 2008).

As RBPs são proteínas reguladoras que interagem com os mRNAs formando estruturas macromoleculares denominadas complexos ribonucleoproteicos mensageiros (mRNPs) (Keene, 2001; Moore, 2005). As RBPs reconhecem e se ligam a transcritos funcionalmente relacionados para regular de forma coordenada seu processamento, localização celular e tradução (Moore, 2005). A base destas redes de regulação mencionadas anteriormente são as mRNPs, sendo, portanto sua caracterização fundamental para a compreensão dos mecanismos reguladores da expressão gênica.

Muitas das RBPs foram anotadas em genomas de mamíferos com base na presença de domínios de ligação ao RNA (RBDs – "RNA-binding domains"), mas as funções e as especificidades das ligações *in vivo* da maior parte das RBPs não são bem compreendidas (Müller-McNicoll & Neugebauer, 2013). Muitas RBPs foram inferidas a partir da homologia de sequência, e até recentemente, apenas uma pequena fração foi validada a propriedade de ligação ao RNA *in vivo*. Os domínios de ligação ao RNA são conservados e reconhecem sequências curtas contendo de 4-6 nucleotídeos ou elementos estruturais em seus RNAs alvos (Ankö & Neugebauer, 2012).

A biologia estrutural das RBPs tem proporcionado alguns detalhes moleculares e princípios de reconhecimento de RNA por um único RBDs. No entanto, muitas RBPs requerem múltiplos RBDs para a sua função *in vivo*, pois permitem que a proteína possa reconhecer longos trechos de RNA e combinar múltiplas interações fracas para atingir alta afinidade e especificidade (Mackereth & Sattler, 2012). A multimerização também permite às RBPs reconhecerem sequências de RNA que pertencem a diferentes RNAs ou que estão separados por longas sequências de nucleotídeos (Wahl et al, 2009).

Já foram anotadas mais de 40 RBDs nos bancos de dados (Kishore et al, 2010), dentre os mais conhecidos estão: motivo de reconhecimento de RNA (RRM), K-homology (KH), RGG (Arg-Gly-Gly) Box, domínio Sm, DEAD/DEAH Box, dedo de zinco (ZnF), domínio de

ligação à RNA dupla fita (dsRBD); domínio de choque térmico; domínio Pumilio/FBF e domínio Piwi/Argonaute/Zwille (PAZ) (Figure 1.3).

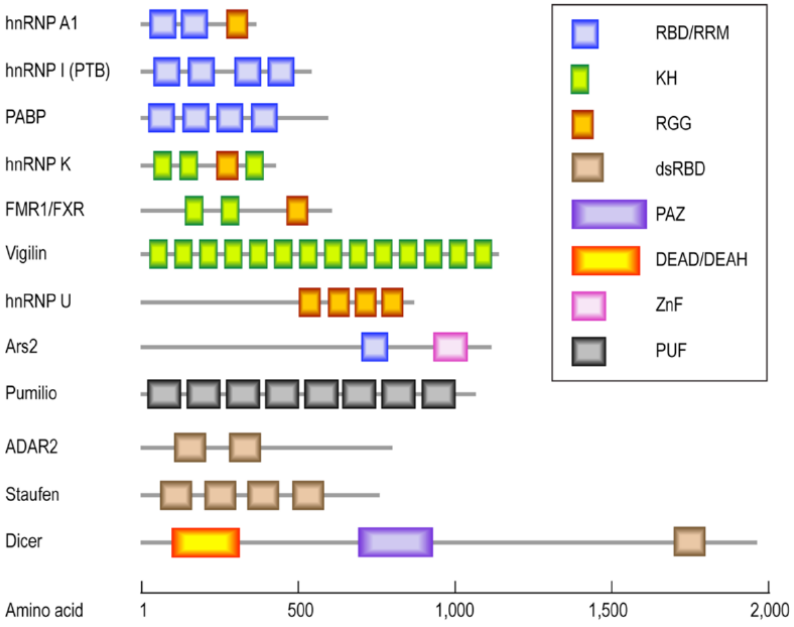

Figura 1.3 Proteínas de união ao RNA e seus domínios. Essas proteínas podem conter vários domínios de ligação ao RNA. Na esquerda estão representadas as diferentes RBPs com retângulos / quadrados coloridos que representam os domínios de união ao RNA. No quadro à direita estão denominados os respectivos domínios que inclui: o motivo de reconhecimento de RNA (RRM), domínio KH, RGG, domínio de ligação ao RNA dupla fita (dsRBD), domínio *Piwi/Argonaute/Zwille* (PAZ), *RNA helicase DEAD/DEAH*, dedo de zinco de ligação ao RNA (ZnF) e repetições PUF de ligação ao RNA (PUF). FONTE: (Glisovic et al, 2008).

O motivo de reconhecimento de RNA dedo de zinco (ZnF - zinc-finger) compreende dois resíduos de histidina e dois resíduos de ácidos aminados cisteína associados a um íon de zinco (CCHH). Domínios de dedo de zinco do tipo CCHH são domínios de ligação ao DNA mais comuns dentro do genoma eucarioto. A fim de alcançar um elevado reconhecimento específico da sequência de DNA, vários dedos de zinco são utilizados de uma forma modular. Apesar do amplo reconhecimento ao DNA, descobertas recentes identificaram que os domínios dedos de zinco também têm a capacidade de reconhecer o RNA. Os domínios dedos de zinco CCCH foram recentemente descobertos reconhecendo sequências de RNA de cadeia simples de forma específica. Em geral, os dedos de zinco podem reconhecer DNA diretamente através da ligação à sequência de DNA dupla fita e RNA através de ligação a sequência RNA simples fita (Stefl et al, 2005).

O motivo de ligação ao RNA dupla fita (dsRBM) contém 70-75 aminoácidos e desempenha um papel crítico no processamento e localização do RNA, interferência de RNA e repressão da tradução. Apenas três estruturas de dsRBMs foram descritas até o presente,

todas possuem características de união ao RNA dupla fita. Os dsRBMs interagem ao longo do RNA dupla fita através de ambas as alfa hélices e folhas β1-β2. Apesar das características estruturais comuns entre dsRBMs, cada domínio reconhece sequências de RNA específicas (Stefl et al, 2005).

O motivo de reconhecimento de RNA (RRM), que é o motivo de ligação ao RNA mais comum, é um domínio com 75-85 aminoácidos que forma duas alfa-hélices em quatro cadeias de folha beta de modo a possibilitar o reconhecimento de RNA e proteína (Stefl et al, 2005). Este motivo de reconhecimento exerce o seu papel em várias funções celulares, especialmente em processamento de mRNA e rRNA, regulação da tradução, exportação e estabilidade do RNA. A alta versatilidade estrutural das interações RRM explica por que proteínas contendo esse motivo têm diversas funções biológicas (Cléry et al, 2008).

1.5 Família "Deleted in Azoospermia" (DAZ)

As proteínas da família DAZ têm uma estrutura comum que consiste em um domínio RRM e pelo menos uma cópia de um motivo rico em aminoácidos básicos, denominado repetições DAZ (Reijo et al, 1995b) (Saxena et al, 1996).

Várias evidências sugerem que os genes da família DAZ têm funções essenciais na manutenção das células-tronco das linhagens germinativas e embrionárias humanas (Moore et al, 2003). Homens que não possuem o *cluster* do gene DAZ do cromossomo Y perdem todas as células-tronco germinativas e têm defeitos na espermatogênese (Reijo et al, 1995a).

A família de proteínas DAZ consiste em três membros: BOULE (BOLL), DAZ-Like (DAZL) e DAZ. O gene DAZ apresenta quatro cópias das repetições DAZ e está localizado no cromossomo Y, enquanto que DAZL e BOLL são cópias localizadas no cromossomo 3 e 2, respectivamente (Saxena et al, 2000). As proteínas da família DAZ são detectadas em células-tronco das linhagens germinativas masculinas e femininas assim como no plasma germinativo na fase inicial de embriões de anfíbios (Houston & King, 2000; Karashima et al, 2000; Ruggiu et al, 1997).

As proteínas DAZ se ligam aos RNAs *in vitro* e *in vivo* e estão envolvidas na regulação pós-transcricional, como na ativação da tradução, transporte e estabilidade de mRNAs alvos (Figura 1.4) (Reynolds & Cooke, 2005; Vangompel & Xu, 2011; Yen, 2004).

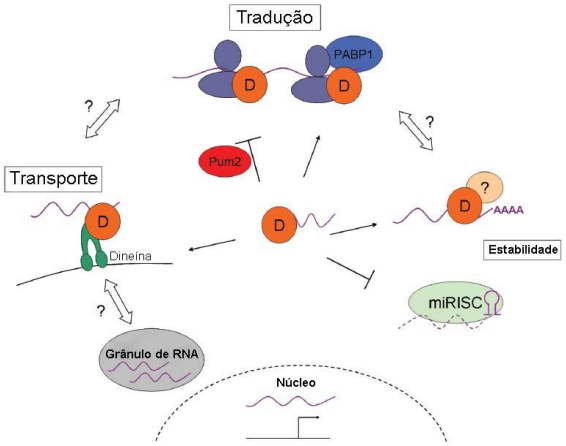

Figura 1.4 Modelo para as funções de genes da família DAZ. Proteínas dessa família funcionam através de mecanismos similares e o modelo representa suas funções citoplasmáticas. Uma proteína da família DAZ genérica (circulo com letra "D") ligada a um RNA é representada no centro da figura. Essas proteínas têm multiplas funções, provavelmente dependendo das proteínas parceiras associadas. A ligação a PABP (proteínas de ligação a poli-A) promove associação com ribossomos e tradução, enquanto que a ligação ao repressor PUM2 inibe a tradução. Interações com dineínas podem mediar o transporte de mRNAs alvos para grânulos de estresse, assim como corpos cromatóides ou polissomos para ativação traducional. As proteínas da família DAZ podem promover estabilidade através da inibição da degradação mediada por miRNA, ou promoção da poliadenilação com ligação a fatores desconhecidos. Linhas sólidas representam mecanismos conhecidos, enquanto as setas vazadas representam especulações entre funções conhecidas. Adaptado de (Vangompel & Xu, 2011).

DAZL desempenha um papel chave no desenvolvimento de células germinativas em animais, tais como *Caenorhabditis elegans* (Karashima et al, 2000), *Drosophila melanogaster* (Eberhart et al, 1996), *Xenopus laevis* (Houston & King, 2000) e camundongo (*Mus musculus*) (Ruggiu et al, 1997). Em Xenopus e peixe-zebra, o mRNA de *dazl* está presente no germoplasma e em células progenitoras germinativas durante o início da embriogênese (Hashimoto et al, 2004; Houston & King, 2000). A função de DAZL está associada a manutenção da pluripotência e no mecanismo de diferenciação de células germinativas primordiais *in vivo* e *in vitro* (Haston et al, 2009). DAZL ativa a tradução de mRNAs alvo através da ligação direta em elementos *cis* na porção 3´-UTRs (Vasudevan et al, 2006). Além disso, DAZL de Xenopus interage com proteínas de ligação a poli-A, (PABPs), que são críticas para a iniciação da tradução (Collier et al, 2005).

DAZL é uma proteína de ligação ao RNA e interage com um conjunto de mRNAs específicos, como o homólogo *vasa* de camundongo, *Mvh*, e o componente do complexo sinaptinemal, *Sycp3* (Reynolds et al, 2007; Reynolds et al, 2005b). A função de DAZL foi proposta como sendo um adaptador para transporte de mRNA e como um ativador da tradução (Collier et al, 2005; Lee et al, 2006). Takeda e seus colaboradores (2009) utilizaram

um mRNA repórter com proteína verde fluorescente (GFP- “Green fluorescence protein”) fusionada com 3´UTR de *tdrd7*, e mostraram que DAZL antagoniza a repressão mediada pelo miR-430 do mRNA *tdrd7* em embriões de peixe-zebra. Além disso, a adição de elementos de ligação de DAZL a um mRNA sintético alvo do miR-430 conduziram à estabilização do mRNA de maneira específica em células progenitoras germinativas. DAZL induz a poliadenilação do mRNA repórter independentemente da função do miRNA. DAZL foi descrito como um "fator anti-miRNA" durante desenvolvimento das células germinativas em vertebrados (Figura 1.5) (Takeda et al, 2009).

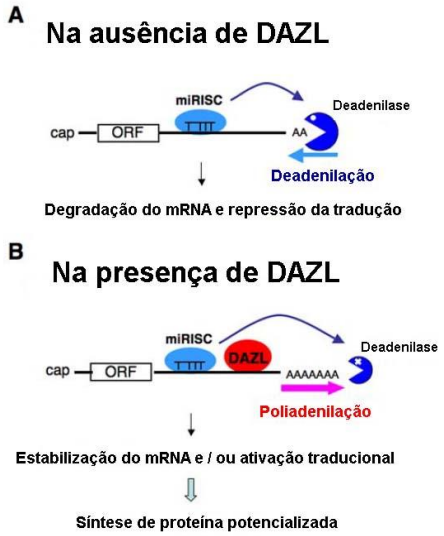

Figura 1.5 Modelo para a função de DAZL. (A) Na ausência de DAZL (células somáticas), miRISC se liga ao mRNA alvo e induz a deadenilação, degradação do mRNA e repressão da tradução. (B) Na presença de DAZL (células progenitoras germinativas), o mRNA com DAZL é poliadenilado. Esse efeito pode superar o efeito inibitório de miRISC, resultando na síntese de proteína ativa, mesmo na presença do miRNA. Adaptado de (Takeda et al, 2009).

Além disso, DAZL colocaliza com TIA1, um marcador de grânulos de estresse, em células HeLa sob estresse oxidativo (Kim et al, 2012). Essa descoberta levou a especulações sobre uma nova função de DAZL em células sob estresse térmico. Kim e seus colaboradores (2012) revelaram que grânulos de estresse são formados em células germinativas masculinas de camundongo sob estresse térmico e que DAZL é um componente essencial nos grânulos de estresse (Figura 1.6). Há evidências de que em células germinativas masculinas, os grânulos de estresse têm função de proteção contra a apoptose (Kim et al, 2012).

Lee e colaboradores (2006) demonstraram a interação de DAZL com a cadeia leve da dineína, um componente do complexo motor dineína-dinactina, e a distribuição subcelular de Dazl apresentou dependência de microtúbulos. Baseado nesses resultados foi proposto que

Dazl tem função envolvendo o transporte de mRNAs específicos via complexo motor contendo dineína em células germinativas masculinas de camundongo (Figura 1.7).

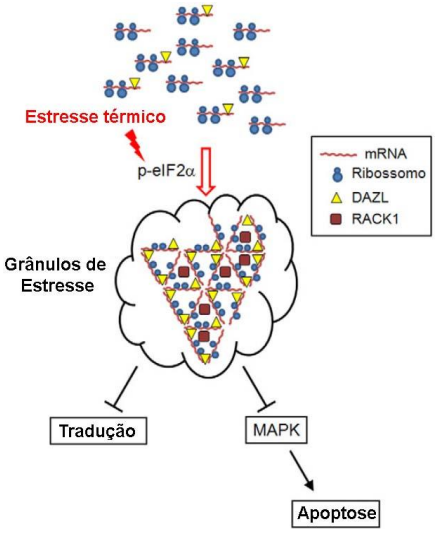

Figura 1.6 Modelo da formação de grânulos de estresse em células germinativas de mamíferos. DAZL está envolvido com o transporte e tradução de mRNAs específicos durante o desenvolvimento dessas células. Com as células sob estresse térmico, eIF2 alpha é fosforilado e os grânulos formados. DAZL é essencial para a formação desses grânulos e pode recrutar mRNAs para os grânulos de estresse. Esses grânulos não somente reduzem a atividade traducional global, mas também previnem a apoptose das células por sequestrar RACK1 e subsequente suprimir a via apoptotica MAPK. Adaptado de Kim et al, 2012.

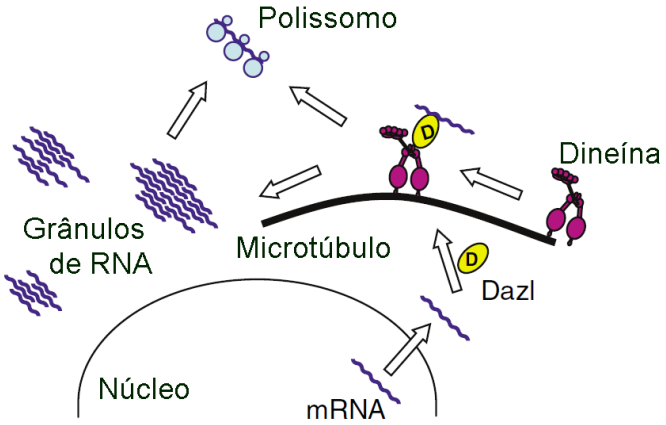

Figura 1.7 Modelo representativo da função de Dazl. Dazl reconhece um conjunto de mRNAs específicos no citoplasma formando um complexo com a proteína motora dineína. Esse complexo é responsável pelo transporte dos mRNAs para os grânulos de RNA ou diretamente para ribossomos. Adaptado de Lee et al, 2006.

As proteínas da família DAZ interagem com outras proteínas estabelecendo complexos de regulação e agem no controle da tradução de mRNAs específicos (Reynolds &

Cooke, 2005). Na tabela 1.1 estão descritas as proteínas que apresentam interação com DAZ ou contém potencial de interação com essa proteína.

Gene	Expressão	Motivo(s)
PUM2	CTEs e células germinativas	Repetições PUF
HQK3	Super regulado em ovários e testículos	Nenhum
BOU	Células germinativas masculinas	RRM, Repetições DAZ
DZIP1	Tecidos específicos e testículos	Zinc Finger
DZIP2	Células germinativas masculinas	Zinc Finger
DZIP3	Não há conhecimento	Nenhum
DAZL	Células germinativas	RRM, Repetições DAZ

Tabela 1.1 - Genes que codificam proteínas que interagem com DAZ. FONTE: (Moore et al, 2003).

1.6 Proteína DZIP1 ("DAZ-interacting protein")

A proteína que interage com DAZ, DZIP1, co-localiza com as proteínas DAZ ou DAZL em células-tronco embrionárias e germinativas e estas apresentam interações entre si formando um complexo de proteínas que se liga a mRNA (Moore et al, 2004). Moore e seus colaboradores (2004) analisaram o perfil de expressão de DZIP e DAZL em células-tronco embrionárias humanas. Em contraste a DAZL, a expressão de DZIP (isoforma 1) se manteve constante no curso de diferenciação dos corpos embrióides (Fig.1.8) (Moore et al, 2004).

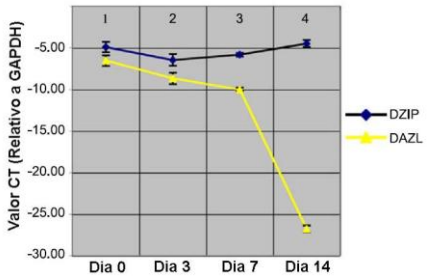

Figura 1.8 Perfil de expressão de DZIP1 e DAZL durante diferenciação de corpos embrióides. Adaptado de Moore et al, 2004.

O gene *DZIP1* está localizado no cromossomo 13 e codifica três isoformas de proteínas diferentes que contêm um domínio zinc-finger (C2H2) (Moore et al, 2004). A comparação dessas isoformas revela uma extensiva identidade das sequências de nucleotídeos, o transcrito da isoforma 1 contém um éxon alternativo de 57 nucleotídeos, que resulta na adição de 19 aminoácidos (Figura 1.9).

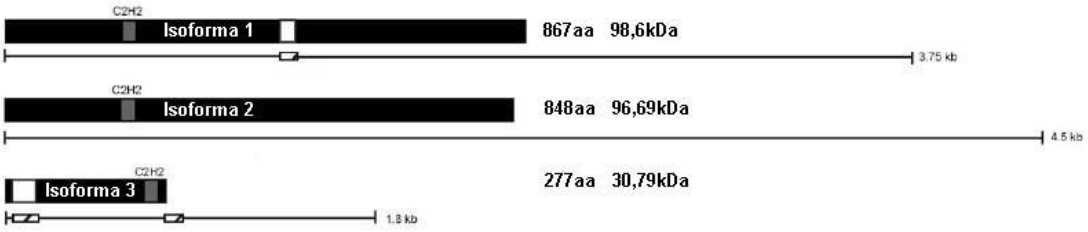

Figura 1.9 Esquema do alinhamento de nucleotídeos das três isoformas de DZIP1 e as proteínas codificadas. Linha fina na horizontal representa o cDNA dos diferentes transcritos e retângulos representam os éxons alternativos. Acima dos cDNAs estão as proteínas codificadas. Regiões pretas representam aminoácidos em comum, regiões brancas representam os aminoácidos adicionais únicos para cada isoforma e regiões cinza representa o domínio "zinc-finger" C2H2. Adaptado de (Moore et al, 2004).

Moore e seus colaboradores (2004) demonstraram que DAZ co-imunoprecipita com as isoformas 1 e 2. Além disso, descobriram que o domínio zinc-finger C2H2 é requerido para a interação com a proteína DAZ. O gene DZIP1 é conservado em humanos, chimpanzé, macaco, cachorro, bovinos, camundongo, ratos, galinha e peixe-zebra (Tabela 1.2).

Gene		**Identidade (%)**	
Espécie	**Símbolo**	**Proteína**	**DNA**
H.sapiens	**DZIP1**		
vs. P.troglodytes	DZIP1	99.0	99.3
vs. M.mulatta	DZIP1	96.5	97.2
vs. C.lupus	DZIP1	80.8	85.7
vs. B.taurus	DZIP1	80.3	85.6
vs. M.musculus	Dzip1	69.6	75.5
vs. R.norvegicus	Dzip1	68.2	75.6
vs. G.gallus	DZIP1	51.5	64.4
vs. D.rerio	dzip1	37.3	51.0

Tabela 1.2 Porcentagem de identidade do gene DZIP1 de Homo sapiens com o gene em outras espécies. (Dados obtidos do banco de dados NCBI HomoloGene).

DZIP1 também tem sido descrito como um dos reguladores da via de sinalização *Hedgehog* (Hh), essa via é responsável pelo desenvolvimento embrionário desde *D. melanogaster* a humanos (Ingham & McMahon, 2001). A interferência dessa via em humanos pode causar problemas como holoprosencefalia (Wallis & Muenke, 2000), polidactilia

postaxial (Radhakrishna et al, 1997) e leva ao desenvolvimento de alguns tipos de câncer (carcinoma e meduloblastoma), conforme citado por (Goodrich & Scott, 1998).

1.7 Via de sinalização Hedgehog e DZIP1

A via de sinalização Hedgehog (Hh) tem função em muitos processos durante o desenvolvimento embrionário e permanece ativa durante a fase adulta onde está envolvida no controle do crescimento, sobrevivência e destino celular (Taipale & Beachy, 2001). A via de sinalização Hh em mamíferos consiste em três diferentes ligantes: Sonic Hh, Indian Hh e Desert Hh (Figura 1.10). Essas três proteínas podem se ligar à proteína transmembranar Patched (PTCH) (Stone et al, 1996). Uma vez que a proteína Hh está ligada, PTCH libera a atividade de Smoothened (SMO) para realizar a transdução da via de sinalização (Frank-Kamenetsky et al, 2002). Os mediadores principais dessa via são fatores transcricionais membros da família de proteínas GLI que contém domínios zinc-finger (Alexandre et al, 1996). Gli1 é um efetor positivo dessa via de sinalização, Gli3 é um inibidor transcricional e Gli2 tem ambas as funções (Sasaki et al, 1999). O sinal de Hh ativa a resposta transcricional, principalmente por modulação de modificações, processamento e tráfego nuclear das proteínas Gli (Bai et al, 2004). Recentemente descobriram que o cílio primário é requerido para a sinalização Hh em vertebrados (Eggenschwiler & Anderson, 2007). O cílio primário é uma estrutura baseada em microtúbulos e está presente na superfície de algumas células. Essa estrutura funciona como uma antena da célula e é responsável pela transdução de sinais importantes para o desenvolvimento embrionário e para a homeostase dos tecidos adultos (Wilson & Stainier, 2010). Algumas vias de sinalização precisam de cílios primários para a transdução do sinal correto, pois há diversos componentes dessas mesmas vias de sinalização presentes no cílio. As vias que dependem do cílio primário são: Hedgehog, PDGFRα (Platelet-Derived Growth Factor Receptor α) (Eggenschwiler & Anderson, 2007) e a via não canônica de Wnt (Wingless-Int), designada de PCP (Planar Cell Polarity) (Satir et al, 2010).

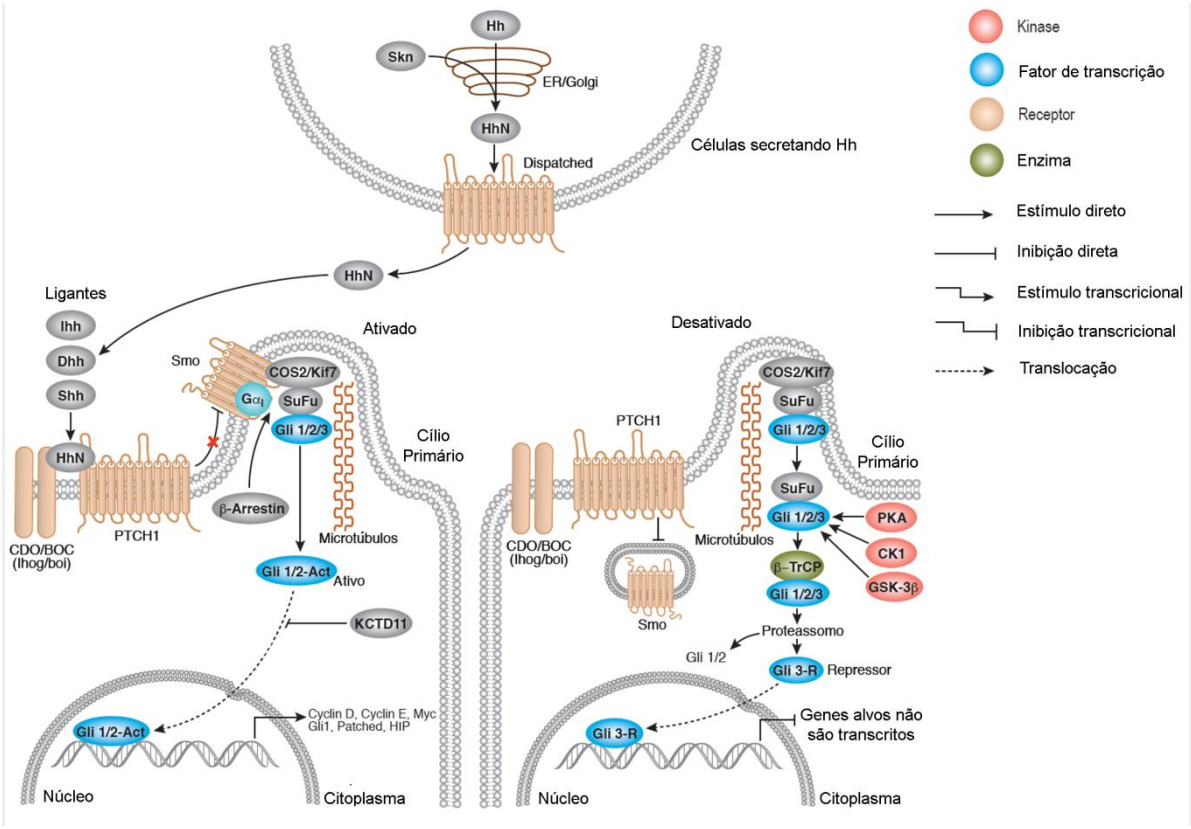

Figura 1.10 Via de sinalização Hedgehog em vertebrados. Células específicas secretam ligantes da família Hh (Ihh, Dhh ou Shh). No estado ligado, a molécula Hh se liga a Ihog/Patch que permite a incorporação de Smoothened à membrana do cílio primário. No cílio primário, a atividade da proteína G associada a Smoothened alivia a associação de Gli aos microtúbulos, permite a translocação nuclear e ativação dos genes-alvo da via, que incluem ciclina D, ciclina E, Myc, e Patched. Na ausência do ligando de Hedgehog (estado desligado), o receptor Patched está associado com Smoothened e impede a sua incorporação à membrana. No estado desligado permite SuFu e COS2/Kif7 sequestrar o fator de transcrição Gli, permitindo assim a sua fosforilação pela PKA, CK1 e de GSK-3. Isto resulta numa degradação dos ativadores Gli (Gli1 e Gli2) mediada por β-TRCP ou produção do repressor Gli3, levando a repressão dos genes alvo da via. Adaptado de http://www.cellsignal.com/reference/pathway/Hedgehog.html.

Mais recentemente, a proteína Igu/Dzip1, codificada pelo gene *iguana*, foi associada à ciliogênese (Glazer et al, 2010; Tay et al, 2010). Em peixe-zebra, o mutante *iguana* perde completamente os cílios primários (Glazer et al, 2010). A distribuição sub-celular de iguana é exclusivamente citoplasmática, porém, quando a PKA (cAMP *dependent protein kinase*) é inativada há uma translocação nuclear de iguana (Sekimizu et al, 2004; Wolff et al, 2004). Em contraste, Glazer e seus colaboradores (2010) identificaram a proteína Igu/Dzip1 localizado no corpo basal do cílio primário.

A proteína Dzip1, uma proteína *zinc finger* com domínios *coiled-coil*, é essencial à transdução de sinal da via Hh em peixe-zebra (Sekimizu et al, 2004). O mutante *iguana* foi

primeiramente analisado e associado à via de sinalização Hh devido ao seu fenótipo semelhante ao do mutante *sonic you* (*syu*), um dos genes envolvido nessa via (Brand et al, 1996; Odenthal et al, 2000). A proteína Igu/Dzip1 é um componente da via Hh que atua jusante de Smo e montante aos fatores de transcrição Gli, atuando na modulação destes (Sekimizu et al, 2004; Wolff et al, 2004). Em 2011, Jin e seus colaboradores descobriram que DZIP1 está envolvido no mecanismo de degradação de Gli dependendo de seu estado fosforilativo. DZIP1 possui quatro sítios de fosforilação. A enzima PP2As contendo a subunidade B56 (Fosfatase) é responsável pela remoção dos grupos fosfatos nesses sítios enquanto que Casein Kinase 2 é responsável pela fosforilação (Jin et al, 2011). Análises de mutagênese demonstraram que a forma não fosforilada de DZIP1 é mais potente na degradação de Gli (Jin et al, 2011), no entanto a forma como DZIP1 regula Gli não está entendida, uma vez que essas proteínas parecem não ter interações físicas (Sekimizu et al, 2004).

Apesar desses dados da literatura, as funções de DZIP1 em células humanas não estão descritas e há poucos dados sobre os mecanismos em que essa proteína participa. Dessa forma, esse trabalho tem como principal objetivo estudar a função de DZIP1 em células humanas por meio da identificação da localização de DZIP1 em diferentes condições (bloqueio da via Hh e estresse oxidativo), proteínas parceiras, mRNAs presentes no complexo, interação com RNA, funções biológicas e entre outros.

1.8 Modelos Biológicos

Um dos modelos biológicos utilizados nesse trabalho foi a linhagem celular HeLa, uma linhagem estabelecida em 1951 a partir da biópsia do tumor do cérvix (colo do útero) de Henrietta Lacks, uma mulher afro-americana que vivia próximo à Baltimore, Estados Unidos. As células foram obtidas sem o conhecimento ou permissão dela ou de sua família, e essas foram as primeiras células humanas cultivadas em laboratório, denominadas células imortais (Callaway, 2013). Essa linhagem celular contribuiu para o desenvolvimento da vacina contra a poliomielite, quimioterapia, a descoberta das telomerases humanas e entre outros avanços. Uma busca pelo banco de trabalhos científicos “PubMed” com a palavra “HeLa” retorna mais de 75 mil resultados. Por mais que essa linhagem possua características de células cancerígenas, ela tem sido usada para decifrar os mecanismos celulares e moleculares que regem as células humanas de maneira geral. Por isso, essa linhagem celular foi utilizada por nós para desvendar o papel molecular da proteína DZIP1.

Outro tipo celular utilizado nesse trabalho foram as células-tronco derivadas de tecido adiposo. As células-tronco são encontradas na maioria dos metazoários e estão presentes por toda a fase embrionária e adulta de um organismo. As células-tronco são definidas como células sem especialização (também conhecidas como indiferenciadas) que se renovam por meio da divisão celular e podem se diferenciar em tipos celulares especializados (Ivanova et al, 2002). As células-tronco utilizadas nesse trabalho são classificadas como adultas, pois são células não diferenciadas, multipotentes e se encontram distribuídas nos diferentes tecidos do corpo. A principal função das células-tronco adultas no organismo é a manutenção e reparo do tecido em que se encontram. As células-tronco derivadas de tecido adiposo podem dar origem a vários tipos de células: osteoblastos, condrócitos e adipócitos (Gimble et al, 2007); e possuem propriedades físicas de aderência ao plástico e morfologia alongada semelhante aos fibroblastos (Pittenger et al, 1999).

A função de DZIP1 foi estudada em células de linhagem HeLa e em células-tronco derivadas de tecido adiposo com o propósito inicial de comparar a função dessa proteína em cultura de linhagem celular e cultura primária, respectivamente. No entanto, a via de sinalização Hedgehog (Hh) está relacionada com processos de proliferação celular, diferenciação, angiogênese, remodelamento da matriz celular e homeostase de células-tronco (Varjosalo & Taipale, 2008). Vários autores descrevem o papel dessa via no processo de diferenciação de células-tronco (Cai et al, 2012; Fontaine et al, 2008; Ghanbari et al, 2013; James et al, 2010; Warzecha et al, 2006; Wu et al, 2013; Wu et al, 2004). Dessa forma, as células-tronco adultas utilizadas no estudo da função de DZIP1 ajudaram a preencher a lacuna referente a essa característica peculiar às células-tronco: o processo de diferenciação.

2. OBJETIVOS

2.1 Objetivo principal:

O objetivo geral desse trabalho é caracterizar a função celular e molecular da proteína DZIP1 em células da linhagem HeLa e células-tronco derivadas de tecido adiposo humano.

2.2 Objetivos específicos:

1. Identificar os mRNA associados a DZIP1 em células HeLa e células-tronco derivadas de tecido adiposo;
2. Definir redes gênicas e vias metabólicas e de sinalização reguladas por DZIP1;
3. Definir e caracterizar a interação da proteína DZIP1 com homoribopolímeros.
4. Verificar a participação de DZIP1 em complexos protéicos.
5. Identificar as proteínas parceiras de DZIP1;
6. Caracterizar o fenótipo celular quando silenciada a expressão de DZIP1;
7. Avaliar o acúmulo de alguns mRNA alvos em células com expressão silenciada de DZIP1;

3. ARTIGO

3.1 Título

Ribonomic analysis of human DZIP1 reveals involvement in ribonucleoprotein complexes and stress granules

3.2 Autores

Patrícia Shigunov, Jose Sotelo-Silveira, Marco Augusto Stimamiglio, Crisciele Kuligovski, Florencia Irigoín, Jose Badano, David Munroe, Alejandro Correa, Bruno Dallagiovanna.

3.3 Relação do artigo com a tese

Esse artigo contempla a maior parte dos objetivos dessa tese, sendo: Identificação dos mRNAs associados a DZIP1 em células HeLa; estabelecimento das redes gênicas e vias metabólicas e de sinalização reguladas por DZIP1; caracterização da interação da proteína DZIP1 com RNA; caracterização do fenótipo celular quando silenciada a expressão de DZIP1; avaliação do acúmulo de alguns mRNA alvos em células com expressão silenciada de DZIP1.

3.4 Situação do artigo

Artigo submetido à revista Nucleic Acids Research (NAR-00852-Y-2013).

RIBONOMIC ANALYSIS OF HUMAN DZIP1 REVEALS INVOLVEMENT IN RIBONUCLEOPROTEIN COMPLEXES AND STRESS GRANULES

Patrícia Shigunov[1], Jose Sotelo-Silveira[2], Marco Augusto Stimamiglio[1], Crisciele Kuligovski[1], Florencia Irigoín[3,4], Jose Badano[3], David Munroe[5], Alejandro Correa[1], Bruno Dallagiovanna[1*]

[1] Stem Cells Basic Biology Laboratory. Instituto Carlos Chagas, FIOCRUZ. Algacyr Munhoz Mader 3775, Curitiba 81350-010, Brazil

[2] Department of Genetics, Instituto de Investigaciones Biologicas Clemente Estable and Department of Cell and Molecular Biology, School of Sciences, UdelaR, Avenida Italia 3318. CP 11600. Montevideo, Uruguay

[3] Institut Pasteur Montevideo, Mataojo 2020, Montevideo 11400, Uruguay

[4] Department of Histology and Embryology, Facultad de Medicina, Universidad de la República, Avenida General Flores 2125 C.P. 11800 Montevideo - Uruguay

[5] Advanced Technology Program, SAIC-Frederick, Inc., Frederick National Laboratory for Cancer Research, Frederick, MD, 21702, USA

*****To whom correspondence should be addressed**:** Tel: +55 41 3316 3237; Fax: +55 41 3316 3267; E-mail: brunod@tecpar.br

Running title: DZIP1 in RNPs complexes and stress granules

Keywords: DZIP1, ribonucleoprotein, stress granules, polysome, Hedgehog signaling.

ABSTRACT

DZIP1 (DAZ-interacting protein 1), has been described as a component of the Hh signaling pathway with a putative regulatory role in ciliogenesis. DZIP1 interacts with DAZ and DAZL RNA binding proteins in embryonic stem cells and human germ cells suggesting a role in mRNA regulation. We therefore investigated DZIP1 function in HeLa cells and its involvement in ribonucleoprotein complexes. DZIP1 was found predominantly in granules in the cytoplasm. The number of DZIP1-containing granules increased when cells were subjected to cold shock. Under oxidative stress conditions, DZIP1 was re-localized to stress granules. We identified the mRNAs associated with DZIP1, by carrying out immunoprecipitation assays with antibodies against DZIP1 and microarray hybridization. The genetic networks formed by the DZIP1-associated mRNAs were involved in cell cycle and gene expression regulation. DZIP1 is involved in the Hedgehog signaling pathway. We used cyclopamine, a specific inhibitor of this pathway, to analyze the expression of DZIP1 and its associated mRNAs. Transcripts expression increased with treatment; however the silencing or overexpression of DZIP1 in HeLa cells had no significant effect on the accumulation of the associated mRNAs. Polysomal profile analysis by sucrose gradient demonstrates the presence of DZIP1 in the polysomal fraction. Our results suggest that DZIP1 is part of an RNA transport complex involved in regulating the cellular distribution of a defined subpopulation of mRNAs.

INTRODUCTION

The Hedgehog (Hh) signaling pathway is involved in many processes during embryonic development and remains active in adults, in which it is involved in controlling cell growth, survival and fate (Taipale & Beachy, 2001). The Hh signaling pathway in mammals involves three directly related ligands: Sonic Hh, Indian Hh and Desert Hh. All these Hh proteins bind to the transmembrane protein Patched (Ptch) (Stone et al, 1996). Ligand binding release the inhibition, by Ptch, of the positive effector Smoothened (Smo), resulting in signal transduction (Frank-Kamenetsky et al, 2002). The principal mediators of the transcriptional response to Hh are members of the zinc finger-containing GLI protein family (Alexandre et al, 1996). Gli1 is a positive effector of signaling, Gli3 is principally a transcription inhibitor and Gli2 can fulfill both these roles (Sasaki et al, 1999). Hh signals elicit their transcriptional responses principally by modulating the modification, processing and nuclear trafficking of Gli proteins (Bai et al, 2004). In vertebrates, Gli processing requires an intact primary cilium, a microtubule-based organelle on the cell surface. The integrity of the primary cilium is essential for mammalian Hh signaling (Eggenschwiler & Anderson, 2007).

The zebrafish *iguana* gene, also referred to as *DZIP1* (DAZ-interacting protein 1) (Moore et al, 2004), has been described as a component of the Hh signaling pathway with a putative regulatory role in Hh signaling and ciliogenesis (Glazer et al, 2010) (Kim et al, 2010) (Wilson & Stainier, 2010). The DZIP1 protein has three different protein isoforms, each with a single C2H2 zinc finger domain (Moore et al, 2004). Its phosphorylation regulates a Gli turnover mechanism (Jin et al, 2011). A B56-containing PP2A (protein phosphatase) dephosphorylates all four phosphorylation sites of DZIP1. Analyses based on mutagenesis further demonstrated that the unphosphorylated form of DZIP1 promoted Gli turnover more strongly than the phosphorylated forms (Jin et al, 2011), but the way in which DZIP1 regulates Gli turnover is unknown. There is also evidence to suggest that DZIP1 plays a role in ciliogenesis. DZIP1 has been localized to the basal body of the primary cilium (Kim et al, 2010) (Glazer et al, 2010). Kim *et al.* (2010) suggested that DZIP1 might be an essential component of a protein complex involved in the biogenesis of the primary cilium. The role of DZIP1 in Hh signaling may thus relate to its function in the regulation of ciliogenesis (Kim et al, 2010) (Glazer et al, 2010).

A potential role in mRNA regulation has also been suggested, on the basis of the association of human DZIP1 with the RNA-binding protein DAZ, in embryonic stem cells and germ cells (Moore et al, 2004). The proteins of the DAZ family (DAZ, DAZ-like and BOULE) activate the translation of specific mRNAs in metazoan germ cells (Maegawa et al, 2002) (Collier et al, 2005) (Reynolds et al, 2005a) (Smith et al, 2011), by interacting with the poly(A)-binding

protein (PABP) (Collier et al, 2005). It has also been suggested that proteins of the DAZ family transport target transcripts to RNA granules (Vangompel & Xu, 2011). Moreover, DAZL is an essential component of stress granules, which prevent male germ cells from undergoing apoptosis in conditions of heat stress (Kim et al, 2012). This observation suggests that DZIP1 may be a component of ribonucleoprotein (RNP) complexes.

We show here that DZIP1 is located predominantly in the cytoplasm, in granules, and that it is a component of ribonucleoprotein complexes in HeLa cells. DZIP1 colocalized with TIA-1 in stress granules, but not with p-bodies, suggesting a role in the localization of mRNAs within the body of the cell. A ribonomic analysis of associated mRNAs identified networks of genes involved principally in the cell cycle and gene expression. Knockdown of the expression of the DZIP1 gene did not affect the stability of the associated mRNAs. However, DZIP1 is associated with polysomes. Our results suggest that DZIP1 is part of an RNA transport complex involved in regulating the cellular cycling of a defined subpopulation of mRNAs.

RESULTS

DZIP1 is found predominantly in the cytoplasm of HeLa cells

We investigated the subcellular distribution of DZIP1 in HeLa cells, by carrying out indirect immunofluorescence analysis with an anti-DZIP1 antibody and amino-GFP or carboxy-YFP-tagged hDZIP1 proteins. A granular pattern of DZIP1 labeling was observed in the cytoplasm, with a slightly stronger signal in the perinuclear region (Fig. 1 A-C). Furthermore, some nuclear staining was observed when the anti-DZIP1 antibody was used. For the confirmation of these results, we transfected the cells with a vector encoding a carboxy-GFP-tagged DZIP1 and observed them 24 h later. The tagged-DZIP1 protein was also found mostly in the cytoplasm (Fig. 1 D-F). A similar pattern was observed when HEK293 cells were transfected with this construct, although the granular distribution was less evident (Fig. 1G-I). We also obtained similar results by transfecting cells with an amino-YFP-tagged DZIP1 construction (see Supplementary Fig. S1 I-L). We used the pGFP or pYFP plasmid as a control (see Supplementary Fig. S1 A-H)

Zebrafish Iguana proteins (DZIP1 and DZIP1L) have been shown to localize to the basal bodies of primary cilia (Kim et al, 2010). The human DZIP1 protein has also been reported to be present in the basal body of hTERT-RPE1 cells (Epithelial cells immortalized with hTERT) (Glazer et al, 2010). We therefore investigated the distribution of GFP-tagged DZIP1 in hTERT-RPE1 cells, and the primary cilium was visualized by incubation with an anti-acetylated tubulin antibody (Vorobjev & Chentsov YuS, 1982) (Fig. 1 J-O). Some GFP-

tagged DZIP1 localized to discrete puncta at the base of cilia, potentially compatible with a basal body localization (Fig. 1 M-O, arrows), but most of the signal formed foci distributed throughout the cytoplasm (Fig. 1 J-O). Similar results were obtained with the YFP construct, but the signal was less intense (see Supplementary Fig. S1 M-O). The combination of diffuse and granular patterns in the cytoplasm observed for DZIP1 suggests that at least some of the protein is present in high molecular weight protein complexes. We determined the mobile/immobile fraction of GFP-tagged DZIP1, by carrying out fluorescence recovery after photobleaching (FRAP) assays. The mean mobile fraction was 0.64 (± 0.19) and the immobile fraction was 0.36 (± 0.19) (see Supplementary Fig. S1 P-S). The immobile fraction was larger if photobleaching was carried out close to the nucleus (not shown). These findings indicate that the DZIP1 protein is partitioned between soluble and insoluble forms.

DZIP1 is recruited to stress granules in cells subjected to oxidative stress

DAZL colocalizes with TIA1, a stress granule marker, in HeLa cells under oxidative stress conditions (Lee et al, 2006). DZIP1 interacts with the DAZ and DAZL proteins in embryonic stem cells and germ cells (Moore et al, 2004). This raises the possibility of DZIP1 being a component of regulatory RNA granules. DZIP1-GFP-expressing cells were subjected to cold-shock treatment and observed *in vivo*. Within a few minutes, DZIP1 was found to be concentrated in cytoplasmic granules, the number and intensity of which increased over time (see Supplementary Fig. S2A, movie 1). We investigated whether these granules corresponded to the well studied stress granules, by performing immunofluorescence assays with anti-DZIP1 and anti-TIA1 antibodies, in transfected HeLa subjected to oxidative stress (Fig. 2A-B, S2B). Arsenite treatment induced the formation of stress granules in concentration 0.5mM - 2mM, as demonstrated by labeling for TIA-1. DZIP1 mostly colocalized with TIA-1-containing granules (Fig. 2A-B, S2B). In normal condition, no colocalization of DZIP1 with TIA-1-containing granules was observed (see Supplementary Fig. S2C). Interestingly there are DZIP1-containing granules that are not stress granules and we note that the stress granules more robust colocalizes with DZIP1. We certified that TIA-1 signal was not leaking back into the FITC channel (Fig. 2C). We investigated whether DZIP1 was present in other RNA granules, such as p-bodies, by labeling the cells for DCP1, a p-body marker. No colocalization of DZIP1 with this marker was observed in HeLa cells in normal condition (Fig. 2D-E) nether under oxidative stress (Fig. S2D). These results suggest that DZIP1 could be involved in ribonucleoprotein complexes under normal and stress condition.

DZIP1 is a component of ribonucleoprotein complexes and is associated with a specific subpopulation of mRNAs

DZIP protein interacts with DAZ (deleted in azoospermia) in embryonic stem cells and germ cells (Moore et al, 2004). The genes of the *DAZ* family encode RNA-binding proteins (Vangompel & Xu, 2011). We therefore carried out immunoprecipitation assays with anti-DZIP1 antibodies, to determine whether DZIP1 was present in ribonucleoprotein complexes in HeLa cells in normal condition and to identify the mRNAs with which it was associated. The presence of DZIP1 in the immunoprecipitates was confirmed by western blotting (Fig. 3A). The mRNAs present in the immunoprecipitates were identified by microarray hybridization, with a GeneChip Affymetrix Human Genome U133 Plus 2.0 Array (Fig. 3B). A rabbit isotype IgG antibody (IP-Control) was used as a control. All signals corresponding to a two-fold increase with respect to the control were considered to be positive. In total, 585 genes displayed four-fold enrichment, and 1737 displayed two-fold enrichment in the DZIP1 elutes (see Supplementary Table S2 – ANEXO 1). We validated our microarray results, by testing six microarray-positive candidates by quantitative RT-PCR (Fig. 3C). We also transfected Hela cells with a plasmid encoding GFP-tagged DZIP1 (Fig. S3A) and carried out immunoprecipitation assays with an anti-GFP antibody. Cells transfected with pGFP alone were used as a negative control. The mRNAs associated with the immunoprecipitated GFP-tagged DZIP1 were reverse transcribed and the same six microarray-positive candidates were confirmed by quantitative PCR (Fig. 3D).

We analyzed the functional relationships between DZIP1-associated mRNAs, by assigning biological functions on the basis of Gene Ontology terms, and using IPA to identify the gene networks formed by the transcripts. GO analysis showed enrichment in regulatory proteins. IPA identified gene networks involved in the control of cell growth, gene expression and cellular compromise (Table 1).

DZIP1 contains a single C2H2 zinc finger domain. Zinc finger proteins are generally thought of as DNA-binding transcription factors. However, some classes of zinc finger proteins, including the common C2H2 zinc fingers, function as RNA-binding proteins (Hall, 2005). We investigated the ability of DZIP1 to interact directly with RNAs in EMSA. A Myc-tagged protein was produced in 293T cells and purified by affinity chromatography (see Supplementary Fig. S3B). EMSA was performed using four homoribopolymers as probes. Under the conditions used, DZIP1 did not interact robustly with the RNA probes, even in the most permissive conditions tested (see Supplementary Fig. S2C).

As stated above, DZIP1 is required for the correct regulation of Hedgehog signaling (Sekimizu et al, 2004). We investigated the role of DZIP1 in the Hh signaling pathway, by

cross-referencing data for the mRNA targets of hDZIP1 with data for known elements of the Hh pathway. The mRNAs associated with DZIP1-containing complexes included some corresponding to the Hh pathway, such as the *PTCH1, CSNK1E, STK36, DISP1* and *NPC1* mRNAs.

The expression of DZIP1 and its mRNAs targets is affected by inhibition of the Hh pathway

DZIP1 has been described as a component of the Hh signaling cascade. Cyclopamine is a specific Hh inhibitor that blocks Hh pathway activation by binding directly to Smo (Chen et al, 2002). We first incubated HeLa cells with various concentrations of cyclopamine and determined the shortest time and the minimum concentration required to inhibit cell proliferation (see Supplementary Fig. S4A). Proliferation was evaluated by BrdU incorporation. Levels of cell proliferation were found to have decreased after incubation for 24 hours with 300 nM or 600 nM cyclopamine. The molecular effect of cyclopamine treatment was evaluated by analyzing the amount of mRNA for Gli1 (see Supplementary Fig. S4B-C), a positive effector of Hh signaling (Alexandre et al, 1996). Gli1 levels decreased considerably after incubation with 300 nM cyclopamine. We determined the optimal concentration for blocking the Hh pathway without modifying the cell cycle or viability, by evaluating these parameters after treatment with 300 nM cyclopamine for 24 hours. Cell cycle progression and apoptosis levels were similar in treated and untreated control cells (see Supplementary Fig. S4D-G). We therefore used incubation with 300 nM cyclopamine for 24 hours in subsequent experiments.

We investigated the effect on the subcellular distribution of DZIP1 of blocking the Hh pathway, by treating HeLa cells with cyclopamine and carrying out immunolocalization assays with anti-DZIP1 antibody. Fewer granules were present in the cytoplasm in cells in which the Hh pathway was blocked with cyclopamine than in untreated control cells (Fig. 4A-D). Moreover, the nuclear signal was completely absent after treatment. The decreased of granules and absence nuclear signal could be connected with transduction of Hh signaling pathway.

We investigated the levels of *DZIP1* and *GLI1* transcripts and of two DZIP1-associated mRNAs (*BRD8* and *PTCH1*) after treatment with cyclopamine for 24, 48 and 72 hours. The levels of the *DZIP1* and *GLI1* transcripts were markedly decreased by blockade of the Hh pathway (Fig. 4E-F). This treatment also resulted in a marked increase in the accumulation of *PTCH1* and *BRD8* transcripts (Fig. 4G-H). The increase in the amount of *PTCH1* and *BRD8*

mRNA could be a direct effect of blocking the Hh pathway or due to decrease in mRNA expression DZIP1.

Knockdown of DZIP1 expression affect cell proliferation

We investigated the role of DZIP1 in relation to its associated mRNAs, by determining whether gene silencing with DZIP1-specific siRNA molecules resulted in phenotypic changes or altered the levels of associated mRNAs. We screened for gene-specific silencing, by transfecting HeLa cells with a mixture of DZIP1 siRNAs at a concentration of 1 nM. *DZIP1* expression was assessed 24, 48, and 72 h after transfection (see Supplementary Fig. S5A). We confirmed by western blot the silencing of more than 50% of DZIP1 in protein extracts from transfected cells after 72 h, as demonstrated by comparison with cells transfected with a scrambled control (siNC1 – negative control) (Fig. 5A-B). *DZIP1* knockdown had no significant effect on cell morphology. We evaluated the survival rates of *DZIP1*-knockdown cells in Annexin V assays 72 hours after transfection, by determining the percentages of living, apoptotic and dead cells. No significant differences were found between *DZIP1*-knockdown cells and control cells (see Supplementary Fig. S5B-C). Propidium iodide staining also showed no differences in the percentages of the cells in the G1, S and G2 phases of the cell cycle (see Supplementary Fig. S5D-E).

Kikuyama *et al*. (2012) recently described DZIP1 as a putative tumor supressor gene. *DZIP1*-knockdown in breast cancer cell lines results in an increase in cell growth. We assessed the putative role of DZIP1 in controlling cell proliferation, by evaluating the effect of *DZIP1* knockdown on proliferating HeLa cells. Growth curves showed that the knockdown population contained a higher number of cells than the control population, as previously reported in tumor cells (Fig. S5F).

***DZIP1* knockdown and overexpression do not affect the accumulation or stability of mRNAs associated with DZIP1-containing complexes**

RNP complexes control the expression of bound mRNAs by regulating their stability, translation or subcellular localization (Moore, 2005). We evaluated mRNA levels for *IFT80, SNX2, BRD8* and *PTCH1* in *DZIP1*-knockdown cells. The level of *GLI1* mRNA was used as a control non-target. In all cases (*IFT80, SNX2, PATCH1*, *BRD8* and *GLI1*), although knockdown cells tended to show higher levels of transcript accumulation, no statistically significant differences were observed (Fig. 5C).

We confirmed the relationship between the amount of DZIP1 and the accumulation of associated mRNAs in DZIP1-containing complexes in cells over expressing DZIP1-GFP

protein (Fig. S3A). We then analyzed the mRNA levels for *DZIP1, IFT80, SNX2, BRD8, PTCH1* and *GLI1*. *DZIP1* was strongly overexpressed, but no significant difference in the levels of the DZIP1-associated mRNAs was observed. (Fig. 5D).

We investigated the potential role of DZIP1 in regulating the stability of the mRNA targets of RNP complexes, by determining the half-lives of the associated mRNAs by actinomycin D treatment and quantitative RT-PCR. Cells were transfected with siDZIP1 or siNC1 and after 72 hours were treated with the transcriptional inhibitor (10 μg/ml actinomycin D) for 0, 1, 2 or 4 hours. Mean relative mRNA levels, as determined by quantitative RT-PCR at each time point after the addition of Act D, were plotted and used to calculate the half-life of *BRD8, IFT80, SNX2* and *PTCH1* mRNA. The DZIP1 silencing had no significant effect on the half-lives of the four targets of DZIP1-containing complexes analyzed, as shown by comparison with the control (Fig. 5E, see Supplementary Fig. S6).

DZIP1 is found associated with polysomes.

To analyze the association of DZIP1 with macromolecules involved in translation, we evaluated the presence of DZIP1 in the polysomal fraction. Cells transfected with pDZIP1-GFP were treated with cycloheximide to stabilize ribosome-mRNA complexes or puromycin to disassembled ribosomes and cytoplasmatic extracts were separated by sucrose gradient sedimentation to isolate distinct ribosome populations (Fig. 6A-B). Distribution of DZIP1-GFP was examined by Western blot analysis in both conditions using an antibody against GFP. The set of Western blots shown in Fig. 6A and B were used for quantification (Fig. 6C). We observed the presence of DZIP1-GFP in fractions 1-13 comprising 40S, 60S, 80S or monosomes and polysome fractions. When cells were treated with puromycin, the presence of GFP-DZIP1 was only detected in the ribosome-free fractions (fractions 1-3), demonstrating that DZIP1-GFP is associated to translationally active ribosomes.

DZIP1 protein complexes might regulate the translation of the associated mRNAs. We tested this hypothesis by carrying out western blots with extracts of cells overexpressing GFP-tagged pDZIP1 or pGFP, with anti-SNX2, anti-GFP and anti-GAPDH antibodies. The amount of SNX2 protein was similar to that in cells transfected with the control pGFP alone (Fig. 6D).

Our results suggest that DZIP1 is a component of ribonucleoprotein complexes. DZIP1 is not regulating the expression of its associated mRNAs but probably being responsible for the subcellular localization of these transcripts to different kinds of ribonucleoprotein complexes (Fig. 7). Thus, DZIP1 could be involved in the cycling of its targets mRNAs within the cell, i.e nucleus, cytoplasm, stress granules and polysomes.

DISCUSSION

In this study, we found that DZIP1 was present principally in the cytoplasm of HeLa cells and that this subcellular distribution was modified by external stimuli. Ribonomic analysis showed that DZIP1 was present in RNP complexes and associated with a population of mRNAs involved principally in cell cycle regulation and the response to Hedgehog signaling.

Human DZIP1 and DZIPL have been shown to be required for the formation of primary cilia (Glazer et al, 2010). DZIP1 has been localized to the basal body of cilia and its knockdown has been shown to impair ciliogenesis (Kim et al, 2010). Cilia have been shown to be necessary for Hh signaling in vertebrates (Eggenschwiler & Anderson, 2007). Several Hedgehog signaling components are localized to cilia in vertebrates, including the Patched and Smoothened transmembrane proteins (Corbit et al, 2005) and Gli transcription factors (Haycraft et al, 2005). These observations led to the suggestion that DZIP1 may be involved in regulating the biogenesis of primary cilia and that its role in Hh signaling is related to its specific location in this cellular structure. Our data do not exclude the possibility that DZIP1 is present in the basal body of primary cilia, but we found that DZIP1 was present throughout the cytoplasm and, to a certain extent, in the nuclear compartment. Moreover, half the protein appeared to be immobilized in granular structures, suggesting that this protein might be a component of macromolecular complexes. This observation is consistent with the original report by Moore *et al*. (2004), who also observed the presence of DZIP1 in the cytoplasm of germ cells and reported that its translocation to the nucleus was dependent on its PKA-regulated phosphorylation (Wolff et al, 2004).

Many aspects of the RNA regulon model (Keene, 2007) are reflected in the results presented here. Posttranscriptional regulation involves multifunctional proteins, which form ribonucleoprotein complexes that are assembled in a combinatorial manner. A single protein or mRNA may, therefore, be involved in multiple RNA regulons. Our ribonomic analysis showed that DZIP1 was associated with a vast subpopulation of mRNAs. These transcripts mostly encoded proteins involved in the control of the cell cycle and gene expression. DZIP1 has recently been identified as a putative tumor suppressor involved in controlling cell proliferation (Kikuyama et al, 2012). DZIP1 is also known to be involved in the regulation of Hedgehog signaling (Sekimizu et al, 2004), a pathway activated in several types of human cancers (Gupta et al, 2010). Thus, the greater cell growth observed following *DZIP1* knockdown may reflect a non repression of mRNA targets by DZIP1-containing regulatory RNP complexes. Interestingly, several transcripts involved in the Hh response and in the biogenesis of primary cilia were identified as associated with DZIP1. Various authors have

suggested that DZIP1 plays an essential role in regulating ciliogenesis and as a structural component of the primary cilium (Glazer et al, 2010; Kim et al, 2010). We have demonstrated that the activation state of the Hh signaling pathway determines DZIP1 levels and cellular distribution. Thus, DZIP1 may be indirectly involved in and the formation of cilia and in Hh signaling, through an effect on the fate of transcripts encoding the various components of the two pathways.

However, we detected no direct binding of DZIP1 to its associated mRNAs. The stability and translatability of the identified transcripts also seemed to be unaffected by changes in DZIP1 levels. However DZIP1 is clearly associated to polysomes. RNP complexes can also regulate the expression of target mRNAs by determining their distribution in specific foci in the cytoplasm, enhancing translation or leading to controlled degradation (Martin & Ephrussi, 2009). The granular pattern of DZIP1 labeling was abolished by blockade of the Hh pathway. Moreover, DZIP1 was mobilized to RNA stress granules in response to heat or oxidative stress RNA. DAZ family proteins (with which DZIP1 interacts) have also been reported to be associated with RNA granules in the stress response (Kim et al, 2012).

Our results suggest that DZIP1 is part of an RNA transport complex involved in regulating the subcellular distribution of a defined subpopulation of mRNAs. We propose a model in which DZIP1 interacts with various RNA-binding proteins, to transport mRNAs from the nucleus, through the cytoplasm and there to polysomes or storage/degradation complexes. As part of the stress response, DZIP may transport associated mRNAs to stress granules. The diversity of the mRNAs associated with DZIP1 suggests that this protein may be a component of different regulatory RNPs responsible for transporting mRNAs to translating polysomes or to the degradation machinery.

According to the RNA regulon model, the protein and mRNA contents of RNPs are dynamic, varying in response to changing cellular conditions. It would therefore be of interest to determine the protein composition of these RNPs and to investigate how the stability, distribution and translation of DZIP1 target messages change in response to cell stress. It remains to be determined whether DZIP1 is essential for stress granule formation and which proteins act as partners in which conditions: normal, oxidative stress, blockade and activation of the Hedgehog pathway.

MATERIALS AND METHODS

Plasmids

All DZIP1 constructs were derived from human DZIP1 Ultimate™ ORF Clone -IOH27736 (Invitrogen). Bacterial expression constructs and DZIP1 mammalian expression plasmids (pEGFP, pEYFP and pSECTAG2B – Invitrogen) were constructed by PCR amplification and standard cloning methods. Cloning details will be available on request.

Cell culture, transfection and treatments

HeLa cells were maintained in RPMI-1640 medium supplemented with 10% heat-inactivated FCS, 100 U/ml penicillin and 100 U/ml streptomycin, at 37°C, under a humidified atmosphere containing 5% CO_2. The Nucleofector® kit, program I-013, was used to transfect 10^6 cells with 5 μg plasmid DNA in 100 μl Opti-MEM® (Invitrogen). The Hh pathway was inhibited by incubating cultures with 300 nM cyclopamine for 24 h, after which RNA was extracted from the cells. Oxidative stress was induced by incubating the cells with 0.5 or 2.0 mM sodium arsenite (Sigma-Aldrich) for 10 minutes. Cold shock was performed by incubating the cells at 20^oC and monitored until 30 minutes.

Measurement of mRNA half-life

We assessed mRNA stability, by adding actinomycin D (Sigma, cat #A-9415) to the medium at a concentration of 10 mg/ml, to block transcription. Cells were harvested 0, 1, 2 and 4 h after the addition of actinomycin D. Total RNA was isolated and its concentration determined. The first-strand cDNA was synthesized from 1 μg of total RNA (DNase-treated). The mean relative amounts of cDNA obtained by quantitative RT-PCR at each time point after the addition of Act D were used to estimate the half-life of the transcript (t1/2) from a first-order decay model based on the equation, $\gamma = \beta_0 e^{\beta_1 t} + \varepsilon$, where γ is the mean relative amount of mRNA at time t after the addition of Act D, β_0 is the initial amount, β_1 is a decay parameter related to half-life ($t1/2 = \pm \ln 2/ \beta_1$) and e is an error term (Raghavan et al, 2002; Sharova et al, 2009).

Immunofluorescence and FRAP (fluorescence recovery after photobleaching)

Cells seeded on glass coverslips were fixed by incubation with 4% formaldehyde solution for 10 minutes and washed with PBS. They were then permeabilized by incubation with 0.5% Triton X-100 in PBS for 30 min. Nonspecific binding sites were blocked by incubating with 5% BSA for 1 h, and the cells were then incubated for 1 h at 37°C with the primary antibodies

diluted in PBS containing 1% BSA: anti-DZIP1 antibody (rabbit polyclonal, Santa Cruz Biotechnology) was used at a dilution of 1:30, anti-acetylated tubulin antibody (mouse monoclonal, Sigma) was used at a dilution of 1:1000, anti-DCP1a antibody (mouse monoclonal, Santa Cruz Biotechnology) was used at a dilution of 1:30, and anti-TIA1 antibody (goat polyclonal Santa Cruz Biotechnology) was used at a dilution 1:50. The cells were incubated for 1 h at 37°C with secondary antibodies: anti-rabbit Alexa Fluor 488 (donkey) or anti-rabbit Alexa Fluor 546 (goat) at a dilution 1:500, anti-mouse rhodamine (goat) at a dilution of 1:1000, anti-mouse Alexa Fluor 594 (goat) at a dilution of 1:500, or anti-goat Alexa Fluor 546 (donkey) at a dilution of 1:500. Cell nuclei were stained with DAPI. Images were obtained with a Nikon E-600 microscope or with a Leica SP5 laser scanning confocal microscope. FRAP experiments were performed on a Leica SP5 confocal microscope with a 100×/1.3 NA oil-immersion objective and a 40 mW argon laser. Cells were imaged in LabTek II chambers (Nalgene) *in vivo*. Recovery data were binned logarithmically, generating a relatively uniform spacing of points along the FRAP curve, so as not to bias one phase of the curve when fitting the FRAP model (Sprague et al, 2004).

Total RNA extraction and quantitative reverse transcription-polymerase chain reaction

RNA was extracted with the RNeasy mini kit (Qiagen). RT-PCR and quantitative RT-PCR were performed as previously described (Rebelatto et al, 2008). For a list of the primers used, see supporting Table S1. GAPDH was used as an internal control. Experiments were performed with technical triplicates. Student's *t* test was used to assess the significance of differences between the cells populations analyzed. *P*-values ≤ 0.05 were considered to be statistically significant.

Western blotting

Protein extracts were obtained as previously described (Shigunov et al, 2012). The rabbit anti-hDZIP1 antibody (1:200; Santa Cruz Biotechnology, CA, USA), rabbit anti-GFP (1:1000; Novus Biologicals), rabbit anti-GAPDH (1:200; Cell Signaling Technology) and mouse anti-SNX2 (1:1000; BD Bioscience) antibodies were used. Western blots were probed with anti-mouse and anti-rabbit dy680 secondary antibodies, and were then scanned and analyzed with the Odyssey infrared imaging system (Li-Cor Biosciences, Bad Homburg, Germany).

Immunoprecipitation

Immunoprecipitation (IP) reactions were performed as described by Shigunov *et al.* (2012). For IP assays, we used 2 µg of anti-DZIP1 antibody (rabbit polyclonal, Santa Cruz

Biotechnology, CA, USA) or 2 µg of anti-GFP antibody (NB600-308, rabbit polyclonal, Novus Biologicals, CO, USA) bound to protein A-agarose beads (Sigma, Deisenhofen, Germany) in three independent assays. HeLa cells were lysed by incubation in polysome lysis buffer (15 mM Tris-HCl pH 7.4, 15 mM $MgCl_2$, 0.3 M NaCl, 1% Triton X-100, 1 mM DTT, 100 U/ml RNase Out, 1 mM PMSF and 10 µM E64) for 1 h at 4°C. The beads were washed, buffer and cell lysate were added, and the reaction mixtures were rotated vertically for 2 h at 4°C. The beads were then thoroughly washed again with polysome lysis buffer and then either boiled in denaturing buffer for western blots or used for RNA extraction for microarray and quantitative RT-PCR experiments. Identical IP experiments were performed with beads precoated with rabbit IgG as a negative control or with anti-GFP antibody for HeLa cells transfected only with pGFP.

Microarray analysis

RNA was processed for hybridization with GeneChip 3' IVT Express (Affymetrix - Santa Clara, USA), in accordance with the manufacturer's instructions. Briefly, cDNA was synthesized from immunoprecipitated RNA by reverse transcription, followed by second-strand synthesis to generate double-stranded cDNA. An *in vitro* transcription reaction was used to generate biotinylated cRNA. The cRNA was purified and fragmented, and then hybridized onto GeneChip Affymetrix Human Genome U133 Plus 2.0 arrays. Post hybridization washes were performed with an Affymetrix GeneChip® Fluidics Station 450. Arrays were scanned on an Affymetrix GeneChip® Scanner 3000. Scanned arrays were normalized with the GCRMA in Partek software (Partek Incorporated. St. Louis, MO). Signal intensity ratios were calculated and a list of genes displaying a fold-change in expression (IP-DZIP1/ IP-negative) of at least 2.0 was generated. The list obtained was used as an input for Ingenuity pathway analysis (IPA), to determine the functional relationships between the genes for which enrichment was detected in associations with DZIP1 protein. All microarray data were submitted to the GEO database and can be found under accession number GSE28882.

RNA interference assays

The chemically synthesized dsRNA sequences for the Dicer-substrate 27-mers used in this study were synthesized and purified by HPLC (Integrated DNA Technologies, Coralville, IA). The non silencing dsRNA controls (NC1) included 27mers (Integrated DNA Technologies). Transfections were performed in 6-well plates, with Lipofectamine™2000 reagent (Invitrogen) used to deliver dsRNA into HeLa cells; in accordance with the manufacturer's protocol. The final concentration of three DZIP1-specific dicer-substrate dsRNA mixtures and

of the NC1 dsRNA was 1 nM and the lipid concentration was 5 μl/ml of medium. We determined mRNA levels 24-72 h after transfection.

Sucrose gradient analysis

Cells were then treated with 100 μg/ml cycloheximide for 10 min at 37°C followed by two washes on ice with cold PBS containing 100 μg/ml cycloheximide. Lysates were prepared, and gradient separation and fractionation were performed as previously described (Holetz et al, 2007). Cell lysis was performed for 10 minutes on ice with polysome buffer (15 mM Tris-Hcl pH 7,4, 1% triton x100, 15 mM $MgCl_2$, 0,3M NaCl, 0,1 ug/ml cycloheximide, 1mg/ ml heparin). Then cell lysate was centrifuged for 12000g for 10 minutes at 4^oC temperature. Lysate supernatant was carefully isolated and seeded onto 10% to 50% sucrose gradients and centrifugated at 39000 rpm sw40 rotor (HIMAC CP80WX HITACHI) for 160 minutes at 4^oC. The sucrose gradient was fractionated using the ISCO gradient fractionation system (ISCO Model 160 Gradient former) connected to a UV detector to monitor absorbance at 254 nm and to record polysome profile.

Cells were then treated with 2mM puromycin for 2 hours at 37°C followed by two washes on ice with cold PBS. Cells were lysed in buffer containing: 15 mM Tris- Hcl pH 7,4, 1% triton x100, 15 mM $MgCl_2$, 0,3M NaCl, 1mg/ ml heparin, 2 mM puromycin. Following incubation on ice for 10 min, subunits were separated at 37°C for 20 min. Gradient separation and fractionation were performed as cycloheximide treatment.

ACKNOWLEDGMENTS

We thank Carlos A. Palacios for generously providing expression plasmids and Eloise Pavão Guerra-Slompo for generously providing TcRBP40 protein. This work was supported by grants from Ministério da Saúde and Conselho Nacional de Desenvolvimento Cientifico e Tecnológico — CNPq (CT- Saúde/MS/SCTIE/DECIT/MCT/CNPq No. 17/2008), Fundação Araucária and FIOCRUZ. This project has been funded in part with federal funds from the National Cancer Institute, National Institutes of Health, under contract HSN261200800001E. The content of this article does not necessarily reflect the views or policies of the Department of Health and Human Services, nor does mention of trade names, commercial products, or organizations imply endorsement by the U.S. Government. B.D. received fellowships from CNPq and P.S. from CAPES.

REFERENCES

1. Taipale J and PA Beachy. (2001). The Hedgehog and Wnt signalling pathways in cancer. Nature 411:349-54.
2. Stone DM, M Hynes, M Armanini, TA Swanson, Q Gu, RL Johnson, MP Scott, D Pennica, A Goddard, H Phillips, M Noll, JE Hooper, F de Sauvage and A Rosenthal. (1996). The tumour-suppressor gene patched encodes a candidate receptor for Sonic hedgehog. Nature 384:129-34.
3. Frank-Kamenetsky M, XM Zhang, S Bottega, O Guicherit, H Wichterle, H Dudek, D Bumcrot, FY Wang, S Jones, J Shulok, LL Rubin and JA Porter. (2002). Small-molecule modulators of Hedgehog signaling: identification and characterization of Smoothened agonists and antagonists. J Biol 1:10.
4. Alexandre C, A Jacinto and PW Ingham. (1996). Transcriptional activation of hedgehog target genes in Drosophila is mediated directly by the cubitus interruptus protein, a member of the GLI family of zinc finger DNA-binding proteins. Genes Dev 10:2003-13.
5. Sasaki H, Y Nishizaki, C Hui, M Nakafuku and H Kondoh. (1999). Regulation of Gli2 and Gli3 activities by an amino-terminal repression domain: implication of Gli2 and Gli3 as primary mediators of Shh signaling. Development 126:3915-24.
6. Bai CB, D Stephen and AL Joyner. (2004). All mouse ventral spinal cord patterning by hedgehog is Gli dependent and involves an activator function of Gli3. Dev Cell 6:103-15.
7. Eggenschwiler JT and KV Anderson. (2007). Cilia and developmental signaling. Annu Rev Cell Dev Biol 23:345-73.
8. Moore F, J Jaruzelska, D Dorfman and R Reijo-Pera. (2004). Identification of a novel gene, DZIP (DAZ-interacting protein), that encodes a protein that interacts with DAZ (deleted in azoospermia) and is expressed in embryonic stem cells and germ cells. Genomics 83:834-43.
9. Glazer AM, AW Wilkinson, CB Backer, SW Lapan, JH Gutzman, IM Cheeseman and PW Reddien. (2010). The Zn finger protein Iguana impacts Hedgehog signaling by promoting ciliogenesis. Dev Biol 337:148-56.
10. Kim HR, J Richardson, F van Eeden and PW Ingham. (2010). Gli2a protein localization reveals a role for Iguana/DZIP1 in primary ciliogenesis and a dependence of Hedgehog signal transduction on primary cilia in the zebrafish. BMC Biol 8:65.
11. Wilson CW and DY Stainier. (2010). Vertebrate Hedgehog signaling: cilia rule. BMC Biol 8:102.
12. Jin Z, W Mei, S Strack, J Jia and J Yang. (2011). The antagonistic action of B56-containing protein phosphatase 2As and casein kinase 2 controls the phosphorylation and Gli turnover function of Daz interacting protein 1. J Biol Chem 286:36171-9.
13. Maegawa S, M Yamashita, K Yasuda and K Inoue. (2002). Zebrafish DAZ-like protein controls translation via the sequence 'GUUC'. Genes Cells 7:971-84.
14. Collier B, B Gorgoni, C Loveridge, HJ Cooke and NK Gray. (2005). The DAZL family proteins are PABP-binding proteins that regulate translation in germ cells. EMBO J 24:2656-66.
15. Reynolds N, B Collier, K Maratou, V Bingham, RM Speed, M Taggart, CA Semple, NK Gray and HJ Cooke. (2005). Dazl binds in vivo to specific transcripts and can regulate the pre-meiotic translation of Mvh in germ cells. Hum Mol Genet 14:3899-909.
16. Smith RW, RC Anderson, JW Smith, M Brook, WA Richardson and NK Gray. (2011). DAZAP1, an RNA-binding protein required for development and spermatogenesis, can regulate mRNA translation. RNA 17:1282-95.
17. Vangompel MJ and EY Xu. (2011). The roles of the DAZ family in spermatogenesis: More than just translation? Spermatogenesis 1:36-46.
18. Kim B, HJ Cooke and K Rhee. (2012). DAZL is essential for stress granule formation implicated in germ cell survival upon heat stress. Development 139:568-78.
19. Sharova LV, AA Sharov, T Nedorezov, Y Piao, N Shaik and MS Ko. (2009). Database for mRNA half-life of 19 977 genes obtained by DNA microarray analysis of pluripotent and differentiating mouse embryonic stem cells. DNA Res 16:45-58.
20. Raghavan A, RL Ogilvie, C Reilly, ML Abelson, S Raghavan, J Vasdewani, M Krathwohl and PR Bohjanen. (2002). Genome-wide analysis of mRNA decay in resting and activated primary human T lymphocytes. Nucleic Acids Res 30:5529-38.

21. Sprague BL, RL Pego, DA Stavreva and JG McNally. (2004). Analysis of binding reactions by fluorescence recovery after photobleaching. Biophys J 86:3473-95.
22. Rebelatto CK, AM Aguiar, MP Moretão, AC Senegaglia, P Hansen, F Barchiki, J Oliveira, J Martins, C Kuligovski, F Mansur, A Christofis, VF Amaral, PS Brofman, S Goldenberg, LS Nakao and A Correa. (2008). Dissimilar differentiation of mesenchymal stem cells from bone marrow, umbilical cord blood, and adipose tissue. Exp Biol Med (Maywood) 233:901-13.
23. Shigunov P, J Sotelo-Silveira, C Kuligovski, AM de Aguiar, CK Rebelatto, JA Moutinho, PS Brofman, MA Krieger, S Goldenberg, D Munroe, A Correa and B Dallagiovanna. (2012). PUMILIO-2 is involved in the positive regulation of cellular proliferation in human adipose-derived stem cells. Stem Cells Dev 21:217-27.
24. Holetz FB, A Correa, AR Avila, CV Nakamura, MA Krieger and S Goldenberg. (2007). Evidence of P-body-like structures in Trypanosoma cruzi. Biochem Biophys Res Commun 356:1062-7.
25. Vorobjev IA and Chentsov YuS. (1982). Centrioles in the cell cycle. I. Epithelial cells. J Cell Biol 93:938-49.
26. Lee KH, S Lee, B Kim, S Chang, SW Kim, JS Paick and K Rhee. (2006). Dazl can bind to dynein motor complex and may play a role in transport of specific mRNAs. EMBO J 25:4263-70.
27. Hall TM. (2005). Multiple modes of RNA recognition by zinc finger proteins. Curr Opin Struct Biol 15:367-73.
28. Sekimizu K, N Nishioka, H Sasaki, H Takeda, RO Karlstrom and A Kawakami. (2004). The zebrafish iguana locus encodes Dzip1, a novel zinc-finger protein required for proper regulation of Hedgehog signaling. Development 131:2521-32.
29. Chen JK, J Taipale, MK Cooper and PA Beachy. (2002). Inhibition of Hedgehog signaling by direct binding of cyclopamine to Smoothened. Genes Dev 16:2743-8.
30. Moore MJ. (2005). From birth to death: the complex lives of eukaryotic mRNAs. Science 309:1514-8.
31. Corbit KC, P Aanstad, V Singla, AR Norman, DY Stainier and JF Reiter. (2005). Vertebrate Smoothened functions at the primary cilium. Nature 437:1018-21.
32. Haycraft CJ, B Banizs, Y Aydin-Son, Q Zhang, EJ Michaud and BK Yoder. (2005). Gli2 and Gli3 localize to cilia and require the intraflagellar transport protein polaris for processing and function. PLoS Genet 1:e53.
33. Wolff C, S Roy, KE Lewis, H Schauerte, G Joerg-Rauch, A Kirn, C Weiler, R Geisler, P Haffter and PW Ingham. (2004). iguana encodes a novel zinc-finger protein with coiled-coil domains essential for Hedgehog signal transduction in the zebrafish embryo. Genes Dev 18:1565-76.
34. Keene JD. (2007). RNA regulons: coordination of post-transcriptional events. Nat Rev Genet 8:533-43.
35. Kikuyama M, H Takeshima, T Kinoshita, E Okochi-Takada, M Wakabayashi, S Akashi-Tanaka, T Ogawa, Y Seto and T Ushijima. (2012). Development of a novel approach, the epigenome-based outlier approach, to identify tumor-suppressor genes silenced by aberrant DNA methylation. Cancer Lett 322:204-12.
36. Gupta S, N Takebe and P Lorusso. (2010). Targeting the Hedgehog pathway in cancer. Ther Adv Med Oncol 2:237-50.
37. Martin KC and A Ephrussi. (2009). mRNA localization: gene expression in the spatial dimension. Cell 136:719-30.

Table 1. Molecular and cellular functions associated with DZIP1 targets

Category[a]	Top-ranked functions	Enrichment score
Binding function	Protein binding	28.69
	Nucleic acid binding	21.78
	Chromatin binding	4.37
Molecular function	Binding	23.48
	Catalytic activity	7.19
	Transcription regulator activity	3.2
	Molecular transducer activity	2.45
	Structural molecule activity	2.08
Components	Extracellular region	16.22
	Cell part	11.21
Associated network functions[b]	***p*-value**	**No. molecules**
Cell cycle	3.07E-12 - 4.89E-02	127
Gene expression	1.22E-10 - 4.65E-02	153
Cellular compromise	1.35E-10 - 2.95E-02	107
DNA replication, recombination, and repair	1.06E-09 - 3.61E-02	113
RNA posttranscriptional modification	7.52E-09 - 1.65E-02	44

[a]GO annotations of DZIP1 mRNA targets.

[b]Ingenuity pathway analysis networks: Functions associated with the networks regulated by DZIP1.

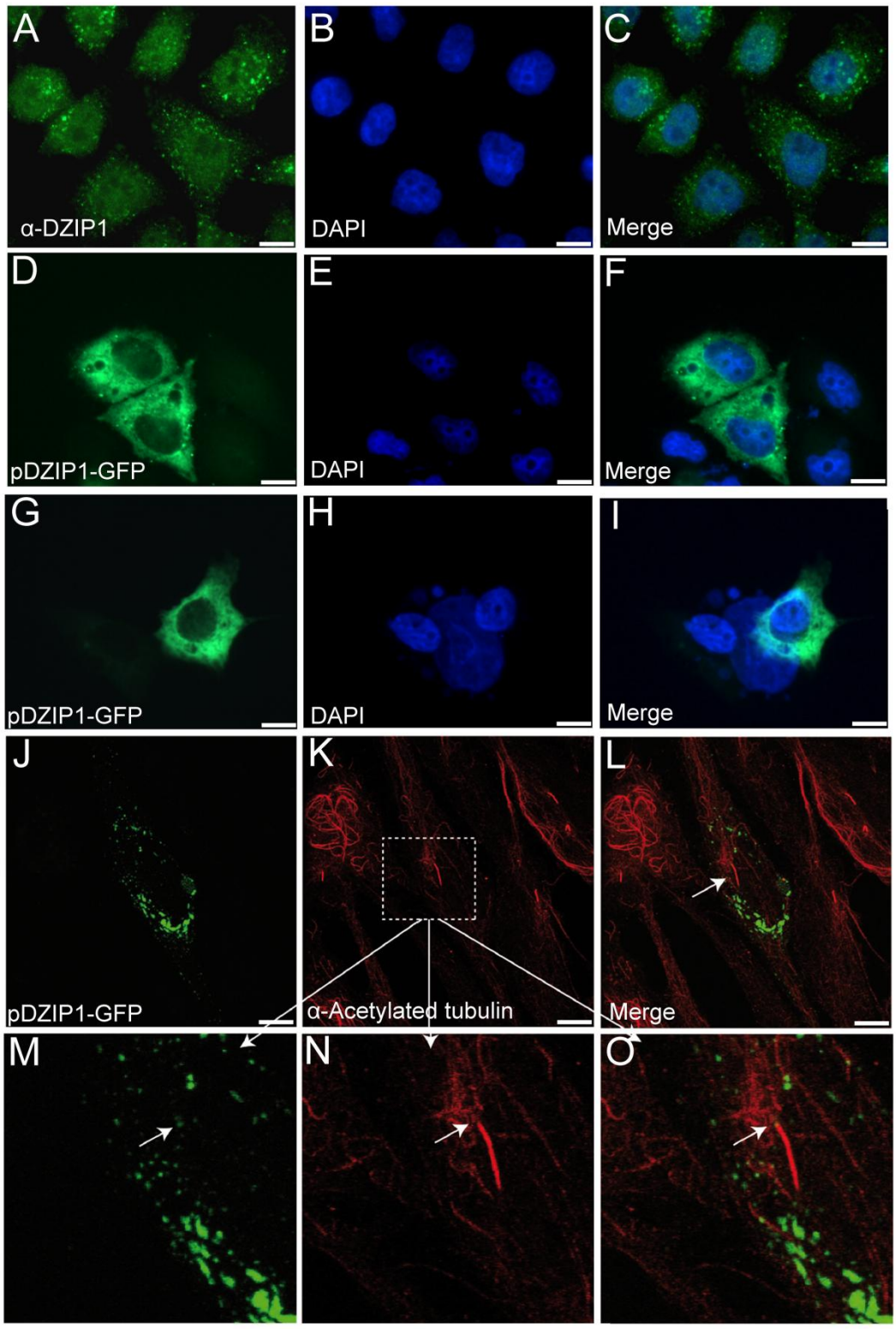

Fig. 1 DZIP1 is located predominantly in the cytoplasm, in a granular pattern. (A) Indirect immunofluorescence staining of DZIP1 (green) in HeLa cells. (B) Nuclei counterstained with DAPI (blue) and (C) merged image. HeLa (D-F), HEK293 (G-I) and hTERT-RPE1 (J-O) cells were transfected with pDZIP1-GFP. (J-O) Ciliary axonemes were labeled with anti-acetylated tubulin antibodies (red). (M-O) are magnified sections from (K) (white boxes). Arrow = basal bodies of primary cilia. Scale bar: 10 μm.

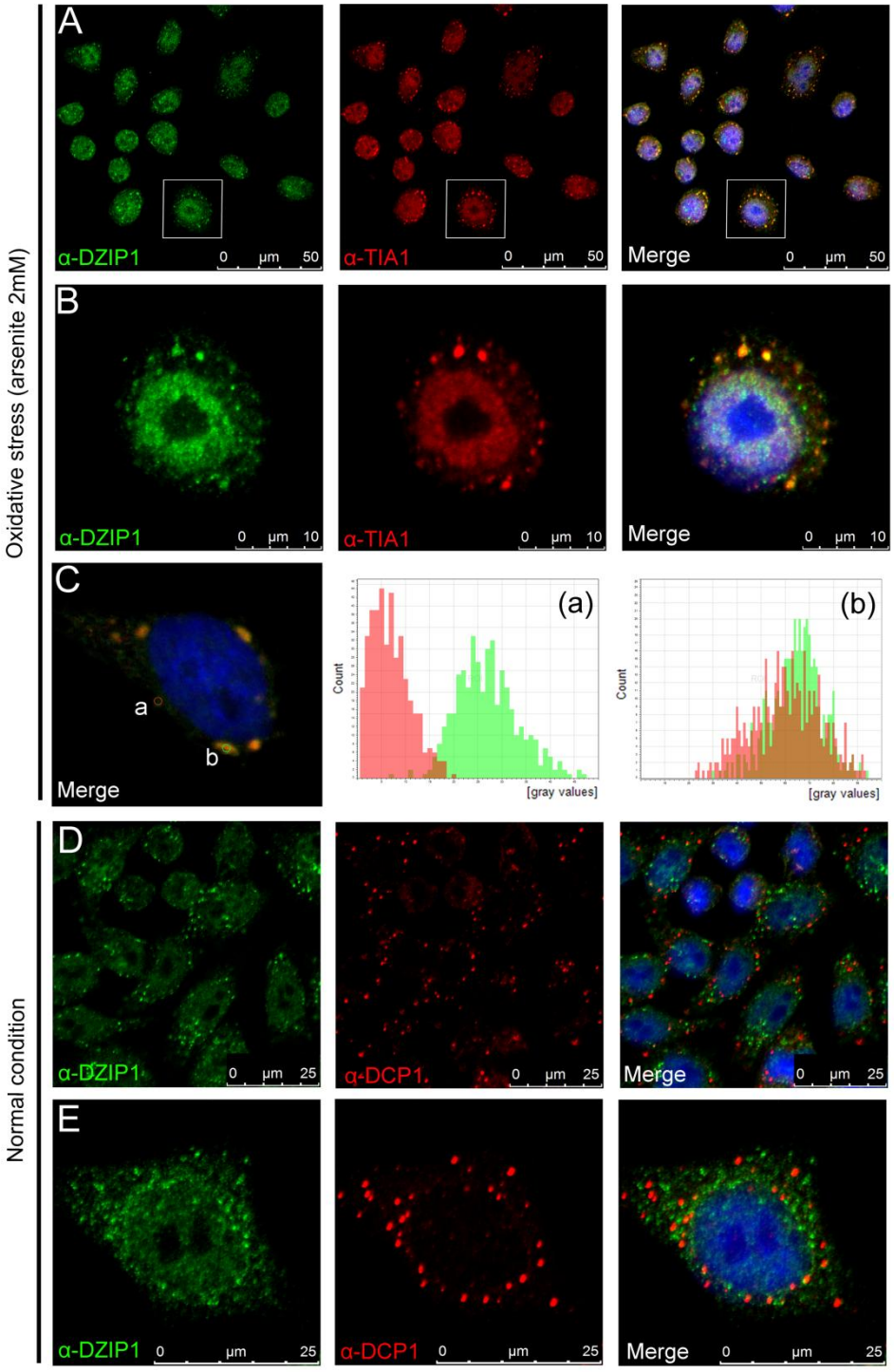

Fig. 2 DZIP1 is recruited to stress granules in oxidative-stressed cells

(A) Indirect immunofluorescence staining was carried out to detect the colocalization of DZIP1 (green) and TIA1 (red) in HeLa cells. Nuclei were counterstained with DAPI (blue). (B) Images are magnified sections from A (white boxes). (C) Fluorescence intensities of DZIP1 (green) and TIA1 (red) were measured on selected region the merged images (left) without colocalization (a) and with colocalization (b) of HeLa cells under oxidative stress. (D) Indirect immunofluorescence staining of DZIP1 (green) and DCP1 (red) antibody was used to detect colocalization with p-bodies. (E) Enlarged area shows a cell in detail.

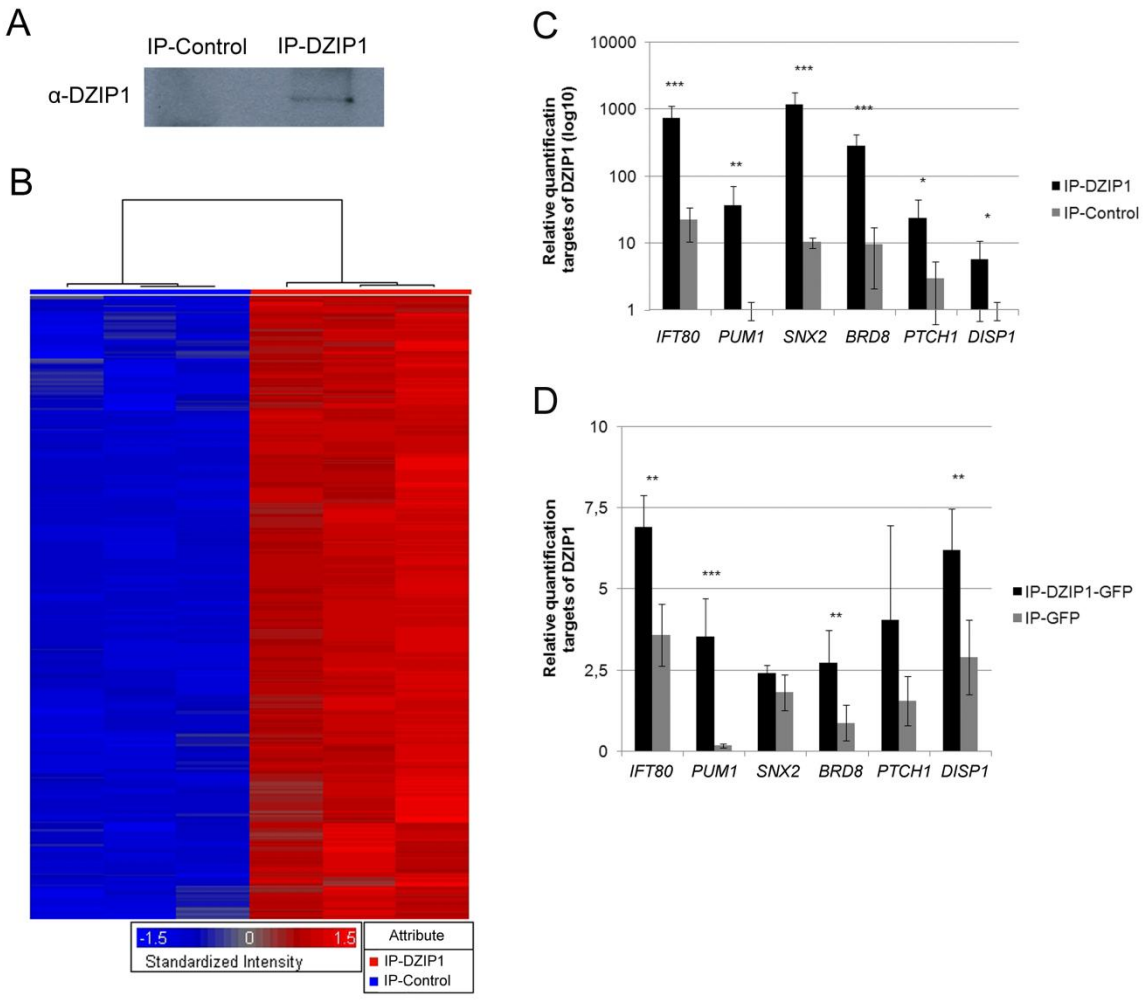

Fig. 3 Identification of DZIP1-associated mRNAs in HeLa cells. (A) Western blot of the HeLa cells proteins immunoprecipitated with a specific anti-DZIP1 antibody and a control IgG, probed with a specific anti-DZIP1 antibody; (B) mRNAs associated with DZIP1. Microarray analysis of the immunoprecipitated RNA fractions. Rows correspond to individual transcripts and the color code indicates the degree of enrichment. Three independent assays, with anti-DZIP1 antibody and negative controls, are shown. (C) Quantitative RT-PCR analysis of Transcript levels in IP-DZIP1 (DZIP1 immunoprecipitate) versus negative IP (IP-Control), normalized with respect to concentration. Analysis of the mRNAs (*IFT80, PUM1, SNX2, BRD8, PTCH* and *DISP1*) enrichment of IP-DZIP1. Mean of technical triplicates. (D) Quantitative RT-PCR of transcript levels in IP-DZIP1-GFP versus those for negative IP (IP-GFP), normalized with respect to concentration. Analysis of the mRNAs (*IFT80, PUM1, SNX2, BRD8, PTCH* and *DISP1*) enrichment of IP-DZIP1-GFP. Mean of technical duplicates.

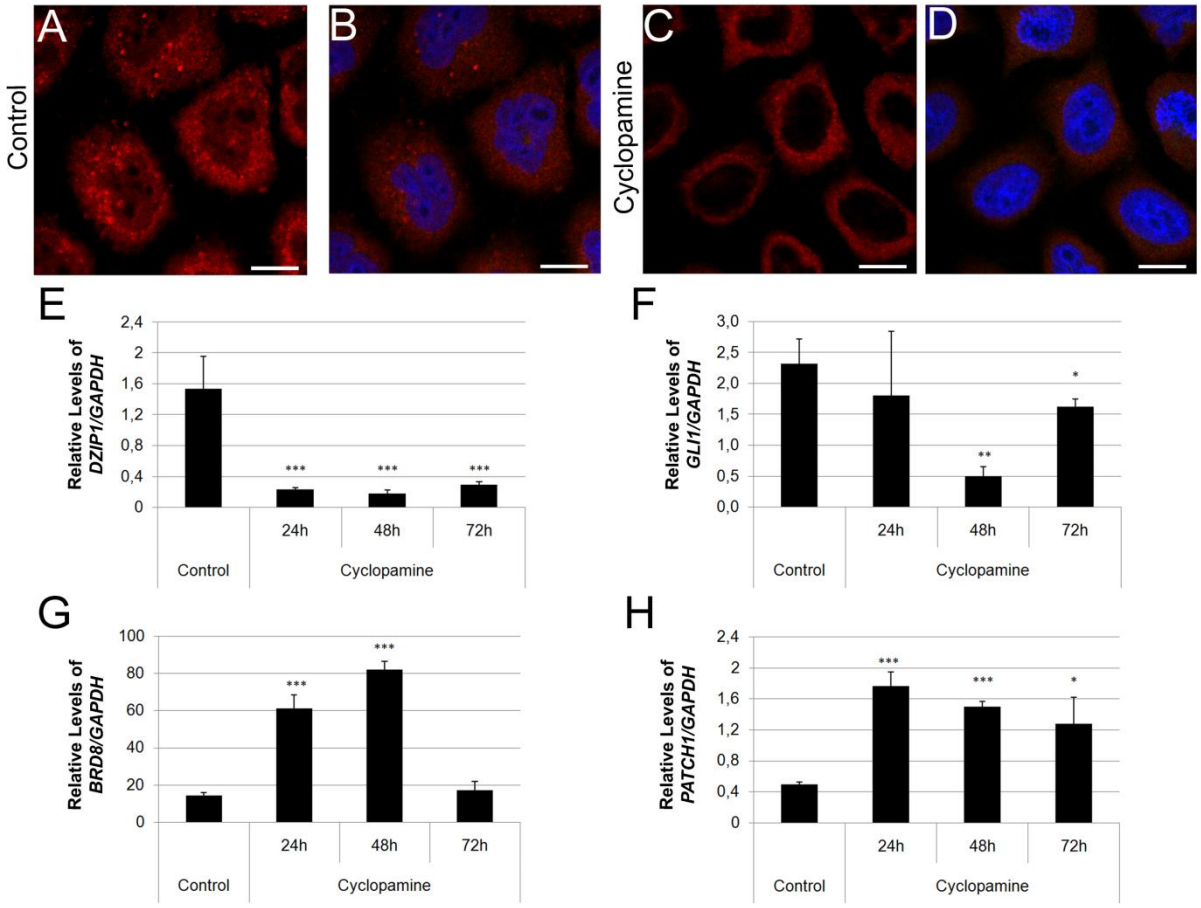

Fig. 4 The expression of DZIP1 and its mRNA targets is affected by Hh pathway blockade. Indirect immunofluorescence staining was used to detect DZIP1 (red), and nuclei were counterstained with DAPI (blue). (A-B) HeLa cells without cyclopamine treatment. (A) DZIP1 and (B) Merge DZIP1/DAPI. (C-D) HeLa cells treated with 300 nM cyclopamine for 24 h. (C) DZIP1 and (D) Merge DZIP1/DAPI. (E-H) Quantitative RT-PCR analysis of *DZIP1*, *GLI1*, *BRD8* and *PTCH1* mRNA levels in HeLa cells treated with cyclopamine for 24, 48 and 72 h. *GAPDH* was used as an internal housekeeping gene control. *$P \leq 0.05$, **$P \leq 0.01$, ***$P \leq 0.001$. Scale bar: 10 μm.

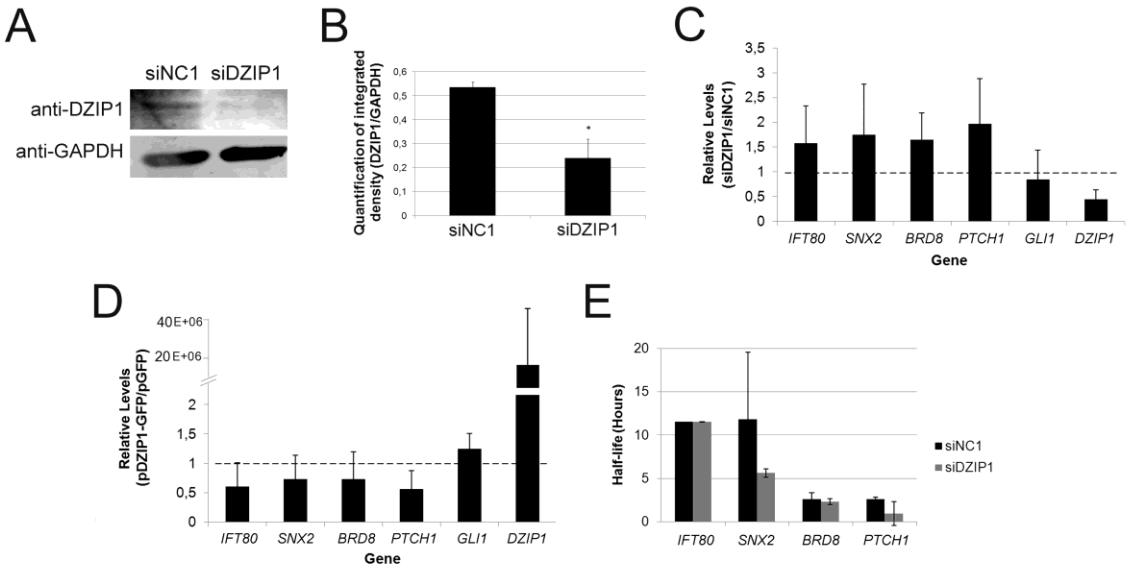

Fig. 5 *DZIP1* knockdown and overexpression do not affect the accumulation or stability of mRNAs associated with DZIP1-containing complexes. (A) Protein extracts from *DZIP1* knockdown (siDZIP1) and negative control (siNC1) cells were analyzed by western blotting with antibodies against DZIP1 and GAPDH. (B) The set of Western blots shown in (A) were used for the shown quantitation and are representative for results from two experiments. (C) Quantitative RT-PCR analysis of *DZIP1*, *GLI1*, *PTCH1*, *BRD8*, *SNX2* and *IFT80* mRNA levels in *DZIP1* knockdown cells. (D) Quantitative RT-PCR analysis of *DZIP1*, *GLI1*, *PTCH1*, *BRD8*, *SNX2* and *IFT80* mRNA levels in HeLa cells transfected with pDZIP1-GFP or pGFP alone. *GAPDH* was used as an internal housekeeping gene control. (E) Mean half-life for some of the mRNA targets of DZIP1 (*IFT80*, *SNX2*, *BRD8* and *PTCH1*) in HeLa cells transfected with siDZIP1 and siNC1. Mean of two independent experiments are shown. $*P \leq 0.05$.

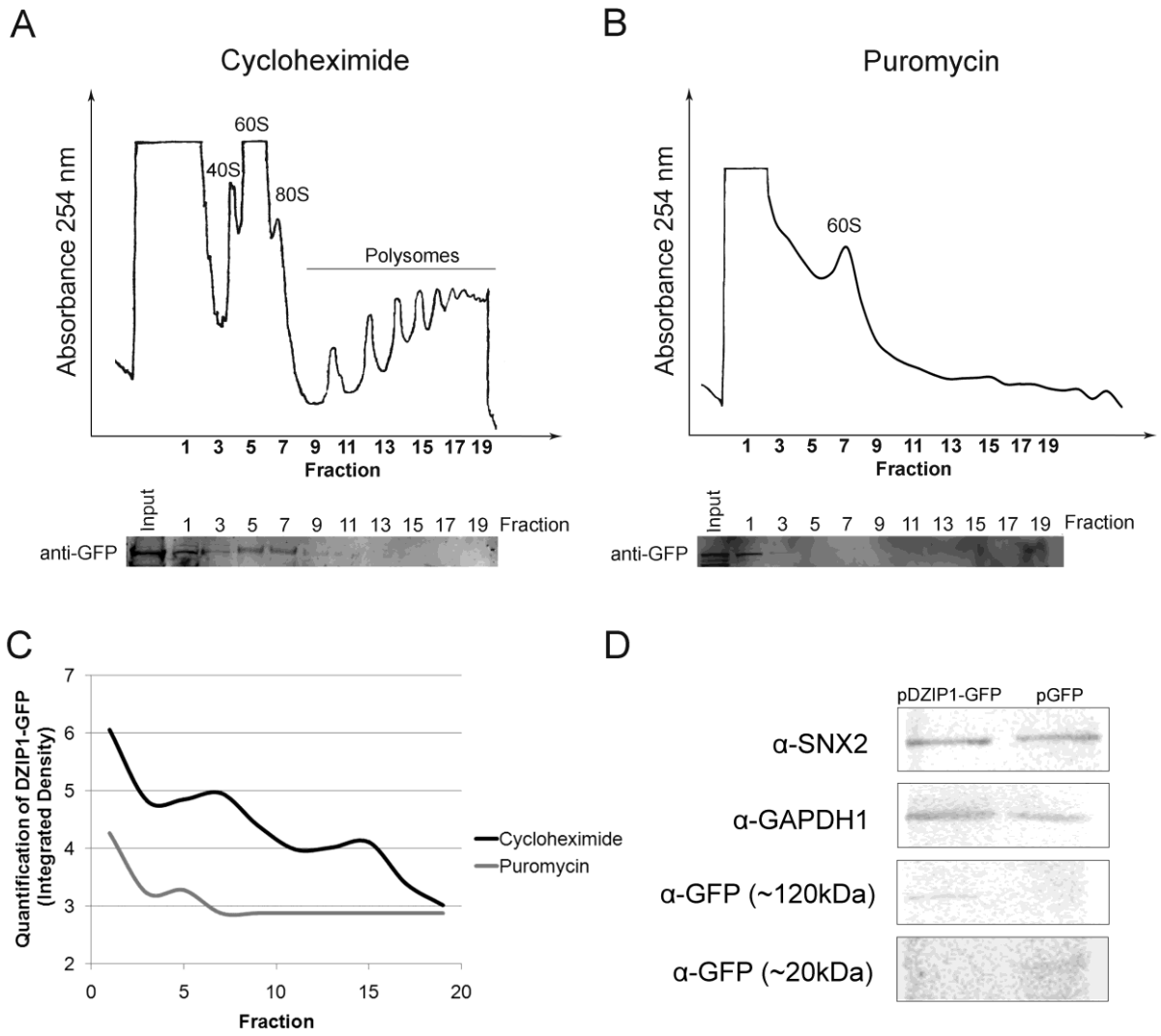

Fig. 6 Polysomal distribution of DZIP1-GFP. (A) HeLa cells were treated with cycloheximide, lysates prepared, separated in a 10–50% sucrose gradient. Distribution of DZIP1-GFP was examined by Western blot analysis. (B) HeLa cells were treated with puromycin, extracts prepared and processed as in (A). (C) Quantitation of the distribution of DZIP1-GFP after cycloheximide and puromycin treatment. The set of Western blots shown in (A) and (B) were used for quantitation. (D) Protein extracts of Hela cells transfected with pDZIP1-GFP or pGFP alone (control sample) were analyzed by western blotting with antibodies against SNX2, GAPDH and GFP.

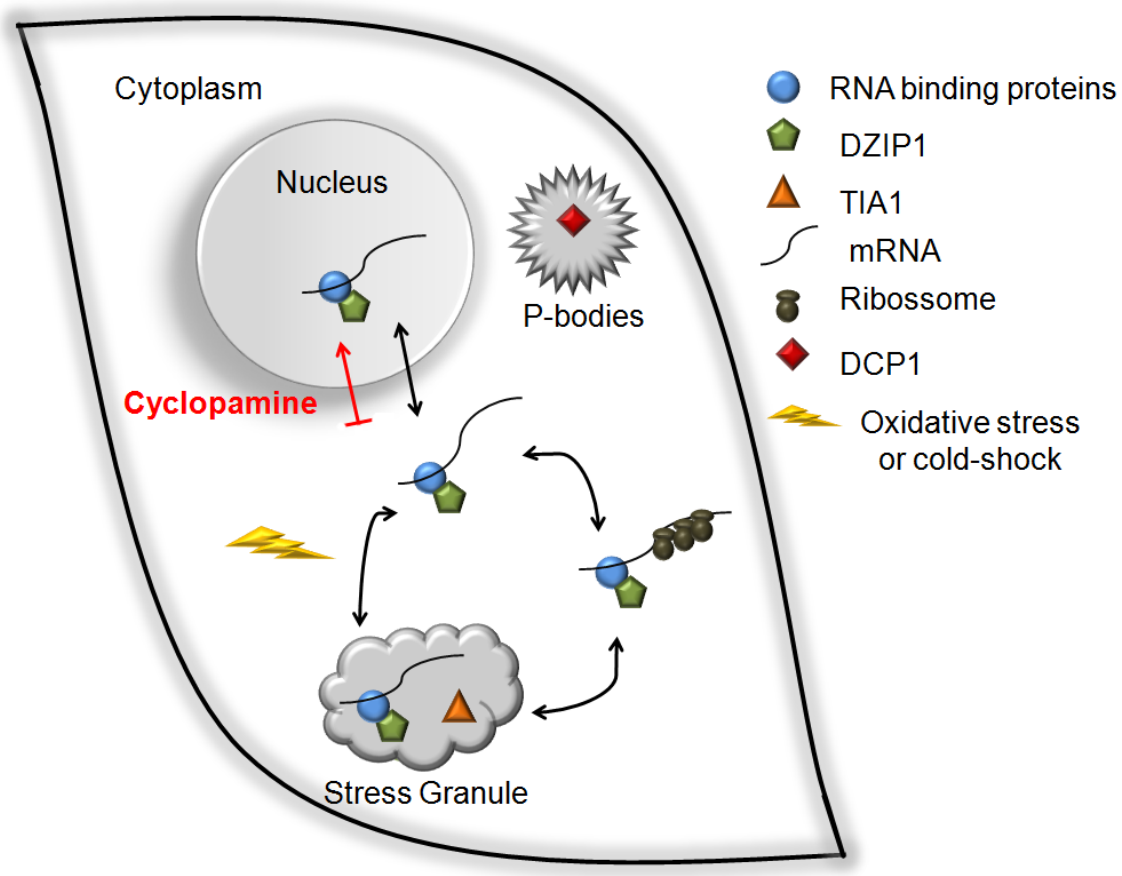

Fig. 7 Model of ribonucleoprotein complexes containing DZIP1 in stress granules. DZIP1 is located mainly in the cytoplasm, where it is involved in ribonucleoprotein complexes related to mRNA networks involved primarily in controlling cell cycle and gene expression in HeLa cells. Inhibiting the Hedgehog pathway with cyclopamine, blocked its translocation to the nucleus. DZIP1 is found associated with polysomes and when HeLa cells are exposed to oxidative stress, DZIP1 is translocated to stress granules but not to processing bodies (p-bodies).

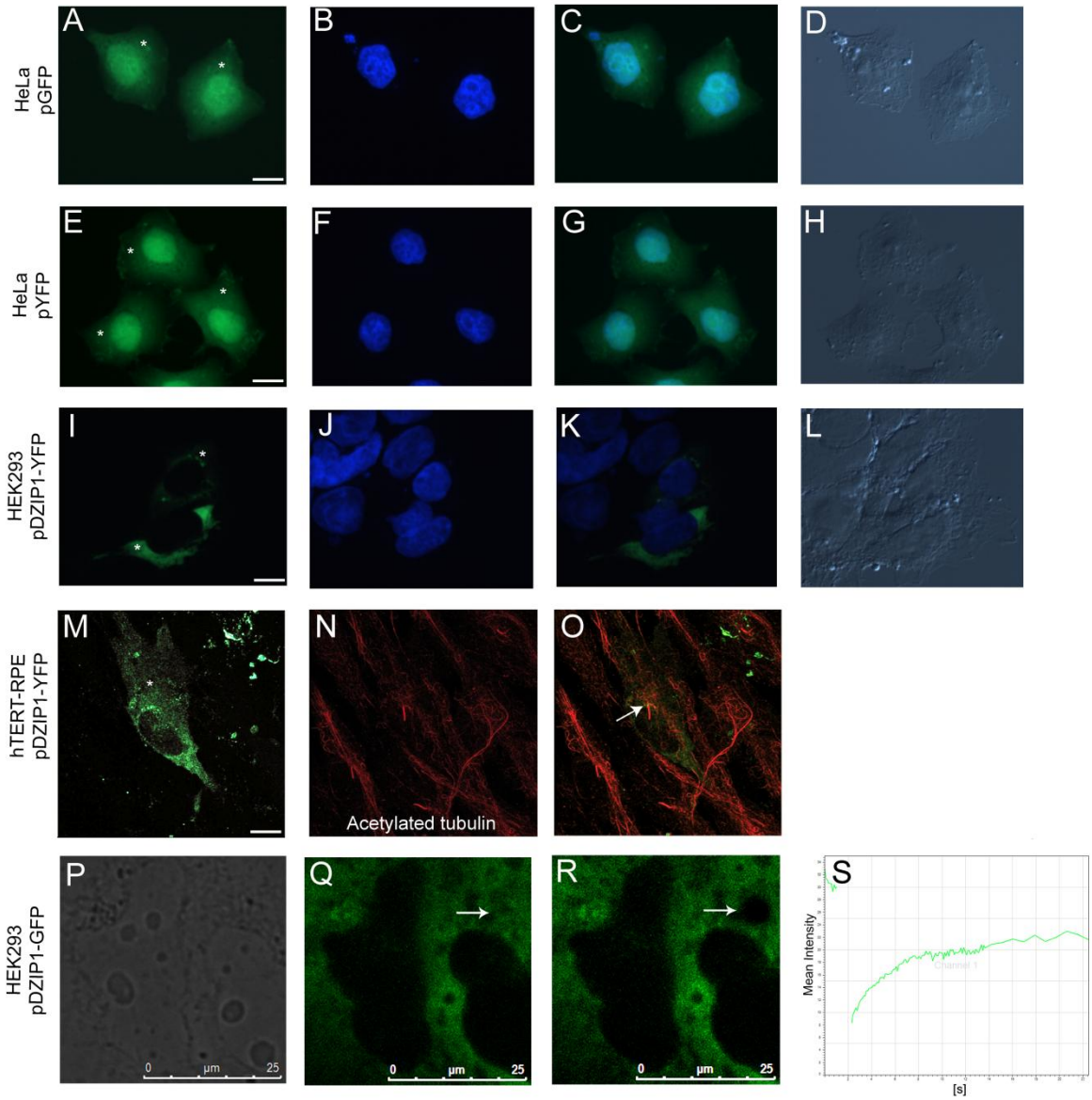

Supplementary Fig. S1 DZIP1 is located predominantly in the cytoplasm, in a granular pattern. HeLa was transfected with pGFP (A-D) or pYFP (E-H). Nuclei were counterstained with DAPI (blue). (I-L) HEK293 and (M-O) hTERT-RPE1 cells were transfected with pDZIP1-YFP (green). (N-O) Ciliary axonemes were labeled with anti-acetylated tubulin antibodies (red). Arrow = basal bodies of primary cilia. (P-R) HEK293 cells were transfected with pDZIP1-GFP. Fluorescence images of a section that was photobleached in a living cell; the fluorescence intensity of the bleached area was monitored. (P) Cells in phase contrast. (Q) Cells before photobleaching (arrow). (R) Cells two seconds after photobleaching (arrow). (S) Fluorescence recovery graph. An asterisk indicates a cell containing a plasmid. Scale bar: 10 µm.

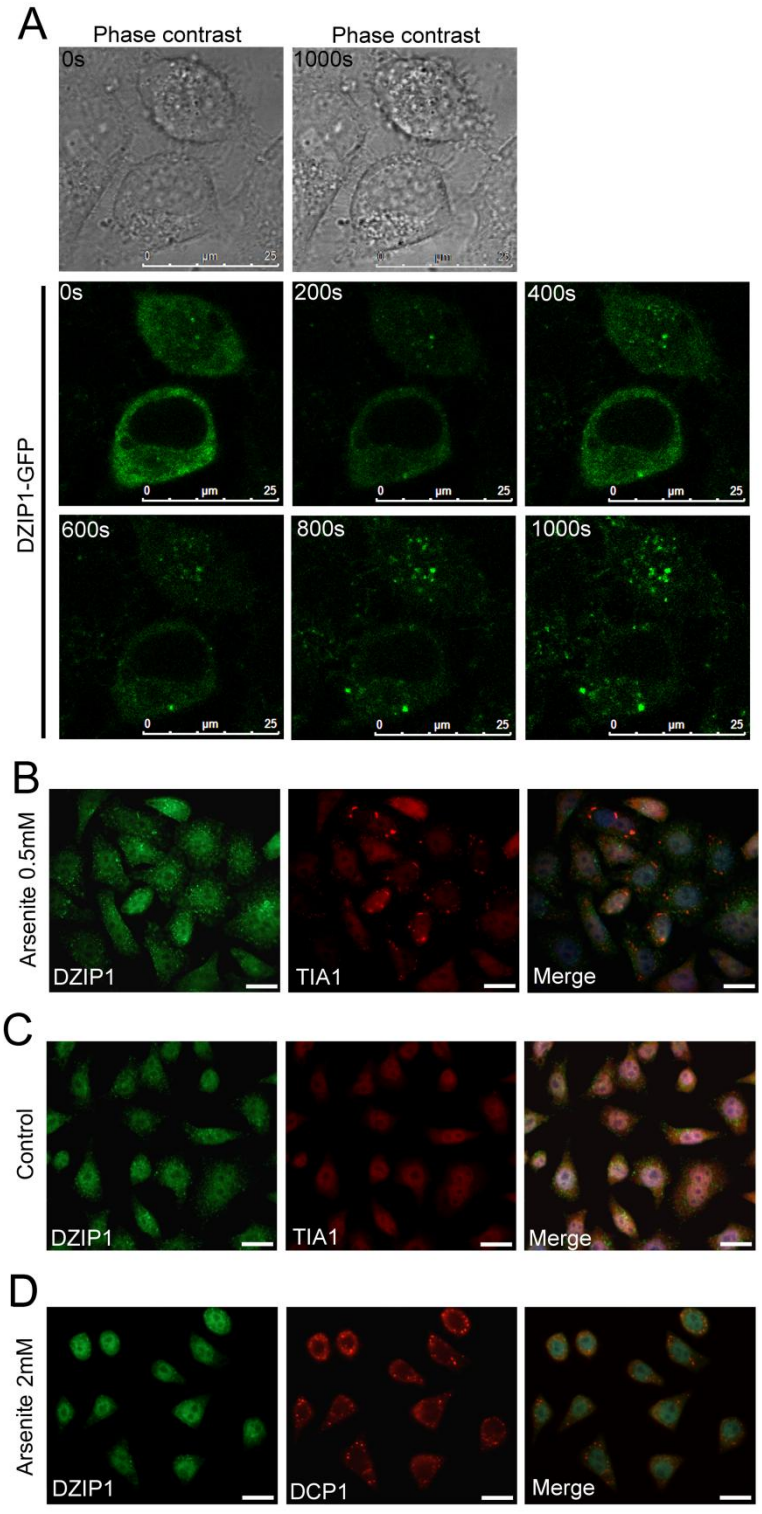

Supplementary Fig. S2 Real-time imaging of DZIP1-GFP aggregation with granules. (A) HeLa cells were transfected with DZIP1-GFP and cultured for 18 hours at 37°C, and were then shifted to 20°C. Fluorescence images were taken at one-second intervals (the time after the temperature shift is indicated in each panel). (B-D) Indirect immunofluorescence staining was carried out to detect the colocalization of DZIP1 (green) and TIA1 (red) or DCP1 (red) in HeLa cells. Nuclei were counterstained with DAPI (blue). (B) Oxidative stress with 0,5mM sodium arsenite. (C) Normal condition. (D) Oxidative stress with 2mM sodium arsenite. Scale bar: 10 μm.

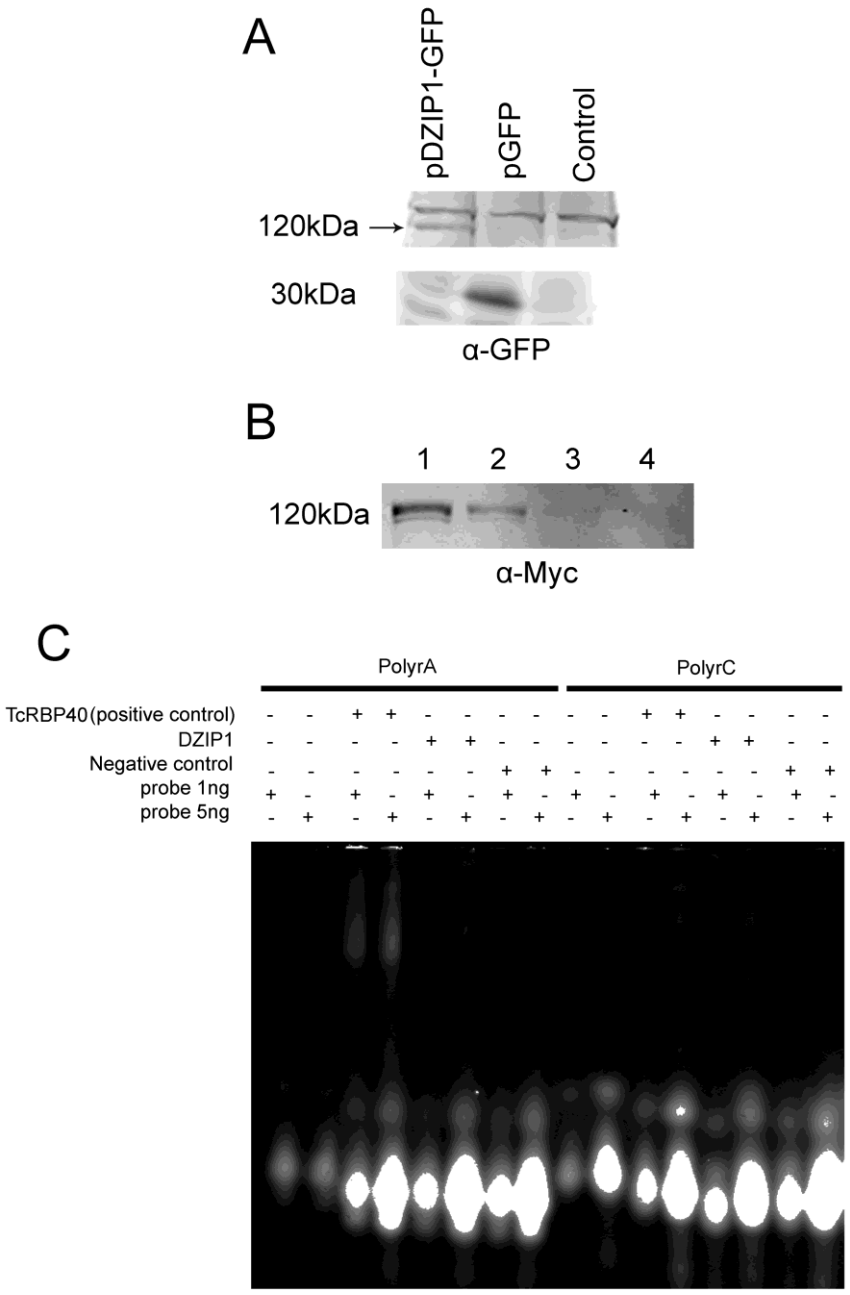

Supplementary Fig. S3 DZIP1 did not interact robustly with the RNA probe. (A) Western-blot analysis of DZIP1-GFP and GFP levels in protein extracts from cells transfected with the corresponding plasmids. The band detected proximally at 120 kDa corresponds to DZIP1-GFP and the band detected at 27 kDa corresponds to free GFP. (B) Western-blot analysis against MYC tag: eluates (1-4) for affinity purification from cells transfected with a construct encoding DZIP1 fused to a histidine tail and a MYC tag (pSECTAG2). These eluates were used in electrophoretic mobility shift assays (EMSA). (C) We investigated whether DZIP1 interacted directly with these RNAs, by performing EMSA with purified DZIP1 protein and polyr A and C (U and G – not shown) probes. TcRBP40 is an RNA-binding protein used as a positive control. IP, immunoprecipitation.

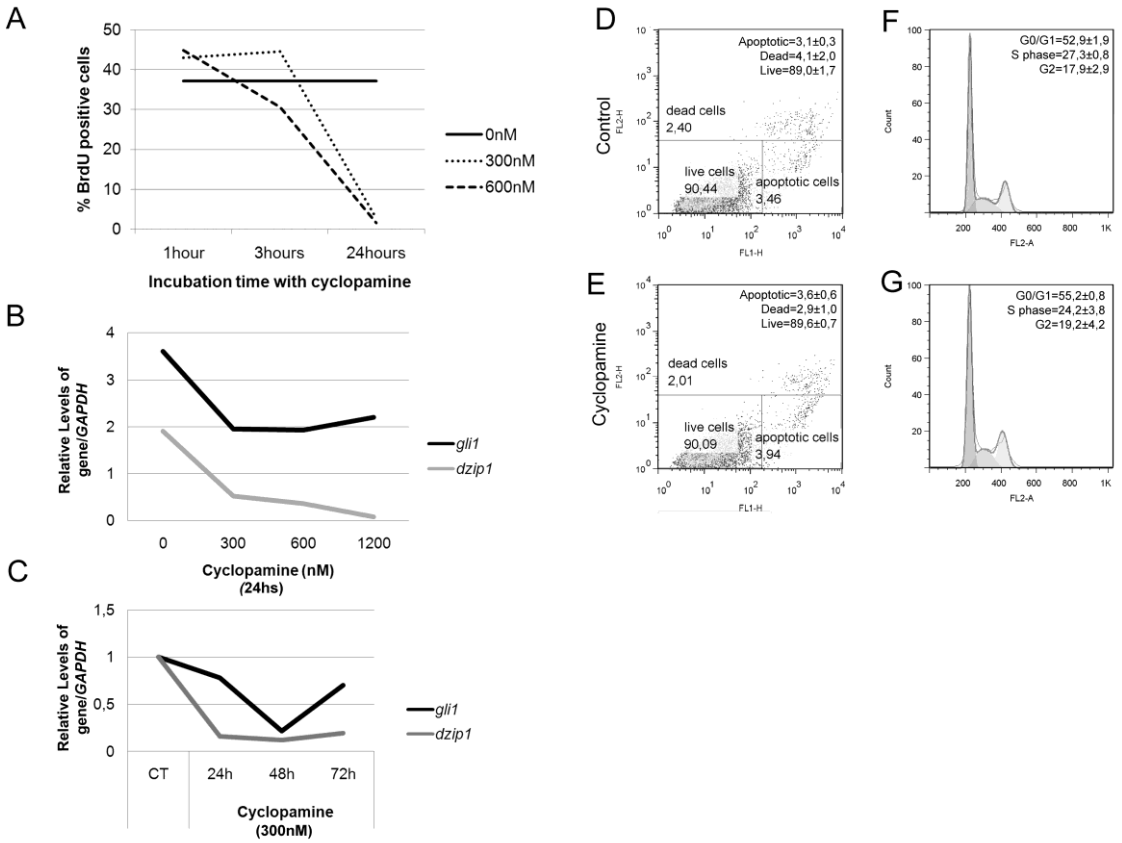

Supplementary Fig. S4 Expression of *DZIP1* and its mRNAs targets is affected by Hh pathway blockaded. (A) HeLa cells were incubated for several time periods, with various concentrations of cyclopamine. Proliferation was evaluated by BrdU incorporation. (B-C) We analyzed gli1 mRNA levels in cells treated with various concentrations of cyclopamine for various times, by quantitative RT-PCR. (D-E) No change in the percentage apoptotic cells was observed after treatment of the cells with 300 nM cyclopamine for 24 hours. FACS-based apoptosis analysis showed that cyclopamine caused no significant change in the percentages of live, apoptotic and dead cells with respect to control cells. Dot plots for (D) control and (E) cyclopamine-treated cells. Cells were treated with Alexa Fluor 488 annexin V and propidium iodide (Molecular Probe), and subjected to flow cytometry. (F-G) FACS-based cell cycle analysis demonstrated that cyclopamine treatment did not affect the percentages of cells in the G1, S and G2 phases of the cell cycle. A representative histogram of control cells (F) and cyclopamine-treated cells (G) based on the ‘‘Dean-Jett-Fox’’ model.

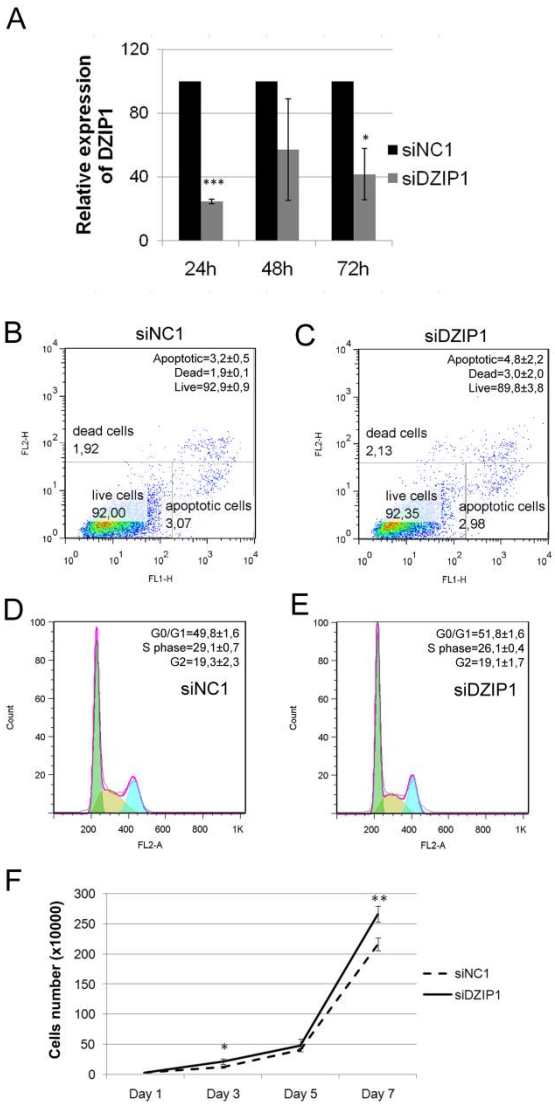

Supplementary Fig. S5 *DZIP1* knockdown and overexpression do not affect the accumulation or stability of mRNAs associated with DZIP1-containing complexes. (A) Quantitative RT-PCR analysis of *PTCH1*, *BRD8* and *DZIP1* expression 24, 48 and 72 h after the transfection of cells with 1 nM DZIP1 duplex mix (siDZIP1) or 1 nM Scrambled-negative control duplex (siNC1). (B-C) The percentage of apoptotic cells was similar in *Dzip1*-knockdown cells and control cells. FACS-based apoptosis analysis showed that *DZIP1* knockdown caused no significant change in the percentages of live, apoptotic and dead cells with respect to control cells (siNC1). Dot plot of (B) control and (C) *DZIP1*-knockdown cells. Cells were treated with Alexa Fluor 488 annexin V and propidium iodide (Molecular Probe), and subjected to flow cytometry analysis. (D-E) FACS-based cell cycle analysis demonstrated that *DZIP1* knockdown had no effect on the percentages of cells in the G1, S and G2 phases of the cell cycle. A representative histogram of control cells (D) and *DZIP1*-knockdown cells (E) based on the ‘‘Dean-Jett-Fox’’ model. (F) Greater growth of HeLa cells following *DZIP1* knockdown. Cells were counted at the indicated time points and the mean ±SD values of three independent experiments are shown.

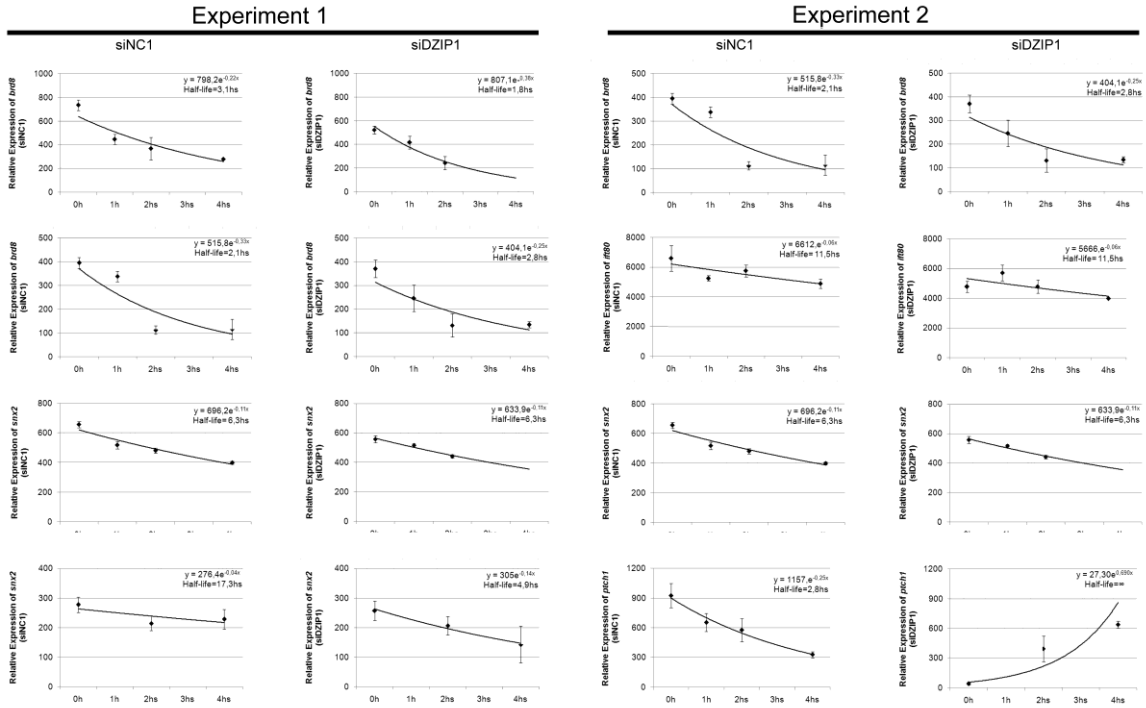

Supplementary Fig. S6 Half-life of *BRD8, IFT80, SNX2* and *PTCH* mRNAs in *DZIP1*-knockdown and control cells. HeLa cells transfected with siDZIP1 and siNC1 were treated with Act-D for various times, to block mRNA synthesis. Total RNA extraction, cDNA production, and real-time PCR amplification were performed as described in the text. The values shown are the means and standard deviations (SD) of RNA copy number per µg of total RNA from two independent experiments run in triplicate.

Supplementary Table S1. Primer Sets Used for Quantitative Reverse Transcription–Polymerase Chain Reaction Analyses

Official symbol	NCBI ID	Primer sequence (5´–3´)	Amplicon (bp)
DZIP1	NM_014934	Forward GCCATCGACGTGGACAAGGTGGC	205
		Reverse TGTGACTTTGTAGAAAAGCTTGG	
GAPDH	NM_002046.3	Forward: GGCGATGCTGGCGCTGAGTAC	149
		Reverse: TGGTTCACACCCATGACGA	
SNX2	NM_003100.2	Forward: GACGGAGAGGACCTGTTCAC	240
		Reverse CAGGTGTGACTGCAGGAGAA	
PTCH1	NM_001083606.1	Forward: ATCCATGTGGCTGCCCTCTT	223
		Reverse CACAGCTCCTCCACGTTGGT	
IFT80	NM_020800.1	Forward: GGGATGCTTAGATCAACTTTAGCTC	159
		Reverse: GCCATCATGAGCTTTCCAC	
BRD8	NM_006696.3	Forward: GCGACGGGAACGGGCAAACA	157
		Reverse: TCTGGAGGGCGGCCAGGTTC	
GLI1	NM_005269.2	Forward: CCCGCCCTTCTGCCACCAAG	182
		Reverse: ACCGTCTGCAGGTCCAGGCT	
PUM1	NM_001020658.1	Forward: AAACCTGAGAAGTTTGAATTG	351
		Reverse: GCAAGACCAAAAGCAGAGTTG	
DISP1	NM_032890.2	Forward: GAGCTGCGCCTGCCAACTCA	231
		Reverse: CAGGGGGTGAGGGGACTCGG	

DZIP1, DAZ interacting protein 1; GAPDH, glyceraldehyde-3-phosphate dehydrogenase; SNX2, sorting nexin 2; PTCH1, patched homolog 1 (Drosophila); IFT80, intraflagellar transport 80 homolog; BRD8, bromodomain containing 8; GLI1, GLI family zinc finger 1; PUM1, pumilio homolog 1; DISP1, dispatched homolog 1;

4. MATERIAIS E MÉTODOS

Essa seção compreende os materiais e métodos referentes aos resultados (Capítulo 5) que não estão inclusos no artigo (Capítulo 3).

4.1 Lista de soluções

Solução de lise: Hepes 20 mM (pH 7,4), NaCl 100 mM, NaF 50 mM, 1% Triton x-100, 10% glicerol, 1 mM dithiothreitol, 1 μl cocktail de inibidores de protease;
Tampão de amostra para DNA 10x: Ficoll 25%, azul de bromofenol 0,25%, xilenocianol 0,25%;
TBE: tris-base 89 mM, ácido bórico 89 mM, EDTA 2 mM;
Solução de brometo de etídeo: solução 5 μg/mL de brometo de etídeo em água Destilada
PBS 10x: KCl 2,7 mM, KH2PO4 1,5 mM, $Na_2HPO_4.7H_20$ 4,3 mM, NaCl 137 mM;
Tampão de amostra de proteína 4x: Tris-HCl 160 mM pH 6,8, SDS 4%, β-mercaptoetanol 10%, glicerol 24%, azul de bromofenol 0,02%;
Tampão de lise celular para técnica da palitagem: glicerol 5%, SDS 0,5%, EDTA 5 mM, NaOH 50 mM, azul de bromofenol 0,01%;
Tampão para SDS-PAGE: tris-base 25 mM, glicina 192 mM, SDS 0,1%;
Meio LB (Luria-Bertani): 10 g/L bacto-triptona, 5 g/L NaCl, 5 g/L extrato de levedura.
Cepa de bactéria: *E. coli* DH5α – Promega.

4.2 Clonagem clássica

Os métodos de clonagem clássica envolvem enzimas de restrição para inserção de segmentos de DNA em vetores. Estas enzimas clivam ou digerem especificamente regiões dentro da seqüência de DNA, podendo produzir extremidades coesivas. Isso permite a ligação de segmentos de DNA como a inserção de genes em vetores. Para isso, é necessária a digestão tanto do vetor quanto do gene a ser clonado com enzimas que gerem extremidades compatíveis. Os sítios para estas enzimas podem ser inseridos nos genes por PCR, através de iniciadores desenhados para esta finalidade.

4.2.1 Reação em cadeia da polimerase (PCR)

Os oligonucleotídeos foram desenhados com base nas seqüências dos genes humanos disponíveis no NCBI (www.ncbi.nlm.nih.gov) e sintetizados pela companhia *The midland certified Reagent* (Midland, Texas). A enzima de alta processividade, *Taq* DNA Polimerase (InvitrogenTM, NY, USA), foi utilizada nas reações. Para cada reação em cadeia da polimerase foi utilizado: Tampão de PCR 1x; 2,5 mM $MgCl_2$ (somente quando utilizado *Taq* DNA polimerase); 1,25 mM dNTPs; 1 U DNA polimerase; 10 ρmol iniciador "foward", 10 ρmol iniciador "reverse" e 20 ng DNA (exceto para a PCR de colônia e os controles sem DNA molde). Os iniciadores utilizados para amplificar o gene DZIP1 foram: primer "forward" (5´AGATCTATGCAAGCTGAGGCAGCG3´) e "reverse" (5´ GGATCCTTGACATCTGAAGTGTCGC3´) com temperatura de anelamento de 60^{o}C de temperatura. As reações foram incubadas em termociclador (Termociclador Biocycler MyGeneTm – Series Peltier Thermal Cycler, Perkin-Elmer 9700 ou MWG de Biotech) com o seguinte programa: 94 ^{o}C por 2 minutos; 30 ciclos de 94 ^{o}C por 15 segundos; 60 ^{o}C por 30 segundos e 72 ^{o}C por 3 minutos.

4.2.2 Purificação de produto de PCR

O produto de PCR foi purificado com o kit de Purificação de PCR (PROMEGA), segundo instruções do fabricante. Resumidamente, os produtos passam através de coluna com resina, a coluna foi lavada com isopropanol e o produto purificado foi eluido com água ultra pura. A qualidade da purificação foi conferida por eletroforese em gel de agarose e a concentração determinada por espectrofotometria.

4.2.3 Eletroforese de DNA

Os fragmentos de DNA foram separados de acordo com a massa molecular por meio de eletroforese em gel de agarose. A concentração do gel variou de acordo com o tamanho dos fragmentos de DNA analisados. As amostras foram preparadas com adição de tampão de amostra de DNA e submetidas ao gel submerso em tampão TBE e voltagem de 80 V. Após a migração do DNA no gel, o mesmo foi incubado em brometo de etídeo (0,2 mg/L) por 30 minutos e visualizado em sistema de fotodocumentação.

4.2.4 Digestão enzimática

As reações de digestão foram realizadas a partir de 2 a 5 µg de DNA e 10U de endonuclease de restrição, num volume final de 10 a 50 µl. O vetor pEGFP (Figura 4.1) e pGEM-T easy contendo DZIP1 foram abertos por dupla digestão utilizando as enzimas BglII e BamHI, tampão NEB3 e BSA, conforme especificações do fabricante. A reação foi incubada a 37 ^{o}C por duas horas. As digestões de pEGFP e pGEM-T easy contendo DZIP1 foram submetidas a eletroforese em gel de agarose para purificação das bandas correspondentes ao plasmídeo aberto e gene DZIP1. Estas bandas foram preservadas do contato com brometo de etídio e luz UV, utilizando-se como guias para os cortes uma pequena quantidade das mesmas digestões, aplicadas nas canaletas adjacentes do gel. Os géis foram cortados, corando-se apenas as amostras guias, então fez-se a excisão das bandas de interesse com bisturi. O DNA foi separado da agarose através de purificação em ponteiras com filtro, centrifugando-se a 6.000 rpm por 5 min. Por fim, estas amostras foram concentradas por sistema microcon.

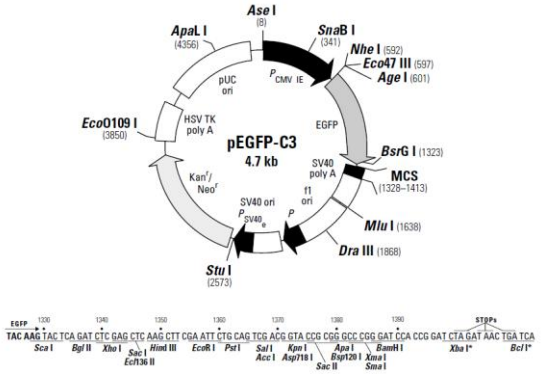

Figura 4.1 Mapa do vetor pEGFP-C3 – (BD Biosciences Clontech).

4.2.5 Reação de Ligação

Após a digestão dos insertos (gene DZIP1) e do plasmídeo pEGFP, procedeu-se a ligação dos mesmos catalisada pela enzima T4 DNA ligase. As reações foram realizadas com 30 ng de vetor, excesso molar de 10 vezes do inserto, 1 U de ligase, tampão para ligase 1 x e H_2O para 10 µl de reação. A incubação foi realizada a 16 ºC em banho seco durante 16 horas.

4.2.6 Preparação de células cálcio-competentes

O método com cloreto de cálcio (SAMBROOK et al, 1989) foi utilizado para a preparação das células cálcio-competentes. A preparação se inicia com a seleção de uma

colônia da cepa DH5α de *E. coli* que foi inoculada em 5 ml de meio LB. A cultura foi incubada por 16 horas a 37 ^{o}C sob agitação constante. Um ml desta cultura foi transferido para 100 ml de meio LB (inóculo de 1:100) pré-aquecido a 37 ºC. As células foram incubadas a 37 ^{o}C sob agitação constante até a fase de crescimento exponencial (densidade óptica 600 = 0,5). A cultura foi então centrifugada a 5000 x *g* por 10 minutos a 4 ^{o}C e o pellet obtido foi suspendido em 50 ml de $CaCl_2$ 100 mM frio e mantido no gelo por 10 minutos. A suspensão foi submetida a uma nova centrifugação de 5.000 x *g* e as células foram suspendidas em 2,0 ml de $CaCl_2$ 50 mM e, posteriormente, 20% de glicerol foi adicionado. Alíquotas foram feitas e armazenadas a -70^{o}C.

4.2.7 Transformação de bactérias pelo método de choque-térmico

O volume de 1-5 µl das reações de ligação foi incubado com 50-200 µl de bactérias competentes por 30 minutos no gelo. Após este tempo, a mistura foi incubada a 42 ^{o}C durante 30 segundos (choque térmico) e colocada novamente no gelo. Em seguida, meio LB foi adicionado ao tubo e as células foram cultivadas a 37 ^{o}C por 1 hora antes da incubação em meio sólido. Volumes de 100 e 200 µl da cultura de bactérias transformadas foram espalhados em placas de Petri contendo meio de cultura seletivo (LB, Agar 15%, e antibiótico). As placas foram incubadas por 18 horas a 37 ^{o}C. Clones contendo plasmídeos recombinantes foram selecionados de acordo com o resultado da técnica de palitagem ou por PCR de colônia.

4.2.8 PCR de colônia

As colônias foram coletadas e suspendidas em 50 µl de água ultra pura, em tubo de 1,5 ml. Da suspensão, cerca de 1 µl foi transferido para tubos de 0,5 ml com a mistura: Tampão de PCR 1x (Invitrogen); 25 mM MgCl2; 1,25 mM dNTPs; 1U Taq polimerase (Invitrogen); 2 ρmol iniciador *foward*, 2 ρmol iniciador *reverse* num volume de 10 µl de reação. As reações foram incubadas no termociclador (Termociclador Biocycler MyGeneTm – Series Peltier Thermal Cycler**,** Perkin-Elmer 9700 ou MWG de Biotech) com o seguinte programa: 94^{o}C por 2 minutos; 30 ciclos de 94^{o}C por 15 segundos; 60 ^{o}C por 30 segundos e 72 ^{o}C por 40 segundos; 72 ^{o}C por 3 minutos. Ao término da reação, as amostras foram submetidas à eletroforese em gel de agarose e visualizadas em trans-iluminador de UVP (Biorad).

4.2.9 Técnica de palitagem (tooth-pick)

As colônias foram coletadas com o auxílio de palitos de dente estéreis e transferidas para o fundo de tubos de 1,5 mL numerados e em seguida para a superfície do meio LB solidificado em placa de petri (placa-mãe) com mapa numérico correspondente ao número dos tubos. Esse procedimento teve como objetivo a obtenção de uma réplica das colônias que foram analisadas. A cada um dos tubos foram acrescentados 10 µl do tampão de lise (5 µl NaOH 10 M, 50 µl Glicerol, 10 µl EDTA 15 M, 50 µl SDS 10 % e 885 µl água ultra pura e azul de bromofenol). Os tubos foram incubados em banho-maria a 65 ºC por 10 min. As amostras foram analisadas por eletroforese em gel de agarose a 1 %, usando o plasmídeo original como controle. Ao fim da eletroforese, o gel foi corado com brometo de etídeo (0,5 µg / ml) por aproximadamente 20 minutos, lavado com água ultrapura e analisado em luz ultravioleta. O gel foi fotografado no sistema de foto-documentação UVP (Biorad).

4.2.10 Mini-Preparação dos plasmídeos com insertos (miniprep)

As colônias selecionadas foram adicionadas em 5 ml de meio LB contendo o antibiótico apropriado e cultivadas por 18 h a 37 ^{o}C sob constante agitação. As células obtidas foram centrifugadas a 12.000 x *g* por 1 minuto e o sedimento obtido foi utilizado para a extração dos plasmídeos através do sistema "QIAprep spin miniprep" (QIAGEN) conforme orientações do fabricante. Após a obtenção dos plasmídeos, fez-se a mensuração da concentração por espectrofotometria.

4.3 Clonagem pelo sistema PGEM®-T Easy (Promega)

O sistema pGEM®-T (Figura 4.2) foi desenhado especificamente para a clonagem de produtos de PCR amplificados com a enzima Taq DNA polimerase (Polimerase de DNA de *Termus aquaticus*), a que adiciona um desoxi-nucleotídeo adenina nas extremidades 5´ do fragmento amplificado. Dessa forma, o nucleotídeo timina presente na extremidade 3´ do vetor interage com a adenina do produto da PCR e possibilita a ligação dos mesmos com a T4 DNA Ligase (Promega).

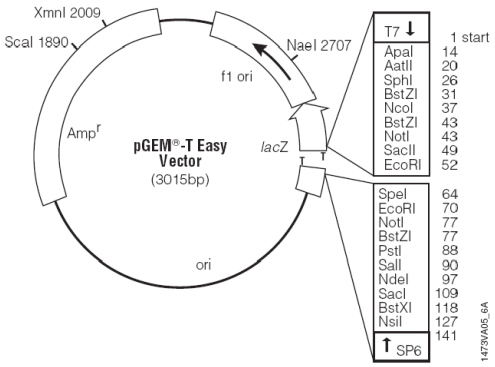

Figura 4.2 - Sítio de múltiplas clonagens do vetor pGEM®-T Easy . O sítio de clonagem se encontra dentro da sequência codificante para a enzima β- galactosidase, que hidrolisa o substrato X-gal (análogo da lactose) e gera um produto precipitado de cor azul nas bactérias. No entanto, quando o fragmento de DNA é inserido no sítio de clonagem, a sequência da enzima é interrompida e não gera o produto final azul. Dessa forma, a identificação dos clones é facilitada pela coloração: brancas são as colônias que contém o vetor com o inserto e as azuis são bactérias com o vetor sem o inserto.

Para a clonagem no sistema p-GEM®-T, os produtos de PCR foram purificados e quantificados. A ligação ao vetor de clonagem pGEM®-T Easy foi dada pela reação da tabela 4.1. A reação foi incubada a 16 ^{o}C por 18 horas. Ao fim da incubação, uma fração dessa reação (1- 5µl) foi utilizada para transformar bactérias competentes. Após esse procedimento, essas células transformadas foram cultivadas em placas contendo LB / ágar com ampicilina, IPTG (isopropil-tio-galactopiranosideo) e X-GAL e mantidas por aproximadamente 18 horas em estufa a 37 ^{o}C. Colônias brancas foram selecionadas e a presença do vetor com o inserto foi conferida por PCR de colônia ou pela técnica de palitagem .

Reação	**Quantidade**
2x Rapid Ligation Buffer (Promega)	10µl
pGEM® -T Easy Vector (50ng/µl)	1µl
Produto de PCR purificado	x µl
T4 DNA Ligase (Promega, 3U/µl)	1µl
Água deionizada	x µl
Volume Total	20µl

Tabela 4.1 Reação de ligação do vetor p-GEM®-T.

4.4 Cultura de células da linhagem HeLa

A linhagem celular HeLa (código ATTC - CCL-2) utilizada para a realização dos experimentos foi cultivada em meio RPMI suplementada com 10% de soro fetal bovino, 100 µg/mL de estreptomicina e 100 U/mL de penicilina (todos da GIBCO). O sub-cultivo celular

foi realizado duas vezes por semana, numa proporção de 1:6. As células foram mantidas em estufa a 37 ºC contendo 5% de CO2 e umidade controlada.

4.4.1 Bloqueio e ativação da via Hedgehog

As células foram incubadas com 300nM de ciclopamina ou 3μM de purmorfamina durante 24 horas. Após esse período, as células foram fixadas com paraformaldeído 4% ou submetidas ao estresse oxidativo.

4.4.2 Estresse oxidativo

Para o estresse oxidativo, a concentração final de 2mM de arsenito de sódio foi adicionado á cultura de células e incubado por 10 minutos em estufa a 37 ºC. As células submetidas ao estresse oxidativo foram lavadas uma vez com PBS 1x a 37 ºC e fixadas com paraformaldeído 4% por 10 minutos. As células foram lavadas três vezes com PBS 1x e submetidas à imunofluorêscencia.

4.4.3 Transfecção de DNA

As células foram semeadas em frascos de 75 cm^2 de área (TPP, Suíça) em 75-80% de confluência. O DNA plasmidial (20 μg) foi diluído em 2 mL de meio Opti-MEM e homogeneizado. Cerca de 80μl de X-tremeGENE HP (Roche) foi adicionado à mistura, homogeneizada e incubada por 20 minutos à temperatura ambiente. Após a incubação a mistura contendo DNA plasmidial, reagente de transfecção (X-tremeGENE HP) e meio são espalhados sobre a monocamada de células aderidas. Após 24 horas, as células são suspensas por ação da enzima tripsina e plaqueadas em lamínulas pra visualização em microscópio de fluorescência ou em frascos de cultura para expansão da cultura transfectada.

4.5 Imunoprecipitação de DZIP1-GFP

Células da linhagem HeLa foram transfectadas com plasmídeo que expressa a proteína verde fluorescente (“Green Fluorescent proteín” – GFP) ou com o plasmídeo que expressa a proteína DZIP1 fusionada a GFP. Após 48 horas, as células foram suspensas com a enzima tripsina, contadas e lavadas com PBS 1x. Cerca de 1 mL de Tampão de lise (Tris-HCl pH 7,4 15mM, $MgCl_2$ 15 mM, NaCl 0,3 M, 0,5% NOTC (N-Octyl), 1 mM DTT, 100 U / ml RNase

Out, PMSF 1mM e E-64 10uM) foi utilizado para lisar 2 x 10^6 células por 2 horas à 4^oC sob agitação. As células lisadas foram centrifugadas a 10000 x g por 20 minutos e o sobrenadante foi incubado com "beads" magnéticas contendo proteína A para a etapa de pré-lavagem por 1 hora a 4 ^oC sob agitação. Os tubos contendo o sobrenadante e "beads magnéticas" foram encaixadas em suporte com ímã por 2 minutos, o sobrenadante foi transferido para outro tubo e incubado com "beads" magnéticas contendo anticorpo anti-GFP (coelho) por 2 horas a 4 ^oC sob agitação. As "beads" magnéticas foram lavadas 5x por 5 minutos sob agitação. As proteínas foram eluídas com 50 µl de glicina 0,2M pH 2,5 por 5 minutos e neutralizadas com 5 µl TrisHCl pH 9,5. As amostras foram realizadas em triplicata técnica e armazenadas à -20 ^oC. A imunoprecipitação de GFP e DZIP1-GFP foram confirmadas por western blot e quantificadas por nanodrop.

4.6 Identificação das proteínas parceiras por espectrometria de massa

Essas proteínas foram digeridas com tripsina e concentradas com o sistema *stage tip*. Os peptídeos foram analisados utilizando um sistema de análise em espectrômetro de massas Orbitrap XL (*Thermo*, San José). Os dados obtidos por espectometria de massa foram analisados por Mascot para comparação e identificação das proteínas em banco de dados, International Protein Índex (IPI).

4.7 Eletroforese de proteína em gel de acrilamida desnaturante (SDS-PAGE)

As proteínas foram desnaturadas com tampão de amostra de proteína 1x por 10 minutos á 94 ^oC e submetidas a eletroforese em gel de poliacrilamida, conforme descrito por (Laemmli, 1970). Após a eletroforese, as proteínas foram coradas por coloração com nitrato de prata.

4.8 Coloração com nitrato de prata

A coloração com nitrato de prata compreende quatro etapas: (1) fixação do gel com uma solução de fixação (etanol 50%; ácido acético glacial 12% e 50 µl de formaldeído 37% em volume final de 100 mL) por 30 minutos; (2) sensibilização do gel com solução de sensibilização (0,02% de tiossulfato de sódio em água) por 2 minutos; (3) coloração das proteínas com solução de prata (0,2% de nitrato de prata, 50 µl de formaldeído 37% em 100 mL de água) por 30 minutos, o gel foi lavado três vezes por 15 minutos em água destilada e

(4) revelado em solução de revelação (3% de carbonato de sódio, 2 mL de solução de sensibilização e 75 µl de formaldeído 37% em 100 mL de água) por tempo suficiente para as bandas aparecerem. A reação foi inativada pela solução de parada (etanol 50%; ácido acético glacial 12%).

4.9 Coleta e isolamento das células-tronco derivadas de tecido adiposo

Este projeto foi realizado no Instituto Carlos Chagas em colaboração com o Núcleo de Tecnologia Celular da PUCPR que foi responsável pela coleta e isolamento das células-tronco. A coleta foi realizada após o esclarecimento dos objetivos do projeto de pesquisa aos doadores e obtenção do termo de consentimento livre e esclarecido dos mesmos (ANEXO 2). Todo o procedimento está de acordo com as normas para pesquisa envolvendo seres humanos e com a aprovação do Comitê de Ética da Fundação Oswaldo Cruz (número de aprovação 419/07, ANEXO 3).

O tecido adiposo foi adquirido de pacientes submetidos à cirurgia bariátrica com dermolipectomia. As células-tronco derivadas de tecido adiposo foram isoladas usando digestão enzimática. Logo após a retirada do tecido adiposo, os fragmentos foram removidos com auxílio de pinça e bisturi, lavados com PBS para remover o excesso de hemácias, mascerados e digeridos com 1 mg/mL de colagenase tipo I (InvitrogenTM, NY, USA) numa proporção de 1 parte de tecido adiposo para 4 partes de colagenase por 30 minutos a 37ºC sob agitação constante. Para eliminar os fragmentos não digeridos, o material foi filtrado duas vezes com filtro de 100 µm de membrana de nylon (BD FALCONTM, BD Biosciences Discovery Labware, Bedford, USA). Em seguida, a suspensão de células foi centrifugada a 800 x g por 10 minutos e descartado o sobrenadante. O tampão hemolítico (NH4CL 155 mmol / L e Tris 20 mmol / L pH 7,3) foi adicionado ao precipitado por 10 minutos para lise das hemácias e centrifugado novamente à 800 x g por 10 minutos. O sedimentado foi suspendido em PBS e filtrado (filtro com poro de 40 µm). As células foram centrifugadas novamente e ressuspendidas em meio DMEM/F12 com 10% SBF e 100 µg/mL de estreptomicina e 100 U/mL de penicilina. As células foram contadas usando câmara de Neubauer e plaqueadas em uma concentração de 1,4 x 10^5 células / cm^2 em frascos de cultura de 75 cm^2. Os frascos foram incubados em estufa umidificada a 37 ^oC com 5% de tensão de CO_2. O meio de cultura foi trocado duas vezes por semana até alcançar a confluência celular. Quando confluentes, as células aderentes foram dissociadas utilizando tripsina - EDTA 0,25 % e novamente plaqueadas numa concentração de 1,3 x 10^4 células por cm^2 (primeira passagem).

As células-tronco isoladas foram previamente caracterizadas imunofenotipicamente por citometria de fluxo (*FACS Calibur, BD Biosciences*). As células foram positivas para CD105, CD90, CD73, CD166, CD29 e CD44; negativas para marcadores de linhagem hematopoética (CD14, CD45 e CD31 e CD34) (Rebelatto et al, 2008). As células foram capazes de diferenciar em três linhagens (condrócito, osteoblasto e adipócito), atendendo os critérios exigidos para serem caracterizadas como células-tronco (Dominici et al, 2006).

4.10 Imunoprecipitação de Ribonucleopartículas associadas com DZIP1

A imunoprecipitação das ribonucleopartículas contendo DZIP1 em células-tronco de tecido adiposo foi realizada com proteína A acopladas a esferas (Sigma Aldrich P3296). A proteína A tem afinidade com a região constante de anticorpos provenientes de coelhos e a proteína G tem afinidade com anticorpos derivados de camundongo, galinha, cabra, cavalo entre outros. Uma parcela de 50 µl da resina de proteína A acoplada a esferas foi adicionada em um tubo de 1,5 ml, em seguida o tubo foi centrifugado a 600 x g por 1 minuto, o sobrenadante foi retirado, adicionou-se 500µl de PBS 1x (*RNAse free*) e 2 µg de anticorpo (como controle foi usado isotipo IgG). Essa mistura foi incubada durante a noite a 4 ^{o}C sob agitação constante. As células ($1x10^6$ a $5x10^6$ células) foram incubadas com 500 µl de tampão de lise (Tris-HCl pH 7,4 15mM, $MgCl_2$ 15 mM, NaCl 0,3 M, 1% Triton X-100, 1 mM DTT, 100 U / ml RNase Out, PMSF 1mM e E64 10uM), em condições livres de RNAses, por 1 hora sob agitação constante. Em seguida, as células foram centrifugadas por 20 minutos a 10000 x g a 4^{o}C. O sobrenadante foi incubado com proteína A por 1 hora a 4^{o}C sob agitação para "pre-cleaning". A mistura contendo anticorpo ligado a proteína A foi bloqueada com 1% leite a 4ºC por 2-3 horas sob agitação. Logo após, Esses complexos foram lavados 3 x com o tampão de lavagem (Tris-HCl pH 7,4 15mM, $MgCl_2$ 15 mM, NaCl 0,3 M, 1% Triton X-100). Por fim, o sobrenadante contendo os complexos celulares que transpôs pelo pré-cleaning foi incubado com anticorpo ligado a proteína A a 4^{o}C por duas horas sob agitação. Em seguida, esses complexos foram lavados três vezes com tampão de lavagem contendo RNase Out (100U/ml) por 5 minutos a 4^{o}C sob agitação. A extração de RNA total foi realizada com o Kit RNeasy (QIAGEN), seguindo instruções do fabricante.

4.11 Identificação dos transcritos alvos do complexo contendo DZIP1 em células-tronco

O RNA total imunoprecipitado foi inicialmente digerido com RNase III. Os fragmentos resultantes foram hibridizados com o mix de adaptadores SOLiD™ para posterior

retrotranscrição. A transcrição reversa foi realizada utilizando o kit *SOLiD™ Total RNA-Seq* (água livre de nuclease, 10x RT Buffer, dNTP Mix, SOLiD™ RT Primer, ArrayScript Reverse Transcriptase) de acordo com as instruções do fabricante. O cDNA resultante foi purificado utilizando o kit *Mini Elute PCR Purification* (Qiagen) e os cDNAs foram submetidos à eletroforese em *Novex® Pre-Cast Gel*. Os cDNAs de tamanho apropriado (150-250 nt) foram excisados do gel e amplificados utilizando o kit *SOLiD™ Total RNA-Seq* (água livre de nuclease, 10x PCR Buffer, dNTP Mix, SOLiD™ 5'PCR Primer, AmpliTaq® DNA Polymerase). Por ser uma biblioteca multiplex também foi utilizado o kit SOLiD™ RNA Barcoding para substituir SOLiD™ 3'PCR Primer. O programa utilizado para amplificação consiste em manter as amostras a 95°C por 5 min, 18 ciclos de amplificação (95°C 30 seg, 62°C 30 seg, 72°C 30 seg) e, finalmente, 72°C a 7 min. O produto da PCR foi purificado de acordo com as instruções do fabricante utilizando *PureLink® Micro Kit Column* (Invitrogen) e quantificados com *Qubit® dsDNA HS Assay Kit*. A concentração final da biblioteca submetida ao sequenciamento foi de 50 pg/µl.

4.12 Microscopia de imunofluorescência (IF)

A imunolocalização das proteínas nas células foi realizada por imunofluorescência indireta. As células foram lavadas três vezes com PBS pH 7,3 por 5 minutos e fixadas com paraformaldeído 4% durante 10 minutos. As células foram lavadas três vezes com PBS 1x durante 5 minutos e permeabilizadas com triton X-100 0,5% diluído em PBS por 10 minutos a temperatura ambiente. As células foram novamente lavadas por três vezes com PBS durante 5 minutos e incubadas com 5% BSA em PBS por 1 horas em temperatura ambiente. Em BSA 1%, os anticorpos foram diluídos 1:50 anti-TIA1 (cabra) e 1:30 anti-DZIP1(coelho) e incubados por 1 hora a 37 ^{o}C. Posteriormente, as células foram lavadas três vezes por 5 minutos com PBS e incubadas com o anticorpo secundário anti-coelho Alexa Fluor 488 (produzido em asno) e anti-cabra Alexa Fluor 546 (produzido em asno) diluído 1:400 por 30 minutos. As células foram lavadas três vezes por 5 minutos e incubadas com DAPI (1 µg/µl) diluído em PBS por 5 minutos, lavadas três vezes em PBS por 5 minutos e montadas com n-propil-galato (200 µg/ml) e seladas com esmalte sobre uma lâmina de microscopia óptica. As lâminas foram observadas no microscópio de fluorescência Nikon Eclipse E600 com objetivas de 40x. Imagens digitais foram capturadas usando-se a câmara CoolSnap (Media Cybernetics).

5. RESULTADOS

Os resultados referentes aos objetivos que não foram contemplados no artigo (Capítulo 3) estão organizados nessa seção.

5.1 Clonagem do gene DZIP1 em vetor de expressão em eucariotos

A introdução do gene DZIP1 de humano em vetor de expressão em eucariotos foi realizada pelo método de clonagem clássica, onde o gene foi amplificado por PCR a partir do clone comercial DZIP1 humano Ultimate™ ORF (IOH27736 - Invitrogen). Os iniciadores utilizados contêm sequências específicas para enzimas de restrição e flanqueiam as extremidades do gene inteiro. O produto da PCR foi incorporado no vetor pGEM-T easy para facilitar a visualização do processo de digestão das extremidades do gene. O plasmídeo peGFP-C3 foi digerido por dupla digestão e certificado que estava aberto por eletroforese de DNA (Figura 5.1 A). O gene DZIP1 no vetor pGEM-T easy foi digerido com as mesmas enzimas, ligado ao peGFP aberto e clonado em bactérias *E. coli* DH5α. Os clones foram analisados pela técnica de palitagem (Figura 5.1 B).

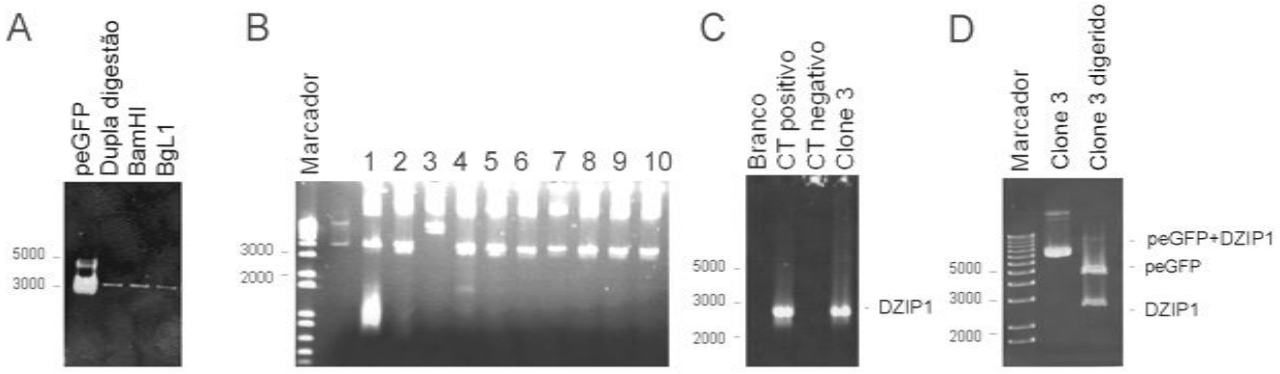

Figura 5.1 Clonagem de DZIP1 em peGFP. Eletroforese em gel de agarose 1% corado com brometo de etídeo para resolver: (A) Digestão do pEGFP com as enzimas BamHI e BgL1; (B) Análise dos clones 1-10 pela técnica de palitagem; (C) PCR de colônia; (D) Digestão do plasmídeo obtido do clone 3. CT- Controle;

O clone 3 foi positivo na técnica de palitagem, ou seja, o plasmídeo peGFP contém o gene DZIP1, dessa forma esse clone foi confirmado por PCR de colônia e digestão enzimática do plasmídeo (Figura 5.1 C-D). O plasmídeo derivado do clone 3 foi seqüenciado e a fase de leitura do gene GFP com DZIP1 está correta (Figura 5.2). A expressão de DZIP1 fusionada a GFP foi avaliada em microscopia de fluorescência e por western blot (Capítulo 3).

Figura 5.2 Verificação da sequência e fase de leitura do gene GFP e DZIP1 do clone 3. Observa-se que o fim da sequência do gene GFP (último códon é AAG) está em fase de leitura com o início do gene DZIP1 (códon de início é ATG). Dados obtidos a partir de software DNASTAR (MapDraw).

5.2 Identificação das proteínas parceiras de DZIP1 em células HeLa

DZIP1 interage com a proteína DAZ (Moore, 2004), além disso, os resultados expostos no artigo (Capítulo 3) indicam que DZIP1 participa de um complexo ribonucleoprotéico. Dessa forma, a identificação das proteínas parceiras de DZIP1 complementam as informações sobre a função dessa proteína. Para isso, imunoprecipitações de DZIP1 fusionada a proteína GFP (pDZIP-GFP) em células HeLa foram realizadas com anticorpo contra GFP. Como controle negativo das imunoprecipitações, células foram transfectadas com o plasmídeo que possui apenas a proteína GFP (pGFP) e todo o processo de imunoprecipitação foi realizado em triplicata técnica sob as mesmas condições (Figura 5.4).

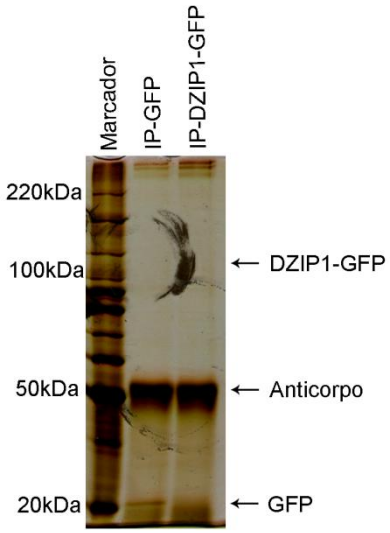

Figura 5.4 Imunoprecipitação de DZIP1-GFP e GFP representativa resolvido em gel SDS-PAGE corado com nitrato de prata. Marcador de massa molecular em kDa (BenchMark™ *Protein Ladder*);

Após as imunoprecipitações, as amostras foram processadas e as proteínas identificadas por espectrometria de massas LTQ-Orbitrap. Na tabela 5.1 estão descritas as proteínas identificadas nesse ensaio preliminar. Observa-se a presença da proteína DZIP1 em todas as triplicatas técnicas e ausência nas amostras controle (GFP). Dessa forma, a proteína de interesse está sendo imunoprecipitada nas condições utilizadas no ensaio. Mesmo sendo um ensaio preliminar, observa-se a presença de proteínas características de complexos ribonucleoprotéicos como proteína de união ao RNA, proteína de transporte e citoesqueleto. Contudo novos testes serão necessários para aperfeiçoar a imunoprecipitação do complexo contendo DZIP1, pois não há reprodutibilidade das proteínas parceiras o que pode estar associada as condições estringentes da lise celular ou lavagens.

		Intensidade					
REFSEQ	**Descrição**	**DZIP_1**	**DZIP_2**	**DZIP_3**	**GFP_4**	**GFP_5**	**GFP_6**
NP_055749	DZIP1 Isoform 2 of Zinc finger protein DZIP1	5881100	2008100	10698000	0	0	0
NP_005338	78 kDa glucose-regulated protein precursor	0	0	7074100	0	0	0
NP_001164040	UPF0428 protein CXorf56 isoform 2	0	0	1365100	0	0	0
NP_001156759	RNA-binding protein EWS isoform 5	0	0	284220	0	0	0
NP_001013865	SAFB-like transcription modulator isoform b	0	0	187020	0	0	0
NP_001188267.1	SAFB cDNA FLJ54744, highly similar to Scaffold attachment factor B	0	0	1669500	0	0	0
NP_777549	Mimitin, mitochondrial	0	0	1003000	0	0	0
NP_116294.1	RBM17 Uncharacterized protein	0	0	1379400	0	0	0
NP_057234	Ankyrin repeat and SOCS box protein 2 isoform 2	0	0	1689500	0	0	0
NP_006378	Calcium homeostasis endoplasmic reticulum protein	0	0	3434300	0	0	0
NP_001073884	U2SURP Isoform 3 of U2 snRNP-associated SURP motif-containing protein	821890	0	0	0	0	0
NP_003676.2	KHSRP cDNA FLJ51330, highly similar to Far upstream element-binding protein 2	1082700	0	0	0	0	0
NP_006799	Protein transport protein Sec61 subunit beta	801260	0	0	0	0	0
NP_036365	Rab3 GTPase-activating protein catalytic subunit isoform 2	27888000	0	0	0	0	0
NP_899195.1	SEC13 Uncharacterized protein	662720	0	0	0	0	0
NP_004003	Dystrophin Dp260-2 isoform	0	330760	0	0	0	0

Tabela 5.1 Proteínas identificadas nas amostras de imunoprecipitações de DZIP1-GFP (1-3) e GFP (4-6) em células HeLa. O experimento foi realizado em triplicata técnica.

5.3 Localização de DZIP1 em células HeLa sob ativação e bloqueio da via Hedgehog.

A localização de DZIP1 em células HeLa é nuclear e granular no citoplasma (ver Capítulo 3). DZIP1 colocaliza com TIA1 (marcador característico de grânulos de estresse). Após o bloqueio da via Hedgehog, o padrão de localização granular de DZIP1 é reduzido (ver Imunofluorescência em imagem confocal no Capítulo 3 Figura 5A-D). Com o propósito de investigar a relação entre os grânulos de estresse, a via Hedgehog e a localização de DZIP1, imunofluorescência indireta foi realizada para avaliar a localização de DZIP1 e TIA1 em células HeLa com a via Hedgehog bloqueada (ciclopamina), ativada (purmorfamina) e nas duas condições sob estresse oxidativo (arsenito de sódio).

As células foram expostas a concentração de 300 nM de bloqueador da via Hedgehog (ciclopamina) durante 24 horas. Após esse período, o estresse oxidativo foi provocado pela adição de 2 mM de arsenito de sódio por 10 minutos. Na figura 5.5 A pode-se verificar que o bloqueio da via Hedgehog não induziu a formação de grânulos de estresse, representado pela proteína TIA1. No entanto, as células sob estresse oxidativo e via Hedgehog bloqueada resultou em formação de grânulos de estresse e mudanças morfológicas significativas (Figura 5.5 B).

As células foram expostas a concentração de 3 μM de ativador da via Hedgehog (purmorfamina) durante 24 horas. Após esse período, estresse oxidativo foi provocado pela adição de 2 mM de arsenito de sódio por 10 minutos. Na figura 5.5 C pode-se verificar que a ativação da via Hedgehog não induziu a formação de grânulos de estresse, representado pela proteína TIA1. As células sob estresse oxidativo e via Hedgehog ativada resultou na formação de grânulos de estresse e sem mudanças morfológicas significativas (Figura 5.5 D). Dessa forma, a via Hedgehog não afetou a formação de grânulos de estresse em células HeLa. No entanto, a alteração morfológica ocasionada pela ciclopamina e o estresse oxidativo não é observada quando a via está ativada com purmorfamina e sob estresse. Isso sugere que a via Hh ativada é capaz de proteger ou recuperar o arranjo citoesqueletal das células sob estresse.

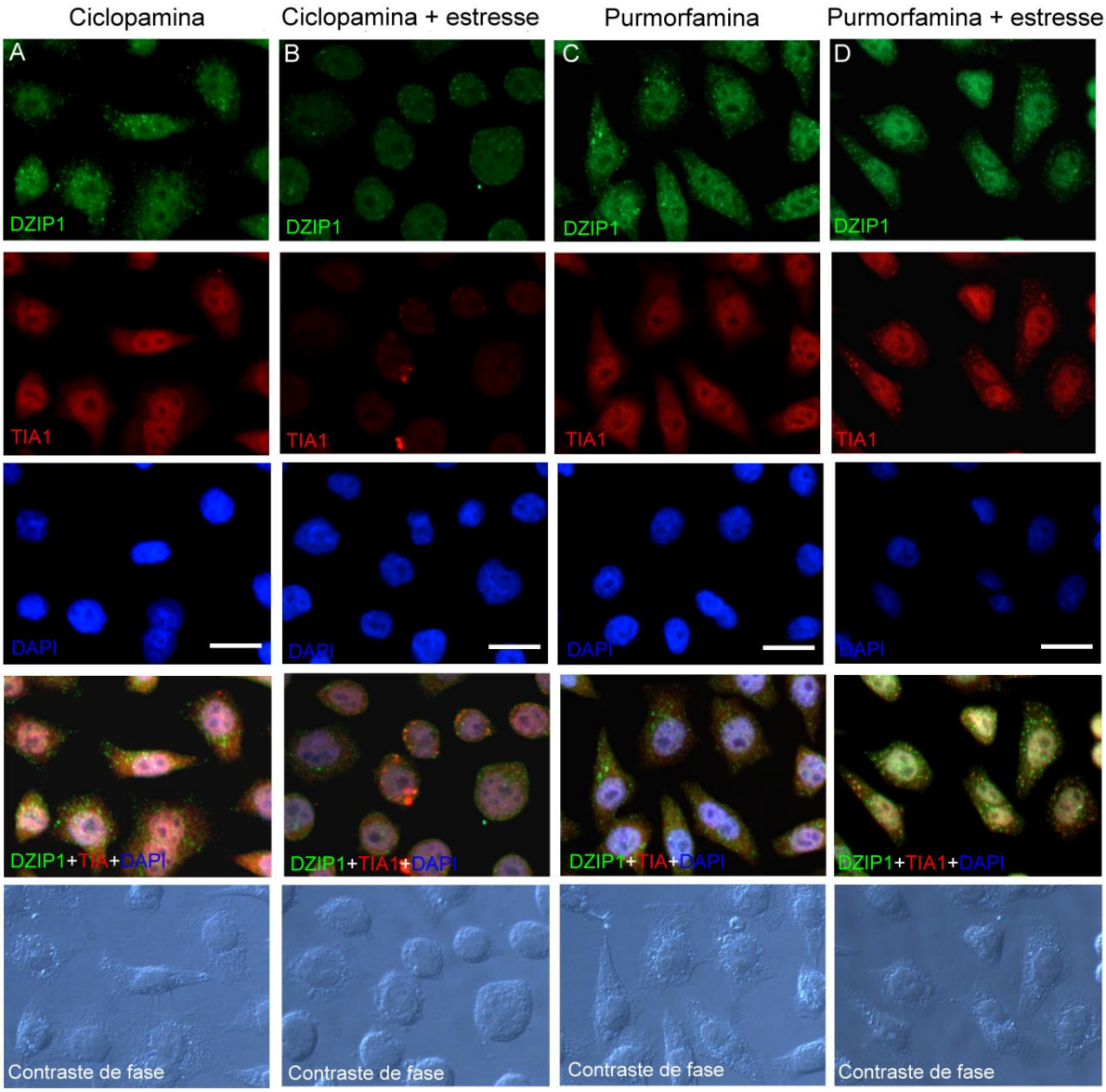

Figura 5.5 Imunolocalização de DZIP1 e TIA1 (marcador de grânulos de estresse) em células HeLa com a via Hedgehog bloqueada (ciclopamina), ativada (purmorfamina) e esses estados sob estresse oxidativo. (A) Tratamento com 300 nM de ciplopamina por 24 horas; (B) Tratamento com 300 nM de ciclopamina por 24 horas e estresse oxidativo induzido com 2 mM de arsenito de sódio por 10 minutos; (C) Tratamento com 3 μM de purmorfamina por 24 horas; (D) Tratamento com 3 μM de purmorfamina por 24 horas e estresse oxidativo induzido com 2 mM de arsenito de sódio por 10 minutos; Barra representa 20 μm.

5.4 DZIP1 em células-tronco derivadas de tecido adiposo

A proteína DZIP1 foi inicialmente identificada em células-tronco germinativas e embrionárias humanas (Moore et al, 2004), no entanto pouco se sabe sobre essa proteína em células-tronco adultas. Dessa forma, decidimos avaliar a localização de DZIP1 em células-

tronco derivadas de tecido adiposo humano sob estresse oxidativo, ativação e bloqueio da via Hedgehog. Dados não publicados do grupo do Laboratório de Biologia Básica de Células-Tronco (ICC-FIOCRUZ) demonstram a presença de grânulos de estresse em células-tronco de tecido adiposo sem qualquer tipo de estresse. Dessa forma, a localização de DZIP1 e TIA1 foi avaliada nessas células em diferentes condições: controle sem estresse, sob estresse oxidativo (Arsenito de sódio 2 mM por 30 minutos), com a via Hedgehog bloqueada (ciclopamina) ou ativada (purmorfamina).

As células-tronco de tecido adiposo apresentam poucos grânulos de estresse (Figura 5.6 A) e mesmo sob estresse oxidativo (2 mM por 30 minutos – condições estringentes) parece não haver aumento considerável (Figura 5.6 B). Nota-se que alguns grânulos de estresse contem a proteína DZIP1 na condição sem e com estresse. O mesmo fenômeno é observado no tratamento com ciclopamina e purmorfamina (Figura 5.7 e 5.8). Dessa forma, a via Hedgehog não parece interferir na formação de grânulos de estresse e DZIP1 continua presente em grânulos de estresse em células-tronco derivadas de tecido adiposo.

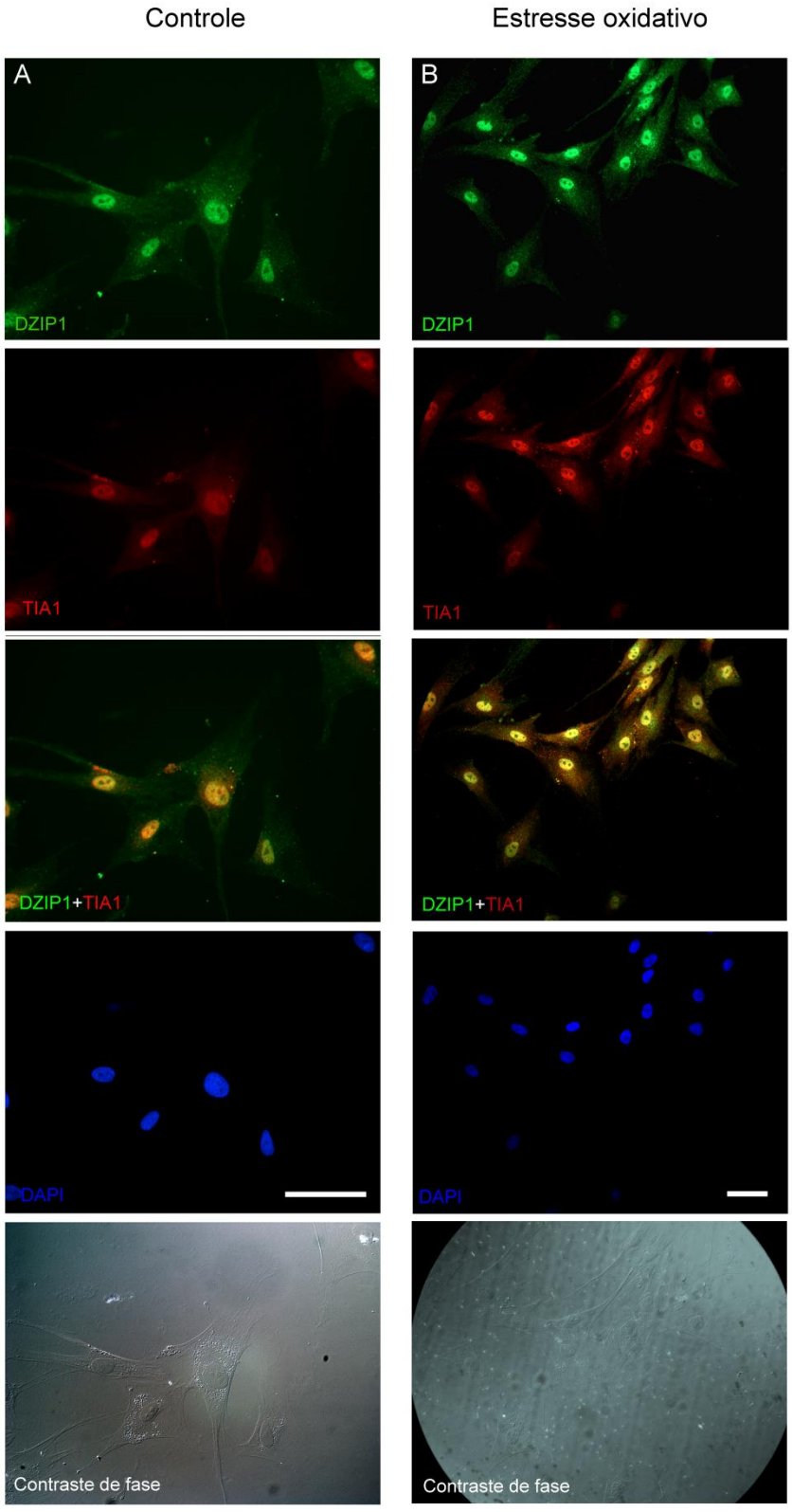

Figura 5.6 Imunolocalização de DZIP1 (diluição 1:30) e TIA1 (diluição 1:50) em células-tronco de tecido adiposo. (A) Células sem tratamento (Controle) e (B) Células sob estresse oxidativo (arsenito de sódio). Barra representa 100 μm.

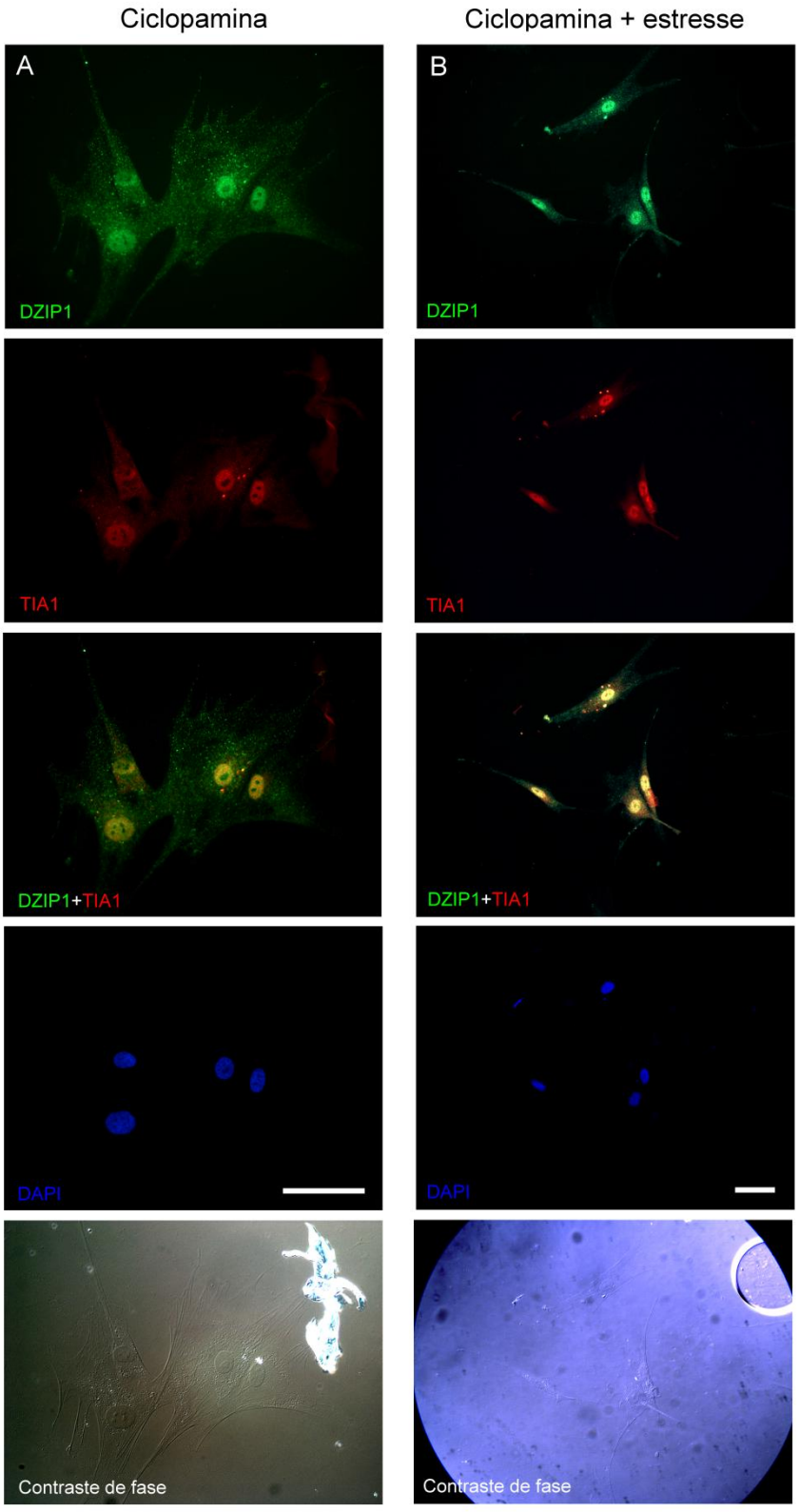

Figura 5.7 Imunolocalização de DZIP1 (diluição 1:30) e TIA1 (diluição 1:50) em células-tronco de tecido adiposo com a via Hedgehog bloqueada com ciclopamina. (A) Células tratadas com ciclopamina por 24 horas; (B) Células tratadas com ciclopamina e sob estresse oxidativo (arsenito de sódio). Barra representa 100 μm.

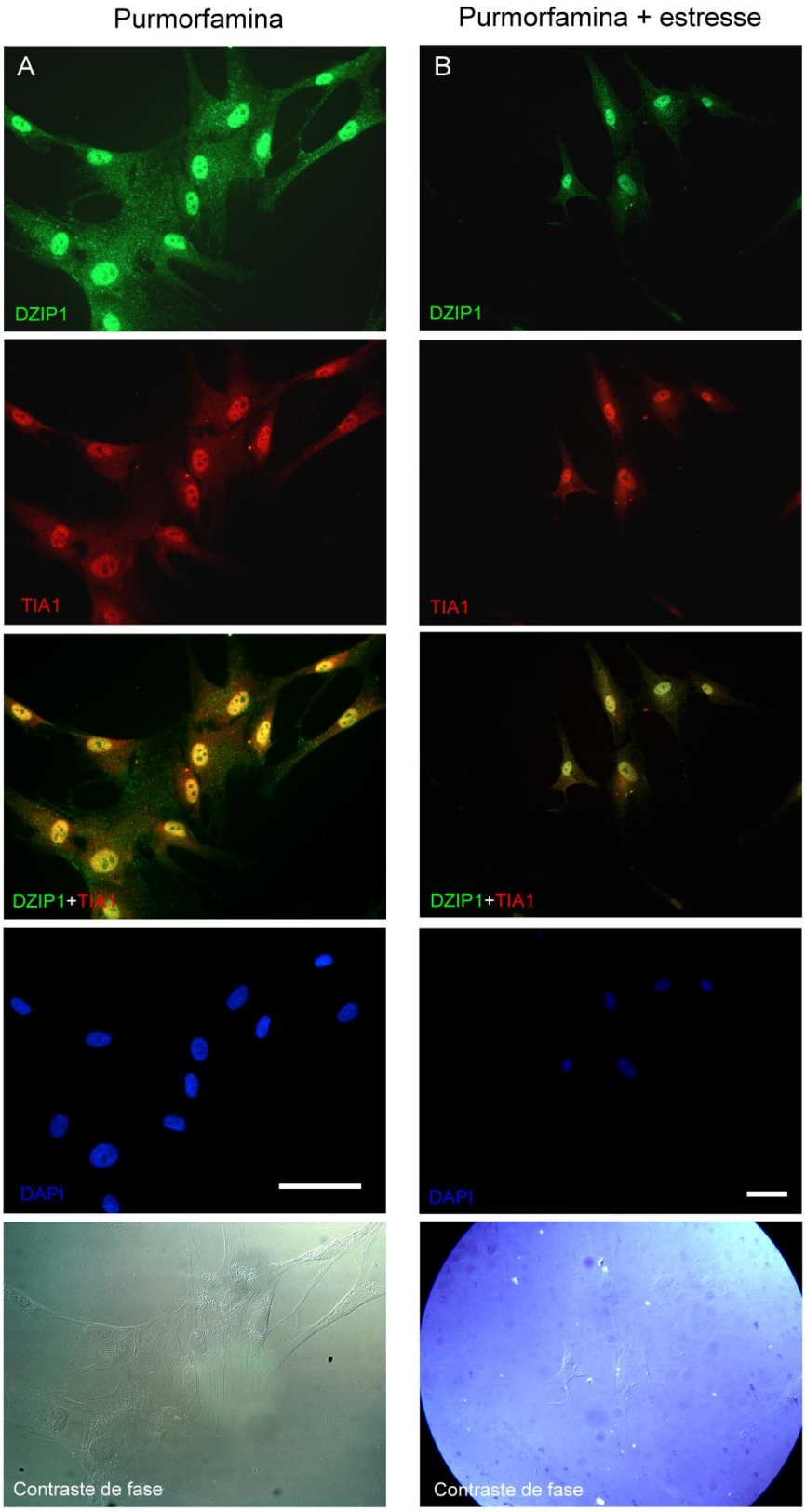

Figura 5.8 Imunolocalização de DZIP1 (diluição 1:30) e TIA1 (diluição 1:50) em células-tronco de tecido adiposo com a via Hedgehog ativada com purmorfamina. (A) Células tratadas com purmorfamina por 24 horas; (B) Células tratadas com purmorfamina e sob estresse oxidativo (arsenito de sódio). Barra representa 100 μm.

6. DISCUSSÃO

Nessa seção segue a discussão dos resultados do capítulo 5 em relação aos obtidos no artigo (Capítulo 3).

6.1 Localização subcelular de DZIP1

Ao longo do desenvolvimento desse trabalho foram realizados diversos experimentos a fim de caracterizar a função da proteína DZIP1. A localização de DZIP1 foi avaliada por duas técnicas diferentes (imunofluorescência indireta e superexpressão utilizando construções com DZIP1 fusionada a proteínas fluorescentes - GFP e YFP) e em diferentes tipos de células humanas: HeLa, HEK293, hTERT-HPE e células-tronco derivadas de tecido adiposo. O padrão de localização granular no citoplasma celular foi uma característica geral. Enquanto que o sinal nuclear não prevaleceu quando utilizadas as construções de fusão. Provavelmente pelo fato do sinal de localização nuclear da proteína DZIP1 estar sendo afetado pelo peptídeo fusionado de aproximadamente 27 kDa.

6.2 DZIP1 e a via de sinalização Hedgehog

A localização de DZIP1 foi avaliada em células com a via de sinalização Hedgehog bloqueada com ciclopamina. Em células HeLa, as imagens de imunofluorescência em microscópio confocal (Figura 4 do artigo) demonstram claramente a ausência de sinal no núcleo e marcação difusa no citoplasma. Embora os níveis de mRNAs de DZIP1 tenham diminuido com o tratamento com ciclopamina, a quantidade em nível protéico não foi averiguado. Apesar disso, o padrão de localização granular de DZIP1 foi afetado com o tratamento com ciclopamina. Esse comportamento não foi tão evidente em células-tronco derivadas de tecido adiposo. As células-tronco apresentam grânulos de estresse (marcação com TIA1) sem qualquer estímulo de estresse prévio. E quando adicionado 2 mM de arsenito de sódio por 30 minutos (condição estringente) para gerar o estresse oxidativo nas células-tronco, a quantidade desses grânulos não aumentam. Em contrapartida, as células HeLa com 0,5 mM de arsenito de sódio apresentam grande quantidade de grânulos de estresse (Lee et al, 2006). Integrantes do grupo do LABCET têm estudado a função de TIA1 em células-tronco adultas e testado anticorpos originados a partir de diferentes epítopos. Dados preliminares apresentam distinções na localização de TIA1 de acordo com o anticorpo em células-tronco.

A avaliação das células HeLa sob bloqueio da via Hedgehog e estresse oxidativo (Figura 5.5) demonstrou alteração morfológica. Enquanto que as células com a via Hedgehog ativa e sob estresse oxidativo não foram afetadas. Isso sugere que essa via de sinalização poderia ter um efeito sobre o citoesqueleto ou citoproteção. Sasaki (2010) demonstrou o envolvimento dessa via de sinalização na regulação do citoesqueleto de actina via cascata Tiam1-Rac1 (Sasaki et al, 2010). DZIP1 poderia estar associado a um complexo dependente do citoesqueleto e talvez a mudança na localização de DZIP1 após o bloqueio da via Hedgehog se deve ao fato da via regular o citoesqueleto.

As proteínas DZIP1 e DZIPL humanas tem sido requeridas para a formação do cílio primário (Glazer et al, 2010). DZIP1 foi encontrada no corpo basal do cílio e o silenciamento afeta a ciliogenesis (Kim et al, 2010). O cílio primário é necessário para a transdução da via de sinalização Hedgehog em vertebrados (Eggenschwiler & Anderson, 2007). Diversos components da via Hedgehog estão localizados no cílio em vertebrados, incluindo as proteínas transmembranas Patched e Smoothened (Corbit et al, 2005) e os fatores transcricionais Gli (Haycraft et al, 2005). Essas observações sugerem que DZIP1 poderia estar envolvida regulando a biogenesis do cílio primário e que sua função na via de sinalização Hedgehog está relacionada a sua localização específica nessa estrutura celular. Nossos resultados demonstram que DZIP1 está presente no corpo basal do cílio primário, mas nós também encontramos DZIP1 presente em todo o citoplasma e no compartimento nuclear. Além disso, metade da quantidade de proteína parece imobilizada em estruturas granulares, sugerindo que esta proteína poderia ser um componente de complexos macromoleculares. Essas observações corrobora com o artigo original de Moore e seus colaboradores (2004) que também observa a presença de DZIP1 no citoplasma de células germinativas e com relatos da translocação de DZIP1 para o núcleo dependendo da fosforilação regulada pela PKA (Wolff et al, 2004). Além disso, a proteína Igu/DZIP1 tem localização citoplasmática com padrão vesicular em células NIH3T3. Essas vesículas são enriquecidas com a proteína lisosomal Lamp1 (Sekimizu et al, 2004). A presença do domínio PEST na sequência da proteína DZIP1 sugere que a proteína poderia ser alvo de degradação rápida que consiste com a localização dessa proteína com lisossomos em culturas de células (Sekimizu et al, 2004).

6.3 Via de sinalização Hedgehog em células-tronco

A via de sinalização Hedgehog (Hh) está relacionada com processos de proliferação celular, diferenciação, angiogênese, remodelamento da matriz celular e homeostase de

células-tronco (Varjosalo & Taipale, 2008). Vários autores descrevem o papel dessa via no processo de diferenciação de células-tronco (Cai et al, 2012; Fontaine et al, 2008; Ghanbari et al, 2013; James et al, 2010; Warzecha et al, 2006; Wu et al, 2013; Wu et al, 2004).

A via de sinalização Hh inibe o potencial de diferenciação osteo/dentinogênico das células-tronco mesenquimais da papila apical (Jiang et al, 2013), a diferenciação para osteoblasto (Plaisant et al, 2009) e a maturação de adipócitos de células-tronco mesenquimais humanas (Fontaine et al, 2008). Todavia, Xu Wu e seus colaboradores (2004) demonstraram que a ativação dessa via de sinalização com purmorfamina induz a osteogênese de células progenitoras mesenquimais pluripotentes (C3H10T1/2). A via de sinalização Hh promove proliferação de células-tronco epiteliais da bexiga (Shin et al, 2011). Por sua vez, a inibição dessa via de sinalização diminui a proliferação e clonogenecidade de células-tronco mesenquimais humanas (Plaisant et al, 2011), além de induzir as células-tronco embrionárias de camundongo à diferenciação em células da endoderme (Ghanbari et al, 2013) e reduzir a diferenciação condrogênica de células-tronco mesenquimais (Wu et al, 2013). Interessantemente, a localização de DZIP1 durante a adipogênese é predominantemente nuclear (Shigunov, 2009). Dessa forma, a localização de DZIP1 pode mudar de compartimento de acordo com o estado celular. E se DZIP1 participa de um complexo ribonucleoprotéico que poderia estar envolvido no transporte de mRNAs, dependendo do estado de diferenciação carregaria conjuntos distintos de mRNAs.

A proteína Sonic Hh promove proliferação e diferenciação condrogênica e osteogênica de células-tronco mesenquimais derivadas de medula óssea in vitro (Cai et al, 2012; Warzecha et al, 2006) e diferenciação de células-tronco embrionárias humanas em subtipos neurais (Wu et al, 2012). Assim como Indian Hh induz condrogênese em células-tronco mesenquimais (Steinert et al, 2012).

Apesar da via de sinalização Hh estar envolvida na autorrenovação e diferenciação de células-tronco, há poucas informações sobre os mecanismos moleculares que envolvem essa via. O melhor entendimento desses mecanismos poderia auxiliar na descoberta de novas terapias para potencializar a formação de osso, cartilagem e adipócitos.

6.4 Função de DZIP1

Muitos aspectos do modelo de “regulon” do RNA (Keene, 2007) são refletidos nos resultados presentes aqui nesse trabalho. A regulação pós-transcricional envolve proteínas multifuncionais, que formam complexos ribonucleoproteicos que são montados de maneira combinatorial. Uma única proteína ou mRNA pode, portanto, estar envolvida em múltiplos “regulons” de RNA. Nossas análises de ribonômica mostram que DZIP1 está associada com

uma vasta subpopulação de mRNAs. A maioria desses transcritos codificam a proteínas envolvidas no controle do ciclo celular e expressão gênica. DZIP1 tem recentemente sido identificada como um supressor de tumor envolvido no controle da proliferação celular (Kikuyama et al, 2012). DZIP1 está também envolvida na regulação da via Hedgehog (Sekimizu et al, 2004), uma via ativa em diferentes tipos de cancers humano (Gupta et al, 2010). Nós demonstramos que o silenciamento de DZIP1 resultou no aumento no número de células durante do crescimento celular, o que poderia ser um reflexo da ausência de repressão dos mRNAs alvos pelo complexo ribonucleoproteíco contendo DZIP1. Interessantemente, vários transcritos envolvidos na resposta da via Hedgehog e na biogênese do cílio primário foram identificados associados ao complexo contendo DZIP1. Vários autores tem sugerido que DZIP1 tem função essencial na regulação da ciliogenesis e como um componente estrutural do cílio primário (Glazer et al, 2010; Kim et al, 2010). Nós demonstramos que o estado ativo da via de sinalização Hedgehog determina os níveis de DZIP1 e distribuição celular. Dessa forma, DZIP1 poderia estar envolvido indiretamente na formação do cílio e na via Hedgehog através do efeito no destino dos transcritos que codificam em vários componentes das duas vias.

Nesse trabalho, demonstramos que a proteína DZIP1 não possui interação com poliribopolimeros. Esse resultado não exclui totalmente a possibilidade da DZIP1 interagir diretamente com mRNAs, mas sugere que o complexo contendo DZIP1 poderia necessitar de proteínas de união ao RNA. A estabilidade e tradutibilidade dos transcritos identificados não foram afetados com a mudança nos níveis de DZIP1. No entanto, DZIP1 está claramente associada aos polissomos. Complexos de ribonucleoproteínas podem também regular a expressão dos mRNAs alvos determinando sua distribuição em locais específicos no citoplasma, potencializando a tradução ou levando para degradação (Martin & Ephrussi, 2009). O padrão de localização granular de DZIP1 foi reduzida com o bloqueio da via Hedgehog. Além disso, DZIP1 foi mobilizado pra grânulos de estresse contendo RNA em resposta ao choque térmico ou estresse oxidativo. Contudo, nossos resultados sugerem que DZIP1 poderia fazer parte de um complexo de transporte envolvido na regulação da distribuição subcelular de uma subpopulação definida de mRNAs.

Nós propomos um modelo em que DZIP1 interage com proteínas de união do RNA, para transportar mRNAs do núcleo, através do citoplasma incluindo polissomos ou complexos de degradação ou estocagem. Em resposta ao estresse celular, DZIP1 poderia transportar mRNAs associados para grânulos de estresse. A diversidade de mRNAs associados com DZIP1 sugere que essa proteína poderia ser um componente de diferentes complexos

ribonucleoprotéicos regulatórios transportando mRNAs para tradução nos polissomos ou maquinaria de degradação ou estocagem.

De acordo com o modelo de “regulon” de RNA, as proteínas e mRNAs contidos nas ribonucleoproteínas são dinâmicos, variam em resposta as mudanças das condições celulares. Por conta disso, seria de interesse determinar a composição de proteínas desses complexos e investigar como a estabilidade, distribuição e tradução dos mRNAs alvos de DZIP1 mudam em resposta ao estresse celular. Resta determinar se DZIP1 é essencial para a formação dos grânulos de estresse e quais proteínas agem como parceiras em cada condição: normal, estresse oxidativo, bloqueio e ativação da via Hedgehog.

7. CONCLUSÕES

Com base nos resultados desse trabalho, podemos concluir que a proteína DZIP1 possui localização subcelular nuclear e citoplasmática e sob estresse celular co-localiza em grânulos de estresse. O bloqueio da via de sinalização Hedgehog com ciclopamina torna a localização de DZIP1 predominantemente citoplasmática e difusa em células HeLa.

O bloqueio da via de sinalização Hedgehog afeta a expressão do mRNA de DZIP1, enquanto aumenta os níveis de expressão dos mRNAs associados ao complexo contendo DZIP1. Dessa forma, DZIP1 responde à via de sinalização Hedgehog.

DZIP1 não possui interação com homoribopolímeros e não afeta o acúmulo e a meia vida dos mRNAs associados ao complexo contendo DZIP1 (BRD8, SNX2, PATCH1 e IFT80).

O silenciamento de DZIP1 não afeta a morfologia, ciclo celular e viabilidade das células HeLa, apesar de proporcionar o aumento do número de células durante curva de crescimento celular.

DZIP1 participa de um complexo ribonucleoprotéico contendo mRNAs envolvidos no ciclo celular, expressão gênica e compromisso celular (degeneração ou dano celular). Essa proteína está presente em complexos dependentes de polissomos e pode estar associado a um complexo protéico envolvido no transporte de mRNAs.

8. PERSPECTIVAS

Os resultados desse trabalho possibilitaram o surgimento de novas perspectivas de investigação da função de DZIP1 e da via de sinalização Hedgehog:

- Avaliar a associação de DZIP1 com microtúbulos (nocodazol) e a técnica de fluorescência *in situ* para avaliar a localização dos mRNAs associados;
- Identificar as proteínas parceiras de DZIP1 e caracterizar o complexo que contém DZIP1;
- Identificar os mRNAs associados ao complexo contendo DZIP1 em células-tronco derivadas de tecido adiposo e quais estão associados aos polissomos (cruzar dados da ribonômica de DZIP1 com a ribonômica polissomal de células-tronco de tecido adiposo (Spangenberg et al, 2013));
- Identificar os mRNAs associados ao complexo contendo DZIP1 em condições de estresse celular;
- Identificar os mRNAs diferencialmente expressos em células-tronco derivadas de tecido adiposo com a via de sinalização bloqueada com ciclopamina e ativada com purmorfamina;

9. REFERÊNCIAS

Alekhina OM, Vassilenko KS (2012) Translation initiation in eukaryotes: versatility of the scanning model. *Biochemistry (Mosc)* **77:** 1465-1477

Alexander RP, Fang G, Rozowsky J, Snyder M, Gerstein MB (2010) Annotating non-coding regions of the genome. *Nat Rev Genet* **11:** 559-571

Alexandre C, Jacinto A, Ingham PW (1996) Transcriptional activation of hedgehog target genes in Drosophila is mediated directly by the cubitus interruptus protein, a member of the GLI family of zinc finger DNA-binding proteins. *Genes Dev* **10:** 2003-2013

Ankö ML, Neugebauer KM (2012) RNA-protein interactions in vivo: global gets specific. *Trends Biochem Sci* **37:** 255-262

Auweter SD, Oberstrass FC, Allain FH (2006) Sequence-specific binding of single-stranded RNA: is there a code for recognition? *Nucleic Acids Res* **34:** 4943-4959

Bai CB, Stephen D, Joyner AL (2004) All mouse ventral spinal cord patterning by hedgehog is Gli dependent and involves an activator function of Gli3. *Dev Cell* **6:** 103-115

Brand M, Heisenberg CP, Warga RM, Pelegri F, Karlstrom RO, Beuchle D, Picker A, Jiang YJ, Furutani-Seiki M, van Eeden FJ, Granato M, Haffter P, Hammerschmidt M, Kane DA, Kelsh RN, Mullins MC, Odenthal J, Nüsslein-Volhard C (1996) Mutations affecting development of the midline and general body shape during zebrafish embryogenesis. *Development* **123:** 129-142

Brennecke J, Stark A, Russell RB, Cohen SM (2005) Principles of microRNA-target recognition. *PLoS Biol* **3:** e85

Cai JQ, Huang YZ, Chen XH, Xie HL, Zhu HM, Tang L, Yang ZM, Huang YC, Deng L (2012) Sonic hedgehog enhances the proliferation and osteogenic differentiation of bone marrow-derived mesenchymal stem cells. *Cell Biol Int* **36:** 349-355

Callaway E (2013) Deal done over HeLa cell line. *Nature* **500:** 132-133

Chen CZ, Lodish HF (2005) MicroRNAs as regulators of mammalian hematopoiesis. *Semin Immunol* **17:** 155-165

Chen JK, Taipale J, Cooper MK, Beachy PA (2002) Inhibition of Hedgehog signaling by direct binding of cyclopamine to Smoothened. *Genes Dev* **16:** 2743-2748

Cléry A, Blatter M, Allain FH (2008) RNA recognition motifs: boring? Not quite. *Curr Opin Struct Biol* **18:** 290-298

Collier B, Gorgoni B, Loveridge C, Cooke HJ, Gray NK (2005) The DAZL family proteins are PABP-binding proteins that regulate translation in germ cells. *EMBO J* **24:** 2656-2666

Corbit KC, Aanstad P, Singla V, Norman AR, Stainier DY, Reiter JF (2005) Vertebrate Smoothened functions at the primary cilium. *Nature* **437:** 1018-1021

De Conti L, Baralle M, Buratti E (2013) Exon and intron definition in pre-mRNA splicing. *Wiley Interdiscip Rev RNA* **4:** 49-60

Djebali S, Davis CA, Merkel A, Dobin A, Lassmann T, Mortazavi A, Tanzer A, Lagarde J, Lin W, Schlesinger F, Xue C, Marinov GK, Khatun J, Williams BA, Zaleski C, Rozowsky J, Röder M, Kokocinski F, Abdelhamid RF, Alioto T, Antoshechkin I, Baer MT, Bar NS, Batut P, Bell K, Bell I, Chakrabortty S, Chen X, Chrast J, Curado J, Derrien T, Drenkow J, Dumais E, Dumais J, Duttagupta R, Falconnet E, Fastuca M, Fejes-Toth K, Ferreira P, Foissac S, Fullwood MJ, Gao H, Gonzalez D, Gordon A, Gunawardena H, Howald C, Jha S, Johnson R, Kapranov P, King B, Kingswood C, Luo OJ, Park E, Persaud K, Preall JB, Ribeca P, Risk B, Robyr D, Sammeth M, Schaffer L, See LH, Shahab A, Skancke J, Suzuki AM, Takahashi H, Tilgner H, Trout D, Walters N, Wang H, Wrobel J, Yu Y, Ruan X, Hayashizaki Y, Harrow J, Gerstein M, Hubbard T, Reymond A,

Antonarakis SE, Hannon G, Giddings MC, Ruan Y, Wold B, Carninci P, Guigó R, Gingeras TR (2012) Landscape of transcription in human cells. *Nature* **489:** 101-108

Dominici M, Le Blanc K, Mueller I, Slaper-Cortenbach I, Marini F, Krause D, Deans R, Keating A, Prockop D, Horwitz E (2006) Minimal criteria for defining multipotent mesenchymal stromal cells. The International Society for Cellular Therapy position statement. *Cytotherapy* **8:** 315-317

Eberhart CG, Maines JZ, Wasserman SA (1996) Meiotic cell cycle requirement for a fly homologue of human Deleted in Azoospermia. *Nature* **381:** 783-785

Eggenschwiler JT, Anderson KV (2007) Cilia and developmental signaling. *Annu Rev Cell Dev Biol* **23:** 345-373

Esau C, Kang X, Peralta E, Hanson E, Marcusson EG, Ravichandran LV, Sun Y, Koo S, Perera RJ, Jain R, Dean NM, Freier SM, Bennett CF, Lollo B, Griffey R (2004) MicroRNA-143 regulates adipocyte differentiation. *J Biol Chem* **279:** 52361-52365

Filipowicz W, Bhattacharyya SN, Sonenberg N (2008) Mechanisms of post-transcriptional regulation by microRNAs: are the answers in sight? *Nat Rev Genet* **9:** 102-114

Fontaine C, Cousin W, Plaisant M, Dani C, Peraldi P (2008) Hedgehog signaling alters adipocyte maturation of human mesenchymal stem cells. *Stem Cells* **26:** 1037-1046

Frank-Kamenetsky M, Zhang XM, Bottega S, Guicherit O, Wichterle H, Dudek H, Bumcrot D, Wang FY, Jones S, Shulok J, Rubin LL, Porter JA (2002) Small-molecule modulators of Hedgehog signaling: identification and characterization of Smoothened agonists and antagonists. *J Biol* **1:** 10

Frazer KA (2012) Decoding the human genome. *Genome Res* **22:** 1599-1601

Ghanbari A, Khazaei M, Hashemi-Tabar M, Rabzia A, Fathi F, Bayat PD (2013) Sonic hedgehog inhibition induces mouse embryonic stem cells to differentiate toward definitive endoderm. *Indian J Exp Biol* **51:** 201-207

Gimble JM, Katz AJ, Bunnell BA (2007) Adipose-derived stem cells for regenerative medicine. *Circ Res* **100:** 1249-1260

Glazer AM, Wilkinson AW, Backer CB, Lapan SW, Gutzman JH, Cheeseman IM, Reddien PW (2010) The Zn finger protein Iguana impacts Hedgehog signaling by promoting ciliogenesis. *Dev Biol* **337:** 148-156

Glisovic T, Bachorik JL, Yong J, Dreyfuss G (2008) RNA-binding proteins and post-transcriptional gene regulation. *FEBS Lett* **582:** 1977-1986

Goodrich LV, Scott MP (1998) Hedgehog and patched in neural development and disease. *Neuron* **21:** 1243-1257

Gupta S, Takebe N, Lorusso P (2010) Targeting the Hedgehog pathway in cancer. *Ther Adv Med Oncol* **2:** 237-250

Hall TM (2005) Multiple modes of RNA recognition by zinc finger proteins. *Curr Opin Struct Biol* **15:** 367-373

Hashimoto Y, Maegawa S, Nagai T, Yamaha E, Suzuki H, Yasuda K, Inoue K (2004) Localized maternal factors are required for zebrafish germ cell formation. *Dev Biol* **268:** 152-161

Haston KM, Tung JY, Reijo Pera RA (2009) Dazl functions in maintenance of pluripotency and genetic and epigenetic programs of differentiation in mouse primordial germ cells in vivo and in vitro. *PLoS One* **4:** e5654

Haycraft CJ, Banizs B, Aydin-Son Y, Zhang Q, Michaud EJ, Yoder BK (2005) Gli2 and Gli3 localize to cilia and require the intraflagellar transport protein polaris for processing and function. *PLoS Genet* **1:** e53

Holetz FB, Correa A, Avila AR, Nakamura CV, Krieger MA, Goldenberg S (2007) Evidence of P-body-like structures in Trypanosoma cruzi. *Biochem Biophys Res Commun* **356:** 1062-1067

Houston DW, King ML (2000) A critical role for Xdazl, a germ plasm-localized RNA, in the differentiation of primordial germ cells in Xenopus. *Development* **127:** 447-456

Ingham PW, McMahon AP (2001) Hedgehog signaling in animal development: paradigms and principles. *Genes Dev* **15:** 3059-3087

Ivanova NB, Dimos JT, Schaniel C, Hackney JA, Moore KA, Lemischka IR (2002) A stem cell molecular signature. *Science* **298:** 601-604

James AW, Leucht P, Levi B, Carre AL, Xu Y, Helms JA, Longaker MT (2010) Sonic Hedgehog influences the balance of osteogenesis and adipogenesis in mouse adipose-derived stromal cells. *Tissue Eng Part A* **16:** 2605-2616

Janga SC (2012) From specific to global analysis of posttranscriptional regulation in eukaryotes: posttranscriptional regulatory networks. *Brief Funct Genomics* **11:** 505-521

Jansen RP, Niessing D (2012) Assembly of mRNA-protein complexes for directional mRNA transport in eukaryotes--an overview. *Curr Protein Pept Sci* **13:** 284-293

Jiang Q, Du J, Yin X, Shan Z, Ma Y, Ma P, Fan Z (2013) Shh signaling, negatively regulated by BMP signaling, inhibits the osteo/dentinogenic differentiation potentials of mesenchymal stem cells from apical papilla. *Mol Cell Biochem*

Jin Z, Mei W, Strack S, Jia J, Yang J (2011) The antagonistic action of B56-containing protein phosphatase 2As and casein kinase 2 controls the phosphorylation and Gli turnover function of Daz interacting protein 1. *J Biol Chem* **286:** 36171-36179

Jones KB, Salah Z, Del Mare S, Galasso M, Gaudio E, Nuovo GJ, Lovat F, LeBlanc K, Palatini J, Randall RL, Volinia S, Stein GS, Croce CM, Lian JB, Aqeilan RI (2012) miRNA signatures associate with pathogenesis and progression of osteosarcoma. *Cancer Res* **72:** 1865-1877

Karashima T, Sugimoto A, Yamamoto M (2000) Caenorhabditis elegans homologue of the human azoospermia factor DAZ is required for oogenesis but not for spermatogenesis. *Development* **127:** 1069-1079

Keene JD (2001) Ribonucleoprotein infrastructure regulating the flow of genetic information between the genome and the proteome. *Proc Natl Acad Sci U S A* **98:** 7018-7024

Keene JD (2007) RNA regulons: coordination of post-transcriptional events. *Nat Rev Genet* **8:** 533-543

Keene JD (2010) The global dynamics of RNA stability orchestrates responses to cellular activation. *BMC Biol* **8:** 95

Kikuyama M, Takeshima H, Kinoshita T, Okochi-Takada E, Wakabayashi M, Akashi-Tanaka S, Ogawa T, Seto Y, Ushijima T (2012) Development of a novel approach, the epigenome-based outlier approach, to identify tumor-suppressor genes silenced by aberrant DNA methylation. *Cancer Lett* **322:** 204-212

Kim B, Cooke HJ, Rhee K (2012) DAZL is essential for stress granule formation implicated in germ cell survival upon heat stress. *Development* **139:** 568-578

Kim HR, Richardson J, van Eeden F, Ingham PW (2010) Gli2a protein localization reveals a role for Iguana/DZIP1 in primary ciliogenesis and a dependence of Hedgehog signal transduction on primary cilia in the zebrafish. *BMC Biol* **8:** 65

Kim VN (2005) MicroRNA biogenesis: coordinated cropping and dicing. *Nat Rev Mol Cell Biol* **6:** 376-385

Kishore S, Luber S, Zavolan M (2010) Deciphering the role of RNA-binding proteins in the post-transcriptional control of gene expression. *Brief Funct Genomics* **9:** 391-404

Kozomara A, Griffiths-Jones S (2011) miRBase: integrating microRNA annotation and deep-sequencing data. *Nucleic Acids Res* **39:** D152-157

Laemmli UK (1970) Cleavage of structural proteins during the assembly of the head of bacteriophage T4. *Nature* **227:** 680-685

Lee KH, Lee S, Kim B, Chang S, Kim SW, Paick JS, Rhee K (2006) Dazl can bind to dynein motor complex and may play a role in transport of specific mRNAs. *EMBO J* **25:** 4263-4270

Mackereth CD, Sattler M (2012) Dynamics in multi-domain protein recognition of RNA. *Curr Opin Struct Biol* **22:** 287-296

Maegawa S, Yamashita M, Yasuda K, Inoue K (2002) Zebrafish DAZ-like protein controls translation via the sequence 'GUUC'. *Genes Cells* **7:** 971-984

Martin KC, Ephrussi A (2009) mRNA localization: gene expression in the spatial dimension. *Cell* **136:** 719-730

Matoulkova E, Michalova E, Vojtesek B, Hrstka R (2012) The role of the 3' untranslated region in post-transcriptional regulation of protein expression in mammalian cells. *RNA Biol* **9:** 563-576

Mazumder B, Seshadri V, Fox PL (2003) Translational control by the 3'-UTR: the ends specify the means. *Trends Biochem Sci* **28:** 91-98

Moore F, Jaruzelska J, Dorfman D, Reijo-Pera R (2004) Identification of a novel gene, DZIP (DAZ-interacting protein), that encodes a protein that interacts with DAZ (deleted in azoospermia) and is expressed in embryonic stem cells and germ cells. *Genomics* **83:** 834-843

Moore FL, Jaruzelska J, Fox MS, Urano J, Firpo MT, Turek PJ, Dorfman DM, Pera RA (2003) Human Pumilio-2 is expressed in embryonic stem cells and germ cells and interacts with DAZ (Deleted in AZoospermia) and DAZ-like proteins. *Proc Natl Acad Sci U S A* **100:** 538-543

Moore MJ (2005) From birth to death: the complex lives of eukaryotic mRNAs. *Science* **309:** 1514-1518

Müller-McNicoll M, Neugebauer KM (2013) How cells get the message: dynamic assembly and function of mRNA-protein complexes. *Nat Rev Genet* **14:** 275-287

Odenthal J, van Eeden FJ, Haffter P, Ingham PW, Nüsslein-Volhard C (2000) Two distinct cell populations in the floor plate of the zebrafish are induced by different pathways. *Dev Biol* **219:** 350-363

Pichon X, Wilson LA, Stoneley M, Bastide A, King HA, Somers J, Willis AE (2012) RNA binding protein/RNA element interactions and the control of translation. *Curr Protein Pept Sci* **13:** 294-304

Pittenger MF, Mackay AM, Beck SC, Jaiswal RK, Douglas R, Mosca JD, Moorman MA, Simonetti DW, Craig S, Marshak DR (1999) Multilineage potential of adult human mesenchymal stem cells. *Science* **284:** 143-147

Plaisant M, Fontaine C, Cousin W, Rochet N, Dani C, Peraldi P (2009) Activation of hedgehog signaling inhibits osteoblast differentiation of human mesenchymal stem cells. *Stem Cells* **27:** 703-713

Plaisant M, Giorgetti-Peraldi S, Gabrielson M, Loubat A, Dani C, Peraldi P (2011) Inhibition of hedgehog signaling decreases proliferation and clonogenicity of human mesenchymal stem cells. *PLoS One* **6:** e16798

Radhakrishna U, Wild A, Grzeschik KH, Antonarakis SE (1997) Mutation in GLI3 in postaxial polydactyly type A. *Nat Genet* **17:** 269-271

Raghavan A, Ogilvie RL, Reilly C, Abelson ML, Raghavan S, Vasdewani J, Krathwohl M, Bohjanen PR (2002) Genome-wide analysis of mRNA decay in resting and activated primary human T lymphocytes. *Nucleic Acids Res* **30:** 5529-5538

Rebelatto CK, Aguiar AM, Moretão MP, Senegaglia AC, Hansen P, Barchiki F, Oliveira J, Martins J, Kuligovski C, Mansur F, Christofis A, Amaral VF, Brofman PS, Goldenberg S, Nakao LS, Correa A (2008) Dissimilar differentiation of mesenchymal stem cells from bone marrow, umbilical cord blood, and adipose tissue. *Exp Biol Med (Maywood)* **233:** 901-913

Reijo R, Lee TY, Salo P, Alagappan R, Brown LG, Rosenberg M, Rozen S, Jaffe T, Straus D, Hovatta O (1995a) Diverse spermatogenic defects in humans caused by Y chromosome deletions encompassing a novel RNA-binding protein gene. *Nat Genet* **10:** 383-393

Reijo R, Lee TY, Salo P, Alagappan R, Brown LG, Rosenberg M, Rozen S, Jaffe T, Straus D, Hovatta O (1995b) Diverse spermatogenic defects in humans caused by Y chromosome deletions encompassing a novel RNA-binding protein gene. *Nat Genet* **10:** 383-393

Reynolds N, Collier B, Bingham V, Gray NK, Cooke HJ (2007) Translation of the synaptonemal complex component Sycp3 is enhanced in vivo by the germ cell specific regulator Dazl. *RNA* **13:** 974-981

Reynolds N, Collier B, Maratou K, Bingham V, Speed RM, Taggart M, Semple CA, Gray NK, Cooke HJ (2005a) Dazl binds in vivo to specific transcripts and can regulate the pre-meiotic translation of Mvh in germ cells. *Hum Mol Genet* **14:** 3899-3909

Reynolds N, Collier B, Maratou K, Bingham V, Speed RM, Taggart M, Semple CA, Gray NK, Cooke HJ (2005b) Dazl binds in vivo to specific transcripts and can regulate the pre-meiotic translation of Mvh in germ cells. *Hum Mol Genet* **14:** 3899-3909

Reynolds N, Cooke HJ (2005) Role of the DAZ genes in male fertility. *Reprod Biomed Online* **10:** 72-80

Ruggiu M, Speed R, Taggart M, McKay SJ, Kilanowski F, Saunders P, Dorin J, Cooke HJ (1997) The mouse Dazla gene encodes a cytoplasmic protein essential for gametogenesis. *Nature* **389:** 73-77

SAMBROOK J, FRITSHC EF, MANIATIS T. (1989) Molecular Cloning: A laboratory manual. Cold Spring Harbor, NY, USA.

Sasaki H, Nishizaki Y, Hui C, Nakafuku M, Kondoh H (1999) Regulation of Gli2 and Gli3 activities by an amino-terminal repression domain: implication of Gli2 and Gli3 as primary mediators of Shh signaling. *Development* **126:** 3915-3924

Sasaki N, Kurisu J, Kengaku M (2010) Sonic hedgehog signaling regulates actin cytoskeleton via Tiam1-Rac1 cascade during spine formation. *Mol Cell Neurosci* **45:** 335-344

Satir P, Pedersen LB, Christensen ST (2010) The primary cilium at a glance. *J Cell Sci* **123:** 499-503

Saxena R, Brown LG, Hawkins T, Alagappan RK, Skaletsky H, Reeve MP, Reijo R, Rozen S, Dinulos MB, Disteche CM, Page DC (1996) The DAZ gene cluster on the human Y chromosome arose from an autosomal gene that was transposed, repeatedly amplified and pruned. *Nat Genet* **14:** 292-299

Saxena R, de Vries JW, Repping S, Alagappan RK, Skaletsky H, Brown LG, Ma P, Chen E, Hoovers JM, Page DC (2000) Four DAZ genes in two clusters found in the AZFc region of the human Y chromosome. *Genomics* **67:** 256-267

Schwarz DS, Hutvágner G, Du T, Xu Z, Aronin N, Zamore PD (2003) Asymmetry in the assembly of the RNAi enzyme complex. *Cell* **115:** 199-208

Sekimizu K, Nishioka N, Sasaki H, Takeda H, Karlstrom RO, Kawakami A (2004) The zebrafish iguana locus encodes Dzip1, a novel zinc-finger protein required for proper regulation of Hedgehog signaling. *Development* **131:** 2521-2532

Sharova LV, Sharov AA, Nedorezov T, Piao Y, Shaik N, Ko MS (2009) Database for mRNA half-life of 19 977 genes obtained by DNA microarray analysis of pluripotent and differentiating mouse embryonic stem cells. *DNA Res* **16:** 45-58

Shigunov P. (2009) Caracterização da expressão de DZIP1 e PUM2 em células-tronco mesenquimais humanas durante o processo de diferenciação celular. Dissertação de Mestrado - Instituto Oswaldo Cruz, Biologia Celular e Molecular.

Shigunov P, Sotelo-Silveira J, Kuligovski C, de Aguiar AM, Rebelatto CK, Moutinho JA, Brofman PS, Krieger MA, Goldenberg S, Munroe D, Correa A, Dallagiovanna B (2012) PUMILIO-2 is involved in the positive regulation of cellular proliferation in human adipose-derived stem cells. *Stem Cells Dev* **21:** 217-227

Shin K, Lee J, Guo N, Kim J, Lim A, Qu L, Mysorekar IU, Beachy PA (2011) Hedgehog/Wnt feedback supports regenerative proliferation of epithelial stem cells in bladder. *Nature* **472:** 110-114

Smith RW, Anderson RC, Smith JW, Brook M, Richardson WA, Gray NK (2011) DAZAP1, an RNA-binding protein required for development and spermatogenesis, can regulate mRNA translation. *RNA* **17:** 1282-1295

Spangenberg L, Shigunov P, Abud AP, Cofré AR, Stimamiglio MA, Kuligovski C, Zych J, Schittini AV, Costa AD, Rebelatto CK, Brofman PR, Goldenberg S, Correa A, Naya H, Dallagiovanna B (2013) Polysome profiling

shows extensive posttranscriptional regulation during human adipocyte stem cell differentiation into adipocytes. *Stem Cell Res* **11:** 902-912

Sprague BL, Pego RL, Stavreva DA, McNally JG (2004) Analysis of binding reactions by fluorescence recovery after photobleaching. *Biophys J* **86:** 3473-3495

Stefl R, Skrisovska L, Allain FH (2005) RNA sequence- and shape-dependent recognition by proteins in the ribonucleoprotein particle. *EMBO Rep* **6:** 33-38

Steinert AF, Weissenberger M, Kunz M, Gilbert F, Ghivizzani SC, Göbel S, Jakob F, Nöth U, Rudert M (2012) Indian hedgehog gene transfer is a chondrogenic inducer of human mesenchymal stem cells. *Arthritis Res Ther* **14:** R168

Stone DM, Hynes M, Armanini M, Swanson TA, Gu Q, Johnson RL, Scott MP, Pennica D, Goddard A, Phillips H, Noll M, Hooper JE, de Sauvage F, Rosenthal A (1996) The tumour-suppressor gene patched encodes a candidate receptor for Sonic hedgehog. *Nature* **384:** 129-134

Strachan T. (1999) Human Molecular Genetics, 2nd edition. In Read AP (ed.). New York: Wiley-Liss.

Taipale J, Beachy PA (2001) The Hedgehog and Wnt signalling pathways in cancer. *Nature* **411:** 349-354

Takeda Y, Mishima Y, Fujiwara T, Sakamoto H, Inoue K (2009) DAZL relieves miRNA-mediated repression of germline mRNAs by controlling poly(A) tail length in zebrafish. *PLoS One* **4:** e7513

Tay SY, Yu X, Wong KN, Panse P, Ng CP, Roy S (2010) The iguana/DZIP1 protein is a novel component of the ciliogenic pathway essential for axonemal biogenesis. *Dev Dyn* **239:** 527-534

Unwin RD, Whetton AD (2006) Systematic proteome and transcriptome analysis of stem cell populations. *Cell Cycle* **5:** 1587-1591

Valencia-Sanchez MA, Liu J, Hannon GJ, Parker R (2006) Control of translation and mRNA degradation by miRNAs and siRNAs. *Genes Dev* **20:** 515-524

Vangompel MJ, Xu EY (2011) The roles of the DAZ family in spermatogenesis: More than just translation? *Spermatogenesis* **1:** 36-46

Vannini A, Cramer P (2012) Conservation between the RNA polymerase I, II, and III transcription initiation machineries. *Mol Cell* **45:** 439-446

Varjosalo M, Taipale J (2008) Hedgehog: functions and mechanisms. *Genes Dev* **22:** 2454-2472

Vasudevan S, Seli E, Steitz JA (2006) Metazoan oocyte and early embryo development program: a progression through translation regulatory cascades. *Genes Dev* **20:** 138-146

Vorobjev IA, Chentsov YuS (1982) Centrioles in the cell cycle. I. Epithelial cells. *J Cell Biol* **93:** 938-949

Wahl MC, Will CL, Lührmann R (2009) The spliceosome: design principles of a dynamic RNP machine. *Cell* **136:** 701-718

Wallis D, Muenke M (2000) Mutations in holoprosencephaly. *Hum Mutat* **16:** 99-108

Warzecha J, Göttig S, Brüning C, Lindhorst E, Arabmothlagh M, Kurth A (2006) Sonic hedgehog protein promotes proliferation and chondrogenic differentiation of bone marrow-derived mesenchymal stem cells in vitro. *J Orthop Sci* **11:** 491-496

Wilson CW, Stainier DY (2010) Vertebrate Hedgehog signaling: cilia rule. *BMC Biol* **8:** 102

Wolff C, Roy S, Lewis KE, Schauerte H, Joerg-Rauch G, Kirn A, Weiler C, Geisler R, Haffter P, Ingham PW (2004) iguana encodes a novel zinc-finger protein with coiled-coil domains essential for Hedgehog signal transduction in the zebrafish embryo. *Genes Dev* **18:** 1565-1576

Wu SM, Tan KS, Chen H, Beh TT, Yeo HC, Ng SK, Wei S, Lee DY, Choo AB, Chan KK (2012) Enhanced production of neuroprogenitors, dopaminergic neurons, and identification of target genes by overexpression of sonic hedgehog in human embryonic stem cells. *Stem Cells Dev* **21:** 729-741

Wu X, Brewer G (2012) The regulation of mRNA stability in mammalian cells: 2.0. *Gene* **500:** 10-21

Wu X, Cai ZD, Lou LM, Chen ZR (2013) The effects of inhibiting hedgehog signaling pathways by using specific antagonist cyclopamine on the chondrogenic differentiation of mesenchymal stem cells. *Int J Mol Sci* **14:** 5966-5977

Wu X, Walker J, Zhang J, Ding S, Schultz PG (2004) Purmorphamine induces osteogenesis by activation of the hedgehog signaling pathway. *Chem Biol* **11:** 1229-1238

Yen PH (2004) Putative biological functions of the DAZ family. *Int J Androl* **27:** 125-129

ANEXOS

ANEXO 1

Supplementary Table S2. mRNA Targets of DZIP1. Ratios of Signal Intensity Were Calculated and Genes that Have Fold Change (IP-DZIP1/ IP-Control) Greater or Equal to 2.0 Were Listed

Gene Title	Gene Symbol	p-value	F(Attribute)	Enrichment (IP-DZIP1 vs. IP-control)
sorting nexin 2	SNX2	4,37E-07	287,272	82,0033
hect domain and RLD 2 pseudogene 2 /// hect domain and RLD 2 pseudogene 3 /// he	HERC2P2 /// HERC2P3 /// LOC440248	1,83E-07	351,022	45,4814
sorting nexin 2	SNX2	5,62E-06	125,296	38,9661
GRIP1 associated protein 1	GRIPAP1	6,17E-08	507,83	35,2246
RNA polymerase II associated protein 2	RPAP2	5,59E-06	132,99	24,8419
leucine-rich PPR-motif containing	LRPPRC	3,02E-07	288,968	23,6286
O-linked N-acetylglucosamine (GlcNAc) transferase (UDP-N-acetylglucosamine:polyp	OGT	2,39E-06	138,821	21,1616
hypothetical protein LOC339047	LOC339047	6,51E-06	72,3266	20,4108
bromodomain containing 8	BRD8	5,24E-05	59,7122	20,396
laminin, alpha 1	LAMA1	3,75E-07	732,77	20,003
exportin 4	XPO4	2,04E-07	338,937	19,407
ATP-binding cassette, sub-family C (CFTR/MRP), member 5	ABCC5	2,64E-08	659,201	18,9958
ataxia telangiectasia and Rad3 related	ATR	2,33E-05	87,6285	18,9586
RNA binding motif protein 5	RBM5	9,50E-07	214,814	18,891
nuclear pore complex interacting protein	NPIP	3,68E-07	189,51	18,6933
golgi autoantigen, golgin subfamily a, 8A	GOLGA8A	4,51E-05	56,1537	16,2527
similar to Uncharacterized protein KIAA0220 /// nuclear pore complex interacting	LOC100132247 /// LOC613037 /// NPIPL3	1,83E-06	166,031	16,1356
Tax1 (human T-cell leukemia virus type I) binding protein 1	TAX1BP1	0,00010145	33,8561	15,9432
BTAF1 RNA polymerase II, B-TFIID transcription factor-associated, 170kDa (Mot1 h	BTAF1	7,63E-05	45,2751	15,5073
hypothetical protein LOC339047	LOC339047	2,46E-05	47,878	15,1338
Tax1 (human T-cell leukemia virus type I) binding protein 1	TAX1BP1	7,79E-07	186,795	14,9951
O-linked N-acetylglucosamine (GlcNAc) transferase (UDP-N-acetylglucosamine:polyp	OGT	6,46E-05	60,0923	14,8399
GPS, PLAT and transmembrane domain-containing protein	LOC399491	9,65E-06	64,0007	13,996
far upstream element (FUSE) binding protein 1	FUBP1	3,90E-05	77,4018	13,9914
WD repeat domain 90	WDR90	2,21E-06	174,461	13,8578
RNA binding motif protein 5	RBM5	2,02E-06	170,405	13,7944
zinc finger, C3H1-type containing	ZFC3H1	8,63E-05	40,9902	13,5453
nuclear transcription factor, X-box binding 1	NFX1	2,07E-06	178,361	13,4847
collagen, type I, alpha 1	COL1A1	1,64E-06	633,613	13,3877
formin binding protein 4	FNBP4	2,73E-05	81,2479	13,3384
extra spindle pole bodies homolog 1 (S. cerevisiae)	ESPL1	1,57E-07	367,818	13,2562
RNA binding motif protein 39	RBM39	3,86E-07	314,921	12,8988
O-linked N-acetylglucosamine (GlcNAc)	OGT	4,63E-06	121,65	12,6921

transferase (UDP-N-acetylglucosamine:polyp				
SWI/SNF related, matrix associated, actin dependent regulator of chromatin, subf	SMARCA5	0,0003071	25,7169	12,4451
structural maintenance of chromosomes 4	SMC4	2,88E-09	1372,6	12,4048
laminin, alpha 5	LAMA5	1,52E-05	96,0168	12,2212
paired immunoglobin-like type 2 receptor beta	PILRB	4,36E-05	94,4153	12,0117
ataxia telangiectasia and Rad3 related	ATR	5,68E-05	52,5225	11,6563
transportin 2	TNPO2	0,00043995	19,5225	11,6396
---	---	6,97E-07	211,764	11,4574
RNA binding motif protein 26	RBM26	1,37E-05	86,4675	11,4534
golgi autoantigen, golgin subfamily a, 8B	GOLGA8B	1,92E-08	728,72	11,4115
centrosomal protein 152kDa	CEP152	1,08E-06	200,506	11,4033
choline kinase beta /// carnitine palmitoyltransferase 1B (muscle)	CHKB /// CPT1B	1,72E-06	159,611	11,3908
REV3-like, catalytic subunit of DNA polymerase zeta (yeast)	REV3L	0,00013617	34,9963	11,324
intraflagellar transport 80 homolog (Chlamydomonas)	IFT80	5,71E-05	40,9424	11,2586
nuclear factor of kappa light polypeptide gene enhancer in B-cells inhibitor, ze	NFKBIZ	1,05E-05	71,0931	10,9007
pleckstrin homology domain containing, family H (with MyTH4 domain) member 1	PLEKHH1	1,73E-06	267,103	10,8817
ankyrin repeat and KH domain containing 1 /// ANKHD1-EIF4EBP3 readthrough transc	ANKHD1 /// ANKHD1-EIF4EBP3 /// EIF4EBP3	5,17E-06	116,866	10,8328
Dmx-like 1	DMXL1	9,84E-05	40,2931	10,8253
PR domain containing 15	PRDM15	1,61E-06	175,386	10,6984
kinetochore associated 1	KNTC1	6,51E-06	109,578	10,4163
SWI/SNF related, matrix associated, actin dependent regulator of chromatin, subf	SMARCA5	3,73E-06	119,369	10,2704
family with sequence similarity 38, member A	FAM38A	3,85E-06	144,688	10,1629
ankyrin repeat and GTPase domain Arf GTPase activating protein 11 /// ArfGAP wit	AGAP11 /// AGAP4 /// AGAP6 /// AGAP7 /// AGAP8	1,15E-07	387,674	10,0682
MYC binding protein 2	MYCBP2	0,00123575	15,4762	9,99133
transcription elongation regulator 1	TCERG1	5,20E-06	146,733	9,97509
vacuolar protein sorting 13 homolog B (yeast)	VPS13B	0,00039514	20,3178	9,94554
RNA binding motif protein 39	RBM39	0,00051342	33,6997	9,75508
ATP-binding cassette, sub-family A (ABC1), member 5	ABCA5	1,37E-06	178,816	9,69132
YTH domain containing 2	YTHDC2	1,04E-05	82,9961	9,68832
extra spindle pole bodies homolog 1 (S. cerevisiae)	ESPL1	2,90E-06	203,982	9,68154
kinesin family member 14	KIF14	1,07E-05	147,541	9,65313
chromosome 6 open reading frame 26 /// mutS homolog 5 (E. coli)	C6orf26 /// MSH5	3,55E-07	269,644	9,55715
rapamycin-insensitive companion of mTOR	RICTOR	0,00177192	19,9477	9,51313
baculoviral IAP repeat-containing 6	BIRC6	0,00016638	28,3152	9,4973
---	---	1,20E-06	175,913	9,47614
inositol 1,4,5-triphosphate receptor, type 1	ITPR1	3,80E-06	166,215	9,43306
polymerase (DNA directed), theta	POLQ	2,21E-07	319,397	9,41963
zinc finger, DHHC-type containing 11	ZDHHC11	6,06E-05	63,2202	9,41939
poly(A) binding protein, cytoplasmic 1-like	PABPC1L	6,54E-08	478,169	9,3845
zinc finger, DHHC-type containing 11	ZDHHC11	0,00031286	86,6149	9,38101
GTF2I repeat domain containing 1	GTF2IRD1	8,62E-05	71,4493	9,36944
KIAA1731	KIAA1731	5,80E-05	62,5272	9,36767

O-linked N-acetylglucosamine (GlcNAc) transferase (UDP-N-acetylglucosamine:polyp	OGT	5,58E-07	229,966	9,18903
myeloid/lymphoid or mixed-lineage leukemia 2	MLL2	5,97E-07	218,411	9,15314
PRP4 pre-mRNA processing factor 4 homolog B (yeast)	PRPF4B	4,32E-07	249,192	9,14371
ubiquitin specific peptidase 34	USP34	0,00066436	18,6289	9,13246
chromodomain helicase DNA binding protein 9	CHD9	0,0013585	13,4325	9,11795
RNA binding motif protein 16	RBM16	0,00058907	20,4284	9,10286
ubiquitin protein ligase E3 component n-recognin 5	UBR5	1,79E-05	72,9817	9,0837
myeloid/lymphoid or mixed-lineage leukemia 3	MLL3	0,00066736	20,9977	9,06722
chromosome 10 open reading frame 137	C10orf137	1,98E-05	72,1398	9,04533
deltex 3-like (Drosophila)	DTX3L	7,37E-06	110,818	9,011
THO complex 2	THOC2	0,00018113	33,4703	8,98682
HEAT repeat containing 5B	HEATR5B	1,76E-05	67,2424	8,96187
KIAA1033	KIAA1033	0,00180582	10,2305	8,90145
carbamoyl-phosphate synthetase 2, aspartate transcarbamylase, and dihydroorotase	CAD	2,47E-06	171,486	8,75138
diacylglycerol kinase, delta 130kDa	DGKD	2,01E-08	928,824	8,73217
cyclin L2	CCNL2	2,60E-07	411,675	8,73053
ring finger protein 160	RNF160	0,00070838	16,4183	8,71933
acetyl-Coenzyme A carboxylase alpha	ACACA	3,32E-06	147,577	8,70831
transformation/transcription domain-associated protein	TRRAP	1,55E-05	72,9169	8,65258
GTPase activating Rap/RanGAP domain-like 1	GARNL1	0,00026454	28,7228	8,6449
cleavage and polyadenylation specific factor 1, 160kDa	CPSF1	0,000191	32,7094	8,63977
membrane-associated ring finger (C3HC4) 6	06/mar	4,72E-05	122,303	8,57924
natural killer-tumor recognition sequence	NKTR	5,76E-06	105,876	8,43622
ubiquitin-like with PHD and ring finger domains 2	UHRF2	0,00035376	24,6628	8,39835
asp (abnormal spindle) homolog, microcephaly associated (Drosophila)	ASPM	0,001021	35,3782	8,36089
natural killer-tumor recognition sequence	NKTR	2,61E-05	115,477	8,32115
similar to TBC1 domain family member 3 (Rab GTPase-activating protein PRC17) (Pr	LOC653498 /// TBC1D3 /// TBC1D3C /// TBC1D3D /// TBC1D3E /// TBC1D3F /// TBC1D3H	2,28E-06	144,271	8,30097
nuclear factor of kappa light polypeptide gene enhancer in B-cells inhibitor, ze	NFKBIZ	2,66E-06	126,725	8,22795
heterogeneous nuclear ribonucleoprotein A1	HNRNPA1	2,73E-05	96,8394	8,22767
cyclin L1	CCNL1	5,31E-05	68,943	8,22235
ArfGAP with GTPase domain, ankyrin repeat and PH domain 10 /// ArfGAP with GTPas	AGAP10 /// AGAP4 /// AGAP5 /// AGAP9 /// RP11-144G6.7	1,95E-05	69,1721	8,21978
Dmx-like 2	DMXL2	3,15E-08	613,386	8,19519
TAR (HIV-1) RNA binding protein 1	TARBP1	1,01E-05	105,198	8,18578
polypyrimidine tract binding protein 2	PTBP2	2,77E-06	139,11	8,18521
SMG1 homolog, phosphatidylinositol 3-kinase-related kinase (C. elegans)	SMG1	3,96E-05	52,0622	8,14921
DENN/MADD domain containing 4C	DENND4C	9,49E-06	86,4897	8,12116
SMG1 homolog, phosphatidylinositol 3-kinase-related kinase pseudogene	LOC641298	1,47E-07	357,128	8,11033

intraflagellar transport 80 homolog (Chlamydomonas)	IFT80	0,00029852	24,3588	8,04209
THO complex 2	THOC2	0,00314026	16,6159	7,97676
nuclear transcription factor, X-box binding-like 1	NFXL1	3,51E-07	286,219	7,94351
RNA-binding region (RNP1, RRM) containing 3	RNPC3	2,80E-07	298,233	7,90221
THO complex 2	THOC2	2,65E-06	167,486	7,86702
Fanconi anemia, complementation group D2	FANCD2	8,46E-06	136,501	7,85347
valyl-tRNA synthetase 2, mitochondrial (putative)	VARS2	8,75E-05	52,0022	7,7994
glutamine-fructose-6-phosphate transaminase 1	GFPT1	0,00045448	29,4615	7,79108
YTH domain containing 2	YTHDC2	2,76E-07	289,377	7,7429
acetyl-Coenzyme A carboxylase beta	ACACB	6,20E-07	320,221	7,73728
structural maintenance of chromosomes 4	SMC4	6,86E-06	165,004	7,7358
ubiquitin protein ligase E3 component n-recognin 5	UBR5	9,67E-06	90,0512	7,72148
WD repeat domain 19	WDR19	0,00243427	10,6469	7,71007
bromodomain and WD repeat domain containing 2	BRWD2	0,00014098	31,5807	7,70599
CDC-like kinase 1	CLK1	3,02E-05	57,1613	7,70261
asparagine-linked glycosylation 13 homolog (S. cerevisiae)	ALG13	2,62E-05	53,8378	7,69793
trophinin associated protein (tastin)	TROAP	3,51E-05	61,1388	7,69096
ankyrin repeat and KH domain containing 1 /// ANKHD1-EIF4EBP3 readthrough transc	ANKHD1 /// ANKHD1-EIF4EBP3	1,53E-06	198,522	7,66178
pumilio homolog 1 (Drosophila)	PUM1	0,00267446	11,0266	7,65605
triple functional domain (PTPRF interacting)	TRIO	0,0004176	20,8902	7,65382
transcription termination factor, RNA polymerase II	TTF2	0,00011435	38,5302	7,64154
heterogeneous nuclear ribonucleoprotein A2/B1	HNRNPA2B1	2,29E-05	121,042	7,64
hect domain and RLD 2 pseudogene 3	HERC2P3	3,97E-07	254,239	7,61118
salt-inducible kinase 1	SIK1	0,00010412	139,029	7,60176
kinesin family member 18B	KIF18B	0,00023	46,2823	7,60104
protein tyrosine phosphatase, receptor type, M	PTPRM	2,74E-05	44,6319	7,59828
hypothetical protein KIAA1434	RP5-1022P6.2	1,40E-05	111,87	7,58863
PAN2 poly(A) specific ribonuclease subunit homolog (S. cerevisiae)	PAN2	5,10E-06	108,153	7,54634
KIAA0802	KIAA0802	0,0001764	42,9624	7,52407
cleavage and polyadenylation specific factor 1, 160kDa	CPSF1	4,38E-05	58,6811	7,51717
exportin 5	XPO5	5,64E-05	55,1121	7,48568
vacuolar protein sorting 13 homolog C (S. cerevisiae)	VPS13C	0,00158136	13,9583	7,44152
phosphoinositide-3-kinase, class 2, beta polypeptide	PIK3C2B	4,80E-06	341,368	7,44105
CUG triplet repeat, RNA binding protein 1	CUGBP1	1,18E-06	280,106	7,38597
Tax1 (human T-cell leukemia virus type I) binding protein 1	TAX1BP1	5,83E-05	47,3196	7,32418
multiple PDZ domain protein	MPDZ	0,0022971	10,1922	7,28894
Myb-like, SWIRM and MPN domains 1	MYSM1	2,26E-06	154,098	7,28349
nischarin	NISCH	0,00114327	13,4475	7,27811
component of oligomeric golgi complex 4	COG4	1,99E-06	151,464	7,27643
myeloid/lymphoid or mixed-lineage leukemia (trithorax homolog, Drosophila); tran	MLLT10	0,0001782	46,8573	7,26341
tetratricopeptide repeat domain 17	TTC17	3,00E-05	65,7225	7,2625
TBC1 domain family, member 8 (with GRAM domain)	TBC1D8	3,37E-07	298,419	7,24693

ash1 (absent, small, or homeotic)-like (Drosophila)	ASH1L	0,00018847	29,4104	7,24256
dedicator of cytokinesis 7	DOCK7	0,00351419	12,4476	7,20647
MAX gene associated	MGA	1,51E-05	73,2317	7,20378
TAF1 RNA polymerase II, TATA box binding protein (TBP)-associated factor, 250kDa	TAF1	0,000377	23,4334	7,15995
lysine (K)-specific demethylase 3B	KDM3B	0,0001108	41,3598	7,15416
PRP4 pre-mRNA processing factor 4 homolog B (yeast)	PRPF4B	1,19E-07	404,788	7,14183
ADAM metallopeptidase with thrombospondin type 1 motif, 6	ADAMTS6	8,28E-07	194,171	7,1395
chromosome 12 open reading frame 30	C12orf30	4,21E-07	272,959	7,1077
hect domain and RLD 2	HERC2	0,00022052	29,1348	7,10662
pumilio homolog 1 (Drosophila)	PUM1	0,00215247	12,8247	7,07853
tetratricopeptide repeat domain 17	TTC17	2,20E-06	138,177	7,05742
integrator complex subunit 8	INTS8	4,28E-05	84,6005	7,04722
transportin 2	TNPO2	0,0026586	11,5279	7,03734
nucleoporin 205kDa	NUP205	0,00151422	18,3086	7,03097
jumonji domain containing 1C	JMJD1C	4,92E-05	41,9499	7,02551
splicing factor 3b, subunit 1, 155kDa	SF3B1	7,86E-05	50,5785	7,01087
acetyl-Coenzyme A carboxylase beta	ACACB	1,38E-06	301,296	6,98492
paired immunoglobin-like type 2 receptor beta	PILRB	3,06E-06	134,084	6,98443
kinesin family member 14	KIF14	9,76E-06	99,9969	6,97039
HLA-B associated transcript 2-like	BAT2L	1,03E-05	75,4685	6,93217
AT hook containing transcription factor 1	AHCTF1	2,80E-06	133,427	6,88681
RNA binding motif protein 6	RBM6	6,56E-06	141,056	6,86587
zinc finger protein 451	ZNF451	6,47E-05	60,023	6,86321
choline kinase beta /// carnitine palmitoyltransferase 1B (muscle)	CHKB /// CPT1B	1,35E-05	81,8806	6,8434
lysine (K)-specific demethylase 3A	KDM3A	0,00037665	24,1394	6,83566
zinc finger protein 335	ZNF335	1,78E-05	71,417	6,82359
RANBP2-like and GRIP domain containing 4 /// RANBP2-like and GRIP domain contain	RGPD4 /// RGPD5 /// RGPD6 /// RGPD8	0,00012262	28,4652	6,80265
host cell factor C1 (VP16-accessory protein)	HCFC1	0,00016102	37,4975	6,79946
fucokinase	FUK	1,65E-06	169,628	6,77176
zinc finger, DHHC-type containing 11	ZDHHC11	0,000108	43,2289	6,72994
phosphoinositide kinase, FYVE finger containing	PIKFYVE	0,00018088	24,6426	6,68197
succinate dehydrogenase complex, subunit A, flavoprotein pseudogene 2	SDHALP2	4,02E-07	255,877	6,67615
PAX interacting (with transcription-activation domain) protein 1	PAXIP1	7,69E-05	62,8307	6,65004
RNA binding motif protein 33	RBM33	1,26E-07	388,732	6,64387
CUG triplet repeat, RNA binding protein 1	CUGBP1	3,34E-05	58,6805	6,63945
tripeptidyl peptidase II	TPP2	8,97E-07	208,635	6,62443
zinc finger, MYND-type containing 8	ZMYND8	0,00017511	39,0894	6,62442
clathrin, heavy chain-like 1	CLTCL1	2,65E-05	67,3935	6,62208
anillin, actin binding protein	ANLN	1,76E-06	302,034	6,59246
hypothetical protein LOC100133781	LOC100133781	0,00037532	60,8968	6,58575
fibronectin type III domain containing 3A	FNDC3A	8,77E-06	85,9623	6,55111
3-hydroxy-3-methylglutaryl-Coenzyme A reductase	HMGCR	1,75E-06	171,2	6,55022
histone deacetylase 4	HDAC4	3,09E-06	132,305	6,52931
inhibitor of kappa light polypeptide gene enhancer in B-cells, kinase complex-as	IKBKAP	9,94E-05	42,978	6,52763
WD repeat domain 44	WDR44	1,80E-05	88,5021	6,52741
WD repeat domain 59	WDR59	0,00020303	43,5639	6,52738

serum/glucocorticoid regulated kinase 1	SGK1	0,00346596	17,3079	6,50758
macrophage stimulating 1 receptor (c-met-related tyrosine kinase)	MST1R	1,99E-06	160,322	6,47159
rotatin	RTTN	1,20E-05	80,2562	6,45689
translocated promoter region (to activated MET oncogene)	TPR	5,21E-05	73,5526	6,4517
polo-like kinase 2 (Drosophila)	PLK2	5,31E-05	61,9007	6,43913
ubiquitin specific peptidase 36	USP36	4,19E-06	220,261	6,3908
ubiquitin protein ligase E3 component n-recognin 4	UBR4	0,00071197	16,1253	6,38839
chromodomain helicase DNA binding protein 1	CHD1	7,72E-06	99,2596	6,36285
DENN/MADD domain containing 4B	DENND4B	9,53E-05	47,4756	6,31696
inositol 1,4,5-triphosphate receptor, type 1	ITPR1	5,86E-05	55,5191	6,31573
unc-84 homolog A (C. elegans)	UNC84A	7,29E-05	38,1841	6,30079
chromosome 12 open reading frame 30	C12orf30	5,06E-06	139,694	6,2972
GCN1 general control of amino-acid synthesis 1-like 1 (yeast)	GCN1L1	0,00071635	24,7118	6,29084
structural maintenance of chromosomes flexible hinge domain containing 1	SMCHD1	9,06E-06	94,5318	6,28981
nucleoporin 160kDa	NUP160	0,00091264	20,2293	6,28927
zinc finger, MYND-type containing 8	ZMYND8	9,35E-06	98,3857	6,2802
tetratricopeptide repeat, ankyrin repeat and coiled-coil containing 1	TANC1	0,00159009	17,5608	6,26352
phosphorylase kinase, alpha 2 (liver)	PHKA2	7,16E-05	50,6395	6,25575
ATP-binding cassette, sub-family C (CFTR/MRP), member 2	ABCC2	2,95E-06	135,811	6,19573
transferrin receptor (p90, CD71)	TFRC	0,00112271	53,13	6,19166
ATP-binding cassette, sub-family C (CFTR/MRP), member 1	ABCC1	8,55E-05	32,3939	6,18973
cyclin L1	CCNL1	0,00012412	42,1941	6,18531
laminin, alpha 3	LAMA3	1,73E-06	155,356	6,1832
exportin 4	XPO4	4,05E-06	116,294	6,17048
sema domain, transmembrane domain (TM), and cytoplasmic domain, (semaphorin) 6D	SEMA6D	1,09E-06	319,482	6,16549
myosin VC	MYO5C	1,06E-06	374,916	6,12541
multiple PDZ domain protein	MPDZ	0,0005159	17,9125	6,11784
TAF4 RNA polymerase II, TATA box binding protein (TBP)-associated factor, 135kDa	TAF4	7,78E-06	96,5667	6,10415
Dedicator of cytokinesis 5	DOCK5	5,06E-05	57,9606	6,09166
baculoviral IAP repeat-containing 6	BIRC6	0,00027956	23,9791	6,07417
zinc finger CCCH-type, antiviral 1	ZC3HAV1	0,00026535	35,7775	6,07255
NLR family, apoptosis inhibitory protein	NAIP	9,67E-06	95,5066	6,06616
eukaryotic translation initiation factor 4 gamma, 3	EIF4G3	0,00200835	10,3898	6,04914
hect domain and RLD 4	HERC4	8,47E-06	92,9691	6,04811
zinc finger protein 692	ZNF692	6,00E-05	63,3276	6,04683
centrosome and spindle pole associated protein 1	CSPP1	7,79E-08	456,596	6,04319
membrane-associated ring finger (C3HC4) 6	06/mar	8,71E-06	106,121	6,0178
eukaryotic translation initiation factor 4A, isoform 2	EIF4A2	8,45E-06	91,106	6,00563
poly(A) binding protein, cytoplasmic 4 (inducible form)	PABPC4	6,58E-06	120,994	6,00225
RAB3 GTPase activating protein subunit 2 (non-catalytic)	RAB3GAP2	0,00097775	14,6045	5,99755
structural maintenance of chromosomes flexible hinge domain containing 1	SMCHD1	5,83E-08	468,523	5,99582
DIP2 disco-interacting protein 2 homolog A (Drosophila)	DIP2A	3,87E-06	122,247	5,99068
Rap guanine nucleotide exchange factor	RAPGEF6	1,38E-05	74,907	5,97361

(GEF) 6				
fibronectin type III domain containing 3B	FNDC3B	0,00068677	17,8086	5,96864
ubiquitin protein ligase E3 component n-recognin 2	UBR2	0,00267388	9,61706	5,96681
HEAT repeat containing 5A	HEATR5A	0,00400186	9,60055	5,96444
U2-associated SR140 protein	SR140	6,47E-07	216,297	5,95907
poly (ADP-ribose) polymerase family, member 6	PARP6	2,50E-05	67,7994	5,95709
poly (ADP-ribose) polymerase family, member 6	PARP6	0,0001913	27,873	5,93011
family with sequence similarity 38, member B	FAM38B	5,94E-07	564,595	5,92784
ash1 (absent, small, or homeotic)-like (Drosophila)	ASH1L	1,34E-05	72,5901	5,92573
mediator complex subunit 23	MED23	0,00092739	15,1899	5,9242
proteasome (prosome, macropain) activator subunit 4	PSME4	0,00296243	10,6442	5,92201
RAB GTPase activating protein 1	RABGAP1	2,47E-05	48,7963	5,92171
KIAA0368	KIAA0368	9,21E-05	41,8752	5,92134
NMDA receptor regulated 1-like	NARG1L	5,52E-05	50,6023	5,91885
Fanconi anemia, complementation group A	FANCA	1,16E-06	189,882	5,91743
NLR family, CARD domain containing 5	NLRC5	6,47E-06	98,7619	5,9136
phosphatidylinositol 4-kinase, catalytic, alpha /// phosphatidylinositol 4-kinas	PI4KA /// PI4KAP1 /// PI4KAP2	0,00285238	9,71018	5,91002
TIA1 cytotoxic granule-associated RNA binding protein	TIA1	4,53E-05	62,5395	5,89851
KIAA0907	KIAA0907	0,0034914	19,6944	5,89728
IQ motif containing GTPase activating protein 3	IQGAP3	4,27E-05	55,8614	5,89386
zinc finger, DHHC-type containing 17	ZDHHC17	0,00050522	21,6908	5,87907
AFG3 ATPase family gene 3-like 1 (S. cerevisiae)	AFG3L1	3,87E-06	119,104	5,86552
nucleoporin 153kDa	NUP153	0,00022319	55,6529	5,85439
splicing factor, arginine/serine-rich 11	SFRS11	0,00022179	57,6398	5,85059
structural maintenance of chromosomes 4	SMC4	0,0002011	146,365	5,84364
hypothetical protein KIAA1434	RP5-1022P6.2	3,19E-06	178,708	5,83975
histocompatibility (minor) HA-1	HMHA1	1,63E-06	165,73	5,82845
MAX gene associated	MGA	1,61E-05	98,84	5,82796
chromosome 6 open reading frame 26 /// mutS homolog 5 (E. coli)	C6orf26 /// MSH5	5,93E-09	1046,43	5,8258
formin-like 2	FMNL2	1,22E-05	141,811	5,82463
ubiquitin associated protein 2	UBAP2	5,37E-05	82,6834	5,81785
chromodomain helicase DNA binding protein 1	CHD1	9,42E-06	96,7162	5,80946
acetyl-Coenzyme A carboxylase beta	ACACB	1,55E-06	203,886	5,75301
chromosome 12 open reading frame 51	C12orf51	9,25E-06	88,2179	5,74309
chromodomain helicase DNA binding protein 7	CHD7	1,10E-05	89,9655	5,72532
leucyl-tRNA synthetase	LARS	0,00012925	64,0562	5,72436
CDC-like kinase 4	CLK4	5,58E-05	51,6389	5,69348
FRY-like	FRYL	1,08E-07	399,129	5,69327
senataxin	SETX	0,00270435	9,99344	5,69327
zinc finger CCCH-type containing 11A	ZC3H11A	0,00033484	25,8124	5,67631
DEAH (Asp-Glu-Ala-His) box polypeptide 9	DHX9	0,00087512	19,2726	5,67606
tripeptidyl peptidase II	TPP2	1,42E-06	158,382	5,67577
nuclear RNA export factor 1	NXF1	0,00038026	29,2966	5,66872
AT hook containing transcription factor 1	AHCTF1	6,78E-05	65,2847	5,65192
3-hydroxy-3-methylglutaryl-Coenzyme A reductase	HMGCR	1,85E-06	169,866	5,63433
chromodomain helicase DNA binding protein 9	CHD9	0,00309448	11,4249	5,62314

transferrin receptor (p90, CD71)	TFRC	0,00122786	51,5476	5,60088
KIAA1012	KIAA1012	0,00160341	12,9964	5,59742
synaptojanin 1	SYNJ1	5,55E-06	101,365	5,59474
ankyrin repeat domain 17	ANKRD17	0,00123173	13,9909	5,59439
tetratricopeptide repeat domain 37	TTC37	0,00111217	14,7008	5,59379
synovial sarcoma translocation gene on chromosome 18-like 1	SS18L1	6,77E-05	56,3387	5,58777
KIAA1033	KIAA1033	0,00094608	14,5966	5,58072
nephronophthisis 3 (adolescent)	NPHP3	0,00213413	9,94415	5,55839
REV1 homolog (S. cerevisiae)	REV1	0,00037722	41,1358	5,55574
Bloom syndrome, RecQ helicase-like	BLM	2,29E-05	85,7099	5,54768
RNA binding motif protein, X-linked	RBMX	0,00013577	101,809	5,54433
tripartite motif-containing 24	TRIM24	4,87E-05	80,7716	5,53808
U2-associated SR140 protein	SR140	5,41E-06	104,758	5,53563
trinucleotide repeat containing 6A	TNRC6A	5,69E-05	40,7714	5,53076
phosphodiesterase 4D, cAMP-specific (phosphodiesterase E3 dunce homolog, Drosoph	PDE4D	0,00014257	61,6694	5,52238
SWI/SNF-related, matrix-associated actin-dependent regulator of chromatin, subfa	SMARCAD1	5,27E-05	48,6127	5,51987
family with sequence similarity 48, member A	FAM48A	1,32E-05	84,4461	5,51119
---	---	0,00028012	51,654	5,50673
---	---	0,00371922	16,8015	5,49481
GCN1 general control of amino-acid synthesis 1-like 1 (yeast)	GCN1L1	3,42E-07	291,99	5,4933
polymerase (DNA directed), alpha 1, catalytic subunit	POLA1	8,48E-06	121,341	5,49282
coiled-coil domain containing 45	CCDC45	1,96E-07	345,515	5,47493
splicing factor proline/glutamine-rich (polypyrimidine tract binding protein ass	SFPQ	2,56E-05	95,067	5,46013
jumonji domain containing 1C	JMJD1C	0,00042586	18,8292	5,45631
solute carrier family 11 (proton-coupled divalent metal ion transporters), membe	SLC11A2	9,61E-06	245,797	5,45252
MON2 homolog (S. cerevisiae)	MON2	0,0021023	12,5012	5,42057
lysine (K)-specific demethylase 3B	KDM3B	0,000185	32,1163	5,40423
zinc finger, SWIM-type containing 6	ZSWIM6	0,00026627	29,709	5,37755
scribbled homolog (Drosophila)	SCRIB	4,36E-07	252,328	5,35553
ribosomal modification protein rimK-like family member B	RIMKLB	6,26E-06	160,655	5,35383
splicing factor 3b, subunit 1, 155kDa	SF3B1	0,00037624	37,8926	5,32796
zinc finger protein 638	ZNF638	3,96E-05	88,6934	5,3234
structural maintenance of chromosomes flexible hinge domain containing 1	SMCHD1	1,92E-05	78,1753	5,31813
---	---	3,66E-05	62,7234	5,29781
REV1 homolog (S. cerevisiae)	REV1	0,00092635	18,1322	5,29086
DIP2 disco-interacting protein 2 homolog B (Drosophila)	DIP2B	3,25E-05	81,599	5,29027
SNF2 histone linker PHD RING helicase	SHPRH	6,07E-06	98,6761	5,28848
chromodomain helicase DNA binding protein 9	CHD9	9,32E-07	193,293	5,28284
---	---	4,88E-05	49,6034	5,27815
ankyrin repeat and FYVE domain containing 1	ANKFY1	0,00321503	10,4846	5,26473
---	---	3,46E-06	127,961	5,26367
neuroblastoma breakpoint family, member 10 /// neuroblastoma breakpoint family,	NBPF10 /// NBPF12 /// NBPF15 /// NBPF16 /// NBPF8 /// NBPF9 /// RP11-94I2.2	5,48E-05	78,7456	5,26335
retinoblastoma binding protein 6	RBBP6	1,23E-05	91,3122	5,25837

phosphodiesterase 10A	PDE10A	0,00061061	26,4372	5,25582
Rap guanine nucleotide exchange factor (GEF) 2	RAPGEF2	0,00179276	12,9409	5,24809
phosphoribosylformylglycinamidine synthase	PFAS	0,00018181	56,3565	5,24795
amylo-1, 6-glucosidase, 4-alpha-glucanotransferase	AGL	0,00224105	21,1859	5,22651
---	---	3,47E-06	125,672	5,22575
TNF receptor-associated factor 5	TRAF5	0,00020197	27,7202	5,22573
nucleoporin 107kDa	NUP107	0,00397063	20,3464	5,21708
leucyl-tRNA synthetase	LARS	0,00026411	31,438	5,21668
chromosome 1 open reading frame 199	C1orf199	7,50E-09	1004,16	5,21409
zinc finger, CCHC domain containing 8	ZCCHC8	2,97E-05	105,467	5,21266
E1A binding protein p400	EP400	0,00016193	30,8596	5,21046
U2-associated SR140 protein	SR140	0,00354817	32,3439	5,20499
phosphoinositide-3-kinase, regulatory subunit 4	PIK3R4	0,00097778	22,8782	5,18973
echinoderm microtubule associated protein like 6	EML6	2,28E-07	311,991	5,18656
phosphodiesterase 7A	PDE7A	0,0002207	36,5891	5,18617
nuclear transcription factor, X-box binding 1	NFX1	1,08E-07	401,866	5,18194
B double prime 1, subunit of RNA polymerase III transcription initiation factor	BDP1	0,00016853	32,2264	5,16497
nucleoporin 214kDa	NUP214	4,62E-06	117,857	5,16004
DNA replication helicase 2 homolog (yeast)	DNA2	5,46E-05	49,0629	5,15962
ring finger and CCCH-type zinc finger domains 1	RC3H1	0,0006424	20,7588	5,1479
zinc finger protein 638	ZNF638	0,00400615	20,2738	5,13809
vacuolar protein sorting 8 homolog (S. cerevisiae)	VPS8	0,00184725	14,63	5,11936
nephronophthisis 3 (adolescent)	NPHP3	0,00037368	19,9438	5,11683
RNA binding motif protein 26	RBM26	4,30E-06	116,005	5,1141
SET domain, bifurcated 1	SETDB1	2,61E-06	132,459	5,114
family with sequence similarity 65, member A	FAM65A	4,96E-07	255,394	5,1069
CTP synthase	CTPS	0,00174739	32,5944	5,10461
RNA binding motif, single stranded interacting protein 2	RBMS2	4,24E-05	44,9979	5,09968
polymerase (DNA directed), delta 1, catalytic subunit 125kDa	POLD1	7,40E-06	102,407	5,09869
cyclin-dependent kinase 10	CDK10	3,63E-05	78,5041	5,0973
senataxin	SETX	0,00211495	10,9924	5,09349
KIAA0368	KIAA0368	0,00030251	32,2451	5,09244
InaD-like (Drosophila)	INADL	6,01E-06	116,015	5,0921
neuron navigator 2	NAV2	7,10E-06	134,378	5,08471
coiled-coil domain containing 93	CCDC93	5,46E-05	43,0005	5,08286
neuroblastoma breakpoint family, member 10 /// neuroblastoma breakpoint family,	NBPF10 /// NBPF11 /// NBPF8 /// RP11-94I2.2	7,69E-06	153,728	5,08208
PAN3 poly(A) specific ribonuclease subunit homolog (S. cerevisiae)	PAN3	0,00246692	8,86859	5,07441
splicing factor, arginine/serine-rich 16	SFRS16	5,72E-06	106,123	5,07183
M-phase phosphoprotein 9	MPHOSPH9	3,75E-06	151,554	5,06311
RNA binding motif protein 33	RBM33	6,56E-05	49,6581	5,06214
oxysterol binding protein-like 3	OSBPL3	3,51E-06	125,444	5,05602
TSR1, 20S rRNA accumulation, homolog (S. cerevisiae)	TSR1	4,96E-06	139,448	5,05404
pogo transposable element with ZNF domain	POGZ	0,00075668	22,4614	5,05199

---	---	1,82E-05	69,7414	5,04364
zinc finger, CCHC domain containing 11	ZCCHC11	2,38E-05	71,3371	5,03715
PRP3 pre-mRNA processing factor 3 homolog (S. cerevisiae)	PRPF3	6,22E-09	1179,61	5,02738
DEAH (Asp-Glu-Ala-His) box polypeptide 9	DHX9	0,00149757	19,5675	5,02184
HECT domain containing 2	HECTD2	1,03E-06	205,805	5,02109
Ewing sarcoma breakpoint region 1	EWSR1	0,00068187	35,5722	5,0171
spastic paraplegia 7 (pure and complicated autosomal recessive)	SPG7	2,80E-06	141,873	4,99551
sperm associated antigen 5	SPAG5	9,39E-06	224,918	4,99354
TTK protein kinase	TTK	5,37E-05	79,5947	4,99286
interleukin enhancer binding factor 3, 90kDa	ILF3	9,01E-06	163,793	4,9819
lipin 1	LPIN1	4,26E-06	116,47	4,97274
Neuroblastoma breakpoint family, member 1	NBPF1	6,22E-06	152,038	4,95986
Nipped-B homolog (Drosophila)	NIPBL	0,00019542	76,2378	4,95553
non-SMC condensin II complex, subunit D3	NCAPD3	2,22E-05	95,3551	4,95452
neuroblastoma breakpoint family, member 10 /// neuroblastoma breakpoint family,	NBPF10 /// NBPF12 /// NBPF15 /// NBPF16 /// NBPF8 /// NBPF9	1,00E-05	148,109	4,95205
centromere protein J	CENPJ	7,23E-08	467,092	4,94831
enhancer of zeste homolog 2 (Drosophila)	EZH2	8,09E-05	108,881	4,94432
Fanconi anemia, complementation group I	FANCI	1,14E-06	472,65	4,93951
calcium channel, voltage-dependent, beta 2 subunit	CACNB2	4,47E-06	209,19	4,93238
topoisomerase (DNA) II binding protein 1	TOPBP1	0,00028866	81,5767	4,93078
anillin, actin binding protein	ANLN	2,28E-07	315,001	4,92545
YEATS domain containing 2	YEATS2	2,74E-05	47,3356	4,90405
CDC-like kinase 2	CLK2	1,88E-05	86,291	4,89422
dpy-19-like 4 (C. elegans)	DPY19L4	3,29E-05	51,6245	4,87759
protein kinase, DNA-activated, catalytic polypeptide	PRKDC	0,00220351	21,6527	4,87471
myeloid/lymphoid or mixed-lineage leukemia 3	MLL3	0,00040976	20,6343	4,85882
PR domain containing 15	PRDM15	0,00025301	27,6296	4,84002
aminoadipate-semialdehyde dehydrogenase	AASDH	0,00039814	26,9073	4,83691
caspase recruitment domain family, member 10	CARD10	4,61E-05	76,5636	4,83435
Pentatricopeptide repeat domain 3	PTCD3	0,00019915	54,3795	4,83381
kinesin family member 23	KIF23	1,15E-06	206,842	4,8324
tripartite motif-containing 33	TRIM33	1,44E-06	257,316	4,83224
splicing factor, arginine/serine-rich 5	SFRS5	0,00124029	35,5146	4,82612
---	---	1,03E-05	82,3077	4,82312
phosphodiesterase 8A	PDE8A	0,00083839	32,4723	4,82253
Ras association (RalGDS/AF-6) and pleckstrin homology domains 1	RAPH1	0,00226767	10,0978	4,80195
hect domain and RLD 4	HERC4	7,12E-05	53,2428	4,80034
zinc finger CCCH-type containing 7A	ZC3H7A	0,00253782	13,3912	4,79997
chromosome 21 open reading frame 66	C21orf66	1,47E-06	179,23	4,79775
inositol 1,4,5-triphosphate receptor, type 3	ITPR3	0,00097451	40,2758	4,78272
anaphase promoting complex subunit 1	ANAPC1	0,00031715	39,343	4,78086
DEAD (Asp-Glu-Ala-Asp) box polypeptide 60-like	DDX60L	0,00031106	22,4624	4,77647
PMS1 postmeiotic segregation increased 1 (S. cerevisiae)	PMS1	0,00033598	39,3481	4,77181
euchromatic histone-lysine N-methyltransferase 1	EHMT1	5,95E-06	103,746	4,75897

SET domain containing 5	SETD5	0,00131422	15,7428	4,757
Eukaryotic translation initiation factor 2C, 4	EIF2C4	9,93E-07	185,985	4,75672
ubiquitin specific peptidase 54	USP54	3,38E-06	165,898	4,75389
thyroid adenoma associated	THADA	4,21E-05	48,8261	4,74011
Ubiquitin specific peptidase 36	USP36	0,00031008	55,3268	4,73752
RAS p21 protein activator 2	RASA2	3,81E-05	51,1999	4,73064
chromosome 4 open reading frame 8	C4orf8	3,31E-05	55,0042	4,73001
programmed cell death 11	PDCD11	1,94E-05	73,9007	4,72714
tubulin folding cofactor E	TBCE	5,16E-05	62,2713	4,72578
nucleoporin 210kDa	NUP210	0,0001033	82,5542	4,72044
WAS protein family homolog 2 pseudogene /// WAS protein family homolog 3 pseudog	WASH2P /// WASH3P /// WASH5P	1,28E-05	82,4472	4,71877
zinc finger CCCH-type containing 7A	ZC3H7A	0,00343494	11,3461	4,71782
KIAA0226	KIAA0226	1,02E-07	396,316	4,70703
tripartite motif-containing 24	TRIM24	8,91E-06	203,671	4,70345
DEAD (Asp-Glu-Ala-Asp) box polypeptide 58	DDX58	1,97E-05	164,317	4,69773
ATPase, class VI, type 11A	ATP11A	0,00199666	21,4444	4,69763
DENN/MADD domain containing 4C	DENND4C	0,00015381	34,2324	4,69004
low density lipoprotein receptor-related protein 6	LRP6	0,0002547	26,4856	4,67883
glomulin, FKBP associated protein	GLMN	7,02E-06	100,182	4,66805
CUG triplet repeat, RNA binding protein 1	CUGBP1	1,72E-07	347,225	4,66531
---	---	7,43E-06	95,0661	4,66526
ataxia telangiectasia mutated	ATM	1,08E-06	175,103	4,66419
aquarius homolog (mouse)	AQR	0,00012497	39,3047	4,66178
tetratricopeptide repeat domain 37	TTC37	0,00018091	26,1939	4,66102
pericentrin	PCNT	0,00015081	43,3723	4,65659
HMG box domain containing 3	HMGXB3	0,00013161	38,2113	4,64993
polymerase (RNA) II (DNA directed) polypeptide B, 140kDa	POLR2B	0,00389661	12,1018	4,64974
splicing factor, arginine/serine-rich 12	SFRS12	0,00097463	21,2523	4,64543
topoisomerase (DNA) II alpha 170kDa	TOP2A	1,41E-06	547,168	4,64064
ubiquitin specific peptidase 7 (herpes virus-associated)	USP7	6,30E-06	100,018	4,61191
inhibitor of kappa light polypeptide gene enhancer in B-cells, kinase beta	IKBKB	0,00010319	39,0667	4,60713
eyes absent homolog 4 (Drosophila)	EYA4	9,47E-06	142,277	4,60288
integrator complex subunit 2	INTS2	1,46E-05	75,4885	4,59727
zinc finger protein 326	ZNF326	1,28E-05	140,279	4,59543
ubiquitin associated protein 2	UBAP2	0,00177668	19,4763	4,59202
BAT2 domain containing 1	BAT2D1	0,00036093	42,3097	4,58992
centrosomal protein 192kDa	CEP192	5,63E-06	103,537	4,58614
zinc finger protein 207	ZNF207	2,58E-06	136,314	4,5795
splicing factor, arginine/serine-rich 15	SFRS15	0,0004298	25,8406	4,57342
poly(A) polymerase gamma	PAPOLG	7,54E-06	102,764	4,56662
ubiquitin specific peptidase 34	USP34	5,40E-05	41,2956	4,566
leucine-rich PPR-motif containing	LRPPRC	0,00077188	44,8567	4,56497
KRIT1, ankyrin repeat containing	KRIT1	4,21E-05	55,2164	4,55593
nuclear transcription factor, X-box binding 1	NFX1	2,43E-06	136,069	4,55547
zinc finger, MYM-type 2	ZMYM2	0,00011582	26,9912	4,54862
tumor protein p53 binding protein 1	TP53BP1	0,00019966	29,832	4,53269
discs, large homolog 5 (Drosophila)	DLG5	6,05E-05	34,2224	4,52713
5-methyltetrahydrofolate-homocysteine methyltransferase	MTR	0,00315112	11,4522	4,52666
non-SMC condensin II complex, subunit G2	NCAPG2	2,61E-05	208,009	4,50083

vacuolar protein sorting 13 homolog A (S. cerevisiae)	VPS13A	2,16E-05	60,9431	4,49397
INO80 homolog (S. cerevisiae)	INO80	2,44E-05	75,8285	4,49186
retinoblastoma binding protein 6	RBBP6	1,41E-07	385,165	4,48845
kinesin family member 21A	KIF21A	1,14E-05	87,9119	4,48768
ubiquitin specific peptidase 19	USP19	0,00022852	29,446	4,46404
family with sequence similarity 65, member A	FAM65A	0,00011295	47,5459	4,46261
nuclear factor related to kappaB binding protein	NFRKB	0,000298	34,0181	4,46146
family with sequence similarity 38, member B	FAM38B	0,00041419	28,9878	4,46079
oral-facial-digital syndrome 1	OFD1	0,00028122	48,8983	4,45876
small nuclear ribonucleoprotein 200kDa (U5)	SNRNP200	0,00023181	29,7997	4,44193
squamous cell carcinoma antigen recognized by T cells 3	SART3	4,21E-06	111,832	4,43281
splicing factor, arginine/serine-rich 14	SFRS14	6,10E-07	252,137	4,41904
ciliary rootlet coiled-coil, rootletin-like 1	CROCCL1	3,38E-07	271,132	4,41249
pleckstrin homology domain interacting protein	PHIP	1,72E-05	183,243	4,4075
pantothenate kinase 4	PANK4	3,36E-07	262,297	4,3981
myeloid/lymphoid or mixed-lineage leukemia (trithorax homolog, Drosophila); tran	MLLT4	1,95E-06	149,968	4,39552
budding uninhibited by benzimidazoles 1 homolog (yeast)	BUB1	1,68E-05	139,249	4,39522
SET domain containing 1B	SETD1B	2,50E-05	60,7573	4,39326
leucine-rich PPR-motif containing	LRPPRC	0,0041848	32,5947	4,39134
serologically defined colon cancer antigen 1	SDCCAG1	0,0018135	14,562	4,38878
centrosomal protein 350kDa	CEP350	0,00052872	19,7109	4,38593
echinoderm microtubule associated protein like 2	EML2	2,08E-05	163,478	4,38122
anaphase promoting complex subunit 4	ANAPC4	0,00377369	9,83165	4,38021
solute carrier family 38, member 1	SLC38A1	2,03E-05	108,939	4,37977
TIA1 cytotoxic granule-associated RNA binding protein	TIA1	0,00019352	28,558	4,37835
dedicator of cytokinesis 9	DOCK9	0,00177275	11,8767	4,37727
AF4/FMR2 family, member 1	AFF1	0,00067558	28,6907	4,37094
5-oxoprolinase (ATP-hydrolysing)	OPLAH	8,72E-06	92,1211	4,36937
rapamycin-insensitive companion of mTOR	RICTOR	4,36E-05	51,7437	4,36677
AT rich interactive domain 4B (RBP1-like)	ARID4B	0,00011849	33,4226	4,3651
tetratricopeptide repeat domain 3	TTC3	3,32E-05	41,8215	4,36413
family with sequence similarity 48, member A	FAM48A	2,57E-06	191,3	4,3633
centromere protein C 1	CENPC1	1,22E-05	78,7794	4,355
TATA box binding protein (TBP)-associated factor, RNA polymerase I, D, 41kDa	TAF1D	0,00170786	32,8675	4,33902
WAS protein family homolog 3 pseudogene	WASH3P	0,00012309	49,5761	4,33565
UDP-glucose ceramide glucosyltransferase-like 2	UGCGL2	0,00321741	9,31526	4,33199
centrosomal protein 164kDa	CEP164	0,0006796	18,524	4,32433
eukaryotic translation initiation factor 4E nuclear import factor 1	EIF4ENIF1	0,00011984	34,8085	4,32301
protein tyrosine phosphatase, receptor type, S	PTPRS	1,49E-06	162,912	4,32155
MMS19 nucleotide excision repair homolog (S. cerevisiae)	MMS19	0,00118357	17,1965	4,32044
neuroblastoma breakpoint family, member 10 /// neuroblastoma breakpoint family,	NBPF10 /// NBPF11 /// NBPF12 ///	0,00061024	54,7444	4,31832

	NBPF14 /// NBPF15 /// NBPF16 /// NBPF8 /// RP11			
KIAA0564	KIAA0564	0,00238678	20,7214	4,31409
LUC7-like (S. cerevisiae)	LUC7L	1,15E-05	132,571	4,31401
Sfi1 homolog, spindle assembly associated (yeast)	SFI1	1,64E-06	156,814	4,31006
vacuolar protein sorting 13 homolog B (yeast)	VPS13B	2,56E-07	291,185	4,309
FK506 binding protein 12-rapamycin associated protein 1	FRAP1	2,64E-05	58,6803	4,30871
RAB GTPase activating protein 1	RABGAP1	2,53E-05	46,2327	4,30621
PDS5, regulator of cohesion maintenance, homolog B (S. cerevisiae)	PDS5B	3,23E-06	127,367	4,30267
mediator complex subunit 17	MED17	0,00048097	36,4281	4,29865
protein tyrosine phosphatase, receptor type, M	PTPRM	0,0001073	33,2798	4,29737
chromosome 15 open reading frame 42	C15orf42	6,42E-06	111,603	4,28586
Vpr (HIV-1) binding protein	VPRBP	4,50E-05	61,895	4,28262
PTK2 protein tyrosine kinase 2	PTK2	0,00087848	17,5289	4,27363
family with sequence similarity 13, member A	FAM13A	3,36E-06	122,524	4,26928
splicing factor 3b, subunit 3, 130kDa	SF3B3	0,00038478	40,8511	4,26756
cysteinyl-tRNA synthetase	CARS	2,54E-05	55,0173	4,25444
nuclear VCP-like	NVL	1,91E-05	205,568	4,24826
family with sequence similarity 21, member A /// family with sequence similarity	FAM21A /// FAM21B /// FAM21C /// FAM21D	0,00311394	12,2403	4,24824
DNA (cytosine-5-)-methyltransferase 3 beta	DNMT3B	6,23E-06	122,581	4,24634
interleukin enhancer binding factor 3, 90kDa	ILF3	6,97E-06	122,664	4,24239
leukemia inhibitory factor receptor alpha	LIFR	1,29E-06	702,002	4,23892
Mov10, Moloney leukemia virus 10, homolog (mouse)	MOV10	0,00136448	19,3603	4,23319
transportin 2	TNPO2	4,24E-05	44,9655	4,23244
leucine-rich repeats and immunoglobulin-like domains 2	LRIG2	5,85E-05	45,5122	4,22787
splicing factor, arginine/serine-rich 5	SFRS5	0,00142263	29,0189	4,21414
CDC42 binding protein kinase alpha (DMPK-like)	CDC42BPA	0,00034043	20,5255	4,20958
DNA (cytosine-5-)-methyltransferase 1	DNMT1	7,40E-05	111,296	4,19923
ankyrin repeat domain 32	ANKRD32	3,07E-06	1072,63	4,1989
hect (homologous to the E6-AP (UBE3A) carboxyl terminus) domain and RCC1 (CHC1)-	HERC1	0,0001014	38,1842	4,19561
microtubule associated monoxygenase, calponin and LIM domain containing 3	MICAL3	3,38E-05	56,4263	4,19524
GTPase activating Rap/RanGAP domain-like 1	GARNL1	4,75E-07	238,382	4,19211
trinucleotide repeat containing 6A	TNRC6A	9,82E-05	32,4373	4,18111
exportin 5	XPO5	4,72E-06	108,052	4,17909
bromodomain adjacent to zinc finger domain, 1A	BAZ1A	1,56E-06	160,689	4,17465
amylase, alpha 1A (salivary) /// amylase, alpha 1B (salivary) /// amylase, alpha	AMY1A /// AMY1B /// AMY1C /// AMY2A /// AMY2B	5,85E-05	46,1677	4,17238
family with sequence similarity 21, member A /// family with sequence similarity	FAM21A /// FAM21B /// FAM21C /// FAM21D	0,00096779	20,8819	4,16913
KIAA1033	KIAA1033	0,00062019	17,4035	4,15887

aminoadipate-semialdehyde dehydrogenase	AASDH	2,76E-05	62,2412	4,1328
ADP-ribosylation factor guanine nucleotide-exchange factor 2 (brefeldin A-inhibi	ARFGEF2	0,00024855	29,0699	4,12937
tensin 3	TNS3	0,00330842	16,7791	4,12782
nuclear autoantigenic sperm protein (histone-binding)	NASP	0,00181593	53,6084	4,12675
zinc finger family member 767	ZNF767	1,62E-05	78,8461	4,12162
gon-4-like (C. elegans)	GON4L	6,31E-05	43,8965	4,1174
ankyrin repeat domain 28	ANKRD28	0,00402341	26,4884	4,11708
Rho-associated, coiled-coil containing protein kinase 2	ROCK2	0,00142476	16,8838	4,11573
FRY-like	FRYL	0,00012705	31,3757	4,11472
CXXC finger 1 (PHD domain)	CXXC1	0,00019129	36,3968	4,11116
muskelin 1, intracellular mediator containing kelch motifs	MKLN1	0,00175509	13,1708	4,10803
SWI/SNF related, matrix associated, actin dependent regulator of chromatin, subf	SMARCA5	0,00019981	30,4823	4,10455
natural killer-tumor recognition sequence	NKTR	9,65E-06	87,6334	4,10387
FCH domain only 2	FCHO2	0,00075057	22,5299	4,09932
serine/threonine kinase 36, fused homolog (Drosophila)	STK36	1,01E-06	188,902	4,09793
glucosidase, beta (bile acid) 2	GBA2	4,32E-06	115,728	4,09519
WD repeat domain 67	WDR67	2,75E-06	154,274	4,09198
WD repeat domain 26	WDR26	5,35E-05	37,1364	4,07639
insulin-like growth factor 1 receptor	IGF1R	0,00164108	11,5613	4,07635
asparagine-linked glycosylation 6, alpha-1,3-glucosyltransferase homolog (S. cer	ALG6	5,02E-06	407,088	4,07594
enolase 3 (beta, muscle)	ENO3	3,45E-05	155,559	4,07215
N-acetyltransferase 10 (GCN5-related)	NAT10	0,00022601	43,9641	4,07012
ring finger protein 160	RNF160	0,00014541	29,4691	4,06776
single stranded DNA binding protein 4	SSBP4	8,16E-05	77,0897	4,06591
Niemann-Pick disease, type C1	NPC1	0,00079448	20,9155	4,06385
KIAA0892	KIAA0892	5,89E-05	47,9112	4,06355
tetratricopeptide repeat domain 3	TTC3	4,48E-05	39,0587	4,06285
PHD finger protein 20	PHF20	0,00041579	28,411	4,05915
myeloid/lymphoid or mixed-lineage leukemia 3	MLL3	7,33E-06	91,8404	4,05367
ras homolog gene family, member T2	RHOT2	0,00019994	34,4148	4,05202
family with sequence similarity 21, member C /// family with sequence similarity	FAM21C /// FAM21D	0,00110244	29,8036	4,04681
DEAD (Asp-Glu-Ala-Asp) box polypeptide 3, X-linked	DDX3X	8,55E-05	38,2586	4,04601
lysine (K)-specific demethylase 4C	KDM4C	0,00023742	25,2881	4,04414
ankyrin repeat domain 27 (VPS9 domain)	ANKRD27	0,00039029	24,3646	4,04267
ATG2 autophagy related 2 homolog A (S. cerevisiae)	ATG2A	0,00169551	12,0463	4,03686
NOP56 ribonucleoprotein homolog (yeast)	NOP56	1,97E-05	209,685	4,03285
transportin 1	TNPO1	0,00167964	11,1887	4,0209
fatty acid synthase	FASN	0,00014001	42,154	4,01759
TRM1 tRNA methyltransferase 1 homolog (S. cerevisiae)	TRMT1	0,00020759	46,9909	4,01343
golgi associated, gamma adaptin ear containing, ARF binding protein 3	GGA3	0,00123699	13,7206	4,00765
PRP39 pre-mRNA processing factor 39 homolog (S. cerevisiae)	PRPF39	3,08E-05	56,4964	4,00221
calpain 7	CAPN7	0,0014415	18,299	4,00115
tripartite motif-containing 33	TRIM33	3,51E-07	271,491	3,97534
WD repeat domain 36	WDR36	0,00182134	13,0288	3,97364
ubiquitin specific peptidase 42	USP42	4,22E-05	47,7804	3,97322
Notch homolog 2 (Drosophila)	NOTCH2	0,00109766	18,0438	3,97136

ankyrin repeat domain 28	ANKRD28	0,00026135	62,0065	3,97123
---	---	0,00041851	22,8909	3,96867
solute carrier family 22, member 15	SLC22A15	0,00084992	15,8483	3,96777
similar to single stranded DNA binding protein 4 /// single stranded DNA binding	LOC646044 /// SSBP4	0,00012533	71,427	3,96383
LON peptidase N-terminal domain and ring finger 3	LONRF3	7,66E-05	97,6472	3,96269
heterochromatin protein 1, binding protein 3	HP1BP3	0,00031595	31,6035	3,96083
polymerase (DNA directed), epsilon	POLE	1,68E-05	82,4018	3,94468
poly (ADP-ribose) polymerase family, member 4	PARP4	0,00010735	44,2354	3,94344
CTF18, chromosome transmission fidelity factor 18 homolog (S. cerevisiae)	CHTF18	2,96E-06	146,653	3,94256
---	---	0,00055571	20,2832	3,94056
tet oncogene family member 3	TET3	4,58E-05	56,702	3,93974
protein disulfide isomerase family A, member 5	PDIA5	0,00077234	16,3394	3,92743
serologically defined colon cancer antigen 1	SDCCAG1	0,00364735	10,0277	3,92521
microtubule associated serine/threonine kinase 2	MAST2	5,24E-05	49,9381	3,92309
RAN binding protein 2	RANBP2	0,00384644	16,5273	3,9181
KIAA1731	KIAA1731	8,66E-07	250,573	3,90741
Nipped-B homolog (Drosophila)	NIPBL	0,0029709	25,7133	3,90717
tetratricopeptide repeat domain 3	TTC3	1,88E-05	55,0812	3,90199
zinc finger, CCHC domain containing 6	ZCCHC6	0,00023618	24,2746	3,8938
chromosome 10 open reading frame 18	C10orf18	0,00417975	18,3095	3,89351
WD repeat and SOCS box-containing 1	WSB1	0,00235244	8,51539	3,89063
TIA1 cytotoxic granule-associated RNA binding protein	TIA1	3,56E-06	136,87	3,88799
nuclear receptor subfamily 2, group C, member 1	NR2C1	0,00011958	41,8355	3,88494
trinucleotide repeat containing 6A	TNRC6A	1,19E-05	81,2568	3,88493
RAB3 GTPase activating protein subunit 2 (non-catalytic)	RAB3GAP2	1,07E-05	99,5692	3,88422
serrate RNA effector molecule homolog (Arabidopsis)	SRRT	0,00052481	41,633	3,88375
ubiquitin protein ligase E3 component n-recognin 2	UBR2	3,19E-07	264,825	3,8767
KIAA1468	KIAA1468	1,63E-05	69,779	3,87347
tetratricopeptide repeat domain 17	TTC17	9,89E-05	39,9774	3,87294
ankyrin repeat domain 20 family, member A1 /// ankyrin repeat domain 20 family,	ANKRD20A1 /// ANKRD20A2 /// ANKRD20A3 /// ANKRD20A4 /// C21orf81 /// LOC10013273	1,19E-05	85,2916	3,87284
REV1 homolog (S. cerevisiae)	REV1	4,56E-07	242,813	3,87139
solute carrier family 11 (proton-coupled divalent metal ion transporters), membe	SLC11A2	0,00016229	115,855	3,86652
M-phase phosphoprotein 9	MPHOSPH9	0,0001414	38,733	3,86383
epithelial splicing regulatory protein 2	ESRP2	4,10E-05	143,091	3,86354
budding uninhibited by benzimidazoles 1 homolog beta (yeast)	BUB1B	9,23E-06	276,178	3,85514
protein phosphatase 4, regulatory subunit 1	PPP4R1	4,81E-05	44,2394	3,8495
pecanex homolog (Drosophila)	PCNX	0,00013878	35,3937	3,84702
transformer 2 beta homolog (Drosophila)	TRA2B	6,05E-07	451,451	3,83926
UTP6, small subunit (SSU) processome component, homolog (yeast)	UTP6	0,00020625	41,8008	3,83788
cullin 9	CUL9	0,00024404	26,8109	3,83574
DNA cross-link repair 1C (PSO2 homolog, S. cerevisiae)	DCLRE1C	4,01E-05	74,7695	3,82301
RAP1 interacting factor homolog (yeast)	RIF1	0,00214079	14,4017	3,81334

general transcription factor IIIC, polypeptide 1, alpha 220kDa	GTF3C1	0,00019821	28,1006	3,80994
mediator of DNA damage checkpoint 1	MDC1	3,93E-05	72,1118	3,80971
myeloid/lymphoid or mixed-lineage leukemia (trithorax homolog, Drosophila); tran	MLLT10	0,00017143	35,7683	3,80766
polymerase (DNA directed), epsilon 2 (p59 subunit)	POLE2	0,00018554	64,7354	3,80651
WEE1 homolog (S. pombe)	WEE1	0,00047047	38,6743	3,79456
interleukin enhancer binding factor 3, 90kDa	ILF3	4,12E-06	233,704	3,78989
EF-hand calcium binding domain 7	EFCAB7	3,90E-07	307,755	3,78788
zinc finger CCCH-type containing 11A	ZC3H11A	0,00048792	19,8474	3,77819
HMG box domain containing 3	HMGXB3	0,00017024	33,6757	3,77431
TATA box binding protein (TBP)-associated factor, RNA polymerase I, D, 41kDa	TAF1D	7,10E-05	92,2369	3,77242
nuclear receptor coactivator 3	NCOA3	0,00059223	21,6546	3,77156
nucleoporin 210kDa	NUP210	0,0001579	67,7017	3,7689
F-box protein 11	FBXO11	0,00103972	14,7975	3,76769
AT rich interactive domain 1A (SWI-like)	ARID1A	0,0006997	18,6094	3,76711
eyes absent homolog 4 (Drosophila)	EYA4	7,19E-07	221,046	3,75617
topoisomerase (DNA) II alpha 170kDa	TOP2A	3,59E-06	934,105	3,75529
splicing factor, arginine/serine-rich 8 (suppressor-of-white-apricot homolog, Dr	SFRS8	1,73E-06	153,191	3,75214
chromosome 14 open reading frame 106	C14orf106	1,91E-05	90,6994	3,75107
Rac GTPase activating protein 1	RACGAP1	5,70E-05	242,859	3,75041
ubiquitin specific peptidase 24	USP24	1,80E-07	316,865	3,74996
phosphoribosylglycinamide formyltransferase, phosphoribosylglycinamide synthetas	GART	0,00095422	46,4999	3,74686
patched homolog 1 (Drosophila)	PTCH1	8,69E-06	98,4161	3,74501
SCY1-like 3 (S. cerevisiae)	SCYL3	2,22E-07	306,319	3,74466
enhancer of zeste homolog 1 (Drosophila)	EZH1	0,00041334	21,9549	3,7409
zinc finger, FYVE domain containing 16	ZFYVE16	0,00045886	18,5281	3,7407
kinesin family member 2C	KIF2C	0,00092433	38,6922	3,7377
HIR histone cell cycle regulation defective homolog A (S. cerevisiae)	HIRA	0,00097777	23,5424	3,73535
valyl-tRNA synthetase	VARS	4,23E-05	69,612	3,73358
carboxylesterase 3	CES3	1,04E-06	548,478	3,72943
cadherin, EGF LAG seven-pass G-type receptor 2 (flamingo homolog, Drosophila)	CELSR2	3,74E-05	66,1731	3,72845
bromodomain containing 1	BRD1	0,00279281	9,84351	3,72744
cysteine sulfinic acid decarboxylase	CSAD	0,0002436	28,154	3,72652
collagen, type IV, alpha 5	COL4A5	1,63E-05	93,7017	3,71811
bromodomain containing 2	BRD2	0,00066697	30,7176	3,71714
interleukin enhancer binding factor 3, 90kDa	ILF3	0,00097959	51,2462	3,71681
CHK2 checkpoint homolog (S. pombe)	CHEK2	0,00037483	43,4352	3,71259
tight junction protein 2 (zona occludens 2)	TJP2	5,04E-05	65,261	3,71125
neuroblastoma breakpoint family, member 10 /// neuroblastoma breakpoint family, ArfGAP with coiled-coil, ankyrin repeat and PH domains 2	NBPF10 /// NBPF11 /// ACAP2	5,59E-06	109,236	3,70935
SET domain containing 5	SETD5	8,82E-06	85,9227	3,70254
mannosidase, alpha, class 2A, member 2	MAN2A2	2,86E-06	207,289	3,69894
tuberous sclerosis 1	TSC1	0,00064085	18,763	3,69792
nuclear transcription factor, X-box binding 1	NFX1	0,00091545	27,9799	3,69251
triple functional domain (PTPRF interacting)	TRIO	0,00050682	20,1613	3,68783
Eukaryotic translation initiation factor 2C, 2	EIF2C2	1,38E-05	102,826	3,68312

chromosome 1 open reading frame 112	C1orf112	0,00016642	39,1213	3,68201
CTP synthase II	CTPS2	0,00010038	57,7538	3,68049
ArfGAP with GTPase domain, ankyrin repeat and PH domain 1	AGAP1	7,62E-05	48,3148	3,67846
Mdm4 p53 binding protein homolog (mouse)	MDM4	0,00178747	21,8609	3,67821
coiled-coil domain containing 132	CCDC132	2,85E-05	66,1813	3,67625
MORC family CW-type zinc finger 2	MORC2	0,00142944	27,1088	3,67121
tetratricopeptide repeat domain 17	TTC17	2,42E-08	668,014	3,67005
protein kinase N2	PKN2	0,00086393	44,0119	3,66974
PH domain and leucine rich repeat protein phosphatase-like	PHLPPL	7,44E-06	91,6103	3,66828
coiled-coil domain containing 18	CCDC18	3,93E-06	121,229	3,66207
Notch homolog 2 (Drosophila)	NOTCH2	0,0005966	23,4395	3,6613
splicing factor, arginine/serine-rich 11	SFRS11	6,59E-06	131,382	3,65794
triple functional domain (PTPRF interacting)	TRIO	0,00013929	33,2249	3,65663
ras homolog gene family, member T2	RHOT2	0,00057106	24,0691	3,65619
TRM1 tRNA methyltransferase 1 homolog (S. cerevisiae)	TRMT1	6,15E-05	94,0553	3,6525
heterogeneous nuclear ribonucleoprotein H1 (H)	HNRNPH1	6,19E-05	91,9112	3,6519
nucleoporin 93kDa	NUP93	0,00122783	40,0257	3,65177
CCR4-NOT transcription complex, subunit 1	CNOT1	0,0008525	58,5631	3,64621
NIMA (never in mitosis gene a)-related kinase 4	NEK4	0,00133744	24,8649	3,64408
sorting nexin 5	SNX5	0,00200469	10,0363	3,6434
peroxisome proliferator-activated receptor gamma, coactivator-related 1	PPRC1	0,000138	45,9145	3,64255
NOP2 nucleolar protein homolog (yeast)	NOP2	0,00107555	39,1623	3,64198
bromodomain PHD finger transcription factor	BPTF	0,00172651	12,0128	3,64054
zinc finger, ZZ-type with EF-hand domain 1	ZZEF1	2,91E-05	62,0716	3,63542
ataxia telangiectasia mutated	ATM	8,69E-06	85,3739	3,63092
Far upstream element (FUSE) binding protein 1	FUBP1	4,85E-05	52,4525	3,62915
tetratricopeptide repeat domain 3	TTC3	0,00031742	18,227	3,6291
transient receptor potential cation channel, subfamily M, member 7	TRPM7	2,15E-05	69,3811	3,62727
programmed cell death 11	PDCD11	1,25E-05	82,7966	3,62686
intersectin 1 (SH3 domain protein)	ITSN1	0,00270773	22,1316	3,62423
leucyl-tRNA synthetase 2, mitochondrial	LARS2	3,27E-07	352,297	3,61944
interleukin enhancer binding factor 3, 90kDa	ILF3	0,00055534	58,5486	3,61891
kinesin family member 2C	KIF2C	2,33E-06	753,845	3,6187
WD repeat and SOCS box-containing 1	WSB1	0,00027812	29,2448	3,61748
ATP-binding cassette, sub-family A (ABC1), member 7	ABCA7	1,41E-05	151,689	3,61669
UHRF1 binding protein 1	UHRF1BP1	0,00238238	44,3228	3,61562
---	---	1,24E-05	86,2699	3,60824
uridine-cytidine kinase 1-like 1	UCKL1	0,00196245	17,363	3,60092
tudor domain containing 9	TDRD9	0,0002694	60,5404	3,60045
KIAA1549	KIAA1549	9,95E-05	50,9675	3,59758
transmembrane and tetratricopeptide repeat containing 4	TMTC4	0,00049841	24,4363	3,59131
sorting nexin 13	SNX13	0,00420809	6,71628	3,58942
KLRAQ motif containing 1	KLRAQ1	8,17E-06	82,1583	3,58876
serologically defined colon cancer antigen 1	SDCCAG1	9,95E-05	39,3904	3,58693
congenital dyserythropoietic anemia, type I	CDAN1	6,81E-06	101,986	3,58416
enhancer of zeste homolog 1 (Drosophila)	EZH1	0,00040044	24,9552	3,58366

SET domain containing 2	SETD2	9,29E-05	46,0255	3,58203
pyruvate dehydrogenase phosphatase regulatory subunit	PDPR	0,00155565	13,4251	3,58152
sterol regulatory element binding transcription factor 1	SREBF1	0,00059841	39,4849	3,57839
bromodomain adjacent to zinc finger domain, 1A	BAZ1A	2,24E-06	155,075	3,56514
enhancer of polycomb homolog 1 (Drosophila)	EPC1	0,00022901	23,9477	3,56238
Janus kinase 1	JAK1	0,00026212	30,4069	3,56085
caprin family member 2	CAPRIN2	3,99E-08	504,275	3,55641
formin-like 2	FMNL2	6,48E-05	44,9996	3,55502
DENN/MADD domain containing 5A	DENND5A	0,00203228	11,3981	3,54946
chromosome 1 open reading frame 27	C1orf27	0,00019182	39,9956	3,54699
chromosome 14 open reading frame 106	C14orf106	0,00074388	19,2468	3,54639
serine/threonine kinase 36, fused homolog (Drosophila)	STK36	1,18E-07	405,814	3,54147
tetratricopeptide repeat domain 13	TTC13	3,07E-05	62,381	3,5412
G kinase anchoring protein 1	GKAP1	0,00014224	51,8048	3,53688
stromal antigen 1	STAG1	4,12E-05	63,3117	3,53539
hook homolog 1 (Drosophila)	HOOK1	7,70E-09	954,875	3,53226
DIS3 mitotic control homolog (S. cerevisiae)	DIS3	0,0003831	22,5611	3,53101
myosin XIX	MYO19	0,00024483	126,035	3,53077
DnaJ (Hsp40) homolog, subfamily C, member 13	DNAJC13	0,00193796	11,8956	3,52868
UTP20, small subunit (SSU) processome component, homolog (yeast)	UTP20	2,47E-05	66,4775	3,5285
nephronophthisis 4	NPHP4	7,72E-08	461,047	3,51995
sorting nexin 14	SNX14	0,00218823	10,2032	3,51995
DEAD (Asp-Glu-Ala-Asp) box polypeptide 17	DDX17	3,18E-05	60,6858	3,51874
ubinuclein 2	UBN2	1,69E-05	87,1555	3,51845
hypothetical protein KIAA1434	RP5-1022P6.2	2,60E-05	68,2994	3,51677
G protein-coupled receptor 133	GPR133	0,00168608	10,9189	3,51592
FtsJ methyltransferase domain containing 2	FTSJD2	0,00349174	9,17377	3,51308
---	---	0,00114377	21,9801	3,5106
RNA polymerase II associated protein 2	RPAP2	2,93E-05	59,2148	3,50535
plakophilin 4	PKP4	0,0020863	9,23178	3,50433
collagen, type XXVII, alpha 1	COL27A1	1,62E-05	71,3924	3,50376
coiled-coil and C2 domain containing 1B	CC2D1B	1,15E-05	81,3249	3,4973
laminin, beta 1	LAMB1	0,00105195	14,122	3,49553
mitochondrial translation optimization 1 homolog (S. cerevisiae)	MTO1	0,00059542	50,2708	3,49445
inversin	INVS	0,00026199	37,3321	3,49406
dynamin binding protein	DNMBP	0,00019163	29,24	3,49115
centrosome and spindle pole associated protein 1	CSPP1	0,00180572	19,6108	3,48889
two pore segment channel 1	TPCN1	3,88E-05	54,2948	3,48847
chaperonin containing TCP1, subunit 6 (zeta) pseudogene 1 /// chaperonin contain	CCT6P1 /// LOC643180	7,82E-05	52,6245	3,48359
intersectin 1 (SH3 domain protein)	ITSN1	0,00049007	24,8328	3,47954
EPS8-like 2	EPS8L2	2,10E-05	68,7621	3,47478
WAS protein family homolog 1 /// WAS protein family homolog 2 pseudogene /// WAS	WASH1 /// WASH2P /// WASH3P /// WASH5P	0,0002995	53,5169	3,47468
coiled-coil domain containing 21	CCDC21	2,29E-08	672,678	3,47157
progestin and adipoQ receptor family member VI	PAQR6	7,75E-05	41,3092	3,46714
cytoplasmic linker associated protein 1	CLASP1	0,00027152	28,4943	3,46646
dpy-19-like 4 (C. elegans)	DPY19L4	0,00093239	13,191	3,46326

sorting nexin 13	SNX13	1,57E-05	70,7662	3,46163
OTU domain containing 4	OTUD4	0,00029222	21,1782	3,46124
vacuolar protein sorting 54 homolog (S. cerevisiae)	VPS54	8,49E-05	58,3592	3,46088
chromosome 14 open reading frame 138	C14orf138	6,85E-06	78,1629	3,45577
MAP kinase interacting serine/threonine kinase 2	MKNK2	2,52E-05	72,2096	3,45505
Hypothetical gene supported by BC029568	MGC39584	1,32E-05	98,4934	3,45045
KIAA0947 protein	KIAA0947	0,00175152	49,882	3,45027
minichromosome maintenance complex component 4	MCM4	0,00035108	39,3344	3,45021
asparagine-linked glycosylation 13 homolog (S. cerevisiae)	ALG13	0,00075349	16,725	3,44921
bromodomain containing 1	BRD1	0,0004566	19,9871	3,44777
ubiquitin specific peptidase 15	USP15	0,00200926	11,492	3,44638
pregnancy-associated plasma protein A, pappalysin 1	PAPPA	0,00224015	11,3119	3,44618
DEAD/H (Asp-Glu-Ala-Asp/His) box polypeptide 11 (CHL1-like helicase homolog, S.	DDX11	1,84E-05	79,363	3,44294
kinesin family member 11	KIF11	2,85E-06	202,805	3,44021
eukaryotic translation initiation factor 2-alpha kinase 3	EIF2AK3	0,00032555	37,3989	3,43816
Wolf-Hirschhorn syndrome candidate 1	WHSC1	0,00063349	28,169	3,43241
TIA1 cytotoxic granule-associated RNA binding protein	TIA1	0,00012414	44,185	3,4297
PIF1 5'-to-3' DNA helicase homolog (S. cerevisiae)	PIF1	0,00010587	47,0498	3,42885
pleckstrin homology domain containing, family G (with RhoGef domain) member 4	PLEKHG4	1,01E-05	92,2686	3,42757
polymerase (RNA) III (DNA directed) polypeptide A, 155kDa	POLR3A	5,76E-06	107,636	3,42704
5'-nucleotidase, cytosolic II	NT5C2	0,00046712	26,7477	3,42524
syntaxin binding protein 3	STXBP3	0,00014892	32,7268	3,42499
IQ motif containing B1	IQCB1	4,03E-05	56,386	3,41889
ATPase family, AAA domain containing 2	ATAD2	3,74E-06	129,749	3,41458
ubiquitin specific peptidase 4 (proto-oncogene)	USP4	7,20E-05	38,4796	3,4138
ubiquitin specific peptidase 37	USP37	3,64E-05	59,0648	3,41298
echinoderm microtubule associated protein like 4	EML4	0,00130778	24,481	3,41136
bromodomain and PHD finger containing, 1	BRPF1	0,00068688	33,8073	3,40933
general transcription factor IIIC, polypeptide 3, 102kDa	GTF3C3	3,08E-06	126,653	3,40775
jumonji, AT rich interactive domain 2	JARID2	2,94E-05	61,7484	3,40653
Myeloid/lymphoid or mixed-lineage leukemia (trithorax homolog, Drosophila)	MLL	2,57E-06	132,224	3,40469
sperm specific antigen 2	SSFA2	0,00019657	36,591	3,40338
E1A binding protein p300	EP300	0,00107624	13,9634	3,3992
ubiquitin specific peptidase 36	USP36	7,85E-05	47,9537	3,39485
cytoskeleton associated protein 5	CKAP5	0,00045035	21,3084	3,39279
nucleoporin 98kDa	NUP98	3,17E-06	170,051	3,39203
ATPase, class II, type 9B	ATP9B	5,99E-05	38,7215	3,39068
ankyrin repeat domain 17	ANKRD17	0,00017409	32,2161	3,39035
nuclear receptor co-repressor 2	NCOR2	0,00032898	18,2242	3,38998
DEAD (Asp-Glu-Ala-Asp) box polypeptide 55	DDX55	0,00179951	35,0561	3,38848
SET binding factor 2	SBF2	0,00325473	7,89144	3,38785
UPF2 regulator of nonsense transcripts homolog (yeast)	UPF2	2,86E-05	81,4823	3,38701
epithelial cell transforming sequence 2 oncogene	ECT2	2,04E-05	310,082	3,38637
potassium intermediate/small conductance	KCNN4	0,00018208	39,7694	3,38577

calcium-activated channel, subfamily N,				
splicing factor, arginine/serine-rich 8 (suppressor-of-white-apricot homolog, Dr	SFRS8	8,03E-05	69,3939	3,38567
laminin, gamma 1 (formerly LAMB2)	LAMC1	0,00376838	42,4843	3,38188
ninein-like	NINL	1,83E-07	326,615	3,38132
KIAA0753	KIAA0753	0,0006035	25,4745	3,3811
family with sequence similarity 160, member A2	FAM160A2	1,42E-06	186,668	3,37906
MAP-kinase activating death domain	MADD	0,00014375	36,1491	3,37604
DEAH (Asp-Glu-Ala-His) box polypeptide 15	DHX15	0,00127369	28,0982	3,37342
WAS protein family homolog 1 /// WAS protein family homolog 2 pseudogene	WASH1 /// WASH2P	8,66E-05	43,5543	3,36036
nuclear transcription factor, X-box binding 1	NFX1	2,22E-07	308,775	3,36026
tripartite motif-containing 37	TRIM37	0,00220038	15,7378	3,35258
atlastin GTPase 2	ATL2	0,00188841	31,7785	3,34905
meningioma expressed antigen 5 (hyaluronidase)	MGEA5	0,0026622	10,3492	3,34696
mitogen-activated protein kinase kinase kinase kinase 5	MAP4K5	0,0027403	8,79414	3,34598
TEL2, telomere maintenance 2, homolog (S. cerevisiae)	TELO2	0,00010198	40,7062	3,33986
ubiquitin specific peptidase 21	USP21	7,72E-06	96,0525	3,33713
protein arginine methyltransferase 7	PRMT7	3,03E-06	148,443	3,33648
chromosome 1 open reading frame 9	C1orf9	6,79E-05	45,3283	3,33579
solute carrier family 6 (neurotransmitter transporter, taurine), member 6	SLC6A6	0,00385272	9,40662	3,3315
small G protein signaling modulator 2	SGSM2	0,00214773	18,38	3,3288
vinculin	VCL	3,61E-06	98,8457	3,32671
unc-51-like kinase 3 (C. elegans)	ULK3	9,14E-05	48,153	3,324
plexin B2	PLXNB2	0,00382343	9,49679	3,32179
---	---	0,00055527	16,8924	3,32168
cancer susceptibility candidate 5	CASC5	9,04E-08	469,613	3,31975
THO complex 1	THOC1	0,00035691	45,9045	3,31972
ArfGAP with GTPase domain, ankyrin repeat and PH domain 3	AGAP3	0,0001824	39,8502	3,31904
inositol polyphosphate-4-phosphatase, type I, 107kDa	INPP4A	0,00039838	19,3447	3,31776
trafficking protein, kinesin binding 1	TRAK1	0,00011002	36,5894	3,31735
vacuolar protein sorting 33 homolog B (yeast)	VPS33B	5,79E-07	222,877	3,31582
ribosomal protein S6 kinase, 52kDa, polypeptide 1	RPS6KC1	8,84E-05	43,2672	3,3148
KIAA1267	KIAA1267	0,00115067	17,364	3,31344
ATPase family, AAA domain containing 2	ATAD2	5,82E-07	243,498	3,30867
Rap guanine nucleotide exchange factor (GEF) 6	RAPGEF6	2,21E-06	136,15	3,30834
K(lysine) acetyltransferase 2A	KAT2A	5,60E-05	110,774	3,30544
eukaryotic elongation factor-2 kinase	EEF2K	1,95E-05	75,6593	3,30504
F-box protein 38	FBXO38	1,25E-05	82,6564	3,30255
importin 9	IPO9	0,00356293	26,4468	3,302
mutY homolog (E. coli)	MUTYH	3,31E-06	274,841	3,30005
ubiquitin specific peptidase 36	USP36	0,00034576	30,7906	3,29863
eukaryotic translation initiation factor 2 alpha kinase 4	EIF2AK4	0,00054608	27,45	3,29807
casein kinase 1, epsilon	CSNK1E	0,00010437	32,5051	3,29635
G kinase anchoring protein 1	GKAP1	8,60E-07	433,033	3,29553
period homolog 2 (Drosophila)	PER2	1,77E-05	71,0906	3,29219
coiled-coil domain containing 14	CCDC14	0,00096293	19,2222	3,29048
insulin-degrading enzyme	IDE	2,78E-06	154,396	3,28246
kinesin family member 21B	KIF21B	9,16E-05	40,7062	3,28014

Nipped-B homolog (Drosophila)	NIPBL	3,77E-05	84,7971	3,27911
zinc finger protein 106 homolog (mouse)	ZFP106	0,00030104	37,3349	3,27695
chromodomain helicase DNA binding protein 7	CHD7	7,36E-05	50,3305	3,27643
polymerase (RNA) III (DNA directed) polypeptide B	POLR3B	0,00015824	32,5565	3,27588
general transcription factor II, i /// general transcription factor II, i, pseud	GTF2I /// GTF2IP1 /// LOC100093631	0,00019394	26,3828	3,27469
Fas (TNFRSF6) binding factor 1	FBF1	0,00016143	33,3552	3,27224
---	---	0,00064602	15,671	3,27073
ATG16 autophagy related 16-like 1 (S. cerevisiae)	ATG16L1	0,00029888	26,1145	3,2673
zinc finger and BTB domain containing 11	ZBTB11	0,00010559	46,5131	3,2646
solute carrier family 38, member 2	SLC38A2	0,00331151	12,6952	3,26231
RNA binding motif protein 25	RBM25	0,00073479	17,2654	3,26133
armadillo repeat containing 8	ARMC8	0,00136587	15,2813	3,25893
Heterogeneous nuclear ribonucleoprotein H1 (H)	HNRNPH1	0,00025168	64,464	3,25519
phosphodiesterase 4D, cAMP-specific (phosphodiesterase E3 dunce homolog, Drosoph	PDE4D	9,37E-05	88,0631	3,25354
phosphoinositide-3-kinase, class 2, alpha polypeptide	PIK3C2A	0,003108	8,88667	3,25325
BMS1 homolog, ribosome assembly protein (yeast)	BMS1	0,00276852	12,1407	3,25158
RecQ protein-like 4	RECQL4	2,81E-05	84,8514	3,25156
MDN1, midasin homolog (yeast)	MDN1	5,00E-05	53,3627	3,25156
ubiquitin specific peptidase 47	USP47	0,00188052	11,8898	3,24698
structural maintenance of chromosomes 5	SMC5	0,00171292	14,4451	3,24465
phosphatidylinositol 4-kinase, catalytic, alpha	PI4KA	0,00140002	12,8333	3,24289
Nipped-B homolog (Drosophila)	NIPBL	6,86E-07	229,341	3,24062
exosome component 10	EXOSC10	0,00022609	33,2571	3,24055
Pyridoxal-dependent decarboxylase domain containing 2	PDXDC2	2,73E-05	72,9761	3,23929
enhancer of polycomb homolog 1 (Drosophila)	EPC1	0,00027719	29,6902	3,2355
transmembrane protein 2	TMEM2	1,85E-06	149,3	3,23385
kinesin light chain 1	KLC1	0,00011964	69,85	3,23159
MAK10 homolog, amino-acid N-acetyltransferase subunit (S. cerevisiae)	MAK10	0,00031784	30,2404	3,22488
testis expressed 15	TEX15	4,91E-05	51,182	3,22383
SVOP-like	SVOPL	2,84E-06	155,135	3,22206
C2 calcium-dependent domain containing 3	C2CD3	0,00011795	32,2628	3,22198
---	---	7,08E-05	38,8975	3,2217
vacuolar protein sorting 13 homolog A (S. cerevisiae)	VPS13A	0,00248068	9,72622	3,22129
phospholipase D1, phosphatidylcholine-specific	PLD1	1,60E-06	171,511	3,21815
retinoblastoma-like 1 (p107)	RBL1	4,57E-05	52,5216	3,21653
DOT1-like, histone H3 methyltransferase (S. cerevisiae)	DOT1L	3,05E-05	60,9989	3,21308
SUMO1/sentrin specific peptidase 6	SENP6	0,00086857	23,4754	3,21272
polymerase (DNA directed), gamma	POLG	8,12E-06	91,2115	3,21208
rapamycin-insensitive companion of mTOR	RICTOR	4,58E-05	49,3899	3,2104
squamous cell carcinoma antigen recognized by T cells 3	SART3	0,00019847	35,2485	3,20946
nucleoporin 155kDa	NUP155	0,00010623	150,582	3,20938
discs, large homolog 1 (Drosophila)	DLG1	0,00011678	40,1553	3,20545
SCY1-like 3 (S. cerevisiae)	SCYL3	2,10E-05	64,9417	3,20506
outer dense fiber of sperm tails 2	ODF2	0,00032549	31,2652	3,20193

ArfGAP with SH3 domain, ankyrin repeat and PH domain 1	ASAP1	2,81E-05	66,0632	3,20054
folliculin interacting protein 1	FNIP1	0,00399874	10,076	3,19859
SECIS binding protein 2	SECISBP2	0,00127968	28,8697	3,19508
ATP-binding cassette, sub-family D (ALD), member 4	ABCD4	0,00104689	13,8689	3,19444
kinesin family member 15	KIF15	0,00022787	43,4135	3,19113
cyclin D binding myb-like transcription factor 1	DMTF1	0,00038403	28,8256	3,19106
ubiquitin-like modifier activating enzyme 3	UBA3	0,00235884	13,4736	3,18971
exportin, tRNA (nuclear export receptor for tRNAs)	XPOT	0,00041383	20,0084	3,18754
family with sequence similarity 48, member A	FAM48A	7,70E-05	57,0592	3,18635
scaffold attachment factor B	SAFB	0,00088263	17,411	3,18565
protein associated with topoisomerase II homolog 1 (yeast)	PATL1	0,00023686	31,0445	3,1854
small nuclear RNA activating complex, polypeptide 4, 190kDa	SNAPC4	7,24E-05	50,0698	3,17766
cadherin, EGF LAG seven-pass G-type receptor 3 (flamingo homolog, Drosophila) /// //	CELSR3 /// SLC26A6	0,00036577	32,5379	3,17619
small nucleolar RNA host gene 12 (non-protein coding)	SNHG12	0,00141884	42,7445	3,17477
cadherin, EGF LAG seven-pass G-type receptor 2 (flamingo homolog, Drosophila)	CELSR2	5,46E-05	49,9685	3,17382
transcription termination factor, RNA polymerase I	TTF1	2,33E-05	81,65	3,17087
ubiquitin specific peptidase 37	USP37	0,00014098	34,4085	3,17003
sema domain, transmembrane domain (TM), and cytoplasmic domain, (semaphorin) 6D	SEMA6D	2,01E-05	78,7465	3,1695
chromosome 9 open reading frame 126	C9orf126	3,52E-07	259,741	3,1683
ubiquitin protein ligase E3B	UBE3B	9,65E-05	34,5438	3,16598
ring finger protein 207	RNF207	3,24E-06	130,382	3,16497
denticleless homolog (Drosophila)	DTL	5,81E-05	131,292	3,1632
TBC1 domain family, member 4	TBC1D4	3,91E-07	285,758	3,15778
lipin 1	LPIN1	0,0003885	31,6272	3,15777
helicase, POLQ-like	HELQ	5,86E-05	49,1875	3,15719
SEC24 family, member B (S. cerevisiae)	SEC24B	0,00245333	10,537	3,15523
centrosomal protein 350kDa	CEP350	0,00059429	31,2299	3,15474
ATPase family, AAA domain containing 2B	ATAD2B	3,15E-06	129,611	3,15129
alanine-glyoxylate aminotransferase 2-like 2	AGXT2L2	3,31E-05	56,4597	3,15067
FK506 binding protein 11, 19 kDa	FKBP11	0,00055404	87,1102	3,14935
diacylglycerol kinase, theta 110kDa	DGKQ	3,61E-06	118,353	3,14876
nucleoporin 214kDa	NUP214	4,69E-07	246,887	3,14091
RNA binding motif protein 10	RBM10	0,00050909	38,3301	3,14025
pericentriolar material 1	PCM1	1,17E-05	90,1024	3,14019
mannosidase, alpha, class 2A, member 2	MAN2A2	5,45E-05	46,9373	3,13852
Transmembrane protein 63A	TMEM63A	0,00013493	34,8238	3,13801
neutral sphingomyelinase (N-SMase) activation associated factor	NSMAF	0,00013336	24,9243	3,13799
nucleolar protein family 6 (RNA-associated)	NOL6	3,33E-05	57,6279	3,13788
cytoplasmic linker associated protein 2	CLASP2	8,84E-05	51,5934	3,13741
---	---	1,48E-06	165,429	3,13599
INO80 homolog (S. cerevisiae)	INO80	7,15E-06	97,8335	3,13527
M-phase phosphoprotein 9	MPHOSPH9	6,70E-07	309,902	3,1335
KIAA0528	KIAA0528	0,00262743	20,7127	3,13065
solute carrier family 26, member 11	SLC26A11	5,17E-06	101,61	3,13062
myosin X	MYO10	0,00070813	17,5612	3,13049

phosphoribosylglycinamide formyltransferase, phosphoribosylglycinamide synthetas	GART	9,70E-06	108,974	3,12921
cysteinyl-tRNA synthetase	CARS	0,00326085	11,5027	3,12899
zinc finger, MYM-type 4	ZMYM4	0,00041125	28,6723	3,12149
transmembrane and tetratricopeptide repeat containing 4	TMTC4	3,07E-06	154,954	3,11505
PWP2 periodic tryptophan protein homolog (yeast)	PWP2	0,00033939	30,7956	3,11499
transmembrane protein 131	TMEM131	0,00060796	16,6437	3,11366
KIAA1529	KIAA1529	6,24E-06	97,0148	3,11321
gon-4-like (C. elegans)	GON4L	1,38E-06	165,258	3,11179
ral guanine nucleotide dissociation stimulator	RALGDS	0,00047623	17,4437	3,11161
polybromo 1	PBRM1	0,00209384	13,0527	3,11107
ATPase type 13A1	ATP13A1	0,00101844	23,4703	3,11038
SWI/SNF related, matrix associated, actin dependent regulator of chromatin, subf	SMARCC1	4,49E-06	149,263	3,1036
Smg-5 homolog, nonsense mediated mRNA decay factor (C. elegans)	SMG5	0,0004602	26,3656	3,1019
myeloid/lymphoid or mixed-lineage leukemia 5 (trithorax homolog, Drosophila)	MLL5	0,00412362	8,12917	3,10185
vacuolar protein sorting 16 homolog A (S. cerevisiae)	VPS16A	0,00264105	10,1397	3,10141
Fanconi anemia, complementation group I	FANCI	1,14E-05	375,546	3,1014
origin recognition complex, subunit 2-like (yeast)	ORC2L	1,60E-06	169,707	3,10125
optic atrophy 1 (autosomal dominant)	OPA1	0,00076369	29,2608	3,10099
heterochromatin protein 1, binding protein 3	HP1BP3	0,00185182	20,2298	3,10014
serologically defined colon cancer antigen 1	SDCCAG1	0,00067873	22,5879	3,09914
Nipped-B homolog (Drosophila)	NIPBL	0,00063113	26,1243	3,09828
ubiquitin specific peptidase 42	USP42	1,83E-06	149,5	3,0972
Fanconi anemia, complementation group A	FANCA	7,13E-05	44,5827	3,09594
Pleckstrin homology domain containing, family A (phosphoinositide binding specif	PLEKHA8	0,00319655	8,24141	3,09552
myeloid/lymphoid or mixed-lineage leukemia (trithorax homolog, Drosophila); tran	MLLT10	1,39E-05	80,6889	3,09472
prematurely terminated mRNA decay factor-like	LOC91431	5,02E-05	45,864	3,09355
minichromosome maintenance complex component 10	MCM10	5,57E-05	55,8933	3,09289
mitogen-activated protein kinase kinase kinase 1	MAP3K1	0,00014773	35,1482	3,09234
protein tyrosine phosphatase, receptor type, f polypeptide (PTPRF), interacting	PPFIA1	0,00362584	8,45988	3,09065
component of oligomeric golgi complex 5	COG5	0,0003744	23,1905	3,09049
tubulin, epsilon 1	TUBE1	0,0022022	10,63	3,08966
enhancer of mRNA decapping 4	EDC4	7,04E-05	45,2295	3,08851
chromodomain helicase DNA binding protein 2	CHD2	8,37E-05	37,9211	3,08626
phosphoinositide-3-kinase, class 2, alpha polypeptide	PIK3C2A	0,00018535	29,8306	3,08469
non-SMC condensin I complex, subunit D2	NCAPD2	0,00167671	43,1278	3,07989
pleckstrin homology-like domain, family B, member 2	PHLDB2	7,14E-05	34,3199	3,07672
mediator complex subunit 13-like	MED13L	0,00359649	7,32372	3,07646
ankyrin repeat domain 32	ANKRD32	6,49E-05	46,0659	3,07375
RecQ protein-like 4	RECQL4	9,56E-05	70,1855	3,07156
WD repeat domain 47	WDR47	4,97E-05	48,1376	3,06719
breast cancer 1, early onset	BRCA1	0,00025558	105,437	3,06642
vacuolar protein sorting 54 homolog (S.	VPS54	0,00256326	30,6463	3,0645

cerevisiae)				
myeloid/lymphoid or mixed-lineage leukemia 4	MLL4	9,05E-06	88,5456	3,06423
insulin-like growth factor 2 mRNA binding protein 3	IGF2BP3	2,29E-05	488,044	3,0634
hypothetical LOC100129637	LOC100129637	1,24E-05	84,746	3,05889
BTG3 associated nuclear protein	BANP	0,00018207	82,5191	3,05754
Rho GTPase activating protein 21	ARHGAP21	0,00049479	17,542	3,05749
WD repeat domain 35	WDR35	0,0001256	33,1154	3,05492
myotubularin related protein 15	MTMR15	9,90E-06	102,474	3,05239
amylase, alpha 2B (pancreatic)	AMY2B	2,47E-07	309,068	3,05201
structural maintenance of chromosomes 5	SMC5	0,00044508	24,1599	3,05107
KIAA0355	KIAA0355	0,0019854	10,6292	3,04997
RAB GTPase activating protein 1-like	RABGAP1L	2,93E-05	75,315	3,04948
DEAD (Asp-Glu-Ala-Asp) box polypeptide 46	DDX46	0,00070949	63,4857	3,04825
AP1 gamma subunit binding protein 1	AP1GBP1	6,84E-06	88,443	3,04677
DEAH (Asp-Glu-Ala-His) box polypeptide 35	DHX35	9,77E-06	88,6364	3,04492
small nucleolar RNA host gene 12 (non-protein coding)	SNHG12	1,14E-05	287,63	3,04445
methyl-CpG binding domain protein 6	MBD6	5,21E-05	56,7908	3,04321
chromosome 6 open reading frame 70	C6orf70	0,00052258	22,0297	3,04065
FAST kinase domains 1	FASTKD1	0,00097864	33,4201	3,03755
GRIP and coiled-coil domain containing 2	GCC2	0,00313767	10,498	3,03701
WNK lysine deficient protein kinase 1	WNK1	0,00042621	25,8978	3,03686
ATP citrate lyase	ACLY	0,00265625	19,6703	3,03614
cell division cycle 7 homolog (S. cerevisiae)	CDC7	0,00026841	111,036	3,0357
SWI/SNF related, matrix associated, actin dependent regulator of chromatin, subf	SMARCA2	0,000118	36,4625	3,03435
general transcription factor II, i /// general transcription factor II, i, pseud	GTF2I /// GTF2IP1 /// LOC100093631	0,00164664	10,4463	3,03119
Scm-like with four mbt domains 1	SFMBT1	0,00025145	43,0744	3,02665
cyclin L2	CCNL2	6,76E-06	99,5047	3,02432
splicing factor, arginine/serine-rich 12	SFRS12	0,00011472	40,4146	3,02328
cyclin-dependent kinase 10	CDK10	2,41E-05	61,2921	3,02282
ubiquitin specific peptidase 31	USP31	2,92E-05	61,5297	3,02198
minichromosome maintenance complex component 8	MCM8	0,0003999	38,5277	3,02132
kinesin family member 4A	KIF4A	1,31E-05	182,349	3,01825
family with sequence similarity 116, member A	FAM116A	0,00129958	32,5834	3,01681
mitogen-activated protein kinase kinase kinase 4	MAP3K4	0,00016371	28,7059	3,0159
fusion (involved in t(12;16) in malignant liposarcoma)	FUS	0,00160755	60,3949	3,01446
hypothetical protein FLJ10404	FLJ10404	4,01E-05	49,3894	3,01398
transferrin receptor (p90, CD71)	TFRC	3,98E-07	260,443	3,01218
alpha thalassemia/mental retardation syndrome X-linked (RAD54 homolog, S. cerevi	ATRX	0,00357242	10,4058	3,01103
casein kinase 1, epsilon	CSNK1E	3,53E-06	122,633	3,01045
son of sevenless homolog 1 (Drosophila)	SOS1	2,60E-05	116,825	3,0104
zinc finger, FYVE domain containing 26	ZFYVE26	0,00148768	12,6676	3,00983
oxysterol binding protein-like 3	OSBPL3	0,00089835	16,6249	3,00516
nardilysin (N-arginine dibasic convertase)	NRD1	0,00076201	17,6045	3,00474
zinc finger protein 207	ZNF207	1,69E-10	3433,99	3,00371
Mdm4 p53 binding protein homolog (mouse)	MDM4	0,00029078	41,5851	3,00121
mitogen-activated protein kinase kinase kinase 4	MAP3K4	0,00012695	32,7608	2,99958

KIAA0319-like	KIAA0319L	0,00041657	27,4865	2,99948
transmembrane channel-like 6	TMC6	0,00061806	42,0653	2,99526
KIAA1671 protein	CTA-221G9.4	8,64E-05	56,9891	2,99297
chromosome 10 open reading frame 76	C10orf76	1,19E-05	79,5657	2,99188
ubiquitin specific peptidase 13 (isopeptidase T-3)	USP13	0,00044256	55,5232	2,99124
transcription factor 12	TCF12	0,00037015	21,0019	2,99121
v-erb-b2 erythroblastic leukemia viral oncogene homolog 2, neuro/glioblastoma de	ERBB2	0,00035192	32,1714	2,99018
ubiquitin specific peptidase 25	USP25	0,00046353	25,8908	2,98505
inositol 1,4,5-triphosphate receptor, type 1	ITPR1	2,52E-05	65,531	2,98168
pyruvate dehydrogenase phosphatase regulatory subunit	PDPR	0,00022953	24,4566	2,98081
chromosome 5 open reading frame 34	C5orf34	3,07E-05	242,069	2,97856
---	---	0,00110229	14,5544	2,97442
signal transducer and activator of transcription 6, interleukin-4 induced	STAT6	0,00144071	17,1751	2,97429
CXXC finger 1 (PHD domain)	CXXC1	1,77E-06	225,579	2,97279
chromosome 4 open reading frame 41	C4orf41	0,00051514	19,4712	2,97079
copine VIII	CPNE8	1,45E-07	384,473	2,96721
DEAD (Asp-Glu-Ala-Asp) box polypeptide 46	DDX46	6,68E-07	224,447	2,96456
family with sequence similarity 40, member A	FAM40A	0,00020005	27,5984	2,9627
ring finger protein 213	RNF213	1,09E-05	84,303	2,96268
MORC family CW-type zinc finger 2	MORC2	5,06E-07	243,299	2,9612
neuralized homolog 4 (Drosophila)	NEURL4	0,0002096	34,5416	2,95937
leukemia inhibitory factor receptor alpha	LIFR	2,65E-05	220,123	2,95795
zinc finger protein 266	ZNF266	2,82E-05	90,3919	2,95625
similar to hCG38149 /// ovostatin /// ovostatin 2	LOC728715 /// OVOS /// OVOS2	1,83E-05	69,6045	2,95443
alveolar soft part sarcoma chromosome region, candidate 1	ASPSCR1	1,76E-06	184,085	2,9515
plexin D1	PLXND1	0,000629	50,4138	2,94995
grainyhead-like 1 (Drosophila)	GRHL1	9,34E-06	89,3555	2,94959
pyruvate dehydrogenase kinase, isozyme 4	PDK4	0,00042192	69,7385	2,94869
RIO kinase 1 (yeast)	RIOK1	0,00148529	44,6054	2,9478
KIAA1219	KIAA1219	0,00417737	8,90889	2,94748
helicase-like transcription factor	HLTF	0,00259232	54,4692	2,94643
RNA binding motif protein 10	RBM10	0,00034772	48,4249	2,94558
mitogen-activated protein kinase kinase kinase 5	MAP3K5	7,54E-06	104,711	2,94424
KIAA0182	KIAA0182	0,00362034	10,3314	2,94391
amyotrophic lateral sclerosis 2 (juvenile)	ALS2	0,00413025	7,99573	2,94144
Rho GTPase activating protein 17	ARHGAP17	0,00148978	11,0126	2,94063
period homolog 1 (Drosophila)	PER1	1,01E-05	100,575	2,94052
signal-induced proliferation-associated 1 like 2	SIPA1L2	2,51E-05	101,148	2,93975
RNA binding motif protein 26	RBM26	6,72E-06	99,5513	2,93848
eukaryotic translation initiation factor 2C, 2	EIF2C2	3,07E-05	84,0121	2,9354
---	---	0,00050783	33,9218	2,93201
Abelson helper integration site 1	AHI1	3,48E-06	124,807	2,9291
Leucine-rich repeats and immunoglobulin-like domains 2	LRIG2	6,09E-05	46,3539	2,92906
thyroid adenoma associated	THADA	0,00014299	31,9304	2,9264
nucleoporin 98kDa	NUP98	7,48E-06	94,6186	2,92434
UPF1 regulator of nonsense transcripts homolog (yeast)	UPF1	0,00140183	14,1021	2,92314
F-box protein 38	FBXO38	0,00034934	27,3055	2,92224

G protein-coupled receptor 126	GPR126	7,98E-09	994,371	2,91604
Janus kinase 1	JAK1	0,00085082	27,8511	2,91603
insulin-like growth factor 2 mRNA binding protein 3	IGF2BP3	0,00044021	105,905	2,91171
chromosome 11 open reading frame 54	C11orf54	0,00049022	30,2365	2,91026
mediator complex subunit 13	MED13	0,0020524	10,6749	2,90985
mitogen-activated protein kinase kinase kinase kinase 5	MAP4K5	6,29E-05	45,4456	2,90946
calcium channel, voltage-dependent, beta 2 subunit	CACNB2	7,68E-05	48,1328	2,90889
DEAH (Asp-Glu-Ala-His) box polypeptide 30	DHX30	0,0039106	20,8988	2,90759
polymerase (RNA) II (DNA directed) polypeptide A, 220kDa	POLR2A	0,00038237	21,3952	2,90744
ArfGAP with RhoGAP domain, ankyrin repeat and PH domain 1	ARAP1	0,0011113	12,5663	2,90568
discs, large homolog 1 (Drosophila)	DLG1	0,00042416	33,0454	2,90421
phospholipase C, gamma 1	PLCG1	0,00110737	16,0295	2,90382
similar to KIF27C	LOC389765	5,02E-05	53,5137	2,90206
---	---	0,00046733	37,7551	2,90108
vacuolar protein sorting 33 homolog B (yeast)	VPS33B	0,00036655	25,2398	2,89942
palmitoyl-protein thioesterase 2	PPT2	4,99E-07	245,74	2,89886
reversion-inducing-cysteine-rich protein with kazal motifs	RECK	0,00022552	187,784	2,89801
tetratricopeptide repeat domain 3	TTC3	0,00209032	9,19536	2,89479
chromosome 5 open reading frame 42	C5orf42	4,24E-07	243,119	2,89441
ubiquitin specific peptidase 28	USP28	0,00130487	17,8703	2,89416
zinc finger and BTB domain containing 40	ZBTB40	0,00010838	40,9028	2,894
ubiquitin associated protein 2-like	UBAP2L	0,00030309	51,8651	2,8938
HEAT repeat containing 6	HEATR6	1,74E-05	65,4152	2,89352
O-linked N-acetylglucosamine (GlcNAc) transferase (UDP-N-acetylglucosamine:polyp	OGT	0,0003472	23,6101	2,89168
tetratricopeptide repeat domain 3	TTC3	0,00012949	37,4186	2,88998
splicing factor, arginine/serine-rich 7, 35kDa	SFRS7	0,00308478	31,5222	2,88826
polymerase (RNA) I polypeptide B, 128kDa	POLR1B	0,00172903	44,0974	2,88759
mediator complex subunit 13-like	MED13L	0,0029855	8,09418	2,88748
phosphodiesterase 8B	PDE8B	3,00E-09	1352,92	2,886
phosphodiesterase 8A	PDE8A	7,75E-05	91,7135	2,88316
discs, large (Drosophila) homolog-associated protein 5	DLGAP5	1,30E-05	120,892	2,88226
spen homolog, transcriptional regulator (Drosophila)	SPEN	0,00113178	18,2183	2,8755
---	---	0,00023392	23,6589	2,87488
KH-type splicing regulatory protein	KHSRP	0,0002272	49,201	2,87373
neuroblastoma breakpoint family, member 10	NBPF10	0,00080454	35,9125	2,87249
mitochondrial translation optimization 1 homolog (S. cerevisiae)	MTO1	2,53E-05	150,533	2,86843
inositol 1,4,5-triphosphate receptor, type 3	ITPR3	0,0001461	67,2478	2,86708
ligase I, DNA, ATP-dependent	LIG1	0,00015049	55,4934	2,86633
NOL1/NOP2/Sun domain family, member 2	NSUN2	0,00026556	202,537	2,86603
nuclear factor of kappa light polypeptide gene enhancer in B-cells inhibitor-lik	NFKBIL2	6,69E-05	43,4284	2,86458
---	---	5,15E-07	298,849	2,86168
tousled-like kinase 2	TLK2	3,41E-05	54,4903	2,85908
golgi autoantigen, golgin subfamily a-like pseudogene /// hypothetical protein L	FLJ40113 /// LOC440295	0,00018011	30,9762	2,85623
myeloid/lymphoid or mixed-lineage leukemia 3	MLL3	0,00272727	9,10746	2,85189

AVL9 homolog (S. cerevisiase)	AVL9	0,00027782	44,8781	2,85164
solute carrier family 7 (cationic amino acid transporter, y+ system), member 6	SLC7A6	0,00013773	55,1003	2,85158
chromosome X open reading frame 15	CXorf15	0,0029365	40,1079	2,85034
tyrosine kinase 2	TYK2	0,00132248	28,5186	2,84938
BAT2 domain containing 1	BAT2D1	0,00319512	21,0829	2,84809
similar to methyltransferase 11 domain containing 1 isoform 2 /// methyltransfer	LOC731602 /// METT11D1	0,00341575	35,373	2,84767
ArfGAP with SH3 domain, ankyrin repeat and PH domain 1	ASAP1	0,00044284	17,3804	2,84692
RAP1 interacting factor homolog (yeast)	RIF1	2,58E-05	63,1139	2,84584
family with sequence similarity 73, member A	FAM73A	5,55E-05	51,3506	2,84501
bromodomain containing 2	BRD2	0,00136143	34,6276	2,84334
polynucleotide kinase 3'-phosphatase	PNKP	0,00010609	76,3614	2,84295
superkiller viralicidic activity 2-like (S. cerevisiae)	SKIV2L	1,57E-06	161,514	2,84053
tankyrase, TRF1-interacting ankyrin-related ADP-ribose polymerase 2	TNKS2	0,00010219	32,7958	2,83974
cytochrome P450, family 27, subfamily B, polypeptide 1	CYP27B1	4,22E-06	116,411	2,83823
RANBP2-like and GRIP domain containing 5 /// RANBP2-like and GRIP domain contain	RGPD5 /// RGPD6 /// RGPD8	0,00131948	13,4185	2,83803
acyl-Coenzyme A dehydrogenase family, member 11	ACAD11	5,18E-06	129,272	2,83783
hypothetical protein LOC283508	LOC283508	7,00E-07	222,533	2,83743
integrator complex subunit 4	INTS4	0,00027218	25,0204	2,83519
KIAA1632	KIAA1632	0,0024275	9,79971	2,83332
SIN3 homolog A, transcription regulator (yeast)	SIN3A	2,58E-05	68,8543	2,83299
optic atrophy 1 (autosomal dominant)	OPA1	0,00030629	37,2327	2,82912
PRP4 pre-mRNA processing factor 4 homolog B (yeast)	PRPF4B	0,00095463	16,5676	2,82826
E4F transcription factor 1	E4F1	0,0037464	33,9216	2,82663
acetoacetyl-CoA synthetase	AACS	0,00145222	11,6539	2,82453
LUC7-like (S. cerevisiae)	LUC7L	7,88E-05	58,3191	2,8221
gon-4-like (C. elegans)	GON4L	4,35E-05	58,6246	2,8203
leucine-rich repeat-containing G protein-coupled receptor 4	LGR4	0,00021516	91,6874	2,81905
mitochondrial translation optimization 1 homolog (S. cerevisiae)	MTO1	2,86E-06	186,42	2,8179
TAF2 RNA polymerase II, TATA box binding protein (TBP)-associated factor, 150kDa	TAF2	0,00079612	16,3235	2,81776
F-box protein, helicase, 18	FBXO18	2,93E-06	127,207	2,81474
zinc finger, MIZ-type containing 2	ZMIZ2	1,70E-05	72,9514	2,81379
CSE1 chromosome segregation 1-like (yeast)	CSE1L	0,00100128	48,7707	2,81303
hypothetical LOC100129637	LOC100129637	1,21E-05	97,8823	2,80781
ankyrin repeat and sterile alpha motif domain containing 1A	ANKS1A	0,00013224	73,6992	2,80659
nuclear receptor coactivator 6	NCOA6	4,82E-05	56,4043	2,80609
SET and MYND domain containing 4	SMYD4	1,81E-05	104,164	2,80296
oxidative-stress responsive 1	OXSR1	0,00400296	8,48576	2,79785
aryl-hydrocarbon receptor repressor	AHRR	5,17E-07	234,908	2,79407
ubiquitin-like with PHD and ring finger domains 1	UHRF1	3,24E-06	819,415	2,79316
alanyl-tRNA synthetase 2, mitochondrial (putative)	AARS2	0,00022699	41,6008	2,79176
Mdm1 nuclear protein homolog (mouse)	MDM1	0,00203332	11,2504	2,79172
PHD finger protein 12	PHF12	0,00073833	20,022	2,79149
---	---	5,43E-08	513,47	2,78938
HEAT repeat containing 1	HEATR1	0,00066299	19,1259	2,78924

adenosine monophosphate deaminase 2 (isoform L)	AMPD2	1,48E-05	77,2912	2,7867
PRP38 pre-mRNA processing factor 38 (yeast) domain containing B	PRPF38B	0,00024788	31,2123	2,78637
ubiquitin-like modifier activating enzyme 6	UBA6	0,00023496	29,374	2,77993
RNA-binding region (RNP1, RRM) containing 3	RNPC3	1,76E-09	1514,73	2,77844
integrator complex subunit 7	INTS7	9,21E-06	162,691	2,77682
zinc finger, CCHC domain containing 2	ZCCHC2	4,17E-06	122,245	2,77513
HECT domain and ankyrin repeat containing, E3 ubiquitin protein ligase 1	HACE1	0,00010088	36,6633	2,77449
MAP-kinase activating death domain	MADD	1,12E-05	84,6106	2,77308
stromal antigen 1	STAG1	0,00024253	23,9204	2,77033
RAD54 homolog B (S. cerevisiae)	RAD54B	0,00015482	36,4319	2,76501
RNA binding motif protein 10	RBM10	0,0005899	53,1591	2,76495
GUF1 GTPase homolog (S. cerevisiae)	GUF1	1,31E-05	84,4767	2,76072
ring finger protein 169	RNF169	0,00066082	29,2992	2,75956
pyridine nucleotide-disulphide oxidoreductase domain 1	PYROXD1	0,00091067	51,4872	2,75942
tubulin folding cofactor D	TBCD	2,26E-05	62,6547	2,75543
zinc finger protein 143	ZNF143	6,31E-06	100,324	2,75252
---	---	0,00090669	14,0614	2,75134
protein kinase N3	PKN3	0,00043352	47,3464	2,75133
integrin-linked kinase-associated serine/threonine phosphatase 2C	ILKAP	0,0004981	29,6404	2,74635
importin 5	IPO5	7,92E-05	43,903	2,74623
intersectin 1 (SH3 domain protein)	ITSN1	8,77E-06	82,6682	2,74589
zinc finger protein 280D	ZNF280D	1,74E-06	150,389	2,74516
RNA polymerase II associated protein 1	RPAP1	0,00070187	20,4795	2,74418
adaptor-related protein complex 3, delta 1 subunit	AP3D1	0,00179117	20,1505	2,74335
similar to methyltransferase 11 domain containing 1 isoform 2 /// methyltransfer	LOC731602 /// METT11D1	1,28E-05	269,567	2,74112
phosphorylase kinase, alpha 1 (muscle)	PHKA1	0,0001691	51,1251	2,73816
DEAD (Asp-Glu-Ala-Asp) box polypeptide 31	DDX31	6,84E-05	40,9332	2,7375
solute carrier family 7 (cationic amino acid transporter, y+ system), member 6	SLC7A6	0,00023813	32,8353	2,73505
protogenin homolog (Gallus gallus)	PRTG	5,81E-06	101,216	2,7341
RAD9 homolog A (S. pombe)	RAD9A	0,00030703	26,3663	2,73037
ubiquitin-conjugating enzyme E2O	UBE2O	3,02E-05	61,4009	2,72764
Pentatricopeptide repeat domain 3	PTCD3	7,31E-07	223,9	2,72698
AF4/FMR2 family, member 4	AFF4	0,00260617	10,537	2,72688
KIAA1468	KIAA1468	6,98E-05	40,0658	2,72664
enolase superfamily member 1	ENOSF1	0,0019313	131,134	2,72663
sulfotransferase family, cytosolic, 1A, phenol-preferring, member 1	SULT1A1	0,00100102	36,514	2,72618
TBC1 domain family, member 4	TBC1D4	0,00013586	44,6969	2,71913
partner and localizer of BRCA2	PALB2	0,00081864	30,0381	2,71846
echinoderm microtubule associated protein like 4	EML4	0,00045217	30,9889	2,71529
---	---	8,53E-05	51,981	2,71495
---	---	3,38E-05	66,1132	2,71332
cyclin G associated kinase	GAK	0,00355508	14,5528	2,71325
ubiquitin specific peptidase 7 (herpes virus-associated)	USP7	0,00082817	23,1854	2,71241
protein tyrosine phosphatase, non-receptor type 4 (megakaryocyte)	PTPN4	5,13E-06	316,499	2,71239
metal response element binding transcription factor 2	MTF2	0,00014859	69,5334	2,71167
hypothetical protein LOC153346	LOC153346	0,00011741	37,2206	2,71152
CCR4-NOT transcription complex, subunit 2	CNOT2	0,00241412	12,9959	2,70973

calpain 7	CAPN7	1,53E-05	80,1661	2,70876
KIAA0999 protein	KIAA0999	0,00073227	16,4324	2,70847
Dedicator of cytokinesis 5	DOCK5	5,84E-05	48,4564	2,70445
integrator complex subunit 3	INTS3	0,00165128	33,2847	2,70343
similar to hCG2042915	LOC100129673	0,00074472	123,752	2,7024
tetratricopeptide repeat, ankyrin repeat and coiled-coil containing 2	TANC2	1,98E-05	68,5334	2,70207
phosphofructokinase, platelet	PFKP	0,00065067	15,9152	2,70137
protein tyrosine phosphatase, receptor type, J	PTPRJ	0,00403285	10,278	2,70106
chromosome 18 open reading frame 8	C18orf8	0,00020649	31,2683	2,69748
WD repeat domain 36	WDR36	5,18E-06	108,019	2,69738
protein kinase, DNA-activated, catalytic polypeptide	PRKDC	0,0021837	15,992	2,69219
---	---	2,63E-05	62,1661	2,69062
La ribonucleoprotein domain family, member 1	LARP1	0,00101271	24,8052	2,68868
roundabout, axon guidance receptor, homolog 1 (Drosophila)	ROBO1	0,00040554	67,4234	2,68805
centrosomal protein 120kDa	CEP120	0,00151872	12,5099	2,68758
aldehyde dehydrogenase 18 family, member A1	ALDH18A1	0,00013943	34,6613	2,68622
G protein-coupled receptor kinase interacting ArfGAP 2	GIT2	0,0008851	13,6489	2,68565
growth arrest-specific 5 (non-protein coding)	GAS5	0,00383876	14,1632	2,68521
ataxin 2	ATXN2	0,00044524	23,1255	2,68187
transducin-like enhancer of split 2 (E(sp1) homolog, Drosophila)	TLE2	2,86E-05	164,693	2,67757
erbb2 interacting protein	ERBB2IP	0,00252572	12,2972	2,67757
---	---	8,55E-07	227,112	2,67628
tubulin, gamma complex associated protein 3	TUBGCP3	5,61E-05	104,09	2,67307
transmembrane and coiled-coil domains 6	TMCO6	7,46E-06	97,6967	2,67268
insulin-like growth factor 1 receptor	IGF1R	4,89E-06	114,511	2,67241
far upstream element (FUSE) binding protein 1	FUBP1	0,00048836	49,749	2,67223
enolase superfamily member 1	ENOSF1	9,72E-05	269,011	2,66972
---	---	5,92E-05	43,4302	2,66894
zinc finger protein 341	ZNF341	1,17E-07	368,934	2,6684
transcription termination factor, RNA polymerase I	TTF1	0,00019853	27,4997	2,66613
YTH domain containing 1	YTHDC1	0,00110736	15,6259	2,66497
integrator complex subunit 6	INTS6	0,00233436	18,0399	2,66225
---	---	0,00049754	21,8851	2,66054
muskelin 1, intracellular mediator containing kelch motifs	MKLN1	0,00013908	32,0132	2,66038
microtubule-associated protein 7	MAP7	0,00036434	168,273	2,65696
heterogeneous nuclear ribonucleoprotein H1 (H)	HNRNPH1	0,00034559	27,1512	2,65163
---	---	7,56E-06	99,7016	2,64832
metal response element binding transcription factor 2	MTF2	0,00039163	158,068	2,64659
pleckstrin homology domain interacting protein	PHIP	1,18E-07	383,696	2,64594
BTG3 associated nuclear protein	BANP	0,00076974	115,309	2,64558
E1A binding protein p300	EP300	0,00010678	35,929	2,64521
AT rich interactive domain 2 (ARID, RFX-like)	ARID2	0,00025722	24,8595	2,64463
PAP associated domain containing 4	PAPD4	1,04E-05	85,5391	2,64252
F-box protein 41	FBXO41	8,73E-06	136,141	2,64173
timeless homolog (Drosophila)	TIMELESS	6,16E-06	482,785	2,64169
exonuclease NEF-sp	LOC81691	1,60E-07	359,538	2,64142

mutS homolog 2, colon cancer, nonpolyposis type 1 (E. coli)	MSH2	5,37E-05	88,2713	2,63812
thymine-DNA glycosylase	TDG	0,00150417	35,6642	2,6367
TAF5 RNA polymerase II, TATA box binding protein (TBP)-associated factor, 100kDa	TAF5	0,00022257	36,415	2,63637
---	---	0,00181684	19,0743	2,63472
chromosome 4 open reading frame 41	C4orf41	0,00028739	24,4894	2,63331
pericentriolar material 1	PCM1	0,00131431	26,5272	2,63153
diaphanous homolog 3 (Drosophila)	DIAPH3	0,00248351	34,8516	2,63119
Serine racemase	SRR	1,83E-07	376,025	2,63103
dipeptidyl-peptidase 8	DPP8	7,58E-06	84,8457	2,63094
salt-inducible kinase 2	SIK2	0,00029669	63,2785	2,62644
serine/threonine kinase 36, fused homolog (Drosophila)	STK36	8,38E-07	205,659	2,62628
Pvt1 oncogene (non-protein coding)	PVT1	9,14E-06	222,853	2,62308
inositol polyphosphate phosphatase-like 1	INPPL1	0,00122344	31,2342	2,62204
Werner syndrome, RecQ helicase-like	WRN	1,99E-05	66,9912	2,62172
zinc finger RNA binding protein	ZFR	7,39E-05	53,4765	2,62153
---	---	0,0002542	31,8254	2,61895
ANKHD1-EIF4EBP3 readthrough transcript /// eukaryotic translation initiation fac	ANKHD1-EIF4EBP3 /// EIF4EBP3	7,65E-05	32,2262	2,61879
DEAD (Asp-Glu-Ala-Asp) box polypeptide 17	DDX17	0,00111315	30,2329	2,61828
sorting nexin 5	SNX5	0,00044481	24,3452	2,61794
CCR4-NOT transcription complex, subunit 2	CNOT2	0,00037295	28,0351	2,61749
E1A binding protein p400	EP400	0,00050116	22,7291	2,61736
TEL2, telomere maintenance 2, homolog (S. cerevisiae)	TELO2	0,00023308	32,1539	2,61521
polymerase (RNA) III (DNA directed) polypeptide E (80kD)	POLR3E	2,40E-05	63,5561	2,6133
eukaryotic translation initiation factor 4 gamma, 3	EIF4G3	0,00012817	27,0057	2,60737
hypothetical protein FLJ11822	LOC440434	0,00217024	21,1489	2,60731
sorting nexin 5	SNX5	0,00118558	14,5763	2,60617
golgi autoantigen, golgin subfamily a, 2-like 1	GOLGA2L1	3,35E-06	120,435	2,60604
ATP/GTP binding protein 1	AGTPBP1	0,00017589	55,4245	2,60596
protein tyrosine phosphatase, non-receptor type 12	PTPN12	0,00194211	9,7258	2,60558
chromosome 3 open reading frame 63	C3orf63	0,00061755	76,1233	2,60556
EPH receptor A2	EPHA2	0,00258324	10,1639	2,60542
kelch-like 2, Mayven (Drosophila)	KLHL2	0,00292937	9,60065	2,60184
sphingomyelin phosphodiesterase 4, neutral membrane pseudogene /// sphingomyelin	LOC150776 /// SMPD4	5,21E-07	265,15	2,59883
non-SMC condensin I complex, subunit H	NCAPH	1,40E-06	236,486	2,59857
coiled-coil domain containing 130	CCDC130	0,00011763	40,9095	2,59693
cell division cycle 25 homolog A (S. pombe)	CDC25A	6,27E-06	476,771	2,59442
importin 9	IPO9	3,11E-05	75,6989	2,59294
mixed lineage kinase 4	KIAA1804	0,00112466	41,3608	2,59288
asp (abnormal spindle) homolog, microcephaly associated (Drosophila)	ASPM	4,10E-05	55,7148	2,59212
cyclin F	CCNF	9,57E-07	214,351	2,59059
SIN3 homolog B, transcription regulator (yeast)	SIN3B	7,73E-06	95,0777	2,59058
cullin-associated and neddylation-dissociated 1	CAND1	0,00419301	8,43161	2,58963
REST corepressor 3	RCOR3	5,52E-05	50,0561	2,58873
DEAD/H (Asp-Glu-Ala-Asp/His) box	DDX11	1,48E-05	108,767	2,58806

polypeptide 11 (CHL1-like helicase homolog, S.				
metal response element binding transcription factor 2	MTF2	0,00040857	57,5785	2,58748
ubiquitin specific peptidase 4 (proto-oncogene)	USP4	0,00158979	11,8029	2,58748
DENN/MADD domain containing 5B	DENND5B	3,83E-05	89,3359	2,587
---	---	0,00258512	9,20989	2,58675
nuclear protein, ataxia-telangiectasia locus	NPAT	2,07E-07	332,701	2,58653
mindbomb homolog 1 (Drosophila)	MIB1	0,00189538	10,1861	2,58606
protein kinase-like protein SgK493	SGK493	0,00024911	39,5926	2,58603
discoidin domain receptor tyrosine kinase 1	DDR1	0,00223013	36,4308	2,58525
exocyst complex component 2	EXOC2	8,98E-05	37,7128	2,58462
DENN/MADD domain containing 3	DENND3	0,00025736	28,8204	2,58183
SCL/TAL1 interrupting locus	STIL	6,19E-05	217,949	2,58129
mbt domain containing 1	MBTD1	0,00082599	18,2775	2,57881
leucyl-tRNA synthetase	LARS	0,00075121	15,5358	2,57759
plakophilin 4	PKP4	0,00014161	32,9128	2,57664
papilin, proteoglycan-like sulfated glycoprotein	PAPLN	1,23E-08	851,202	2,57574
---	---	0,00017424	34,9533	2,5747
neural precursor cell expressed, developmentally down-regulated 4-like	NEDD4L	9,40E-07	222,592	2,57107
fibroblast growth factor receptor 3	FGFR3	2,00E-05	81,0534	2,57013
leucine rich repeat containing 1	LRRC1	0,00015737	36,727	2,56986
proteasome (prosome, macropain) activator subunit 4	PSME4	0,00095488	15,8975	2,56772
tensin 1	TNS1	0,00118427	64,5269	2,56583
RAN binding protein 2	RANBP2	9,26E-06	87,1519	2,56502
transformer 2 beta homolog (Drosophila)	TRA2B	0,00042026	80,2258	2,56447
---	---	0,00144866	17,9826	2,56443
transducin-like enhancer of split 4 (E(sp1) homolog, Drosophila)	TLE4	2,82E-05	83,3729	2,56355
ubiquitination factor E4A (UFD2 homolog, yeast)	UBE4A	7,64E-05	34,1204	2,56346
ArfGAP with SH3 domain, ankyrin repeat and PH domain 1	ASAP1	0,0002617	35,9582	2,55799
nuclear receptor subfamily 2, group C, member 1	NR2C1	0,00011205	42,8861	2,55775
GTPase activating Rap/RanGAP domain-like 4	GARNL4	1,92E-05	228,941	2,5566
ring finger and WD repeat domain 3	RFWD3	0,00042522	62,4387	2,55476
WD repeat domain 26	WDR26	2,86E-05	111,048	2,55455
spastic paraplegia 7 (pure and complicated autosomal recessive)	SPG7	0,00028927	25,4479	2,55122
RAD50 interactor 1	RINT1	0,00023427	38,1856	2,54986
armadillo repeat containing 8	ARMC8	0,00255948	14,5381	2,5493
protein kinase D3	PRKD3	0,00216239	23,7995	2,54902
tumor necrosis factor, alpha-induced protein 3	TNFAIP3	0,00011946	38,8432	2,54715
ubiquitin specific peptidase 13 (isopeptidase T-3)	USP13	0,00057909	29,6873	2,54664
integrator complex subunit 6	INTS6	0,00105229	29,7896	2,54445
ATPase family, AAA domain containing 3B /// similar to AAA-ATPase TOB3	ATAD3B /// LOC732419	0,00130388	22,5982	2,54284
zinc finger protein 106 homolog (mouse)	ZFP106	0,00099301	24,7859	2,54065
myeloid/lymphoid or mixed-lineage leukemia (trithorax homolog, Drosophila); tran	MLLT6	0,00068124	26,3009	2,53893
lysine (K)-specific demethylase 6A	KDM6A	3,65E-05	49,2005	2,53615
MCF.2 cell line derived transforming sequence	MCF2	9,86E-06	90,9737	2,53607
euchromatic histone-lysine N-	EHMT2	2,95E-05	61,2759	2,53585

methyltransferase 2				
Myeloid/lymphoid or mixed-lineage leukemia (trithorax homolog, Drosophila)	MLL	1,29E-05	79,1388	2,53515
ADP-ribosylation factor GTPase activating protein 2	ARFGAP2	0,00132633	27,5458	2,53282
nuclear factor related to kappaB binding protein	NFRKB	1,36E-06	185,413	2,53226
zinc finger protein 592	ZNF592	0,00059165	17,7572	2,53045
---	---	0,00336613	7,36668	2,52955
exportin 5	XPO5	1,42E-05	79,8841	2,52881
interferon induced with helicase C domain 1	IFIH1	0,00266471	17,4815	2,52384
sex comb on midleg homolog 1 (Drosophila)	SCMH1	1,34E-06	197,836	2,52299
PCF11, cleavage and polyadenylation factor subunit, homolog (S. cerevisiae)	PCF11	0,00076132	18,1094	2,5222
ATR interacting protein	ATRIP	2,81E-05	92,5173	2,51636
cell division cycle 27 homolog (S. cerevisiae)	CDC27	0,00010765	40,4866	2,51458
origin recognition complex, subunit 1-like (yeast)	ORC1L	0,00018272	50,9848	2,51331
DIS3 mitotic control homolog (S. cerevisiae)	DIS3	1,12E-05	75,518	2,51256
transmembrane protein 209	TMEM209	9,99E-05	79,8279	2,51227
ubiquitin protein ligase E3 component n-recognin 5	UBR5	8,56E-07	189,372	2,5113
DNA methyltransferase 1 associated protein 1	DMAP1	4,02E-05	160,964	2,51122
WD repeat domain 60	WDR60	1,35E-06	171,105	2,5074
minichromosome maintenance complex component 4	MCM4	7,99E-05	57,9566	2,50241
ral guanine nucleotide dissociation stimulator-like 2	RGL2	3,87E-06	122,403	2,49754
MAX gene associated	MGA	0,0004584	21,4447	2,49736
heterogeneous nuclear ribonucleoprotein D-like	HNRPDL	6,54E-06	210,713	2,49412
nuclear receptor co-repressor 1	NCOR1	0,00270798	17,3654	2,49384
copine I	CPNE1	0,00205718	12,8038	2,49322
A kinase (PRKA) anchor protein 8	AKAP8	0,00024555	31,0493	2,49308
v-abl Abelson murine leukemia viral oncogene homolog 2 (arg, Abelson-related gen	ABL2	2,41E-05	85,8135	2,48979
ATP-binding cassette, sub-family C (CFTR/MRP), member 4	ABCC4	6,74E-05	66,9841	2,4886
RNA binding motif protein 9	RBM9	0,00018998	36,9645	2,48776
trinucleotide repeat containing 18	TNRC18	0,00026442	19,6021	2,48759
EH domain binding protein 1	EHBP1	0,00212992	10,2449	2,48491
family with sequence similarity 120A	FAM120A	6,20E-05	64,9891	2,4842
SET domain containing 2	SETD2	0,00335961	13,4377	2,48191
zinc finger protein 274	ZNF274	0,00028856	46,0584	2,48183
hypothetical protein FLJ11822	LOC440434	2,26E-05	90,881	2,47913
LUC7-like (S. cerevisiae)	LUC7L	0,00138669	15,9804	2,47828
heat shock protein 90kDa beta (Grp94), member 1	HSP90B1	0,00022405	56,4266	2,47824
membrane protein, palmitoylated 5 (MAGUK p55 subfamily member 5)	MPP5	0,00409245	15,9898	2,47821
nuclear receptor co-repressor 1	NCOR1	0,00092777	23,5697	2,47612
coiled-coil domain containing 50	CCDC50	2,44E-05	106,123	2,47513
putative homeodomain transcription factor 1	PHTF1	6,40E-05	51,0281	2,47426
kinesin family member 20A	KIF20A	4,61E-07	1108,35	2,47361
minichromosome maintenance complex component 4	MCM4	0,00029526	87,9655	2,47328
zinc finger E-box binding homeobox 1	ZEB1	0,0024066	33,5057	2,47247

inositol 1,3,4,5,6-pentakisphosphate 2-kinase	IPPK	6,96E-06	182,4	2,47165
ATP-binding cassette, sub-family B (MDR/TAP), member 10	ABCB10	0,00131621	30,4478	2,47131
tubulin, gamma complex associated protein 4	TUBGCP4	1,11E-05	176,505	2,46999
angiogenic factor with G patch and FHA domains 1	AGGF1	0,00032002	42,7491	2,46768
tubulin folding cofactor E	TBCE	0,00039864	28,7858	2,46721
ATPase family, AAA domain containing 2	ATAD2	2,17E-05	79,2897	2,467
MUS81 endonuclease homolog (S. cerevisiae)	MUS81	0,00067119	40,4552	2,4656
inhibitor of Bruton agammaglobulinemia tyrosine kinase	IBTK	0,00171543	10,0605	2,46473
HAUS augmin-like complex, subunit 8	HAUS8	3,49E-06	136,008	2,46426
hypothetical LOC644617	LOC644617	0,00277571	10,6573	2,46319
tripartite motif-containing 66	TRIM66	1,12E-05	84,2915	2,46262
HAUS augmin-like complex, subunit 5	HAUS5	2,09E-06	162,886	2,4619
---	---	0,00028748	30,1538	2,46165
solute carrier family 30 (zinc transporter), member 7	SLC30A7	0,00032671	21,1472	2,46012
chromodomain helicase DNA binding protein 1-like	CHD1L	0,00091816	86,8336	2,45981
gem (nuclear organelle) associated protein 5	GEMIN5	0,00261591	14,0869	2,45777
mediator complex subunit 1	MED1	0,00056429	31,5167	2,45528
methylcrotonoyl-Coenzyme A carboxylase 1 (alpha)	MCCC1	0,00035719	75,8984	2,45446
ArfGAP with SH3 domain, ankyrin repeat and PH domain 1	ASAP1	3,58E-05	43,4838	2,45163
WD repeat domain 70	WDR70	0,00108609	41,7415	2,44974
BAT2 domain containing 1	BAT2D1	0,00173906	18,3812	2,44577
transmembrane protein 194A	TMEM194A	0,00215525	30,5423	2,44365
triple functional domain (PTPRF interacting)	TRIO	0,00058146	18,3538	2,44321
caspase 8 associated protein 2	CASP8AP2	0,00035295	25,4067	2,44194
zyg-11 homolog A (C. elegans)	ZYG11A	9,77E-06	109,219	2,44153
---	---	0,00033345	79,0727	2,44135
DEAH (Asp-Glu-Ala-His) box polypeptide 36	DHX36	0,00043788	35,6824	2,43963
protein regulator of cytokinesis 1	PRC1	0,00106399	163,694	2,43607
STE20-like kinase (yeast)	SLK	0,00146429	18,4011	2,43598
cytoplasmic linker associated protein 2	CLASP2	5,06E-06	116,519	2,4359
AHA1, activator of heat shock 90kDa protein ATPase homolog 2 (yeast)	AHSA2	7,47E-05	57,1383	2,43569
kinesin heavy chain member 2A	KIF2A	0,00382442	12,0822	2,4355
feline leukemia virus subgroup C cellular receptor 1	FLVCR1	3,16E-05	85,1992	2,43424
cytokine-like nuclear factor n-pac	N-PAC	0,00021697	30,3577	2,43376
tRNA splicing endonuclease 2 homolog (S. cerevisiae)	TSEN2	0,00151554	17,6031	2,43151
dishevelled, dsh homolog 3 (Drosophila)	DVL3	0,00128817	11,8447	2,42985
importin 11	IPO11	0,00013767	36,9043	2,42945
WD repeat domain 37	WDR37	3,78E-05	45,9028	2,42589
cell division cycle and apoptosis regulator 1	CCAR1	0,00329887	13,645	2,42496
scaffold attachment factor B2	SAFB2	3,84E-05	58,3944	2,42494
cleavage stimulation factor, 3' pre-RNA, subunit 3, 77kDa	CSTF3	0,00088084	24,0448	2,42347
---	---	0,00020453	29,216	2,42208
PHD finger protein 20-like 1	PHF20L1	0,00027421	27,3586	2,42143
zinc finger, CCHC domain containing 2	ZCCHC2	0,00128965	23,5515	2,4191
leucine-rich PPR-motif containing	LRPPRC	0,00099097	22,35	2,41799

NOP56 ribonucleoprotein homolog (yeast)	NOP56	0,00072594	46,7982	2,41779
protein phosphatase 1, regulatory (inhibitor) subunit 10	PPP1R10	0,001157	15,9129	2,41733
RYK receptor-like tyrosine kinase	RYK	0,0008489	13,9834	2,41429
Fanconi anemia, complementation group L	FANCL	0,00010932	109,932	2,41044
vascular endothelial growth factor A	VEGFA	0,00248891	28,5578	2,41023
Alstrom syndrome 1	ALMS1	1,49E-07	362,98	2,4099
transmembrane channel-like 5	TMC5	0,00045688	166,63	2,40759
TATA box binding protein (TBP)-associated factor, RNA polymerase I, C, 110kDa	TAF1C	0,00059155	28,6552	2,40752
ectonucleoside triphosphate diphosphohydrolase 4	ENTPD4	0,00090433	21,5738	2,40729
quiescin Q6 sulfhydryl oxidase 2	QSOX2	0,00146593	21,3747	2,4071
CDK5 regulatory subunit associated protein 3	CDK5RAP3	0,00120466	38,8959	2,40461
ubiquitin specific peptidase 47	USP47	0,00098688	19,5402	2,40284
DEP domain containing 5	DEPDC5	1,15E-05	87,4264	2,40233
---	---	0,00031527	32,6803	2,40185
helicase, lymphoid-specific	HELLS	1,99E-06	145,887	2,40165
ATPase family, AAA domain containing 3B	ATAD3B	0,00241966	18,8836	2,40161
polybromo 1	PBRM1	0,00149824	13,4231	2,39989
IQ motif containing B1	IQCB1	0,00064184	40,1386	2,39913
cysteine-rich, angiogenic inducer, 61	CYR61	0,00254531	90,9866	2,39806
AT rich interactive domain 2 (ARID, RFX-like)	ARID2	0,003681	14,178	2,39782
---	---	9,21E-05	48,9145	2,39482
RALBP1 associated Eps domain containing 1	REPS1	0,00236325	21,0109	2,39079
Ewing sarcoma breakpoint region 1	EWSR1	0,00026755	41,7223	2,38967
DnaJ (Hsp40) homolog, subfamily C, member 16	DNAJC16	0,00058292	22,067	2,38804
RUN and FYVE domain containing 1	RUFY1	0,00028215	25,9386	2,38694
AT-hook transcription factor	AKNA	0,0021387	14,9926	2,38525
mediator complex subunit 1	MED1	0,00132529	41,5003	2,38481
KIAA0564	KIAA0564	4,13E-05	55,0355	2,38402
Suppressor of cytokine signaling 7	SOCS7	0,00065702	26,9539	2,38274
chaperone, ABC1 activity of bc1 complex homolog (S. pombe)	CABC1	0,00204907	43,2406	2,37966
cadherin, EGF LAG seven-pass G-type receptor 1 (flamingo homolog, Drosophila)	CELSR1	0,0002887	26,082	2,37929
S-phase kinase-associated protein 2 (p45)	SKP2	0,00135891	56,3711	2,37782
ras homolog gene family, member T2	RHOT2	0,00035056	65,495	2,37263
signal-induced proliferation-associated 1 like 2	SIPA1L2	0,00026703	71,6381	2,3726
importin 7	IPO7	0,0002946	29,583	2,37157
ADP-ribosylation factor guanine nucleotide-exchange factor 1(brefeldin A-inhibit	ARFGEF1	0,00122761	13,5086	2,36397
zinc finger, MYM-type 3	ZMYM3	0,00039673	21,1238	2,36249
golgi associated, gamma adaptin ear containing, ARF binding protein 1	GGA1	2,34E-05	134,465	2,36078
sorting nexin 25	SNX25	0,00267748	34,0282	2,35974
poly (ADP-ribose) polymerase family, member 9	PARP9	0,00202184	19,7955	2,35842
solute carrier family 4, sodium bicarbonate cotransporter, member 7	SLC4A7	0,0019883	10,7635	2,35716
interferon-induced protein 44	IFI44	0,00015526	344,004	2,35696
TAF4b RNA polymerase II, TATA box binding protein (TBP)-associated factor, 105kD	TAF4B	0,00015656	49,7825	2,35604
influenza virus NS1A binding protein	IVNS1ABP	0,00028088	123,515	2,35516

anaphase promoting complex subunit 5	ANAPC5	0,00020687	105,157	2,35311
ankyrin repeat and BTB (POZ) domain containing 2	ABTB2	0,00126305	22,2638	2,35167
MKL/myocardin-like 2	MKL2	0,0015429	16,4065	2,35029
---	---	4,03E-05	61,6335	2,34963
KRIT1, ankyrin repeat containing	KRIT1	0,00180681	14,4587	2,34767
RRN3 RNA polymerase I transcription factor homolog (S. cerevisiae)	RRN3	0,00018932	32,4971	2,34716
NMDA receptor regulated 2	NARG2	0,00246953	27,7761	2,34549
SET domain, bifurcated 2	SETDB2	0,00011164	39,4122	2,34431
A kinase (PRKA) anchor protein 8-like	AKAP8L	1,22E-05	77,6056	2,34357
microtubule associated serine/threonine kinase-like	MASTL	0,00107418	26,7344	2,34309
ariadne homolog 2 (Drosophila)	ARIH2	0,00020743	77,4114	2,34138
peptidylprolyl isomerase domain and WD repeat containing 1	PPWD1	0,003386	15,1122	2,34008
chromodomain helicase DNA binding protein 8	CHD8	1,90E-06	155,091	2,33826
---	---	0,00027969	31,5993	2,33818
choline kinase beta	CHKB	0,00050762	37,5774	2,3376
dehydrogenase E1 and transketolase domain containing 1	DHTKD1	5,69E-07	1413,07	2,3363
RNA binding motif protein 25	RBM25	1,80E-06	175,724	2,33621
CAS1 domain containing 1	CASD1	8,95E-05	39,62	2,33589
A kinase (PRKA) anchor protein 13	AKAP13	7,18E-05	42,3661	2,33367
FK506 binding protein 15, 133kDa	FKBP15	0,00258856	9,61015	2,33303
G patch domain containing 1	GPATCH1	0,00019319	34,7352	2,33239
---	---	0,00115833	49,6003	2,33056
growth arrest-specific 5 (non-protein coding)	GAS5	0,00338525	136,221	2,33034
DnaJ (Hsp40) homolog, subfamily C, member 6	DNAJC6	0,00027385	208,663	2,32986
phosphatase and actin regulator 4	PHACTR4	0,00115145	21,7677	2,32864
mediator complex subunit 13-like	MED13L	0,00021157	23,7859	2,32728
transformer 2 alpha homolog (Drosophila)	TRA2A	0,00013131	41,9429	2,32461
Rab geranylgeranyltransferase, beta subunit	RABGGTB	0,00325447	69,7279	2,32451
TIA1 cytotoxic granule-associated RNA binding protein	TIA1	4,13E-06	122,404	2,3218
ClpX caseinolytic peptidase X homolog (E. coli)	CLPX	0,00030777	55,4254	2,32046
cystathionase (cystathionine gamma-lyase)	CTH	0,00152153	244,077	2,31902
WD repeat domain 51A	WDR51A	0,00127482	47,2458	2,31657
nucleolar complex associated 3 homolog (S. cerevisiae)	NOC3L	0,00045254	44,0359	2,31607
ATP-binding cassette, sub-family F (GCN20), member 3	ABCF3	0,00024761	35,4196	2,31131
metal response element binding transcription factor 2	MTF2	1,63E-05	745,059	2,31098
melanoma associated antigen (mutated) 1	MUM1	1,11E-05	80,0583	2,30989
zinc finger protein 195	ZNF195	4,16E-05	75,7651	2,30719
ubiquitin associated protein 2-like	UBAP2L	2,36E-06	143,647	2,30701
adaptor-related protein complex 1, gamma 1 subunit	AP1G1	0,00030215	23,313	2,30684
matrin 3	MATR3	0,00356637	26,4384	2,30571
HAUS augmin-like complex, subunit 6	HAUS6	9,28E-05	143,515	2,30494
dual serine/threonine and tyrosine protein kinase	DSTYK	0,00050728	19,3908	2,30233
GRAM domain containing 1B	GRAMD1B	4,59E-06	219,82	2,30192
fermitin family homolog 2 (Drosophila)	FERMT2	0,00165263	49,4742	2,29987
CDC14 cell division cycle 14 homolog B (S. cerevisiae)	CDC14B	0,00292441	9,65336	2,29982
splicing factor, arginine/serine-rich 14	SFRS14	0,00047092	17,9982	2,29948

transporter 2, ATP-binding cassette, sub-family B (MDR/TAP)	TAP2	8,30E-07	234,306	2,29842
Sin3A-associated protein, 130kDa	SAP130	0,00359446	16,2267	2,29716
family with sequence similarity 133, member B /// similar to FAM133B protein	FAM133B /// LOC728153	0,00416721	14,1418	2,29605
NUF2, NDC80 kinetochore complex component, homolog (S. cerevisiae)	NUF2	0,00150063	31,0615	2,29457
ubinuclein 2	UBN2	1,18E-05	90,376	2,29173
---	---	0,00042616	44,0772	2,28952
ataxin 7	ATXN7	0,00032634	29,98	2,28531
neuroblastoma breakpoint family, member 1 /// neuroblastoma breakpoint family, m	NBPF1 /// NBPF10	0,00212371	15,0555	2,28419
chromodomain helicase DNA binding protein 4	CHD4	0,00227247	10,8445	2,2835
EPH receptor B4	EPHB4	0,00032386	32,0342	2,28266
within bgcn homolog (Drosophila)	WIBG	0,00328395	17,5885	2,28084
zinc finger protein 512B	ZNF512B	0,00021014	34,4887	2,28072
G protein-coupled receptor 64	GPR64	8,54E-05	225,262	2,27996
transmembrane protein 87A	TMEM87A	0,00232421	10,6111	2,27943
retinoblastoma binding protein 4	RBBP4	5,38E-05	113,6	2,27941
cysteine and histidine-rich domain (CHORD)-containing 1	CHORDC1	0,00057941	102,471	2,2791
ring finger protein 145	RNF145	0,00192758	10,213	2,2778
nuclear receptor subfamily 4, group A, member 2	NR4A2	0,00370506	30,6437	2,27512
trichoplein, keratin filament binding	TCHP	0,00304725	11,077	2,27183
sulfotransferase family, cytosolic, 1A, phenol-preferring, member 3 /// sulfotra	SULT1A3 /// SULT1A4	0,00065353	47,6042	2,26618
RAD17 homolog (S. pombe)	RAD17	0,00209103	19,6849	2,26533
dehydrogenase E1 and transketolase domain containing 1	DHTKD1	0,00095867	86,1212	2,26233
transforming, acidic coiled-coil containing protein 3	TACC3	0,00053753	32,389	2,26204
lysophosphatidylcholine acyltransferase 4	LPCAT4	0,00025009	27,1465	2,26181
sulfotransferase family, cytosolic, 1A, phenol-preferring, member 2	SULT1A2	0,00172184	26,9928	2,26159
wings apart-like homolog (Drosophila)	WAPAL	0,00308083	14,0363	2,25986
transformer 2 beta homolog (Drosophila)	TRA2B	0,0034232	67,1927	2,25915
exportin 6	XPO6	2,11E-06	142,38	2,25885
transportin 3	TNPO3	0,00398779	30,9932	2,25873
mediator complex subunit 14	MED14	3,21E-06	116,139	2,25572
KIAA0319-like	KIAA0319L	0,00092522	22,1571	2,25536
cysteine conjugate-beta lyase, cytoplasmic	CCBL1	0,00046708	35,616	2,25212
GTPase activating protein and VPS9 domains 1	GAPVD1	0,000733	28,7083	2,24954
proprotein convertase subtilisin/kexin type 9	PCSK9	3,71E-05	264,089	2,2476
CCR4-NOT transcription complex, subunit 10	CNOT10	0,00069036	48,842	2,24751
MAP/microtubule affinity-regulating kinase 3	MARK3	0,00151752	19,909	2,24627
transforming growth factor, beta receptor III	TGFBR3	0,00211199	86,3195	2,24559
metal response element binding transcription factor 2	MTF2	0,00027949	46,931	2,24157
mitogen-activated protein kinase-activated protein kinase 5	MAPKAPK5	4,56E-05	131,931	2,23966
sulfotransferase family, cytosolic, 1A, phenol-preferring, member 3 /// sulfotra	SULT1A3 /// SULT1A4	5,83E-05	240,62	2,23897
USO1 homolog, vesicle docking protein (yeast)	USO1	0,00150767	16,415	2,23689
DEAD (Asp-Glu-Ala-Asp) box polypeptide 56	DDX56	0,00078545	58,7865	2,23553
elongation factor, RNA polymerase II, 2	ELL2	0,00054055	82,2949	2,23474

translocase of inner mitochondrial membrane 44 homolog (yeast)	TIMM44	0,00056016	27,3587	2,23403
UDP-glucose ceramide glucosyltransferase	UGCG	0,00146002	14,3691	2,23312
anaphase promoting complex subunit 10	ANAPC10	0,00016317	83,8828	2,23187
NMD3 homolog (S. cerevisiae)	NMD3	6,86E-06	103,29	2,23142
sulfotransferase family, cytosolic, 1A, phenol-preferring, member 1	SULT1A1	0,00071771	59,9155	2,22985
cleavage and polyadenylation specific factor 7, 59kDa	CPSF7	0,00241052	23,4224	2,22688
flightless I homolog (Drosophila)	FLII	0,00067496	21,3066	2,22672
TNF receptor-associated factor 2	TRAF2	0,00230425	18,2252	2,22654
cell division cycle 25 homolog A (S. pombe)	CDC25A	1,29E-06	241,453	2,22594
v-ets erythroblastosis virus E26 oncogene homolog 2 (avian)	ETS2	0,0001262	52,9549	2,22515
methylenetetrahydrofolate dehydrogenase (NADP+ dependent) 1, methenyltetrahydrof	MTHFD1	0,00265717	64,4014	2,22067
casein kinase 1, gamma 1	CSNK1G1	0,00414223	9,51717	2,22047
ATP citrate lyase	ACLY	0,00033159	30,8457	2,21849
arrestin domain containing 2	ARRDC2	7,64E-06	99,7953	2,21789
Holliday junction recognition protein	HJURP	0,00070371	29,2076	2,21571
HMG box domain containing 4	HMGXB4	0,0012744	17,4325	2,21429
metal-regulatory transcription factor 1	MTF1	0,000131	29,131	2,21306
cullin 5	CUL5	0,00211246	10,6405	2,20864
tRNA splicing endonuclease 2 homolog (S. cerevisiae)	TSEN2	2,64E-05	139,357	2,20712
WW domain containing E3 ubiquitin protein ligase 1	WWP1	0,00130243	15,1937	2,20606
Transcription factor CP2	TFCP2	5,23E-05	59,7516	2,2037
additional sex combs like 1 (Drosophila)	ASXL1	0,00205102	12,9487	2,20347
solute carrier family 25, member 13 (citrin)	SLC25A13	1,72E-05	396,788	2,20287
X-prolyl aminopeptidase (aminopeptidase P) 3, putative	XPNPEP3	2,52E-05	59,7359	2,20264
mutated in colorectal cancers	MCC	0,00068855	29,3284	2,20122
histidine acid phosphatase domain containing 1	HISPPD1	0,00040422	26,7356	2,20088
AT rich interactive domain 5B (MRF1-like)	ARID5B	0,00094463	188,586	2,19951
RAD54-like (S. cerevisiae)	RAD54L	0,00079346	81,2859	2,19824
Rab geranylgeranyltransferase, beta subunit	RABGGTB	0,00034145	83,6862	2,1982
WD repeat domain 85	WDR85	0,00123263	16,2064	2,1943
SUMO1/sentrin/SMT3 specific peptidase 2	SENP2	0,00207322	33,5776	2,19398
NIMA (never in mitosis gene a)-related kinase 3	NEK3	4,26E-06	121,137	2,18928
ankyrin repeat and IBR domain containing 1	ANKIB1	0,00037609	23,5631	2,18721
---	---	0,00209446	19,215	2,18585
coiled-coil domain containing 88A	CCDC88A	4,73E-06	123,576	2,18537
coiled-coil domain containing 76	CCDC76	1,06E-05	201,003	2,18465
anaphase promoting complex subunit 7	ANAPC7	0,00332705	24,3455	2,18465
additional sex combs like 1 (Drosophila)	ASXL1	2,86E-06	137,804	2,18296
POM121 membrane glycoprotein (rat) /// POM121 membrane glycoprotein C	POM121 /// POM121C	0,00014431	65,0554	2,18262
PMS2 postmeiotic segregation increased 2 (S. cerevisiae) /// PMS2 C-terminal lik	PMS2 /// PMS2CL	0,00017091	102,48	2,17752
nuclear receptor subfamily 4, group A, member 2	NR4A2	0,0011511	63,3226	2,17646
DEP domain containing 1	DEPDC1	0,00329199	105,845	2,17613
WW and C2 domain containing 1	WWC1	0,00014231	135,842	2,17522
DEAD (Asp-Glu-Ala-Asp) box polypeptide 20	DDX20	0,00160436	20,5609	2,17232

guanine nucleotide binding protein-like 3 (nucleolar)-like	GNL3L	0,00029022	25,8602	2,17208
ubiquitin specific peptidase 15	USP15	0,00095502	15,9118	2,17134
desmocollin 2	DSC2	0,00027473	64,842	2,16888
MRE11 meiotic recombination 11 homolog A (S. cerevisiae)	MRE11A	0,00273468	24,073	2,16732
---	---	2,73E-05	175,603	2,167
sema domain, immunoglobulin domain (Ig), transmembrane domain (TM) and short cyt	SEMA4C	0,00034902	23,3207	2,16689
cullin 4A	CUL4A	0,00078268	93,6199	2,16668
discoidin domain receptor tyrosine kinase 1	DDR1	0,00012649	165,919	2,16449
ubiquitin interaction motif containing 1	UIMC1	0,00055976	60,1255	2,16228
wings apart-like homolog (Drosophila)	WAPAL	0,00010204	78,7248	2,16227
heterogeneous nuclear ribonucleoprotein D-like	HNRPDL	0,00188172	37,3114	2,1599
zinc finger, MYM-type 4	ZMYM4	0,00109931	19,5252	2,15928
tetratricopeptide repeat domain 14	TTC14	0,0004189	30,6138	2,15829
SAFB-like, transcription modulator	SLTM	0,00370418	23,0499	2,15735
chromosome 9 open reading frame 97	C9orf97	0,0005475	24,8167	2,15391
zinc finger, DHHC-type containing 13	ZDHHC13	0,00033282	27,8188	2,15346
threonyl-tRNA synthetase 2, mitochondrial (putative)	TARS2	0,00016445	59,9781	2,15256
solute carrier family 25 (mitochondrial carrier; Graves disease autoantigen), me	SLC25A16	0,00144947	16,4771	2,15225
phosphodiesterase 4B, cAMP-specific (phosphodiesterase E4 dunce homolog, Drosoph	PDE4B	0,00234344	45,0811	2,15124
---	---	0,00022863	49,225	2,15114
RNA (guanine-7-) methyltransferase	RNMT	0,00037766	26,1348	2,15032
denticleless homolog (Drosophila)	DTL	0,00040502	294,226	2,14476
cytoskeleton associated protein 5	CKAP5	0,00168027	15,0714	2,14223
structural maintenance of chromosomes 2	SMC2	0,00141654	26,7811	2,14102
mediator complex subunit 24	MED24	4,39E-05	51,207	2,14067
thyroid hormone receptor associated protein 3	THRAP3	0,00411058	9,0831	2,13865
---	---	0,00010013	31,8655	2,13545
ankyrin repeat and zinc finger domain containing 1	ANKZF1	3,76E-08	591,251	2,13478
anaphase promoting complex subunit 5	ANAPC5	0,00208735	81,7204	2,13433
BCL6 co-repressor	BCOR	1,24E-05	109,483	2,13396
additional sex combs like 2 (Drosophila)	ASXL2	0,00072449	20,369	2,13388
Bardet-Biedl syndrome 1	BBS1	0,00412099	10,464	2,13358
endothelial PAS domain protein 1	EPAS1	0,00022825	43,1198	2,13219
myosin VB	MYO5B	0,00126796	26,5601	2,13189
PHD finger protein 14	PHF14	0,00048035	47,0072	2,13159
acyl-Coenzyme A dehydrogenase family, member 9	ACAD9	0,00083432	84,5638	2,13013
lipin 2	LPIN2	0,00134616	20,5321	2,12909
chromosome 12 open reading frame 26	C12orf26	0,00074797	22,4019	2,12851
hyaluronan-mediated motility receptor (RHAMM)	HMMR	0,00122448	26,5651	2,12823
cystathionine-beta-synthase	CBS	0,0009543	31,3423	2,12654
nuclear protein localization 4 homolog (S. cerevisiae)	NPLOC4	0,0005279	17,9849	2,12633
cell division cycle 6 homolog (S. cerevisiae)	CDC6	0,00286272	51,491	2,12622
fibrosin-like 1	FBRSL1	0,00224948	35,5906	2,12558
phosphoinositide-3-kinase, catalytic, beta polypeptide	PIK3CB	0,00330122	36,6384	2,12409
serine/arginine repetitive matrix 1	SRRM1	5,58E-05	63,9009	2,12362
lamin B1	LMNB1	0,00025236	196,89	2,12337

spermatogenesis associated 5-like 1	SPATA5L1	0,00013756	182,332	2,12018
acid phosphatase-like 2	ACPL2	0,00012077	42,3937	2,11926
sphingosine-1-phosphate lyase 1	SGPL1	0,00213448	9,40577	2,11434
zinc finger protein 496	ZNF496	0,00046397	39,0403	2,11313
discoidin domain receptor tyrosine kinase 1	DDR1	0,00400771	54,2644	2,11276
patatin-like phospholipase domain containing 3	PNPLA3	0,00314325	20,5332	2,11069
neural precursor cell expressed, developmentally down-regulated 4	NEDD4	1,46E-05	67,253	2,10985
family with sequence similarity 178, member A	FAM178A	3,76E-06	134,429	2,10856
two pore segment channel 1	TPCN1	0,00056991	21,747	2,10839
---	---	0,00024229	276,859	2,10272
protogenin homolog (Gallus gallus)	PRTG	0,00054699	27,7363	2,09821
cystathionase (cystathionine gamma-lyase)	CTH	1,03E-06	2449,31	2,09704
chromodomain helicase DNA binding protein 1-like	CHD1L	0,00036671	73,8302	2,0943
retinoblastoma binding protein 4	RBBP4	0,00061824	52,8377	2,09418
potassium channel tetramerisation domain containing 3	KCTD3	0,00299987	25,1499	2,0937
prolyl 4-hydroxylase, alpha polypeptide I	P4HA1	0,00030058	186,82	2,09104
histone deacetylase 3	HDAC3	0,00010904	43,7354	2,08981
disabled homolog 2, mitogen-responsive phosphoprotein (Drosophila)	DAB2	0,00011674	90,5238	2,08756
component of oligomeric golgi complex 5	COG5	0,00121932	14,2025	2,08717
chromosome X open reading frame 15	CXorf15	0,00340637	24,4345	2,08301
wings apart-like homolog (Drosophila)	WAPAL	0,00018488	36,5023	2,08158
solute carrier family 43, member 1	SLC43A1	0,00014012	44,6455	2,07963
polypyrimidine tract binding protein 1	PTBP1	0,00082781	91,9357	2,07864
RNA binding motif protein 9	RBM9	0,00021041	28,9637	2,07685
coiled-coil domain containing 72	CCDC72	0,00011634	56,8913	2,07345
pleckstrin homology domain containing, family H (with MyTH4 domain) member 3	PLEKHH3	7,67E-05	54,2778	2,07249
beta-gamma crystallin domain containing 3	CRYBG3	0,00417605	7,22974	2,07161
cell cycle associated protein 1	CAPRIN1	0,0001477	28,93	2,06738
---	---	0,0003656	34,0772	2,06582
kinesin family member 21A	KIF21A	0,00297618	15,8205	2,0652
T-box 3	TBX3	0,00014568	42,7813	2,06518
TSR1, 20S rRNA accumulation, homolog (S. cerevisiae)	TSR1	0,00071959	36,028	2,06492
SIN3 homolog A, transcription regulator (yeast)	SIN3A	0,00073077	24,3196	2,06453
lysine (K)-specific demethylase 1	KDM1	0,00027395	33,7437	2,06428
nucleoporin 35kDa	NUP35	9,65E-05	55,6125	2,06395
poly (ADP-ribose) polymerase family, member 10	PARP10	0,00208472	20,9108	2,06379
dishevelled, dsh homolog 1 (Drosophila) /// hypothetical LOC642469	DVL1 /// LOC642469	0,0005701	22,3335	2,06205
guanine deaminase	GDA	0,00022887	397,845	2,05987
Dispatched homolog 1 (Drosophila)	DISP1	0,0002455	373,441	2,05794
ubiquitin specific peptidase 33	USP33	2,16E-05	318,167	2,0578
cytoplasmic polyadenylation element binding protein 4	CPEB4	0,00105746	22,0183	2,05747
ariadne homolog 2 (Drosophila)	ARIH2	0,00126694	75,305	2,05633
DEAD (Asp-Glu-Ala-Asp) box polypeptide 60	DDX60	0,00010071	48,8019	2,0546
RAD17 homolog (S. pombe)	RAD17	0,00019681	50,8909	2,05333
metastasis associated 1	MTA1	0,00106612	38,5255	2,05305
SEC14 and spectrin domains 1	SESTD1	0,00160798	15,5636	2,05241
Heterogeneous nuclear ribonucleoprotein D-like	HNRPDL	4,80E-05	70,8872	2,05235
ribosomal protein S6 kinase, 90kDa,	RPS6KA3	0,00080637	31,055	2,05131

polypeptide 3				
---	---	0,00134594	56,2238	2,05108
progesterone immunomodulatory binding factor 1	PIBF1	0,0007739	20,4452	2,04599
DAZ associated protein 1	DAZAP1	0,00037446	60,8027	2,0415
golgi autoantigen, golgin subfamily a, 5	GOLGA5	0,00120869	20,7393	2,04068
alanine-glyoxylate aminotransferase 2-like 2	AGXT2L2	0,00089023	23,6084	2,03967
protein kinase D3	PRKD3	0,00026621	42,2479	2,03798
poly(A) binding protein interacting protein 1	PAIP1	0,00129087	186,713	2,03558
exportin 6	XPO6	0,00386138	9,95779	2,03347
tight junction associated protein 1 (peripheral)	TJAP1	7,46E-05	71,9725	2,02889
chromatin assembly factor 1, subunit A (p150)	CHAF1A	7,00E-05	369,307	2,02854
RAB13, member RAS oncogene family	RAB13	5,26E-05	39,0661	2,02816
RNA binding motif, single stranded interacting protein 1	RBMS1	0,00361489	16,8172	2,02515
coiled-coil and C2 domain containing 1A	CC2D1A	0,00122207	11,6419	2,02451
stromal antigen 2	STAG2	0,00022062	58,7018	2,02417
KIAA0240	KIAA0240	0,0011134	19,48	2,02206
DNA cross-link repair 1C (PSO2 homolog, S. cerevisiae)	DCLRE1C	0,00016114	45,4726	2,02198
---	---	0,00030916	68,9493	2,0207
GC-rich promoter binding protein 1-like 1	GPBP1L1	0,00098459	33,0744	2,01839
rhophilin, Rho GTPase binding protein 2	RHPN2	0,00057655	28,1598	2,01594
selenium binding protein 1	SELENBP1	0,0006401	207,34	2,01406
U2 small nuclear RNA auxiliary factor 2	U2AF2	0,00012581	73,6994	2,01365
similar to Solute carrier organic anion transporter family, member 4A1 /// solut	LOC100134295 /// SLCO4A1	8,30E-05	386,594	2,01277
exosome component 7	EXOSC7	0,00169951	12,6963	2,01118
G protein-coupled receptor 89A /// G protein-coupled receptor 89B /// G protein-	GPR89A /// GPR89B /// GPR89C	1,04E-05	639,906	2,00918
RNA binding motif protein 17	RBM17	0,00023276	88,9209	2,00658
NOL1/NOP2/Sun domain family, member 5C	NSUN5C	0,00245163	115,823	2,00379
disabled homolog 2, mitogen-responsive phosphoprotein (Drosophila)	DAB2	0,00074093	27,0644	2,00333
misato homolog 1 (Drosophila) /// misato homolog 2 pseudogene	MSTO1 /// MSTO2P	0,00386697	20,237	2,00041
cystathionine-beta-synthase	CBS	0,00382041	22,0091	2,0003

ANEXO 2

INSTITUTO CARLOS CHAGAS

FUNDAÇÃO OSWALDO CRUZ

Caracterização celular e molecular do potencial de diferenciação de células-tronco mesenquimais adultas

Termo de Consentimento Livre e Esclarecido

1 - Eu,_____, RG,_____estou sendo convidado a participar do projeto chamado: "Caracterização celular e molecular do potencial de diferenciação de células-tronco mesenquimais adultas" e a minha participação é voluntária.

2 – As células-tronco são células que possuem a capacidade de se dividir e de se transformar (num processo também conhecido por diferenciação celular) em outros tecidos do corpo, como ossos, nervos, músculos e sangue. Devido a essa característica, as células-tronco possuim um potencial na aplicação terapêutica, sendo úteis para uso em terapia celular de doenças cardiovasculares, neurodegenerativas, diabetes tipo-1, acidentes vasculares cerebrais, doenças hematológicas, traumas na medula espinhal e nefropatias. O principal objetivo das pesquisas com células-tronco é usá-las para recuperar tecidos danificados. Para isso e necessário comprender os mecanismos que levam a diferenciação dessas células em diferentes tecidos adultos. Eu entendo que este projeto está sendo desenvolvido em conjunto com o Instituto de Biologia Molecular do Paraná e a Pontifícia Universidade Católica do Paraná e que os médicos e pesquisadores estão empenhados na pesquisa básica da capacidade das células-tronco mesenquimais em se transformar em células adultas de diversos tecidos.

3 - Eu entendo que estou sendo submetido à cirurgia bariátrica (bypass hipofuncionante reversível Lazzarotto e Souza) associado à dermolipectomia abdominal no qual serão retirados cerca de **500 gramas do tecido adiposo** para este estudo. As células-tronco mesenquimais obtidas do tecido adiposo serão apenas estudadas em laboratório e **não serão utilizadas para qualquer fim terapêutico ou comercial.**

4 - Eu entendo que no momento da publicação dos resultados obtidos nesta pesquisa, não aparecerá meu nome e sim um código, justamente para preservar minha identidade.

5 – Eu estou ciente que a qualquer momento posso desistir de participar do projeto.

6 - Eu li o texto acima e compreendi a natureza e objetivo do estudo do qual fui convidado a participar e concordo voluntariamente em participar.

Curitiba, ___ / ___/ ___ .

Assinatura do participante = _____

Assinatura do responsável = _____

Assinatura do pesquisador = _____

ANEXO 3

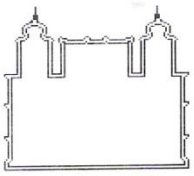

Ministério da Saúde
Fundação Oswaldo Cruz
COMITÊ DE ÉTICA EM PESQUISA-CEP/FIOCRUZ

Rio de Janeiro, 22 de agosto de 2011.

PARECER

Título do Projeto: "Caracterização celular e molecular do potencial de diferenciação de células tronco mesenquimais adultas: aplicação em terapias celulares do sistema cardiovascular"

Protocolo CEP: 419/07

Pesquisador Responsável: Samuel Goldenberg

Instituição: ICC – Instituto Carlos Chagas/Fiocruz/PR

Foram apresentados e submetidos à apreciação do CEP/FIOCRUZ o relatório de atividades, adendo e documentos atualizados ao projeto original do projeto supra mencionado, ambos APROVADOS.

Patricia T. Bozza
Coordenadora do Comitê de Ética em Pesquisa em Seres Humanos
Fundação Oswaldo Cruz

ANEXO 4

Outros trabalhos desenvolvidos durante o doutoramento

Original Research

Are purified or expanded cord blood-derived CD133$^+$ cells better at improving cardiac function?

Alexandra C Senegaglia[1], Laura A Barboza[1], Bruno Dallagiovanna[2], Carlos A M Aita[1], Paula Hansen[1], Carmen L K Rebelatto[1], Alessandra M Aguiar[2], Nelson I Miyague[1], Patrícia Shigunov[2], Fabiane Barchiki[1], Alejandro Correa[2], Marcia Olandoski[1], Marco A Krieger[2] and Paulo R S Brofman[1]

[1]Pontifícia Universidade Católica do Paraná, Institute for Health and Biological Sciences, Rua Imaculada Conceição, 1155 Curitiba, Paraná, 80215901; [2]Instituto Carlos Chagas, Fundação Oswaldo Cruz. Rua Prof. Algacyr Munhoz Maeder, 3775 Curitiba, Paraná 81350010, Brazil

Corresponding author: Alexandra C Senegaglia, Rua Guilherme Pugsley 1760, Apartment 501, Curitiba, Paraná, 80620000, Brazil. Emails: alexandra.senegaglia@pucpr.br; acsenegaglia@hotmail.com

Abstract

Endothelial progenitor cells (EPCs), which express the CD133 marker, can differentiate into mature endothelial cells (ECs) and create new blood vessels. Normal angiogenesis is unable to repair the injured tissues that result from myocardial infarction (MI). Patients who have high cardiovascular risks have fewer EPCs and their EPCs exhibit greater *in vitro* senescence. Human umbilical cord blood (HUCB)-derived EPCs could be an alternative to rescue impaired stem cell function in the sick and elderly. The aim of this study was to purify HUCB-derived CD133$^+$ cells, expand them *in vitro* and evaluate the efficacy of the purified and expanded cells in treating MI in rats. CD133$^+$ cells were selected for using CD133-coupled magnetic microbeads. Purified cells stained positive for EPC markers. The cells were expanded and differentiated in media supplemented with fetal calf serum and basic fibroblast growth factor, insulin-like growth factor-I and vascular endothelial growth factor (VEGF). Differentiation was confirmed by lack of staining for EPC markers. These expanded cells exhibited increased expression of mature EC markers and formed tubule-like structures *in vitro*. Only the expanded cells expressed VEGF mRNA. Cells were expanded up to 70-fold during 60 days of culture, and they retained their functional activity. Finally, we evaluated the therapeutic potential of purified and expanded CD133$^+$ cells in treating MI by intramyocardially injecting them into a rat model of MI. Rats were divided into three groups: A (purified CD133$^+$ cells-injected); B (expanded CD133$^+$ cells-injected) and C (saline buffer-injected). We observed a significant improvement in left ventricular ejection fraction for groups A and B. In summary, CD133$^+$ cells can be purified from HUCB, expanded *in vitro* without loosing their biological activity, and both purified and expanded cells show promising results for use in cellular cardiomyoplasty. However, further pre-clinical testing should be performed to determine whether expanded CD133$^+$ cells have any clinical advantages over purified CD133$^+$ cells.

Keywords: umbilical cord blood, endothelial progenitor cells, transplantation, myocardial infarction

Experimental Biology and Medicine 2010; **235**: 119–129. DOI: 10.1258/ebm.2009.009194

Experimental and Molecular Pathology xxx (2010) xxx–xxx

Contents lists available at ScienceDirect

Experimental and Molecular Pathology

journal homepage: www.elsevier.com/locate/yexmp

Transplantation of SNAP-treated adipose tissue-derived stem cells improves cardiac function and induces neovascularization after myocardium infarct in rats

Gel R.M. Berardi [a,b], Carmen K. Rebelatto [a,b], Heloísa F. Tavares [a], Max Ingberman [c], Patrícia Shigunov [d], Fabiane Barchiki [b], Alessandra M. Aguiar [d], Nelson I. Miyague [b], Julio C. Francisco [b], Alejandro Correa [d], Alexandra C. Senegaglia [b], Paula Hansen Suss [b], José A. Moutinho [b], Vanessa S. Sotomaior [a], Lia S. Nakao [a,c,*], Paulo S. Brofman [b]

[a] Núcleo de Investigação Molecular Avançada, Pontifícia Universidade Católica do Paraná, Rua Imaculada Conceição 1155, Curitiba 80215-901, Brazil
[b] Núcleo de Tecnologia Celular, Pontifícia Universidade Católica do Paraná, Rua Imaculada Conceição 1155, Curitiba 80215-901, Brazil
[c] Departamento de Patologia Básica, Universidade Federal do Paraná, Centro Politécnico, Curitiba 81531-980, Brazil
[d] Instituto Carlos Chagas, FIOCRUZ, Rua Algacyr Munhoz Mader 3775, Curitiba 81350-010, Brazil

ARTICLE INFO

Article history:
Received 17 August 2010
Available online xxxx

Keywords:
Adipose-derived stem cells
SNAP
Nitric oxide
Ejection fraction
Neovascularization
Cardiomyogenesis

ABSTRACT

Stem cell therapy has been considered a promise for damaged myocardial tissue. We have previously shown that S-nitroso-N-acetyl-D,L-penicillamine (SNAP) increases the expression of several muscular markers and VEGF in mesenchymal stem cells, indicating that transplantation of SNAP-treated cells could provide better functional outcomes. Here, we transplanted SNAP-treated adipose tissue-derived stem cells (ADSCs) in rat infarcted myocardium. After 30 days, we observed a significant improvement of the ejection fraction in rats that received SNAP-treated ADSCs, compared with those that received untreated cells ($p = 0.008$). Immunohistochemical reactions showed an increased expression of troponin T–C and von Willebrand factor, and organized vascular units in the infarcted area of tissue transplanted with treated ADSCs. SNAP exposure induced intracellular S-nitrosation, a decreased GSH/GSSG ratio, but did not increase cGMP levels. Collectively, these results indicate that SNAP alters the redox environment of ADSCs, possibly associated with a pre-differentiation state, which may improve cardiac function after transplantation.

STEM CELLS AND DEVELOPMENT
Volume 00, Number 00, 2011

DOI: 10.1089/scd.2011.0143

ORIGINAL RESEARCH REPORT

PUMILIO-2 Is Involved in the Positive Regulation of Cellular Proliferation in Human Adipose-Derived Stem Cells

Patrícia Shigunov,[1] Jose Sotelo-Silveira,[2–4] Crisciele Kuligovski,[1] Alessandra Melo de Aguiar,[1] Carmen K. Rebelatto,[5] José A. Moutinho,[6] Paulo S. Brofman,[5] Marco A. Krieger,[1] Samuel Goldenberg,[1] David Munroe,[2] Alejandro Correa,[1] and Bruno Dallagiovanna[1]

Stem cells can either differentiate into more specialized cells or undergo self-renewal. Several lines of evidence from different organisms suggest that these processes depend on the post-transcriptional regulation of gene expression. The presence of the PUF [Pumilio/FBF (fem-3 binding factor)] domain defines a conserved family of RNA binding proteins involved in repressing gene expression. It has been suggested that a conserved function of PUF proteins is to repress differentiation and sustain the mitotic proliferation of stem cells. In humans, Pumilio-2 (PUM2) is expressed in embryonic stem cells and adult germ cells. Here we show that PUM2 is expressed in a subpopulation of adipose-derived stem cell (ASC) cultures, with a granular pattern of staining in the cytoplasm. Protein levels of PUM2 showed no changes during the differentiation of ASCs into adipocytes. Moreover, RNAi knockdown of *pum2* did not alter the rate of adipogenic differentiation compared with wild-type control cells. A ribonomic approach was used to identify PUM2-associated mRNAs. Microarray analysis showed that PUM2-bound mRNAs are part of gene networks involved in cell proliferation and gene expression control. We studied *pum2* expression in cell cultures with low or very high levels of proliferation and found that changes in *pum2* production were dependent on the proliferation status of the cell. Transient knockdown of *pum2* expression by RNAi impaired proliferation of ASCs in vitro. Our results suggest that PUM2 does not repress differentiation of ASCs but rather is involved in the positive control of ASCs division and proliferation.

Stem Cell Research (2013) 11, 902–912

Available online at www.sciencedirect.com

SciVerse ScienceDirect

www.elsevier.com/locate/scr

Polysome profiling shows extensive posttranscriptional regulation during human adipocyte stem cell differentiation into adipocytes

Lucia Spangenberg[b,1], Patricia Shigunov[a,1], Ana Paula R. Abud[a], Axel R. Cofré[a], Marco A. Stimamiglio[a], Crisciele Kuligovski[a], Jaiesa Zych[a], Andressa V. Schittini[a], Alexandre Dias Tavares Costa[a], Carmen K. Rebelatto[c], Paulo R.S. Brofman[c], Samuel Goldenberg[a], Alejandro Correa[a], Hugo Naya[b], Bruno Dallagiovanna[a,*]

[a] *Instituto Carlos Chagas, Fiocruz-Paraná, Rua Professor Algacyr Munhoz Mader, 3775, Curitiba-PR 81350-010, Brazil*
[b] *Unidad de Bioinformática, Institut Pasteur Montevideo, Mataojo 2020, Montevideo 11400, Uruguay*
[c] *Núcleo de Tecnologia Celular, Pontifícia Universidade Católica do Paraná, Rua Imaculada Conceição, 1155, Curitiba-PR 80215-901, Brazil*

Received 22 December 2012; received in revised form 29 May 2013; accepted 2 June 2013

Abstract Adipocyte stem cells (hASCs) can proliferate and self-renew and, due to their multipotent nature, they can differentiate into several tissue-specific lineages, making them ideal candidates for use in cell therapy. Most attempts to determine the mRNA profile of self-renewing or differentiating stem cells have made use of total RNA for gene expression analysis. Several lines of evidence suggest that self-renewal and differentiation are also dependent on the control of protein synthesis by posttranscriptional mechanisms. We used adipogenic differentiation as a model, to investigate the extent to which posttranscriptional regulation controlled gene expression in hASCs. We focused on the initial steps of differentiation and isolated both the total mRNA fraction and the subpopulation of mRNAs associated with translating ribosomes. We observed that adipogenesis is committed in the first days of induction and three days appears as the minimum time of induction necessary for efficient differentiation. RNA-seq analysis showed that a significant percentage of regulated mRNAs were posttranscriptionally controlled. Part of this regulation involves massive changes in transcript untranslated regions (UTR) length, with differential extension/reduction of the 3′UTR after induction. A slight correlation can be observed between the expression levels of differentially expressed genes and the 3′UTR length. When we considered association to polysomes, this correlation values increased. Changes in the half lives were related to the extension of the 3′UTR, with longer UTRs mainly stabilizing the transcripts. Thus, changes in the length of these extensions may be associated with changes in the ability to associate with polysomes or in half-life.

* Corresponding author. Fax: +55 41 33163267.
E-mail address: brunod@tecpar.br (B. Dallagiovanna).
[1] Both authors contributed equally to this work.

Inibição da via de sinalização Hedgehog com ciclopamina afeta a expressão de miR-20a e miR-31

Luciana Roberge[1], Ana Carolina Origa-Alves[2], Carmen K. Rebelatto[1], Bruno Dallagiovanna[2], Patrícia Shigunov[2*]

[1] Pontifícia Universidade Católica do Paraná, Rua Imaculada Conceição 1155, Curitiba 80215-901, Brasil

[2] Laboratório de Biologia Básica de Células-Tronco, Instituto Carlos Chagas - Fiocruz, Curitiba, Brasil.

*Autor correspondente: Tel: +55 41 3316 3237; Fax: +55 41 3316 3267; E-mail: shigunov@tecpar.br

Artigo aceito para publicação em "Journal of Biotecnology and Biodiversity".

Title: Inhibition of Hedgehog signaling pathway affects the expression of miR-20a and miR-31
Running title: Hedgehog pathway affects miR-20a and miR-31

Abstract

MicroRNAs are small RNA molecules (~ 22 nucleotides) that act as post-transcriptional regulators of gene expression by inhibiting translation of messenger RNAs. MicroRNAs are involved in regulating many biological and pathological processes, as well as the Hedgehog (Hh) signaling pathway. We evaluate the expression of four miRNAs (miR-20a, miR-31, miR-17 and miR-199b5p) in human adipose-derived stem cells under activation and blockade of Hh signaling pathway. Cells were treated with purmorphamine (Hh activator) or cyclopamine (Hh blocker) for 24 hours. RNA extraction and cDNA were performed to analyze of miRNAs expression by quantitative RT-PCR. The expression level of miR-20a and miR-31 increased after blocking Hh signaling pathway, thus these miRNAs may be involved in control of proliferation in stem and cancer cells. MiR-20a and miR-31 are strong candidates for biomarkers of Hh pathway.
Keywords: *MicroRNA, adipose stem cells, purmorphamine, Cyclopamine, Hedgehog.*

Resumo

MicroRNAs são pequenas moléculas de RNA (~ 22 nucleotídeos), que atuam como reguladores pós-transcricional da expressão de genes, inibindo a tradução do RNA mensageiro. MicroRNAs estão envolvidos na regulação de muitos processos biológicos e patológicos, assim como a via de sinalização Hedgehog (Hh). Nós avaliamos a expressão de quatro microRNAs (miR-20a, miR-31, miR-17 e miR-199b5p) em células-tronco derivadas de tecido adiposo humano sob ativação e bloqueio da via de sinalização Hh. As células foram tratadas com purmorfamina (ativador da via Hh) ou ciclopamina (bloqueador da via Hh) durante 24 horas. Extração de RNA e cDNA foram realizadas para fazer a analise da expressão dos miRNAs por RT-PCR quantitativa. O nível de expressão do miR-20a e miR-31 aumentou após o bloqueio da via de sinalização Hh, sendo assim, esses miRNAs podem estar envolvidos no controle da proliferação de células-tronco e câncer. O miR-20a e o miR-31 são fortes candidatos para biomarcadores da via Hh.
Palavras-chave: MicroRNA, Células-tronco de Tecido Adiposo, Purmorfamina, Ciclopamina, Hedgehog.